The Thesis Committee for Mazen Ramzi Abdulbaki
Certifies that this is the approved version of the following thesis:

Simulation Study of Polymer Microgel Conformance Treatments

APPROVED BY
SUPERVISING COMMITTEE:

Supervisor:

Kamy Sepehrnoori

Mojdeh Delshad

Simulation Study of Polymer Microgel Conformance Treatments

by

Mazen Ramzi Abdulbaki, B.S.

Thesis

Presented to the Faculty of the Graduate School of

The University of Texas at Austin

in Partial Fulfillment

of the Requirements

for the Degree of

Master of Science in Engineering

The University of Texas at Austin

August 2012

Dedication

To

my parents

Rima & Ramzi

and my sister

Nora

for their unwavering love and support

Acknowledgements

I would like to thank my supervising professor, Dr. Kamy Sepehrnoori, for his continuous care and guidance. I greatly appreciate having been given the opportunity to be a part of his research group; I enjoyed the experience very much. I would also like to acknowledge Dr. Abdoljalil Varavei for all his help with my simulation work. I am very grateful for his support, patience, and kindness. I learned a great deal from him throughout my time at UT Austin. I would also like to extend a thank you to Dr. Mojdeh Delshad and Dr. Chun Huh; I am very grateful for all their time and support.

In addition, I would like to thank my family and friends for believing in me. Lastly, I would like to thank Natália Saliés and Tarek Hariz for their support and friendship throughout both my undergraduate and graduate studies; I look forward to the day we take on another degree together.

Abstract

Simulation Study of Polymer Microgel Conformance Treatments

Mazen Ramzi Abdulbaki, M.S.E.

The University of Texas at Austin, 2012

Supervisor: Kamy Sepehrnoori

Significant quantities of hydrocarbon are bypassed during conventional waterfloods. This is the direct result of fluid channeling through high permeability zones within the reservoir. Conformance control offers a means of increasing vertical and areal sweep efficiency, thus decreasing the amount of hydrocarbon bypassed. This, in turn, results in increased hydrocarbon production, decreased water cut, and field life extension. This thesis focuses on the use of polymer microgels as a relatively novel conformance control agent. Polymer-microgel-enhanced waterflooding tackles fluid channeling by "plugging" high permeability channels, or thief zones, and diverting trailing flooding fluid to adjacent poorly swept areas of the reservoir.

The first major objective of this thesis was to provide an extensive literature survey on polymer microgel technology, which can serve as the go-to reference on this topic. Colloidal Dispersion Gels (CDGs), Preformed Particle Gels (PPGs), temperature-sensitive polymer microgels (Bright Water), and pH-sensitive polymer microgels are all discussed in detail, and an attempt is made to highlight the potential mechanisms by which they plug thief zones and improve oil recovery.

This thesis then outlines the results of simulating numerous polymer microgel floods, ranging from experimental cases to field cases. Specifically, Colloidal Dispersion Gels (CDGs) were chosen for the simulations undergone. All simulations were run using UTGEL, a newly developed in-house simulator designed exclusively for the simulation of polymer, gel, and microgel floods. The simulations performed provide insight on the polymer microgel flooding process, and also served as a means of validating UTGEL's polymer microgel (CDG) models. The development of the UTGEL simulator was important as it enables the optimization of polymer microgel floods for maximized hydrocarbon recovery efficiency.

The results of a simulation study, using a synthetic field case, are also outlined. This sensitivity study provides additional insight on optimal operational conditions for polymer microgel technology. More specifically, this study aimed to investigate the effectiveness of microgel flooding treatments in layered reservoirs of varying permeability contrasts, vertical-to-horizontal permeability ratios, and under a variety of different injection concentrations.

Table of Contents

List of Tables

List of Figures

Chapter 1: Introduction

With global population consistently on the rise, it is increasingly important to accommodate for subsequent growth in energy demand. By 2040, it is estimated that the world population will be just short of 9 billion people – an increase of approximately 30% from 2011's population (U.S. Census Bureau 2010). And by 2035, it is estimated that yearly global energy consumption will approach 739 quadrillion Btu, roughly twice 2007's energy consumption levels (U.S. Energy Information Administration 2010). In addition, it is important to note that more than 85% of global energy supply stems from fossil fuels (U.S. Energy Information Administration 2010; Sheng 2011). And since fossil fuel is a limited source of energy, it is clear that something must be done in order to address global energy needs. Though much emphasis has been placed on renewable energy sources, these resources currently make only a miniscule fraction of our energy supply. In 2009, renewable energy accounted for a mere 8% of total energy consumption in the U.S. (U.S. Energy Information Administration 2009). Until renewable energy can support the weight of today's energy-intensive society, it is imperative to more efficiently capture and utilize fossil fuels, so as to keep up with increasing energy requirements.

One of the most prominent means of furthering energy supply is to extend the life of mature hydrocarbon reservoirs, through more efficient hydrocarbon capturing techniques. Emerging technologies and different Enhanced Oil Recovery (EOR) processes have rendered this possible. Examples of such means of increasing a reservoir's lifespan include: thermal recovery and chemical flooding – two popular EOR processes, and tertiary production methods. Data obtained from the U.S. Energy Information Administration's 2010 International Energy Outlook can help put EOR's potential into perspective. In 2007, roughly 31 billion barrels of liquid fuel were

produced globally, 29.8 billion barrels of which were conventional liquid fuels (U.S. Energy Information Administration 2010). Given that there are 5.78 million Btu in a barrel of oil (Silverman 2007), it can be determined that approximately 172 quadrillion Btu of energy supplied in 2007 stemmed directly from conventional liquid fuel production. This means that if the use of EOR could have increased global conventional liquid fuel production by 10%, there would have been a resulting incremental energy supply of 17.2 quadrillion Btu. This incremental energy supply is greater than Canada's 2007 energy consumption level of 14.2 quadrillion Btu, and is just short of the African continent's 2007 energy consumption level of 17.8 quadrillion Btu (U.S. Energy Information Administration 2010). It is clear that EOR has significant potential to increase energy supply, and it does so merely by more efficiently extracting hydrocarbons from already mature reservoirs.

One of the primary reasons reservoir life extension is possible is because a large percentage of reservoir hydrocarbon is left behind after the production process. A portion of residual hydrocarbon is left behind because of the capillary forces naturally present in porous reservoirs; however, some hydrocarbon is left behind due to specific limitations in the production process. One such limitation stems from the conventional waterflooding process. After primary production, waterflooding is a common secondary production method. During waterflooding, however, the flooding fluid typically channels through the most permeable zones within the reservoir, leaving a significant quantity of hydrocarbons behind – sometimes as high as 65% - 70% of the original oil in place, depending on the level of heterogeneity (Lake 1989; Sorbie 1991). Polymer microgels, the focus of this thesis, aim to economically remedy this inefficiency in sweeping reservoirs by plugging such high permeability streaks/water channels, diverting injected flooding fluid flow into adjacent low permeability rock that would otherwise be untouched. Thus, adding polymer

microgels to waterflooding fluid can increase macroscopic sweep efficiency and improve hydrocarbon recovery efficiency (by producing otherwise bypassed hydrocarbons).

The focus of this thesis is on such use of polymer microgels in waterflooding processes. The concept of waterflooding, as a secondary production process, is not a new one. Waterflooding currently accounts for over 50% of production in the U.S. (Morrow 2012). However, the addition of polymer microgels to waterflooding fluid is a relatively new concept. Figure 1.1 can aid visualize the different stages of the production process as well as the oil recoveries expected throughout each stage. Polymer-microgel-enhanced waterflooding is classified as a type of chemical EOR process, with potential to produce hydrocarbons above and beyond those recoverable by conventional waterfloods. Using polymer microgels as conformance control agents can prove to be an effective means to further extend the life of oil and gas reservoirs, by more efficiently sweeping hydrocarbons. This will be further elaborated on throughout this thesis.

In addition to improving the hydrocarbon recovery process and thus prolonging the life of hydrocarbon reservoirs, polymer microgels can also serve to decrease associated waste water production. This is also very important as plenty of resources go into disposing water, and such efforts have been estimated to cost up to $40 billion globally per year (Seright et al. 2003). It has been estimated that for every barrel of oil produced worldwide, an average of roughly 3 barrels of water are produced as well; associated waste water production is even more severe in the United States (Seright et al. 2003). As conformance control agents, polymer microgels offer a cost-effective means of increasing hydrocarbon production and decreasing associated water production. It is important to note that polymer microgel flooding has been successfully implemented in many experimental cases as well as field-scale cases worldwide. A number of these cases will be discussed in more detail within this thesis.

This thesis presents an in-depth study of polymer microgels, as well as the results of simulating their use in flooding applications. First, an overview of the necessary background information is provided (Chapter 2). One major objective was to present a literature survey of polymer microgel flooding technology (Chapter 3). Another major objective was to detail the results of simulating several polymer microgel flooding applications, ranging from experimental to synthetic to field cases, and to match simulation results with real results when possible (Chapters 4, 5 and 6). These simulations serve to provide additional insight on the polymer microgel flooding process, as well as to determine optimal conditions for polymer microgel use.

The simulations carried out for this thesis were all run using UTGEL, an in-house reservoir simulator recently developed in the Petroleum & Geosystems Department at The University of Texas at Austin. UTGEL is a spin-off simulator stemming from UTCHEM; it is exclusively designed for the simulation of waterfloods/ polymer floods/ polymer gel floods/ polymer microgel floods. UTGEL enables users to optimize the design of polymer microgel floods, and to forecast the resulting production profiles. It is imperative to fully take advantage of such an EOR process, in order to maximize hydrocarbon recovery efficiency, and thus prolong the life of hydrocarbon reservoirs – our single greatest source of today's energy supply.

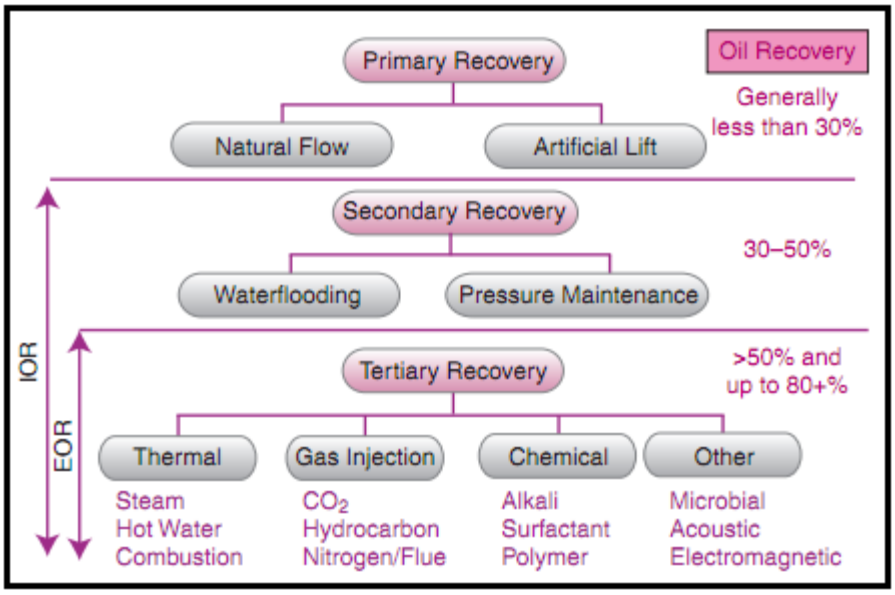

Figure 1.1: Depiction of the Stages Involved in the Production Process

Figure from Al-Mutairi and Kokal (2011). Figure designed based on Stosur (2003) and Stosur et al. (2003).

Chapter 2: Background

Enhanced Oil Recovery (EOR) is the subject of significant attention around the world, largely stimulated by discussions of peak oil. EOR is especially attractive because the global average oil recovery factor is as low as 34% (Schulte 2005). Enhanced Oil Recovery is essentially the recovery of oil brought about by injecting materials/energy not normally present in the reservoir, and it is not necessarily a tertiary recovery process. EOR excludes pressure maintenance efforts such as conventional waterflooding processes. Ultimately, EOR targets residual oil and/or bypassed oil. (Delshad 2012; Lake 2012; Stosur et al. 2003)

Enhanced Oil Recovery can generally be divided into three distinct branches: namely thermal, gas, and chemical processes. In 2004, it was estimated that EOR accounted for approximately 3% of oil production worldwide (Schulte 2005; Oil & Gas Journal 2004). Figure 2.1 demonstrates the relative contribution of each EOR method to incremental oil production in 2004. For more information on EOR, Manrique et al. (2010) can be referred to for a review of thermal, gas, and chemical EOR projects. Mohan et al. (2011) and Al-Mutairi and Kokal (2011) discuss EOR potential in the U.S. and the Middle East respectively. Dickson et al. (2010) provide a methodology for screening EOR processes.

The focus of this thesis is on the use of polymer microgels to increase volumetric sweep efficiency in mature reservoirs, a chemical EOR process that has been drawing noteworthy attention as a potential means of conformance control. Manrique et al. (2010) recognize Colloidal Dispersion Gels (CDGs) and BrightWater, two different polymer microgels, as a “new window of opportunities for EOR chemical methods”.

One of the key take-home messages of this chapter is that conventional polymer flooding, polymer gel flooding, and polymer microgel flooding are three distinct enhanced oil recovery methods. Each of these different enhanced flooding methods is discussed below in detail so as to clarify the divide between them. Polymer gel flooding and polymer microgel flooding are presented as deviations from conventional polymer flooding. The methods are also discussed so as to provide the background information needed to fully understand polymer microgel flooding and its merits.

2.1 CONVENTIONAL POLYMER FLOODING

Sorbie's *Polymer-Improved Oil Recovery* (1991) is an invaluable textbook for those looking to learn about polymer flooding in more depth. Sheng's *Modern Chemical Enhanced Oil Recovery* (2011) is a more recent textbook that can also be referred to for significant detail on polymer flooding. This same work can be referred to for a summary of screening criteria that can be used to determine if polymer flooding is appropriate for a given reservoir. Needham and Doe's *Polymer Flooding Review* (1987) is a reference very well suited for those looking for a more succinct review of polymer flooding.

Polymer flooding is a chemical EOR method that is primarily used in the tertiary recovery stage, though this section should reveal that there are benefits to using it earlier, for e.g. during secondary recovery. Polymer flooding involves the injection of a polymer solution with the primary goal being mobility control. The two most common polymers used in polymer flooding are partially-hydrolyzed polyacrylamide (PHPA) and xanthan gum (Sorbie 1991; Needham and Doe 1987; Sheng 2011). In porous rock, PHPA can demonstrate viscoelastic/shear-thickening/pseudodilatant effects at relatively high shear rates. Xanthan gum, on the other hand, is strictly shear-thinning; it demonstrates pseudoplastic behavior in porous media matching its behavior in a viscometer (Seright et

al. 2008). PHPA is not suitable in conditions of high temperature (decreased chemical stability due to fast hydrolysis rates) or high salinity (compression of polymer chains due to the neutralization of otherwise repelling carboxylic groups). Xanthan gum is more tolerant to high salinities, but has a lower permeability reduction factor (it is adsorbed less, and does not exhibit shear-thickening behavior). (Sheng 2011)

After waterflooding, a portion of oil is left behind due to the trapping action of capillary forces and another portion is left behind due to flooding inefficiencies. The oil left behind due to capillary forces is immobile and is deemed "residual oil". The oil left behind due to waterflooding inefficiencies (namely those resulting from unfavorable mobility ratios and/or reservoir heterogeneity) is potentially mobile oil and is deemed "bypassed oil". This distinction is especially important because it is commonly accepted that polymer flooding does not enable the production of residual oil, since it has only a very slight effect on capillary number. Instead, polymer flooding is aimed at bypassed oil. (Sorbie 1991)

The effects of polymer flooding (mobility control effect/ fractional flow effect/ fluid diversion effect) are discussed in the sub-sections below. This is followed by discussions on polymer retention and residual oil, respectively. Lastly, distinctions are made between conventional polymer floods and polymer gel/polymer microgel floods.

2.1.1 Mobility Control Effect

The leading effect of polymer flooding is that of mobility control. The mobility ratio is the current criterion for polymer flooding mobility control requirements, and it is defined as (Sorbie 1991; Needham and Doe 1987; Sheng 2011):

$$Mobility\ Ratio = M = \frac{\left(\frac{\mu_o}{k_o}\right)}{\left(\frac{\mu_w}{k_w}\right)} \quad \text{(Eqn. 2.1)}$$

Mobility ratio values less than one are favorable; higher mobility ratio values are unfavorable. In one-dimensional floods, mobility ratios greater than five are good candidates for polymer flood consideration (Sorbie 1991). Adding polymer to waterfloods increases the injected aqueous phase's viscosity, and so decreases the mobility ratio. This, in turn, leads to a more uniform areal and vertical displacement of the oil in place and decreased likelihood of viscous fingering. Figures 2.2 and 2.3 can help visualize this increased sweep efficiency. In homogenous one-dimensional cores, an almost piston-like displacement can be reached at mobility ratios that are less than one (Sorbie 1991). Polymer flooding has greater potential if it is used earlier in the production process since there is more mobile oil, and thus k_o is relatively high (Needham and Doe 1987).

Sheng (2011) proposes, and justifies, the use of a new mobility ratio criterion that corrects for movable oil saturation. This is worth further investigating before the design of a polymer flood. Figure 2.4 can help visualize the sensitivity of ultimate oil recovery to mobility ratio (as well as to the degree of heterogeneity).

2.1.2 Fractional Flow Effect

As previously explained, polymer flooding is conventionally thought not to decrease residual oil saturation; it can only enable the production of oil that is bypassed due to unfavorable mobility ratios and/or heterogeneity (Sorbie 1991; Needham and Doe 1987). However, polymer flooding does enable residual oil saturation to be reached more

quickly/economically. This is because polymer floods increase the fractional flow of oil, f_o, where f_o is defined as (Needham and Doe 1987):

$$f_o = \frac{1}{1 + M} \qquad \text{(Eqn. 2.2)}$$

This increase in fractional flow of oil, f_o, is a result of the polymer flood's lowering of the mobility ratio, M. This phenomenon is more significant earlier in the production process when k_o is relatively high, and also in reservoirs where the oil viscosity, μ_o, is low (Needham and Doe 1987).

2.1.3 Fluid Diversion Effect

Heterogeneity, resulting from layering with highly contrasting permeabilities or from the presence of high permeability streaks (thief zones), is another major cause of oil being bypassed after waterflooding. Sorbie (1991) indicates that polymer floods can also remedy this as a result of viscous cross-flow effects, but only at much lower mobility ratios. However, these mobility ratios may be too low to reach economically. Needham and Doe (1987) also indicate that polymer floods can remedy the problem brought about by heterogeneity; they explain that increased flow resistance brought about by the injected polymer can result in fluid diversion away from the naturally preferential water paths.

2.1.4 Polymer Retention

This section serves to introduce the concept of polymer retention in porous media. Dominguez and Willhite (1976), Cohen and Christ (1986) and Huh et al. (1990) are good sources of information on this topic. Sheng (2011) provides a detailed review of the concepts of polymer retention. Polymer retention is important in reservoirs as it results in

the loss of injected polymer and it affects matrix permeability. Polymer retention decreases permeability since it effectively restricts pore space, yielding resistance to flow (Cohen and Christ 1986; Hirasaki and Pope 1974). This can yield fluid diversion affects. A brief background is presented below, and important terms are defined since they become important in subsequent sections.

Mobility reduction as a result of polymer flooding can be quantified using a 'mobility reduction factor', otherwise known as the 'resistance factor' (Chauveteau and Kohler 1974). Jennings et al. (1970) define the resistance factor (RF) as "the decrease in mobility of a polymer solution in comparison with the flow of the water or brine in which it is prepared". The RF, introduced by Pye in 1964, can be expressed as (Dominguez and Willhite 1976; Needham et al. 1987; Pye 1964; Jennings et al. 1970; Chauveteau and Kohler 1974):

$$RF = \frac{\left(\frac{k_w}{\mu_w}\right)}{\left(\frac{k_p}{\mu_p}\right)} = \frac{Mobility\ of\ Flooding\ Water}{Mobility\ of\ Polymer\ Solution} \qquad \text{(Eqn. 2.3)}$$

In a core flood at constant injection rate, this is similar to the ratio of the core pressure drop after polymer flood to the core pressure drop before polymer flood (Pye 1964). The RF is a function of the polymer used, the concentration of the polymer, the solution salinity and the solution hardness (Needham et al. 1987).

Permeability reduction as a result of polymer flooding can be quantified using a 'permeability reduction factor', otherwise known as the 'residual resistance factor' (Chauveteau and Kohler 1974). Jennings et al. (1970) state that the residual resistance factor (RRF) quantifies the "decrease in mobility of water that follows a polymer solution

relative to water flow before the flow of the polymer solution". The RRF can be expressed as (Needham et al. 1987; Jennings et al. 1970; Chauveteau and Kohler 1974):

$$RRF = \frac{\left(\frac{k_w}{\mu_w}\right)_{Initial}}{\left(\frac{k_w}{\mu_w}\right)_{Final}} = \frac{Initial\ Water\ Mobility\ Before\ Polymer\ Flood}{Final\ Water\ Mobility\ After\ Polymer\ Flood} \qquad \text{(Eqn. 2.4)}$$

A higher value of RRF indicates a polymer's increased permeability reduction capabilities; this can render the polymer a more effective conformance control agent. Polymer retention influences permeability reduction capabilities, and this is an incentive for this discussion. The motivation for polymer gel or polymer microgel use is the increased RRF brought about by the presence of a crosslinker (Norman et al. 1999; Smith et al. 2000; Mack and Smith 1994). This will soon be elaborated on further.

Polymer retention can be divided into adsorption, mechanical entrapment, and hydrodynamically induced retention (Cohen and Christ 1986; Sorbie 1991; Dominguez and Willhite 1976). Adsorption is the binding of polymer molecules to solid surfaces. Mechanical entrapment is the trapping of polymer molecules in flow channels that are too narrow for them to pass (Sorbie 1991). Hydrodynamically induced retention is flow-dependent retention brought about by hydrodynamic forces. Sorbie (1991) physically describes it as "polymer molecules that are thought to be trapped temporarily in stagnant flow regions by hydrodynamic drag forces". Higher velocities yield more retention of this type (Dominguez and Willhite 1976). Unlike retention by mechanical entrapment, this retention type is reversible since the hydrodynamically retained polymer molecules do not adsorb to pore walls (Huh et al. 1990). Figures 2.5 and 2.6 can help visualize these three polymer retention mechanisms.

Cohen and Christ (1986) performed a polymer (hydrolyzed polyacrylamide) flooding experiment where they isolated adsorption effects; their results demonstrated 35.2% of polymer retention was attributed to adsorption and 64.8% was attributed to mechanical entrapment and hydrodynamically induced retention. The same experiment also demonstrated that adsorption alone could reduce flow capability by 14%. Dominguez and Willhite (1976) performed a polymer (hydrolyzed polyacrylamide) flooding experiment where they minimized adsorption effects; they compared their results to those in literature and determined that the major source of polymer retention was non-adsorptive retention. The same experiment also demonstrated that mechanical entrapment, RF and RRF all increase with increasing polymer concentrations. Szabo (1975) also concluded that non-adsorptive retention is dominant in low permeability, low surface area sand packs. However, Szabo (1975) demonstrated that this dominance reverses in rocks of higher permeability and surface area (presumably because mechanical entrapment is lessened as effective area open to flow increases). Sorbie (1991) provides support for this phenomenon; adsorption becomes the dominant retention mechanism at higher permeabilities.

Hirasaki and Pope (1974) indicate that adsorption and subsequent permeability reductions are a function of polymer molecular weight, water salinity, rock surface composition, permeability, porosity and flow rate. Hirasaki and Pope (1974) developed a model characterizing polymer adsorption based on the polymer, flooding brine and the rock properties.

Maerker (1973) demonstrated that polymer retention increases reversibly at higher velocities. The results of Dominguez and Willhite's work (1976) support this finding. This dependency is associated with hydrodynamic retention (Sorbie 1991). Stahl and Schulz (1988) outline the conditions required for hydrodynamic retention to occur.

Sheng (2011) provides a review of polymer retention observations, which should be referred to for additional insight. Some observations include:

- Polymer adsorption increases with increasing salinity, lower degrees of hydrolysis, and lower temperatures (Sheng 2011).
- Total retention increases with increasing polymer concentration (Szabo 1975).
- Hydrolyzed polyacrylamide (HPAM) adsorbs to porous media more than xanthan (Sheng 2011).

Additionally, Huh et al. (1990) proposes a polymer retention model that accounts for the different retention mechanisms. Hirasaki and Pope (1972) list adsorption, gel formation, and plugging as mechanisms of permeability reduction. Polymer gels and polymer microgels take additional advantage of gel formation and subsequent plugging to reduce permeability more significantly than conventional polymers can. This deems them more effective conformance control agents.

2.1.5 Residual Oil

It is interesting to note that there is still some investigation of the idea that polymer floods cannot decrease residual oil saturation. Seright (2011) has recently witnessed polymer-flood-induced decreases in residual oil saturation in homogeneous oil-wet cores containing viscous crude. Seright's report (2011) can be referred to for more information on the experiments performed. Sheng (2011) indicates that polymer floods can more effectively produce oil droplets from dead-end pores as a result of polymer viscoelastic behavior, a phenomenon that also sheds some doubt on conventional belief. In addition, Urbissinova et al. (2010) performed polymer flood experiments where they

isolated polymer elasticity as a variable and demonstrated that it can increase displacement efficiency and decrease residual oil saturation.

2.1.6 Distinctions between Polymers and Gels/Microgels

One of the important distinctions between conventional polymer floods and polymer gel/polymer microgel floods is the presence of a crosslinker. Crosslinking agents yield a polymer network which enables a more significant, longer lasting, and more optimizable permeability reduction (RRF); this can result in a long-term increased resistance to flow in high permeability streaks and subsequent fluid diversion effects (Needham and Doe 1987; Smith et al. 2000; Norman et al. 1999). Conventional polymer floods are very effective for mobility control effects (decreasing mobility ratio as a result of polymer viscosity). However, polymer gel/polymer microgel floods are much more suitable for conformance control/water shutoff as they have these enhanced permeability reduction capabilities brought about by the presence of crosslinker (Sheng 2011; Norman et al. 1999).

This suggests that a conventional polymer flood may be ideal in situations with adverse mobility ratios only, while a polymer gel/microgel flood would be ideal in situations with significant heterogeneity/permeability variation only (Norman et al. 1999). Combining different flooding options is often appropriate and is done fairly regularly (Smith et al. 1996; Muruaga et al. 2008). The distinction between polymer gel floods and polymer microgel floods will be made clearer in their respective background sections below.

2.2 POLYMER GEL FLOODING

Kim's dissertation (1995), titled *Simulation Study of Gel Conformance Treatments*, can be referred to for a detailed study of polymer gels and the results of

simulation studies involving their use as conformance control agents. Kim's (1995) study involved three different polymer gels:

1. Polymer/chromium chloride gel.
2. Polymer/chromium malonate gel.
3. Silicate gel.

UTGEL enables the modeling of polymer gels and polymer microgels. Specifically, the simulator enables the modeling of their effect on aqueous-phase viscosity, gel retention on rock matrix, and aqueous phase permeability reduction. Abdo et al. (1984) and Avery et al. (1986) are a couple of articles on polymer gels that can be referenced. The common consensus is that polymer gels can essentially block thief-zones in heterogeneous formations, and divert trailing waterflooding fluid to adjacent under-swept reservoir rock, thus producing otherwise bypassed oil. This results in increased sweep efficiency and incremental oil recovery, an outcome that has been validated with many different field trials (Abdo et al. 1984; Avery et al. 1986). Avery et al. (1986) cite a 75-80% project success history on as many as 600 well treatments over more than 50 fields. Kabir (2001) can be referred to for a review of chemical water shutoff technologies, which includes an overview of polymer gels. Kim's dissertation (1995) can be referred to for a much more extensive list of work on polymer gels. Seright et al. (2003) outline when gels are an effective choice for water shutoff treatments. Seright and Liang (1994) provide a literature review of an extensive number of field applications of polymer gels. Sydansk and Southwell (2000) present the lessons learnt from their experience with a specific polymer gel technology, though some of their learnings extend

to other gels too. Norman et al. (2006) present a review of over 100 polymer gel conformance treatments conducted in Argentina and Venezuela.

2.2.1 Conformance Control

Liu et al. (2006) define conformance control agents as "those technologies in which chemical or mechanical methods are used to reduce or block water/gas production resulting from wellbores or high permeability zones/channels/fractures of reservoirs". Polymer gels and polymer microgels are such conformance control agents. Though they have their distinctions, they both function as plugging agents.

Conformance control can be in the form of water shutoff (producer treatment), profile control (injector treatment), or a combination of the two. Liu et al. (2006) can be referred to for further explanation and illustrations of these difference conformance control treatments. Note that Kabir (2001)'s article can be referred to for a review of different water shutoff technologies. Conformance control can also be in the form of in-depth fluid diversion; as will soon be made clear, polymer microgels can more effectively be used to achieve in-depth fluid profile control. (Liu et al. 2006)

At this point, the difference between conformance control and mobility control should be clear. Huh (2012) elaborates that mobility control is an attempt to improve the *volumetric* sweep efficiency of a reservoir (e.g. through the use of polymers and/or foam), while conformance control is an attempt to improve only the *vertical* sweep efficiency (e.g. through the use of gels, microgels, packers, and/or surfactant foams).

The potential vertical sweep efficiency improvement brought about by conformance control can be demonstrated using a simple reservoir illustration (as was similarly done, for example, by Espinosa 2011). Figure 2.7 is a simplified example of a layered reservoir, with varying permeabilities. In such a layered system, when the wells

are pressure-constrained and when each layer has uniform and similar fluid viscosities, injected flow allocation is determined based on the following equation, derived from Darcy's law:

$$q_i = \frac{k_i * h_i}{\sum_{i=1}^{n}(k_i * h_i)} \ , \qquad \text{(Eqn. 2.5)}$$

where q_i represents the injected flow allocation into layer i; k_i represents the permeability of layer i; h_i represents the thickness of layer i; and n represents the total number of layers.

In the example shown in Figure 2.7, all layers had the same thickness but permeabilities varied. As can be determined using Eqn. 2.5, fluid predominately flooded the layer of highest permeability, which resulted in poor vertical sweep efficiency. In Figure 2.8, it can be seen that the use of a plugging agent, for conformance control, can severely alter injected flow allocation into each layer, increasing vertical sweep efficiency by preferentially flooding layers that were previously poorly swept. Note that in this example, the conformance control agent was assumed to reduce the permeability in the high permeability layer by a factor of ten; in reality, this value would depend on the agent's inherent RRF effects.

2.2.2 Distinctions between Gels and Polymers/Microgels

The primary difference between polymer gels and conventional uncrosslinked polymer is that polymer gels consist of a polymer network developed by the presence of a crosslinker. This renders polymer gels more capable of reducing permeability, and so they can divert fluid more effectively (Needham and Doe 1987). The network formed by

the crosslinking agent also renders polymer gels much more viscous and less flowable than uncrosslinked polymer (Sheng 2011).

Another difference involves their functionality. Both polymer flooding and polymer gel flooding can increase sweep efficiency, yet both do so in different ways. Polymer flooding primarily functions as a means of mobility control/correcting adverse mobility ratios (Norman et al. 1999), and so it is generally ideal to have the polymer sweep as much of the reservoir as possible. Polymer gel flooding, on the other hand, is primarily intended for conformance control/water shut-off, and so gelant should ideally only propagate through high permeability channels/zones. This enables the diversion of subsequent flooding fluid to low permeability zones, without the reduction of permeability in these zones (Seright and Liang 1994).

The primary difference between polymer gels and polymer microgels is the concentration of reactants used in their respective formulations. Polymer microgels are formed using relatively lower concentrations of polymer and crosslinker. This results in the formation of a solution of many separate polymer microgels/colloids, as opposed to a continuous intermolecular bulk gel/polymer gel network. This yields subsequent effects on injectivity and depth of reservoir penetration, to be elaborated on in the polymer microgel background section following shortly.

2.2.3 Injection Mechanisms

Polymer gel injection can be classified as either bulk gel injection (surface-produced) or sequential injection (in-situ). Each of these two injection mechanisms is described in some detail below. The key disadvantages of each mechanism are highlighted and a troublesome dichotomy is made clear. Polymer microgel flooding offers an effective remedy to this dichotomy, as will soon be explained.

Bulk injection involves the injection of a homogeneous gel solution, formulated by mixing high concentrations of polymer and crosslinker at the surface before the injection process takes place. This homogeneous gel solution, injected into the formation, quickly becomes a strong gel in-situ and predominantly affects the near-wellbore region. The large amounts of polymer and crosslinker required for bulk injection, and the resulting rapid intermolecular crosslinking rates deem it both uneconomical and difficult for in-depth placement of the gel solution within the formation. Instead, the gel accumulates primarily in the pore space in the vicinity of the wellbore. In addition, bulk injection can result in weaker gels as a result of shear degradation. (Mack and Smith 1994; Coste et al. 2000; Dovan and Hutchins 1987)

By contrast, sequential injection can be used. This involves the alternating injection of polymer and crosslinker. The injected slugs eventually yield concentrations of polymer and crosslinker that are simultaneously present in the formation matrix (predominantly accumulating on pore walls). This method of injection enables in-depth placement of gels, as there is not much opportunity for crosslinking until both the polymer and crosslinker are present in the formation. Only then will the crosslinking take place yielding a strong gel capable of varying a zone's permeability. The disadvantage of sequential injection, however, is the added difficulty associated with the obvious loss of control. The polymer and crosslinker slugs may not even come into contact with each other if they flood different reservoir zones/strata. (Mack and Smith 1994; Coste et al. 2000)

2.3 POLYMER MICROGEL FLOODING

The primary motivation for polymer microgel-enhanced waterflooding for conformance control is that it offers an alternative to the troublesome dichotomy of

polymer gel flooding, detailed above. Homogeneous polymer microgel solutions can be formulated using relatively low concentrations of polymer and crosslinker. These lower concentrations are what distinguish polymer microgels from polymer gels. The low reactant concentrations enable crosslinks to be primarily intramolecular as opposed to intermolecular, resulting in the formation of many separate polymer microgels and not a continuous bulk gel/polymer gel network. This enables relative ease of injection into the deeper zones of the formation, and also proves to be more economical than the use of bulk polymer gel, due to the lower reactant concentration requirement. The relatively low concentrations of polymer and crosslinker also yield a slower crosslinking reaction rate, enabling the polymer microgel solution to have more time to invade deeper zones within a formation, before their flow begins retarding due to gel formation. Note that the injected low concentration polymer/crosslinker mixture can be referred to as "gelant", and upon gelation within the reservoir, gelant becomes "gel". (Mack and Smith 1994; Diaz et al. 2008)

The presence of polymer colloids/globules in a polymer microgel solution yields a viscosity that is higher than an uncrosslinked polymer solution yet lower than the highly viscous polymer gel network (Sheng 2011). As previously mentioned, polymer microgels are rendered more flowable than polymer gels. This offers clear advantages when it comes to injectivity. In addition, polymer microgels can provide a much higher RRF in high permeability channels than do polymer gels and conventional polymers (Norman et al. 1999; Smith et al. 2000; Mack and Smith 1994).

Polymer microgels, and the different types, will be addressed in much more detail in the literature survey presented in the following chapter.

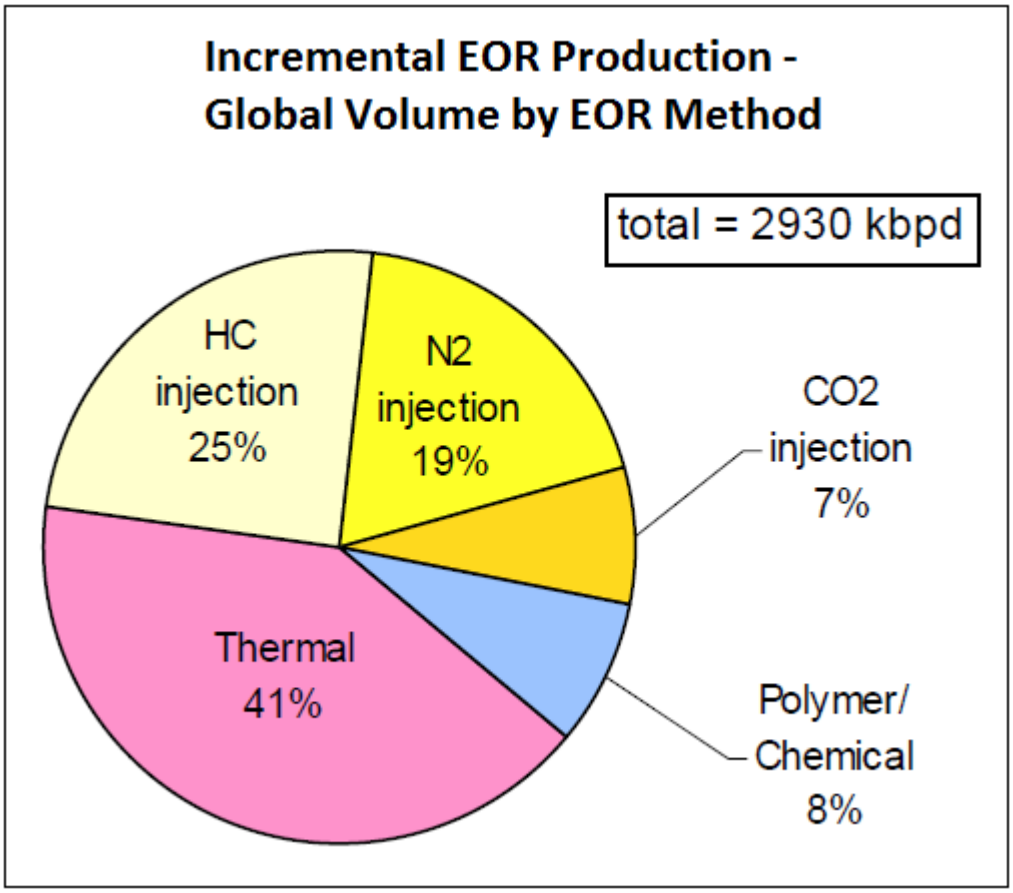

Figure 2.1: 2004 Relative Contribution of EOR Methods to Incremental Oil

Figure from Schulte (2005).

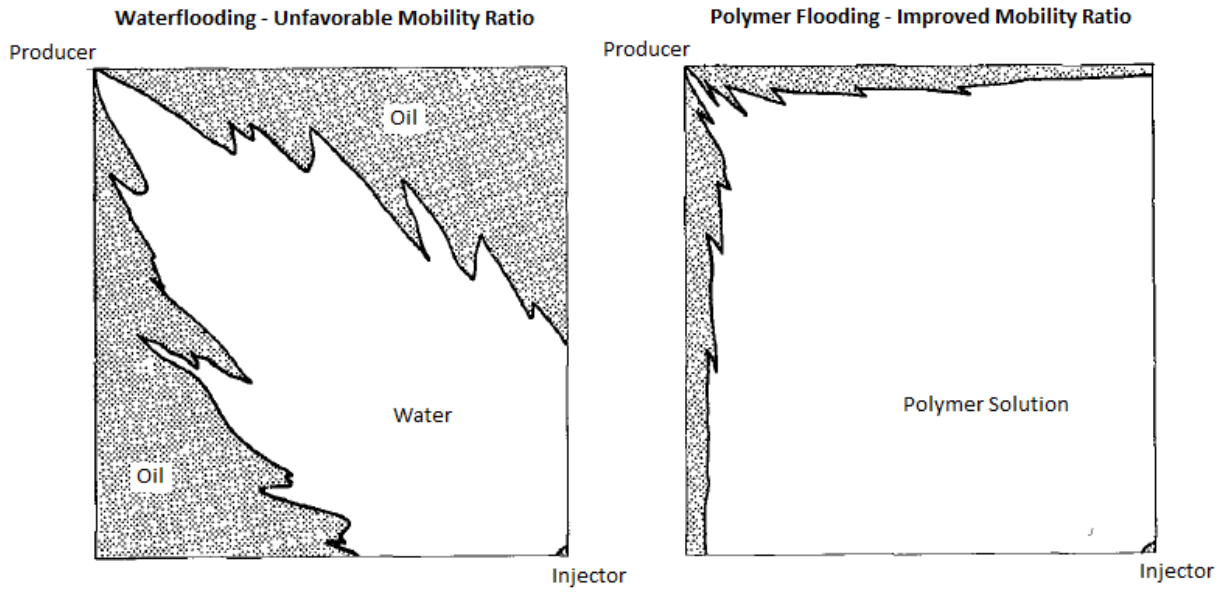

Figure 2.2: Depiction of Polymer Flood Areal Sweep Improvement

Figure from Sorbie (1991).

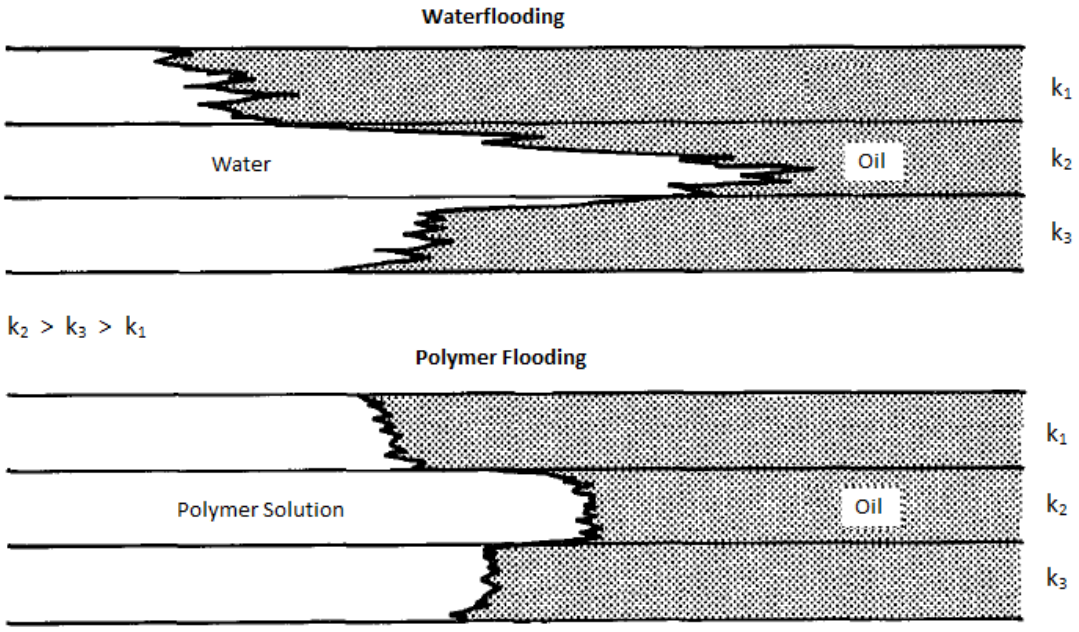

Figure 2.3: Depiction of Polymer Flood Vertical Sweep Improvement

Figure from Sorbie (1991).

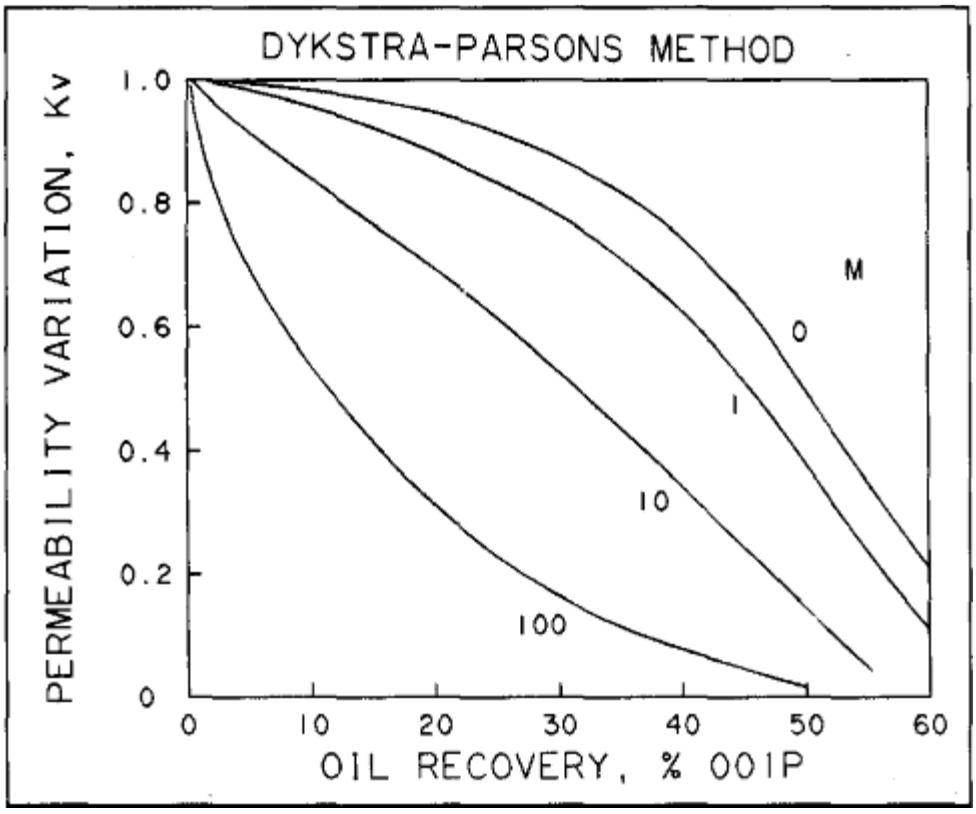

Figure 2.4: Mobility Ratio (M) Influence on Oil Recovery

Figure from Needham and Doe (1987). Water saturation was 35%, and economic limit set as a water-oil-ratio of 25. “M” in the above figure represents the mobility ratio, defined previously in Eqn. 2.1.

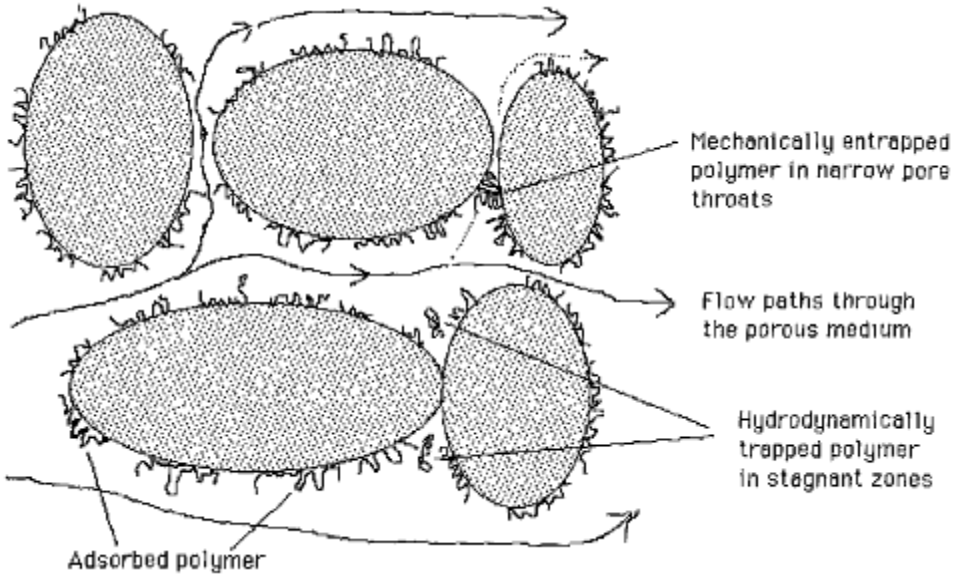

Figure 2.5: Depiction of Polymer Retention Mechanisms in Reservoir (I)

Figure from Sorbie (1991).

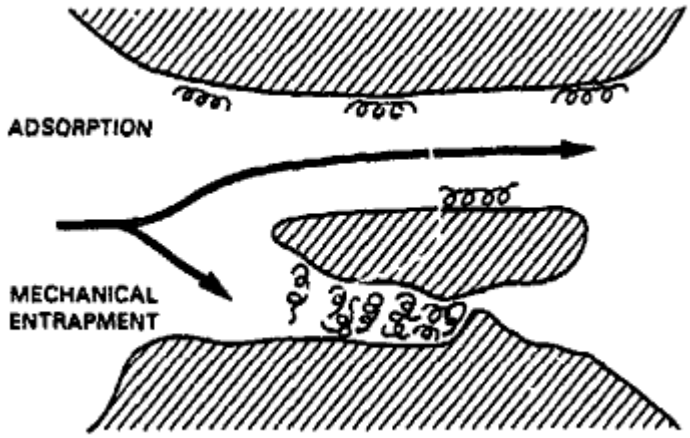

Figure 2.6: Depiction of Polymer Retention Mechanisms in Reservoir (II)

Figure from Huh et al. (1990).

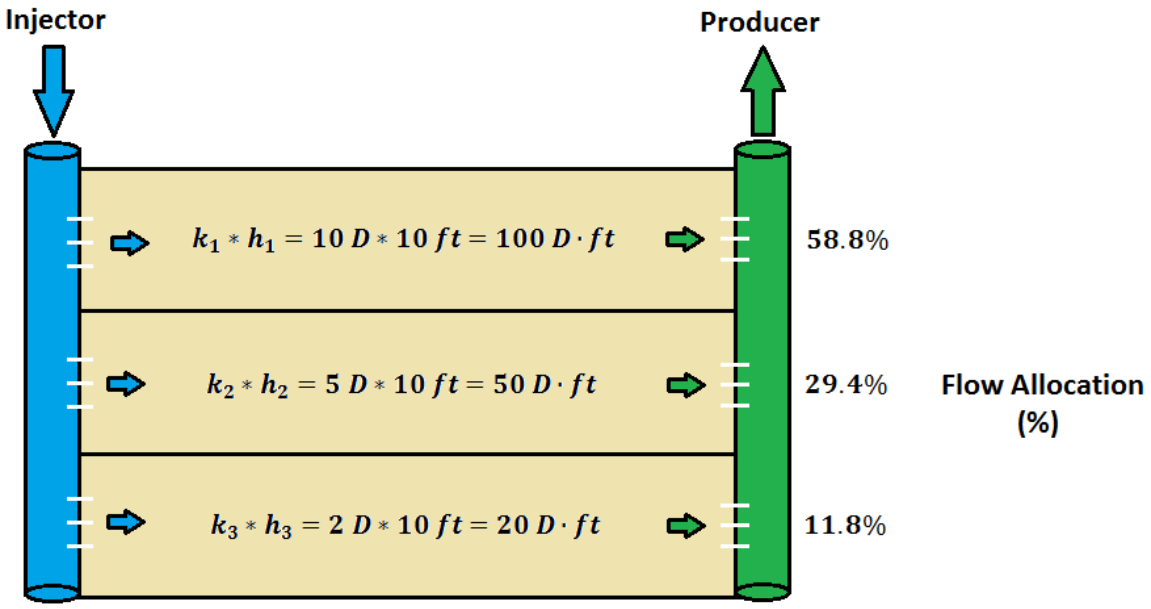

Figure 2.7: Illustration of Flow Allocation into a Layered Reservoir

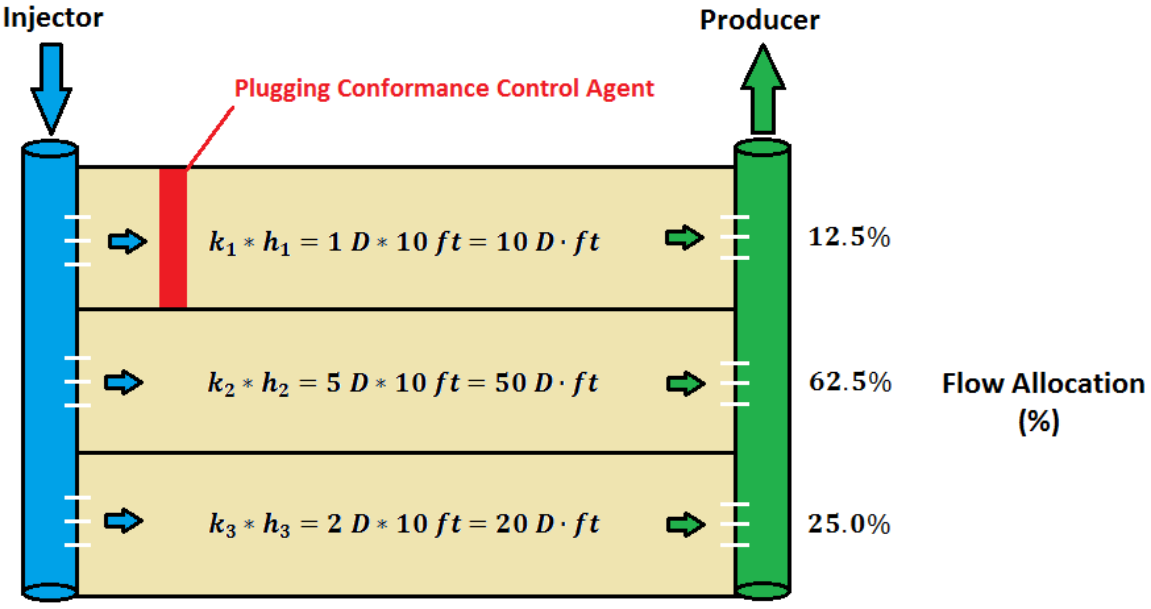

Figure 2.8: Improved Sweep Brought About by Conformance Control

Assumed: Pressure-constrained wells/ uniform layers/ similar fluid viscosities/ RRF=10.

Chapter 3: Polymer Microgel Literature Survey

A polymer microgel literature survey is presented herein. First, polymer microgel flooding is introduced, and the motivation for their use over conventional polymer flooding is outlined. This is followed by a discussion on the characterization of polymer microgels as well as some theories on how they act as conformance control agents. In addition, an extensive survey of four different types of polymer microgels (Colloidal Dispersion Gels, Preformed Particle Gels, Temperature-Sensitive Microgels, and pH-Sensitive Polymer Microgels) is provided. Attention is mainly given to microgel characteristics, laboratory observations, and field applications. The rheology and plugging mechanism of the different polymer microgels are also discussed in some detail.

3.1 INTRODUCTION

Prolonging the life of mature hydrocarbon reservoirs is one of the foremost goals of the energy industry today. This is largely due to our scarce fossil fuel supply and the ever-increasing global energy demand. Half of the hydrocarbon resources worldwide stem from giant fields that are deemed mature (Bourdarot and Ghedan 2011). With the global average oil recovery factor as low as 34% (Schulte 2005), mature fields are appropriate targets for enhanced recovery and field life extension. Extending the life of mature fields enables the maximization of hydrocarbon production as well as the postponement of production decline. There are a variety of different technologies that can facilitate mature field life extension: conformance control, advanced reservoir characterization, artificial-lift optimization, tertiary-recovery schemes, and so on (Ali 2012). The focus of this literature survey is the use of polymer-microgel-enhanced waterfloods as a means of conformance control. Ultimately, polymer microgel flooding is

a form of chemical enhanced oil recovery that primarily targets *bypassed* oil (recall that EOR is generally intended for the recovery of *residual* and/or *bypassed* oil).

Polymer microgels, added to injected waterflooding fluid, serve as water-shutoff, conformance control and/or mobility control agents (Rousseau et al. 2005). This literature survey focuses on their use as conformance control agents. Conformance control is any process by which the sweeping of a reservoir is spread more evenly, approaching the ideal condition of a perfectly conforming drive mechanism (Borling et al. 1994). In the case of a waterflood, the drive mechanism is merely that of the injected aqueous fluid drive. During conventional waterflood processes, the flooding fluid typically follows the path of 'least resistance', i.e. the most permeable path. The most permeable zones, through which injected fluids are channeled, are known as "thief zones". These thief zones are brought about by reservoir heterogeneity (geological layering/ non-uniform depositional history/ presence of natural or induced fractures) and result in poor sweep efficiency and large amounts of unrecovered hydrocarbon (Sorbie 1991; Fletcher et al. 1992; Pritchett et al. 2003). Unfavorable mobility ratios and/or water under-running can also contribute to poor sweep efficiency (Sorbie 1991; Fletcher et al. 1992).

The different types of polymer microgels all fundamentally function to divert injected fluid away from thief zones and into adjacent matrix rock or fractures, thus increasing macroscopic sweep efficiency and improving hydrocarbon recovery efficiency; the polymer microgels do this by either blocking or inhibiting flow through the high permeability thief zone streaks (Borling et al. 1994; Pritchett et al. 2003; Ohms et al. 2009). In addition, the polymer microgels in the aqueous injecting fluid also function to increase the viscosity of the aqueous phase, which in turn improves the mobility ratio in favor of decreased water channeling and delayed breakthrough (Sorbie 1991; Sheng 2011).

The increase in vertical and areal sweep efficiency brought about by the use of polymer microgels not only increases hydrocarbon production, but also yields a subsequent decrease in water production. This direct consequence can be of equal importance nowadays, as regulation on water disposal becomes increasingly strict. It has been estimated that for every barrel of oil produced worldwide, an average of roughly 3 barrels of water are produced as well; associated waste water production is even more severe in the United States (Seright et al. 2003). Efforts to dispose said water have been estimated to cost as high as $40 billion globally per year (Seright et al. 2003). In addition to alleviating environmental concerns and pollution, decreasing water production also prolongs the life of hydrocarbon reservoirs. Decreasing the amount of water produced can also decrease the load on surface facilities, and decrease corrosion and scale levels (Bai et al. 2008).

3.2 POLYMER MICROGEL MOTIVATION OVER POLYMER OR GEL TREATMENTS

Polymer flooding (Needham and Doe 1987; Sorbie 1991; Sheng 2011), polymer gel flooding (Abdo et al. 1984; Avery et al. 1986; Seright and Liang 1994; Kim 1995; Sydansk and Southwell 2000; Kabir 2001; Seright et al. 2003; Norman et al. 2006), and polymer microgel flooding (Mack and Smith 1994; Coste et al. 2000; Chauveteau et al. 2001; Al-Anazi and Sharma 2002; Frampton et al. 2004; Zaitoun et al. 2007; Cozic et al. 2009; Spildo et al. 2009) are three distinct EOR techniques, and it is important to be able to differentiate them from each other.

Polymer flooding stands alone as the EOR technique that is used primarily for *mobility control*. Polymer serves to increase the injecting aqueous fluid's viscosity. This in turn decreases the mobility ratio, as can be seen using the corresponding definition below:

$$Mobility\ Ratio = M = \frac{\left(\frac{\mu_o}{k_o}\right)}{\left(\frac{\mu_w}{k_w}\right)} \qquad \text{(Eqn. 3.1)}$$

Decreasing the mobility ratio through polymer floods leads to a more uniform areal and vertical displacement of oil in place as well as decreased likelihood of viscous fingering. Secondary to this mobility control effect, polymer flooding also improves oil recovery through a fractional flow effect and a fluid diversion effect (Needham and Doe 1987). In a layered system, polymer's effect on mobility ratio leads to viscous crossflow effects that can improve the often poor vertical sweep efficiency (Sorbie 1991). Figure 3.1 illustrates how polymer solution can improve vertical sweep efficiency in such a layered system; the greater the polymer solution viscosity, the lower the mobility ratio, and the greater the induced sweep improvement. However, there is difficulty when permeability contrast in a layered system is very large. If a very high permeability channel exists, polymer may not be enough to mend the water channeling problem. In fact, polymer solution may simply channel through this high permeability zone, yielding very little sweep improvement. In such cases, there is a need to consider conformance control instead.

Polymer gels (bulk gels) and polymer microgels, on the other hand, fit this *conformance control* category, and are ideal for situations where there is high permeability contrast, i.e. great extents of heterogeneity. Note that conformance control primarily involves the improvement of *vertical* sweep efficiency. The fundamental distinction is that polymer gels and polymer microgels make use of a crosslinking agent. Crosslinkers enable polymer gels and polymer microgels to form polymer networks that are much more capable of plugging pores than polymer alone; this enables a more

significant, longer lasting, and more optimizable permeability reduction (Residual Resistance Factor - RRF). This, in turn, can result in a long-term increased resistance to flow in high permeability streaks and subsequent fluid diversion effects, pushing oil out of areas that were previously unswept (Needham and Doe 1987; Smith et al. 2000; Norman et al. 1999). As a result of these enhanced permeability reduction capabilities, polymer gels and polymer microgels are much more suitable for conformance control. (Norman et al. 1999; Sheng 2011)

Polymer gels and polymer microgels are both conformance control agents that function by the strategic plugging of pores. The primary difference between them is the concentration of reactants used in their respective formulations. Polymer microgels are formed using relatively lower concentrations of polymer and crosslinker. This results in the formation of a solution of many separate polymer microgels/colloids (through primarily intramolecular crosslinking reactions), as opposed to a continuous intermolecular bulk gel/polymer gel network. This enables polymer microgels to be more easily injected; this an important motivation for polymer microgel use over polymer gel use. The lower concentration of reactants also yield a slower crosslinking reaction rate, which allows for much deeper reservoir penetration; polymer gels typically form a strong gel in the near-wellbore pore space, while microgels can invade deeper into a formation until their gelation/pore plugging mechanism is triggered (Mack and Smith 1994; Coste et al. 2000; Diaz et al. 2008; Dovan and Hutchins 1987). Thus, polymer microgels are more suited for in-depth conformance control. In addition, polymer microgels can provide a much higher RRF in high permeability channels than do polymer gels and conventional uncrosslinked polymers (Norman et al. 1999; Smith et al. 2000; Mack and Smith 1994).

Liu et al. (2006) outline and illustrate the different forms of conformance control chemical placement treatments, such as water shutoff (production well) treatments and profile control (injector well) treatments. In-depth fluid diversion treatments are an especially attractive form of conformance control as they improve overall sweep more significantly than near-wellbore treatments (especially when there is good communication/crossflow between the different layers/zones), and also yield lower losses in injectivity (Fletcher et al. 1992). Unlike production well treatments, they may also not require shut-in periods. Polymer microgel flooding serves as the most effective means of *in-depth* fluid diversion. Figures 2.7 and 2.8 can help illustrate the dramatic effect plugging agents (such as polymer microgels) can have on layer injected flow allocation. These simplified layered reservoir illustrations demonstrate the potential polymer microgels have to improve vertical sweep efficiency by inducing the preferential flooding of layers that were previously poorly swept. Darcy's law was used to determine each layer's flow allocation - assumptions made are listed below the figures.

3.3 POLYMER MICROGELS

Cozic et al. (2008) define polymer microgels as micrometer-scale, fully water soluble, stable, and non-toxic polymer colloidal particles. They are polymer species with internal crosslinks, making them generally larger, more rigid and more stable than polymer alone. Polymer microgels were developed with the objective of increasing levels of polymer adsorption and resulting RRF values. They evolved from polymer/bulk gels as a more effective/economical means of *in-depth* profile control. Cozic et al. (2009) explain that when injected into multilayered reservoirs "microgels invade the low-permeability zones significantly less because of the low viscosity of their solutions and because of steric effects". Zaitoun et al. (2007) attribute such preferential high perm

penetration to relatively large microgel size. Regardless, polymer microgels primarily penetrate high permeability streaks and adsorb within them, enabling in-depth conformance control through the controlled permeability reduction of these thief zones. Polymer microgels were traditionally formed in-situ, meaning gelant (polymer and crosslinker mixture) was injected and the gelling reaction took place within the reservoir, plugging pores and diverting fluid. However, this was followed by a trend from these microgels that are formed in-situ (such as Colloidal Dispersion Gels) to microgels that are preformed (such as Preformed Particle Gels, BrightWater, and pH Sensitive Polymer Microgels), in order to overcome drawbacks associated with in-situ gelation systems. This will be elaborated on further in their respective sections. (Cozic et al. 2008, 2009; Diaz et al. 2008; Mack and Smith 1994; Zaitoun et al. 2007; Bai et al. 2008; Liu et al. 2006)

There is a vast amount of literature on polymer microgels (Chauveteau et al. 2000, 2001, 2003, 2004; Feng et al. 2003; Rousseau et al. 2005; Cozic et al. 2008, 2009; Zaitoun et al. 2007), demonstrating the growing interest in this technology. Throughout the literature, polymer microgels have a variety of other names. They are also referred to as movable soft microgels, movable gels, weak gels, weak viscoelastic fluid, and deep diverting agents (Sheng 2011). Care should be taken when reading literature to distinguish between microgels, polymer/bulk gels and conventional/uncrosslinked polymers. Sheng (2011) effectively characterizes polymer microgels as a balance between uncrosslinked polymer, which is easy to flow, and polymer gel which is a lot more difficult to flow. Polymer microgels have an intermediate viscosity and are much more readily transported far into a formation than a polymer bulk gel.

3.3.1 Characterization of Microgels and Microgel Dispersions

This section attempts to shed light on the physicochemical aspects of microgels and microgel dispersions. So as to ensure the coherence of this section, some basic definitions and equations need be addressed prior to proceeding:

1. The radius of gyration is one means of quantifying the rough dimensions of a polymer chain. Approximating the polymer chain as a sphere, the radius of gyration would be the distance between the sphere end and its center of mass. (Teraoka 2002)
2. The hydrodynamic radius is another means of quantifying the rough dimensions of a polymer chain. The hydrodynamic radius of a linear polymer chain can be expressed by an extension of the Stokes-Einstein equation. The equation's final form is shown below:

$$R_H = \frac{k_B * T}{6 * \pi * \eta_s * D} \ , \qquad \text{(Eqn. 3.2)}$$

where k_B is the Boltzmann constant, T is the temperature, η_s is the solvent viscosity, and D is the center-of-mass diffusion coefficient of the chain or suspension. (Teraoka 2002; Bjorsvik et al. 2008)

3. The viscosity of a polymer solution can be expressed by the equation below:

$$\eta \approx \eta_s * (1 + [\eta] * c + K_H * [\eta]^2 * c^2) \ , \qquad \text{(Eqn. 3.3)}$$

where η_s is the solvent viscosity, $[\eta]$ is the intrinsic viscosity, c is the concentration, and K_H is the Huggins constant. (Teraoka 2002)

4. Relative viscosity (η_r) is defined as $\frac{\eta}{\eta_s}$, specific viscosity (η_{sp}) as $\eta_r - 1$, and reduced viscosity (η_{red}) as $\frac{\eta_{sp}}{c}$. And so, the following equation holds:

$$\eta_{red} \approx [\eta] + K_H * [\eta]^2 * c \qquad \text{(Eqn. 3.4)}$$

This equation is known as the Huggins equation (Stoffer 1998a; Teraoka 2002; Bjorsvik et al. 2008). Plotting reduced viscosity versus concentration can enable the determination of intrinsic viscosity. The Kraemer equation can also be used to graphically obtain intrinsic viscosity (Stoffer 1998b). Upon determining a polymer solution's intrinsic viscosity, the polymer molecular weight can be obtained using the Mark-Houwink-Sakurada equation (Stoffer 1998c; Teraoka 2002).

5. When viscoelastic materials such as polymer microgels deform, some energy is stored (elastic component) while some energy is lost (viscous component). The Storage or Elastic Modulus (G') and the Loss or Viscous Modulus (G'') are used to represent these different components of viscoelasticity. Their respective values can be measured and used to gauge a viscoelastic fluid's elasticity/structure. (Sheng 2011)

Bjorsvik et al. (2008) define microgels as "non-linked aggregates of finite size" that are formed when "a cross-linker cannot form a connected network". According to Bjorsvik et al. (2008), this occurs when the polymer solution is dilute, i.e. when polymer solution concentration is less than the overlap concentration (c^*). This is because at these low polymer concentrations, cross-linking is primarily intramolecular. However, in the semi-dilute regime, when polymer solution concentration is greater than c^*, crosslinking

is primarily intermolecular, and so a gel is formed instead of a solution of microgels. Note that the overlap concentration can be calculated as the inverse of intrinsic viscosity. (Bjorsvik et al. 2008; Teraoka 2002)

Bjorsvik et al. (2008) determined that the characteristic intrinsic viscosity of an HPAM solution was lower in solutions of greater salinity. This implies that overlap concentrations are larger in solutions of greater salinity. Physically this means that solutions of greater salinity require a greater amount of polymer to fall into the semi-dilute region. One possible explanation for this is that as salinity increases, polymer molecules are more compact. This could be due to the polymer molecules loss of water to the more saline surrounding solution, or could possibly be due to other interactions between the polymer molecules and the surrounding ions. It could also be because greater salinities render it more likely that polymer coils form (Sorbie 1991; Spildo et al. 2009). Bjorsvik et al. (2008) also experimentally showed that polymer solution viscosity decreased with increasing salinity; this supports the idea that polymer molecules are more compact (occupy less space) with greater salinity.

From the storage and loss moduli determined by Bjorsvik et al. (2008), it would appear that a microgel solution formed in saline water is more “fluid”/less “elastic” than a microgel solution formed in fresh water. However, this is likely a result of differences in concentration regime. Recall that more saline solutions are characterized by larger overlap concentrations, thus deeming them more likely to have fewer intermolecular crosslinks at some fixed polymer concentration.

Li et al. (2004) report the results of a study on the size and conformation of linked polymer coils (LPC) in linked polymer solutions (LPS). These LPS are merely microgel suspensions formed using a variety of different polymers and aluminum citrate crosslinker. Li et al. (2004) conducted microfiltration experiments that demonstrated that

LPS had significantly longer filtration times than polymer solutions, despite the polymer solutions possessing higher viscosities and polymer concentrations orders higher than their corresponding LPS. This is evidence of the fact that microgel suspensions are characterized by coil conformations very different from, and with a much greater plugging tendency than, conventional polymer solutions. A scanning electron microscope was used to visualize LPC, and showed that they are rigid, spherical particles. Li et al. (2004)'s microfiltration experiments also enabled them to conclude that LPC size depends on polymer molecular weight and concentration. As molecular weight and/or polymer concentration increases, LPC size in LPS increases, and filtration time of a fixed volume of LPS increases as a result (i.e. plugging tendency increases). The Cage Effect Theory and the Flory-Huggins Theory can help explain these findings: When the polymer concentration is below a certain threshold value, intramolecular cross-linking most likely takes place, as individual polymer molecules are confined to their own unique "cage" - the key difference between microgel suspensions and intermolecular gel networks. This results in each LPC being formed by only one polymer molecule, making their size (hydrodynamic radius) sensitive to molecular weight. In addition, increasing polymer concentration makes intermolecular crosslinking more possible, and thus results in larger mean LPC sizes. (Li et al. 2004)

Chauveteau et al. (2003) offer a detailed look at some of the physicochemical aspects of polymer microgels. In agreement with the previously referenced literature, Chauveteau et al. (2003) describe the effect of polymer concentration regime on the dominant type of crosslinking. They also describe the competition between intramolecular and intermolecular crosslinks in an intermediate regime, between dilute and semi-dilute regimes, as a function of ionic strength. They do this by defining a crosslinking kinetics index and identifying a relationship between this index and Debye

length. A similar relationship was found between elastic modulus and Debye length, supporting Chauveteau et al. (2003)'s interpretation of their findings.

Chauveteau et al. (2003) also made an effort to characterize the interactions between microgels, a very important aspect of polymer microgel flooding. Plotting viscosity against colloid concentration in the dilute regime and under low shear rates enables the determining of the Huggins constant, K_H, using the Huggins equation. When no attractive or repulsive interactions exist between the dispersed microgel colloids, then the Huggins constant depends on particle conformation/solvent quality (Chauveteau et al. 2003; Choi et al. 2006). If the Huggins constant is larger than that which would be expected, then attractive interactions are likely the cause. Interactions between microgels have a significant effect on their transport in porous media. Partly attractive microgels, characterized by higher Huggins constants, form multi-layers on pore walls, and eventually completely plug pores when the multi-layer thickness equals the pore's hydrodynamic radius. Thus, partly attractive microgels make effective diverting agents as they can fully plug pores. Note that even these plugged pores are still very slightly permeable to water as there is flow through the microgels. Strictly repulsive microgels, characterized by Huggins constants lower than 0.3, form only a monolayer of microgels on pore walls. Thus, they function to lower water permeability but without completely plugging pores. As such, they serve as good disproportionate permeability reducers. Note that microgels were found to adsorb more than conventional polymers, and also yielded thicker adsorbed layers than polymers. An effective means of quantifying pore plugging is using the jamming ratio, which is the ratio of mean pore diameter to mean microgel diameter (Cozic et al. 2009; Shi et al. 2011a). Shi et al. (2011a) can be referred to for additional insight on how the jamming ratio can be used to distinguish between

inaccessible pores, plugged pores, and adsorbed pores. (Chauveteau et al. 2003; Choi et al. 2006)

It is important to realize that flow occurs through gels/microgels (Grattoni et al. 2001; Yang et al. 2002; Chauveteau et al. 2003). Grattoni et al. (2001) and Yang et al. (2002) both show that flow occurs through such viscoelastic gel materials as if they are porous media, and also show that the gel internal permeability is velocity dependent. When an imposed pressure gradient is greater than the forces of interaction that hold a gel in place, it was found that aqueous fluid can flow through the gel network. Water essentially flows through spaces between the polymers of the gel. Increased aqueous fluid velocities form larger spaces by deforming the elastic gel, thus increasing permeability. Note that, unlike water, oil simply breaks down the gel yielding a pathway in which it can flow. Thus such gels selectively reduce the permeability to water, but not to oil. This phenomenon is discussed in more detail in subsequent sections. Yang et al. (2002) also demonstrate that the permeability to water in such gels is an intrinsic property of the gel; polymer gel permeability depends on the gel elasticity/storage modulus. (Grattoni et al. 2001; Yang et al. 2002)

Chauveteau et al. (2001), Feng et al. (2003), Rousseau et al. (2005), and Cozic et al. (2009) can be referred to for additional insight on the physicochemical characterization of microgels.

3.3.2 Possible Conformance Control Mechanisms

Recall that the target of polymer microgel flooding is oil bypassed during conventional waterfloods. As previously mentioned, polymer microgels make use of a pore blocking mechanism and serve as conformance control agents; they are not merely intended to reduce mobility ratio like polymer flooding. This section outlines some

theories for polymer microgel possible conformance control mechanisms. Note that the exact mechanism by which they increase sweep efficiency is still uncertain, yet there are some promising ideas.

A point of uncertainty is whether polymer microgels primarily invade high permeability layers, as intended. One chain of thought is that microgels will primarily invade these high permeability zones as long as the microgel solution/gelant is of low viscosity; it is thought that the microgel solutions would essentially act as water does during injection. This, as well as steric effects, would minimize their penetration into other less permeable zones (Cozic et al. 2009; Seright et al. 2011). Another possible reason for minimal microgel penetration of low permeability layers is the relatively large microgel size (Zaitoun et al. 2007). Diaz et al. (2008) provide additional references to works that support both these theories. Either way, if this is in fact the phenomenon taking place during microgel flooding treatments, polymer microgels can proceed to preferentially penetrate and adsorb in-depth within high permeability streaks. Despite distinct microgel types having different triggers, as will soon be revealed, the different types plug pores in similar ways (recall jamming ratio discussion in the previous section). The microgels may adsorb as monolayers or multi-layers, depending on the nature of their interactions with other microgels. Either way, polymer microgels will serve as conformance control agents diverting flooding fluid to lower permeability zones, as long as there are no barriers preventing such diversion. This is one possible means by which polymer microgels improve sweep efficiency and improve oil recovery.

Another possibility is that polymer microgels improve oil recovery even if they significantly penetrate low permeability zones as well. This could be due to their Disproportionate Permeability Reduction (DPR), or Relative Permeability Modification (RPM), effects. This means that the microgels selectively reduce the permeability to

water without reducing the permeability to oil. The microgels are essentially compressed in the presence of water-oil capillary pressure, due to their softness, allowing for oil to pass. Thus, one possibility is that even if polymer microgels invade low permeability zones, they still allow for oil to be produced from those zones without inducing any damage. (Chauveteau et al. 2004; Rousseau et al. 2005)

Other plausible polymer microgel oil recovery mechanisms have been proposed. Spildo et al. (2009) proposed a mechanism of microscopic diversion to explain improved oil recovery in cores after polymer microgel floods. They claimed that rigid polymer microgel colloids even help recover residual (capillary-trapped) oil. They attributed this to the blocking of pores and the redistribution of flow on a microscopic level. Spildo et al. (2009) supported this hypothesis with experiments that demonstrated that residual oil saturations in numerous cores decreased after polymer microgel treatments. They also showed that wider pore radius distributions (greater heterogeneities) yield greater reductions in residual oil saturation, supporting their proposed recovery mechanism. In addition, Sheng (2011) discuss in detail four different displacement mechanisms characteristic of viscoelastic polymers, and likely polymer microgels by extension. These include a pulling mechanism, stripping mechanism, mechanism of oil thread flow, and a mechanism of shear-thickening effect. Sheng (2011) should be referred to for the detailing of each of these mechanisms. Each of these mechanisms could, to some degree, also contribute to polymer microgel-induced improved oil recovery.

3.4 POLYMER MICROGEL TYPES

There are four predominant types of polymer microgels that this literature survey will focus on: Colloidal Dispersion Gels (CDGs), Preformed Particle Gels (PPGs), temperature-triggered polymer microgels, and pH-triggered polymer microgels. The

polymer microgel type that is appropriate for a particular application depends on the situation and the required function.

Note that each of the different microgel types has different characteristics and are triggered by different controls (pressure differential, temperature, pH), but there are a couple of mechanisms common to the different microgels:

1. High viscosity, enabling the microgels to act as mobility control agents as is the case in a conventional uncrosslinked polymer flood (Sheng 2011).
2. High resistance factor (RF) and permeability reduction factor (RRF), upon microgel triggering, enabling the microgels to act as conformance control agents (in a more effective manner than uncrosslinked polymer, and deeper in formations than polymer/bulk gels). (Sheng 2011)
3. Viscoelastic behavior that can potentially reduce residual oil saturation further (Coste et al. 2000; Urbissinova et al. 2010; Sheng 2011).
4. Well-designed microgels (and even gels) may also possess Disproportionate Permeability Reduction (DPR), otherwise known as Relative Permeability Modification (RPM), capabilities. This means that microgel layers, formed by microgel adsorption to pore rock surfaces, can selectively reduce the permeability to water without significantly affecting permeability to oil. This is due to microgel "softness", i.e. their ability to compress/collapse/dehydrate upon the presence of water-oil capillary pressure, so as not to inhibit oil production. This quality is highly beneficial for microgel floods as it minimizes damage to oil-productive zones (and minimizes the need for zonal isolation in water shut off treatments). (Liang et al. 1992; Liang and Seright 1997; Chauveteau et al. 2001, 2004; Kabir 2001; Seright 2009)

The four different polymer microgel types are detailed, one-by-one, in the following sections. The focus is on the polymer microgel properties, suitable conditions for their implementation, and examples of their implementation worldwide. Note that optimal operational criteria and polymer microgel formulations vary on a case-to-case basis. The descriptions below are simply those reported in the literature, and should not necessarily be taken to hold as true for every scenario. Extensive laboratory and pilot testing must be performed before selecting a polymer microgel type for a specific application, and in order to determine the optimal operational criteria/ polymer microgel formulations for the application being considered. Chauveteau et al. (2003) explain that microgels designed for water shutoff or profile control purposes should be:

- Insensitive to shear and reservoir physicochemical conditions
- Size controlled so as to prevent face plugging
- Small enough to ensure in-depth propagation, but large enough to significantly reduce permeability (permeability reduction depends on adsorbed layer thickness and so can be controlled)
- Soft enough to be collapsed onto pore wall by oil-water capillary pressure so as to only reduce water permeability
- Strongly adsorbing, and stable over long periods of time
- Non-toxic

3.4.1 Colloidal Dispersion Gels (CDGs)

Mack and Smith, the pioneers of CDG-use in the field, provide a fairly extensive research paper on CDGs, addressing topics ranging from the characteristics of these microgels to the limits of CDG technology in field applications (1994). They recognized the problems associated with high levels of reservoir heterogeneity, and identified in-depth permeability variation (conformance control) using CDGs as a viable solution.

CDGs are composed of polymer and crosslinker, combined in low concentrations so that a bulk gel cannot form (Mack and Smith 1994; Fielding et al. 1994; Coste et al. 2000; Sheng 2011). The key characteristic of CDGs distinguishing them from polymer bulk gels is that they are not continuous intermolecular gel networks; this is a direct result of the low concentration of reactants required to formulate CDGs. Instead, CDGs are micro-scale separate gels/colloids that came about from primarily intramolecular forces (Mack and Smith 1994; Diaz et al. 2008). Figure 3.2 can help visualize the difference between bulk gels and CDGs. In formulating CDGs, Mack and Smith (1994) recommended the use of a pure, partially hydrolyzed polyacrylamide; this is the most commonly used polymer reported in the literature. The polymer's concentration can vary between 100 and 1200 ppm (Mack and Smith 1994; Sheng 2011). The crosslinker is typically a metal; Mack and Smith (1994) chose to use aluminum citrate specifically, in their earliest work. Fielding et al. (1994), Ranganathan et al. (1998), Smith et al. (2000), Lu et al. (2000), Chang et al. (2004, 2006), and many others chose to use the same crosslinker. Other crosslinker options are possible (Diaz et al. 2008). Mack and Smith (1994) stated that CDGs can be formulated using a ratio of polymer to aluminum crosslinker varying between 20:1 and 100:1. Sheng (2011) specified a range between 30:1 and 60:1.

CDG flow resistance/gelation is triggered by a specific "transition pressure". When subjected to high pressure differentials above the transition pressure, CDGs are in the form of gelant and flow as easily as uncrosslinked polymer. When below the transition pressure, gelation occurs and pore throats are filled/plugged yielding resistance to flow and permeability reductions (Mack and Smith 1994; Sheng 2011). The results of experiments carried out by Smith et al. (2000) support such flow characteristics. The high pressure differential near wellbores is typically above the transition pressure and so CDGs are easily injected even when preformed (CDGs are generally injected as a gelant and form strengthened gels in-situ). Smith (1989) discusses the transition pressure, and describes and exemplifies the method for its determination, using the Transition Gel Unit (TGU) apparatus. The transition pressure is commonly determined as a means of quantifying/characterizing gel strength, higher transition pressures signifying greater gel strength (Smith 1989; Mack and Smith 1994; Ranganathan et al. 1998; Smith et al. 2000; Chang et al. 2004; Muruaga et al. 2008).

Some observations made regarding CDGs include:

- Care must be taken to avoid impurities as they can adversely affect the integrity of CDGs (Mack and Smith 1994).
- The rate of intramolecular crosslinking is a function of polymer concentration, polymer:crosslinker ratio, water salinity, temperature, and shear (Mack and Smith 1994).
- Gelation time is controllable, and can be on the order of hours to weeks. For field applications, it must be ensured that the time is long enough such that gelation occurs far from the wellbore. (Sheng 2011)

- Applying shear can slow down the rate of CDG gel formation (Mack and Smith 1994; Diaz et al. 2008).
- CDGs demonstrate shear-thinning behavior (Mack and Smith 1994).
- CDG strength decreases with increasing salinity (Mack and Smith 1994).
- Resulting gel strength is a function of polymer molecular weight, degree of hydrolysis and presence of impurities (Smith 1995; Spildo et al. 2009).

In the prospect of field application, CDG-enhanced waterflooding can offer distinct advantages. First and foremost, the low reactant concentration requirement enables large quantities of CDGs to be formulated economically. It also enables a relatively slow rate of crosslinking, giving the flooding solution more time to enter the depths of the reservoir formation before crosslinking takes its toll. The shear-thinning behavior of CDGs further guarantees that the CDGs only alter matrix permeability deep in the reservoir. Ultimately, this technology is a potential solution to the problems brought about by high permeability-variance and channeling, offering a viable means of conformance control. (Mack and Smith 1994)

The following are field conditions that are deemed *unsuitable* for CDG-enhanced waterfloods, based on the literature:

1. Fields with high water salinity content. Coste et al. (2000) specified an upper salinity limit of 5000 mg/L. Mack and Smith (1994) specified an upper limit of 30,000 ppm total dissolved solids (TDS).
2. High temperature fields. Coste et al. (2000) specified an upper limit of 90˚C (194˚F). However, Mack and Smith (1994) and Fielding et al. (1994) reported successful CDG applications at temperatures as high as 94.4˚C (202˚F).

3. Fields with already highly mature waterfloods (Mack and Smith 1994). However, some field implementations have been successful despite highly mature waterfloods (Chang et al. 2004, 2006; Diaz et al. 2008).
4. Fields where injection is not within the appropriate zone(s) (Mack and Smith 1994).
5. Fields containing wells with poor wellbore completions (skin and/or very low permeability rock near the wellbore) (Mack and Smith 1994).

CDGs drew significant attention for use in Daqing field in China. Smith et al. (2000) carried out experiments to determine the optimal CDG formulation for a Daqing field pilot, and then ran laboratory core floods to determine the effect of those CDGs on RF, RRF and oil recovery. Results showed that uncrosslinked polymer and polymer microgels yielded similar RF values. However, polymer microgels yielded RRFs 4-5 times larger than uncrosslinked polymer. This demonstrates their more substantial permeability reduction capabilities. The results of the parallel core floods demonstrated that CDGs diverted subsequent injected water to low permeability cores more effectively than uncrosslinked polymers; CDG flooding yielded an ultimate oil recovery almost 10% greater than that resulting from uncrosslinked polymer flooding. The formulated CDGs were easily injected, propagated throughout the length of core, and were stable throughout the one month testing period. (Smith et al. 2000)

Similar merits of the use of CDGs for Daqing field were demonstrated by Lu et al. (2000). In light of these results, a CDG field pilot was carried out, and was deemed successful (Chang et al. 2004). Chang et al. (2004) reported a decrease in water cut by up to 19.8%, and an incremental oil recovery of 10.5% of the original oil in place (OOIP) relative to waterflooding. Chemical costs were reported as $2.72/bbl of incremental oil.

Chang et al. (2006) addresses the same successful pilot and compares a CDG flood to a conventional polymer flood. It was concluded that CDG performed better than a conventional polymer flood; it yielded a long lasting high RRF, lower water cuts and greater incremental oil, all with lower chemical costs as less polymer was required (Chang et al. 2006).

Despite the large number of research articles that support CDG technology, there still lies a great deal of controversy as to whether CDGs are truly superior to conventional polymers or polymer gels. Seright (2006) challenges the results of Chang et al. (2006)'s work. Seright (2006) argues that it is incorrect to claim that "a large amount of CDG would preferentially enter the high-permeability or thief zones and divert polymer or water into medium- and low-permeability zones". Seright claims that this violates Darcy's law, and also argues that polymer microgels would yield more substantial increases in RRF in lower permeability zones. Seright (1992, 2009) and Wang et al. (2006) support this phenomenon. This would cause the polymer microgels to plug low permeability zones more than high permeability zones which would be detrimental to sweep efficiency, directly opposing the positive sweep observations reported by Chang et al. (2004, 2006), Smith et al. (2000) and Lu et al. (2000). Seright (1992, 2006) and Wang et al. (2006) suggest that parallel linear core floods should not be used to investigate fluid diversion, as was done in the experimental studies carried out at Daqing.

Several experiments have shown that CDG gel formation occurs primarily in the front end of cores (Seright 1995; Ranganathan 1998; Lu et al. 2000; Wang et al. 2006). This is another point of controversy. Such front end gel formation/plugging is analogous to the formation of gel near wellbores, which defeats the purpose of CDG in-depth placement and can severely hinder injectivity. Gelation time need be long enough for CDG solution to travel far in-depth before gel formation. Despite these previous

observations, numerous works already discussed have demonstrated successful propagation of CDG solution far in-depth, as well as subsequent improved sweep efficiency. Feng et al. (2003) and Chauveteau et al. (2001)'s work also support that microgels can easily be injected into porous media without front end plugging. It has been argued that high shears near wellbores could have caused delayed CDG gel formation in field applications relative to lab experiments, in an effort to explain the typically longer gelation times witnessed in field applications (Smith et al. 1996; Diaz et al. 2008).

It is clear that significant controversy exists on the subject of CDG use. The main points of debate are the mechanism behind CDG pore-plugging, the CDG gelation time, and the benefits of CDGs over conventional polymers or polymer gels. Despite this controversy, CDGs have demonstrated their capabilities through numerous positive field implementations, even discounting those in Daqing. Mack and Smith (1994) reported the successful use of CDGs in 22 of 29 field projects applied in the Rocky Mountain Region in the U.S.A. Fielding et al. (1994) reported an incremental oil recovery of 5% the OOIP and a decrease in water-oil-ratio (WOR) resulting from the use of CDGs in the North Rainbow Ranch Unit in Wyoming, U.S.A. Other examples of successful implementations of CDG technology include their use in the Comodoro Rivadavia Formation in southern Argentina, in the Loma Alta Sur field in Argentina, as well as in the Adon Road Field in Wyoming, U.S.A. (Muruaga et al. 2008; Diaz et al. 2008; Smith et al. 1996). Figure 3.3 effectively demonstrates the improved/more uniform sweep profile brought about by CDG use in the Loma Alta Sur field in Argentina (Diaz et al. 2008).

Other sources on CDGs, not referenced above, include the works of Li et al. (2004), Al-Assi et al. (2006), Bjorsvik et al. (2008) and Spildo et al. (2010). All in all, it is clear that CDGs can improve sweep efficiency, provide incremental oil recovery and

decrease water production. More objective research need be done in order to clearly identify the mechanism with which CDGs achieve these benefits.

3.4.2 Preformed Particle Gels (PPGs)

Coste et al. (2000), Bai et al. (2004a, 2004b, 2008), Wu and Bai (2008), Zhang and Bai (2010), and Sheng (2011) are prominent resources on Preformed Particle Gels (PPGs), otherwise known as Pre-Gelled Particles. PPGs are polymer microgels that also aim to tackle the problem of water channeling and poor sweep efficiency; they do this by acting as diverting agents, modifying injection profiles for a more uniform sweep. PPGs and CDGs are alike in the sense that they are both *in-depth* gel treatment technologies that act as conformance control agents. PPGs, however, were developed as a more suitable microgel option (than CDGs) for high salinity and/or high temperature formations. Unlike CDGs which are predominantly formed in-situ, PPGs are exclusively formed on the surface (preformed). This enables PPGs to overcome drawbacks inherent to in-situ gelation systems (such as CDGs); PPGs enable greater control on gel formation than CDGs. (Coste et al. 2000; Bai et al. 2004a, 2008)

In forming a PPG, a bulk gel is first formed using polymer and crosslinker, and then the gel is crushed/cut into gel particles of a specific size. The strength of the gel particles is controlled by altering the polymer:crosslinker ratio. These gel particles are size-controlled, strength-controlled, water-swellable, insoluble, environmentally friendly, and are stable for long periods of time (Coste et al. 2000; Bai et al. 2004a, 2004b). For additional information on PPG formulation, Bai et al. (2004a) provide a description of the materials they used as well as their PPG synthesis procedure. Bai et al. (2004a) used an acrylamide monomer and N,N'-methylenebisacrylamide as the crosslinker, and they determined an optimal monomer:crosslinker ratio of 375:1 (by weight) for greatest gel

strength. Bai et al. (2004a) present the results of a systematic study of the effect of PPG composition (polymer, crosslinker, initiator, and additive concentrations) on the resulting PPG strength and swelling capacity. Liu et al. (2006) indicate that PPG injection concentrations are usually between 1000 and 5000 ppm.

As already mentioned, gelation of the PPGs occurs on the surface before injection. This has its advantages over traditional polymer gel or CDG microgel treatments. PPGs offer more control of gelation time and gel strength, since gelation is done on the surface. PPGs can also be used in a wider range of reservoir environments than other gel options. Bai et al. (2004a) present the results of a systematic study of the effect of environmental conditions (temperature, salinity, pH) on the resulting PPG strength and swelling capacity. Coste et al. (2000) and Bai et al. (2004a, 2004b) can be referred to for more extensive lists of advantages of the use of PPGs over other gel options. Table 3.2 can be referred to for a comparison of some of the important characteristics of CDGs and PPGs. Upon injection, the high pressure gradient renders the swollen PPG particles able to deform and flow through porous media. As with CDGs, deep in the reservoir where the pressure differential is below a certain threshold pressure, the PPGs will likely plug pore throats, increasing residual resistance of high-permeability channels and diverting flow to parts of the reservoir that were previously poorly swept. The threshold pressure at which this transition takes place depends on the PPG size relative to pore throat size. (Coste et al. 2000; Bai et al. 2004a, 2004b; He at al. 2004; Wu and Bai 2008)

Through micro-model studies, Coste et al. (2000) identified three mechanisms of PPG particle flow through pore restrictions: particle deformation, particle shrinking through water expulsion, and particle breaking. Coste et al. (2000) also witnessed that PPG particles can reduce residual oil as they can displace all or part of oil trapped in pore

space, depending on their size. Such improved microscopic displacement efficiency can serve as an additional incentive for the use of PPGs for conformance control. Similarly, Bai et al. (2004b) described six different PPG *microscopic* propagation patterns and three different PPG *macroscopic* propagation patterns (pass, broken and pass, and plug). The dominant pattern depends on PPG size relative to pore throat size, PPG strength, as well as differential pressure. Bai et al. (2004b)'s paper should be referred to for more information on PPG transport through porous media. Wu and Bai (2008) present a mathematical model of PPG propagation through porous media. Zhang and Bai (2010) can be referred to for insight on PPG transport through fractures.

PPG particle deformability renders them capable of flowing through porous media even when the particles are larger than pore throats (Coste et al. 2000; Bai et al. 2004b; Wu and Bai 2008). However, there is a limit to their deformability; it is often claimed that PPGs can only flow through porous media if the permeability is very high or if there are fractures (Bai et al. 2004b; Liu et al. 2006). Despite these observations in the laboratory, there have been no reported PPG injectivity problems at a field-scale. Since not all the PPG-flooded reservoirs were fractured, the ease of PPG injectivity may be attributed to the forming of high permeability channels in maturely waterflooded reservoirs (Bai et al. 2004a, 2004b, 2008). This is a point of uncertainty in the literature.

Some observations made regarding PPGs include:

- PPG strength and swelling capacity are a function of PPG composition, temperature, salinity, and pH (Bai et al. 2004a). Bai et al. (2004a) should be referred to for an effective description of how PPGs are affected by said factors.
- PPGs are improved Super Absorbent Polymers (Bai et al. 2008). PPGs can swell in water to a size 20 – 100 times larger than the particles in their dry form (Coste

et al. 2000). Bai et al. (2004a, 2008) state that they can swell up to 200 times their original size (by imbibing water).

- PPG stability is insensitive to high formation water salinity, even when as high as 300,000 mg/L (Bai et al. 2004b).
- PPGs can be used in any conditions of pH or salinity, so long as the temperature is below 110˚C (Coste et al. 2000). Coste et al. (2000) witnessed that a variety of PPG formulations were all stable for up to 6 months at a temperature of 110˚C. Bai et al. (2004a) observed that a thermal stability agent could keep a PPG suspension stable for a year at as high as 120˚C.

Core flood experiments performed by Coste et al. (2000) demonstrated the ability of PPGs to enter and flow through highly permeable porous media, even though the PPG particles used were larger than the pore throats (possible via deformation, shrinking and breaking). The depth of penetration was a function of preformed gel strength; weaker gels penetrated more in-depth. Note that the strength of gels can be characterized using a Gel Strength Code developed by Sydansk (1988). Coste et al. (2000) also performed a one-dimensional core flood that demonstrated that PPGs can reduce residual oil saturation (recovery efficiency increased by 10%). Parallel core floods carried out by Coste et al. (2000) also demonstrated the diverting potential of PPGs (as a result of increased residual resistance in the higher permeability core); Table 3.1 demonstrates the results of two such parallel core flooding tests. It can readily be seen, from Table 3.1, that PPGs enabled flow to be significantly redirected towards the lower permeability core in both tests, greatly increasing ultimate recovery. (Coste et al. 2000)

There are many successful implementations of PPGs for conformance control in the field. Most of these field examples are situated in China, as this is where PPGs were

first introduced back in 1996 (Bai et al. 2004a). Coste et al. (2000) discusses the results of a successful PPG pilot test involving two injectors in Shengli field, China. These pilots yielded improved vertical injection profiles from the two injectors, demonstrated in Figures 3.4 and 3.5, and thus yielded increased oil recovery and decreased water cuts. He et al. (2004) also discusses the results of a successful PPG injector treatment in the north Xingshugang region in the Daqing oil field. The injector treatment economically increased oil production and decreased water production; the improved areal injection profile can be seen in Figures 3.6 and 3.7.

Bai et al. (2004a) report that "preformed particle gel has been successfully applied to correct in-depth reservoir permeability heterogeneity in most China mature oilfields, such as Daqing, Zhongyuan, Liaohe, Shengli, Tuha, Dagang, Jidong, and so on", and also report that "more than 200 wells have been operated by injecting gel in China Oilfields… all without any injectivity problem". Bai et al. (2004a) go on to discuss a few PPG success stories in China's Pucheng and Xingbei oilfields. Both these case studies demonstrated that PPG injector treatments can correct in-depth permeability heterogeneity yielding increased oil recovery and decreased water cut. In addition, Bai et al. (2004a) discuss criteria of well selection for PPG treatment and also outline some important observations on the PPG injection process. Both Bai et al. (2004a) and He et al. (2004) highlight the use of a staged PPG injection process, where the first PPG injection stage aims to increase injection pressure to a point where PPG suspension can invade all layers and face plug the low permeability layers to prevent subsequent plugging/damaging of these low perm zones.

Other examples of successful PPG field implementations include their use in the Anton Irish field in West Texas (Smith et al. 2006; Pyziak and Smith 2007) and the Kelly-Snyder field in Texas (Larkin and Creel 2008). Both of these field cases utilized

PPG (or a similar product) to control carbon dioxide breakthrough in carbon dioxide flooding EOR applications. Cui et al. (2011) experimentally investigated the use of PPGs to enhance Surfactant-Polymer floods, as part of a combination flooding system. Positive results were achieved due to the synergy of the employed chemicals, yielding an increase in both sweep efficiency and displacement efficiency.

Ultimately, PPGs can serve to increase sweep efficiency as well as microscopic displacement efficiency. PPGs are an adequate option where reservoir temperatures are under 120˚C and when the reservoir contains high permeability channels and/or fractures. Though it has been said that PPG particles cannot penetrate consolidated porous media of permeability under 1D (Bai et al. 2004b; Liu et al. 2006), this injectivity issue has not been encountered in field applications. As previously mentioned, this may be attributed to the forming of high permeability channels in maturely waterflooded reservoirs (Bai et al. 2004a, 2004b, 2008). Other possible explanations include the unintentional creation of hydraulic fractures, channeling due to mineral dissolution, and/or the higher injection pressure gradients compared to in the lab (Bai et al. 2004b, 2008; Liu et al. 2006). Regardless, PPGs have proven to be a versatile and increasingly popular conformance control agent; they have been used in thousands of treatments (predominantly in China) of both naturally fractured and unfractured mature reservoirs with temperatures ranging from 20 - 110˚C and salinity ranging from 2,000 - 280,000 mg/L (Liu et al. 2006).

3.4.3 Temperature-Sensitive Microgels

Temperature-Sensitive microgels are a novel deep diverting gel devised as a result of a research project known as Bright Water. This project was carried out roughly a decade ago by an industry consortium between BP, Chevron, Texaco and Nalco. The purpose of the research project was to improve waterflooding sweep efficiency through

the development and use of a time-delayed, highly expandable material. Pritchett et al. (2003) stated that "an essential feature was seen as having only one injected component, so that no separation could occur". As with the other microgels discussed within this survey, the aim was to isolate and plug thief zones *deep* within reservoirs, a goal that cannot be achieved using mechanical plugs, bulk gels, or cement. Instead, a deep diverting temperature-sensitive polymer microgel was designed; the chemical itself was also termed Bright Water. These sub-micron gel particles (often referred to as "kernels") are injected into the reservoir with cool injection water relative to the reservoir temperature itself. The microgel kernels in the cool waterflood travel primarily to thief zones due to their higher permeabilities, slowly picking up heat from the surrounding warmer reservoir rock. At a certain pre-determined critical temperature (a key design parameter), the kernels "pop" like popcorn in the sense that they expand irreversibly. This results in their viscosification and the plugging of the thief zones (through interactions with pore throats/other microparticles), and thus increased residual resistance factor. This, in turn, results in the diversion of subsequent injected water to other relatively unswept portions of the reservoir. Ultimately, as with the other microgels, this yields increased sweep efficiency and hydrocarbon recovery, as well as decreased water production. (Pritchett et al. 2003; Frampton et al. 2004; Morgan 2007; Yanez et al. 2007; Garmeh et al. 2011)

The concept of using a deep diverting gel that takes advantage of the thermal gradient brought about by the injection of cold water into a relatively warm reservoir dates to as long as two decades ago (Fletcher et al. 1992). Bright Water itself was brought into being by the joint efforts of BP's Harry Frampton, BP's James Morgan, and Nalco's Kin-Tai Chang (Chang et al. 2002). Bright Water is a chemical suspension of polymer microparticles of a submicron dimension, when unexpanded, ranging from 0.1 to 1

microns. The microgels are unique in that their conformation is controlled by two types of crosslinking agents, labile and non-labile (stable) crosslinkers. Chang et al. (2002) specified that the microparticle content should ideally contain between 20,000 to 60,000 ppm labile crosslinker (preferably polyethyleneglycol diacrylate) and between 0 to 100 ppm non-labile (stable) crosslinker (preferably methylene bisacrylamide). Chang et al. (2002)'s patent should be referred to for insight on the type of polymers and crosslinkers that are suitable for this application. The same patent dictates that the Bright Water microgels should be prepared using an inverse emulsion process, and continues to briefly describe this process. Frampton et al. (2004) describe this preparation process as well; this is important as it ensures the preparation of individual microparticles and not an aggregate gel, through the use of a dispersing surfactant additive (Frampton et al. 2004; Yanez et al. 2007).

The microgel particles are designed to be able to easily propagate through porous media, and the design should be catered to each specific reservoir. Bright Water's small particle size and low viscosity render it easy to inject (minimal flow resistance) and capable of achieving great depths within a reservoir, before expanding. As soon as the cool injected aqueous Bright Water suspension heats up to a certain pre-determined temperature in the reservoir, the microgels are triggered and the liable crosslinkers begin breaking down which induces microgel swelling through the absorption of water. The swelling leads to the plugging of thief zone pore throats and the diversion of trailing injected fluid. The expanded particle size (and rate of de-crosslinking/swelling) should be designed specific to the target porous media, and can be controlled through the proper selection of polymer as well as the types and degree of labile and non-labile (stable) crosslinkers. The use of Bright Water ideally requires the knowledge of highest permeability thief zone pore size, formation temperature, and microparticle propagation

rate, so as to appropriately design the microparticles (unexpanded size, time to expansion, rate of expansion, expanded size) and to situate the microgel plug at an optimal position deep within the reservoir thief zone. (Chang et al. 2002)

Some observations made regarding Bright Water include:

- Bright Water is insensitive to reservoir salinity when in its unexpanded/kernel form (Chang et al. 2002; Frampton et al. 2004). Salinity does affect Bright Water in its expanded/popcorn form (Frampton et al. 2004; Yanez et al. 2007).
- Bright water kernels are robust throughout a wide range of different reservoir conditions (salinity, pH) and are unaffected by shear (Mustoni et al. 2010).
- Unlike PPGs, Bright Water is not intended for use in fractures (Pritchett et al. 2003; Mustoni et al. 2010).
- Different Bright Water grades are readily available for systems of different temperatures and/or different desired thermal reaction rates (Yanez et al. 2007; Ohms et al. 2009; Husband et al. 2010; Garmeh et al. 2011; Izgec and Shook 2012).
- Activation/triggering temperature of the Bright Water particles depends on the crosslinker selected and its associated mechanism of de-crosslinking (Frampton et al. 2004; Chang et al. 2002).
- Non-labile (stable) crosslinkers keep the expanded microparticles (popcorn) from breaking down into a solution of linear polymers, and so are vital for Bright Water to achieve its intended purpose (Chang et al. 2002; Frampton et al. 2004).
- Bright Water propagation and plugging effects depend on particle concentration. Pritchett et al. (2003) found that Bright Water microparticles (kernels) propagated through porous media with ease when their mean diameter was less than one tenth

the mean pore throat size. Bright Water expanded microparticles (popcorn) were found to yield substantial plugging effects when their mean diameter was greater than one quarter the mean pore throat size. These findings may have been different at different particle concentrations. (Pritchett et al. 2003)

- Pritchett et al. (2003) list nine "preferred target properties" that should be referred to and considered when contemplating the use of Bright Water. Some of these preferred properties include the presence of a porous and permeable thief zone, minimal fracturing, temperature between 50 and 150˚C, and injection water salinity less than 70,000 ppm. (Pritchett et al. 2003)

The first reported trials of Bright Water took place in the Minas field in Indonesia (Pritchett et al. 2003; Frampton et al. 2004). Pritchett et al. (2003) conducted one of these field trials as well as a series of laboratory tests (bottle tests, injectivity tests, propagation tests, and popping tests). This Indonesian field trial showed that Bright Water can be injected without trouble, and that the microparticles can propagate through rock pore space to significant depths (gelation appeared to occur 125 ft from the wellbore). However, oil production response was uncertain for a variety of reasons. Frampton et al. (2004) provide significant more detail on the laboratory tests discussed by Pritchett et al. (2003).

Bright Water's first commercial field implementations followed and were located in BP's Milne Point field in Alaska (Ohms et al. 2009) and in BP's Prudhoe Bay field, also in Alaska (Husband et al. 2010). In the Milne Point field in Alaska, Ohms et al. (2009) reported encouraging results for a Bright Water trial on an isolated compartment containing three wells (1 injector and 2 producers). Over 60,000 barrels of incremental oil were recovered over 4 years, at a cost of under $5/incremental barrel of oil,

demonstrating Bright Water's commercial potential. Certain aspects of the oil response, such as response timing, mimicked simulation predictions. Reduced injectivity (only after a significant period of time – time to in-depth gelation) and decreased permeabilities also suggested that the treatment took place as expected (Ohms et al. 2009). In the Prudhoe Bay field in Alaska, Husband et al. (2010) also reported highly encouraging results that demonstrated Bright Water's commercial potential. The use of Bright Water in a moderate-sized injection pattern (pilot program) led to decreased water cuts and the production of roughly 500,000 incremental barrels of oil, at "competitive cost" (Husband et al. 2010). Figures 3.8 and 3.9, taken from Husband et al. (2010), demonstrate Bright Water's positive effects on vertical sweep efficiency (simulated) and oil rates (actual), respectively. Note that in both Bright Water field implementations discussed above, there was reason to believe in the existence of significant bypassed oil; this is an important prerequisite to utilizing such a technology economically.

Subsequent successful Bright Water field implementations were reported by Pan American in the San Jorge Basin in Argentina (Yanez et al. 2007; Mustoni et al. 2010). Mustoni et al. (2010) reported over 60,000 incremental barrels of oil over six Bright Water pilot treatments, and significant reduction in combined WOR. Yanez et al. (2007) and Mustoni et al. (2010) both provide lists of screening criteria for Bright Water floods. Bright Water has also been used in the Salema field in Brazil (Roussennac and Toschi 2010) and in the El Borma field in Tunisia (Ghaddab et al. 2010).

Garmeh et al. (2011) and Izgec and Shook (2012) are vital references for those considering Bright Water technology. Garmeh et al. (2011) present a workflow for Bright Water treatment design and evaluation, and also discuss different simulation approaches to model Bright Water. Garmeh et al. (2011) also run simulation sensitivities to evaluate the effect of different variables (treatment concentration, slug size, permeability contrast,

k_v/k_h, mobility ratio, and gel activation location) on Bright Water treatment results. Izgec and Shook (2012) more recently performed similar sensitivities, following the simulation approach used by Garmeh et al. (2011). Izgec and Shook (2012) determined that gel placement location and permeability contrast (between the thief zone and surrounding layers) are the most important factors determining the success of a Bright Water treatment. Note that Izgec and Shook (2012)'s sensitivity study should be referred to for insight on the effect of k_v/k_h on incremental recovery; Garmeh et al. (2011)'s study does not take gel placement location into consideration when studying k_v/k_h, rendering this aspect of their study somewhat incomplete. Izgec and Shook (2012) also presented an approach for determining the slug size of a Bright Water treatment.

Ultimately, Bright Water is a conformance control agent with significant potential and a good number of successful field implementations. Their increasing popularity is evident by the almost 60 treatments carried out, to date, in a wide variety of different countries, since the first trial in Indonesia (Garmeh et al. 2011).

3.4.4 pH-Sensitive Polymer Microgels

This final polymer microgel is one of the most recently developed polymer microgels, differing from the previously discussed microgels in that it uses pH change as its activation trigger. Like the other microgels discussed so far, pH-Sensitive Polymer Microgels are conformance control candidates, with the ability to divert flow away from thief zones or high permeability layers towards rock with higher oil saturations. The use of a pH-Sensitive Polymer for conformance control was first proposed by Al-Anazi and Sharma (2002). Al-Anazi and Sharma (2002) noted that polyelectrolytes, such as polyacrylic acid, are very pH sensitive, capable of retaining significant volumes of water and swelling by several orders of magnitude (up to 1000 times original volume) as a

result of pH change. This, in turn, leads to a significant increase in viscosity. Such observations resulted in them experimentally evaluating pH-Sensitive Polymers for conformance control. Huh et al. (2005) took this a step further by proposing similar use of such pH-Sensitive Polymers but in the form of small and elastic microgel globules instead. One important advantage of the use of polyelectrolytes, like polyacrylic acid, for conformance control is their low cost, resulting from their plentiful supply for other applications. Another key advantage is that the swelling of pH-Sensitive Polymer Microgels can be fully reversed by an acid wash. This is a significant advantage over Bright Water, whose swelling/popping cannot be reversed. These polymer microgels are also environmentally benign, which is a consideration of great importance. A disadvantage is the added cost of an acid pre-flush, whose importance will soon be made clear. Note that, throughout the literature, pH-Sensitive Polymer Microgels have also been referred to as pH-Triggered Polymer Microgels, pH-Sensitive Polyelectrolytes, Polyacrylic Acid Hydrogels, and pH-Sensitive Crosslinked Polymers. (Al-Anazi and Sharma 2002; Huh et al. 2005; Benson et al. 2007)

Al-Anazi and Sharma (2002) explain the chemistry involved in the swelling of a pH-Sensitive Polyelectrolyte. It ultimately comes down to the interactions between the ions formed when polyelectrolytes, such as polyacrylic acid, dissociate in solution. When the carboxylic groups (-COOH) in polyacrylic acid are ionized, the resulting negatively charged groups ($-COO^-$) repel each other. This repulsion results in the stretching/uncoiling of the polyacrylic acid polymers, which in turn causes a drastic increase in polyacrylic acid solution viscosity. Figure 3.10 offers an illustration of the uncoiling of polyacrylic acid. Figure 3.11 offers a graphic representation of the resulting viscosity increase, as determined by one of Al-Anazi and Sharma (2002)'s experimental investigations. As can be seen from this figure, at low pH values (around 2) the viscosity

of polyacrylic acid solutions can be very small (less than 10 cP in this example). This is because such low pH values represent acidic conditions where ionized carboxylic groups can be neutralized by protons (H^+), and so polyacrylic acid exists in its coiled low viscosity state. As pH rises, more ionized carboxylic groups will exist and so polyacrylic acid will tend to its uncoiled more viscous state. As can be seen in Figure 3.11, at a somewhat neutral pH (around 6) the viscosity of polyacrylic acid solutions can be orders of magnitude higher (as high as 20,000 cP in this example). Polyacrylic acid solutions have characteristic/critical gelling pH values, at which the solution reaches its maximum viscosity. This is an important aspect of the use of this pH-Sensitive Polymer for conformance control purposes. (Al-Anazi and Sharma 2002)

In order to utilize a pH-Sensitive Polymer such as polyacrylic acid, an acid pre-flush is usually required so as to bring reservoir pH values down as much as possible. Since the polymer exists in its low viscosity state in acidic conditions, the acidic preconditioning enables the subsequent polymer injection to be fairly easy and also allows for the ease of polymer propagation through the porous media. Injected acid and polymer concentrations and rate of injection should be catered to each reservoir's unique rock mineralogy, permeability and salinity (Choi et al. 2006, 2009; Choi 2008). The polymer injection period is followed by a shut-in period, so that the pH can increase as a result of geochemical reactions between the injected acid and carbonate/mineral components (e.g. muscovite, microcline) in the rock. When the pH is above the gelling/critical pH, the polymer will gel. Ideally, the location of this gelation/viscosification will be controlled so as to achieve the desired permeability modification and optimal sweep improvement. Note that the viscosity change is easily and cheaply reversible by use of an acid wash. (Al-Anazi and Sharma 2002; Huh et al. 2005)

Polyacrylic acid gelation depends on pH, polymer concentration, and ionic strength (Al-Anazi and Sharma 2002). Al-Anazi and Sharma (2002) offer a systematic study of the effect of these variables, and temperature, on the pH-Sensitive Polymer's rheological properties. Their findings are very briefly summarized below:

- As polymer concentration increases, the concentration of carboxylic groups increases. This means that larger viscosity values can be attained. Decreasing polymer concentration has the opposite effect.
- As salinity increases, increased cation concentration results in the shielding of the polyacrylic acid negatively charged carboxylic groups and subsequent polymer coil compaction. This means that even though the overall trends of viscosity change with pH are similar to those shown in Figure 3.11, the viscosities are smaller at higher salinities (and are larger at smaller salinities). At a certain high salinity (9 wt% NaCl in this example), polyacrylic acid solution viscosities will be low enough that the polymer ceases to be an effective gelling agent. However, this effect can be offset by increasing polymer concentration (design consideration).
- The polymer rheology was found to be fairly insensitive to temperature, up to 80˚C.
- The polymer was found to be compatible with most commonly used brine types, such as sodium chloride, potassium chloride, and ammonium chloride, and so can be prepared in any of these brine types. However, salts with multivalent cations can yield the formation of precipitates upon contact with ionized polymer. This can be remedied through the use of a different polymer mixing procedure and/or

the use of a pre-flush of a compatible brine to minimize the effect of such multivalent cations.

Al-Anazi and Sharma (2002)'s experiments showed that the pH-Sensitive Polymer, polyacrylic acid, can easily propagate deep into porous media after an acid pre-flush and then gel, yielding substantial and stable permeability reductions. They concluded that the pH-Sensitive Polymer studied "are excellent candidates for conformance control".

As previously mentioned, Huh et al. (2005) first proposed the utilization of such pH-Sensitive Polymers in microgel form. Choi et al. (2006) briefly describe how they formed a homogeneous dispersion of microgel globules. Huh et al. (2005)'s work is a vital reference as they discuss the development of a rheological model for pH-Sensitive Polymer solutions. Huh et al. (2005) used a combination of Brannon-Peppas and Peppas's ionic hydrogel swelling theory, the Mark-Houwink equation, the Martin equation, and the Carreau equation to develop a rheology correlation that can accurately predict apparent viscosity of a polymer solution as a function of pH, salinity, polymer concentration, and apparent shear rate. This is very important as it enables the use of simulation to design pH-Sensitive Polymer Microgel floods for optimal incremental oil recovery and decreased water production. However, the developed rheological model needs to be coupled with a geochemical model that models the pH increase resulting from the reaction between the injected acid and carbonate/mineral components in the rock. Choi et al. (2006)'s experiments and matching attempts provide additional insight on geochemical characterization as well as the transport of pH-Sensitive Polymer Microgels through porous media. Benson et al. (2007) coupled the developed understanding on pH-Sensitive Polymer Microgel rheology, geochemistry, and transport through porous media,

in the development and implementation of pH-Sensitive Polymer simulation capabilities. Benson et al. (2007) also proceeded to use the developed simulation capabilities to model simplified conformance control treatments, and found that pH-Sensitive Polymer Microgel *slug* treatments demonstrated positive vertical conformance improvement capabilities (above and beyond conventional polymer floods). (Huh et al. 2005; Choi et al. 2006; Benson et al. 2007)

Choi (2008) and Choi et al. (2009) propose the use of HPAM instead of the microgels utilized by the previous investigators. However, the concept is essentially the same since HPAM chains portray a similar coiling/uncoiling mechanism when pH changes. HPAM is injected in low pH conditions where the polymer possesses a low viscosity and is easily injected and also easily propagates deep into high permeability zones. Spontaneous geochemical reactions similarly yield increased pH values and polymer solution viscosification and controlled permeability reduction. Chase water is then redirected to lower permeability zones where oil was previously bypassed, increasing overall sweep. Choi (2008) and Choi et al. (2009) extensively discuss their experimental investigation of the use of low pH HPAM for conformance control. Specifically, they studied the rheology and transport of HPAM solutions as well as the pertinent geochemical reactions. Their works should be referred to for the detailing of their experiments and findings. One interesting finding is that a weak acid, such as citric acid, may be preferred over hydrochloric acid since it is less reactive and so pH rise is prolonged, enabling deeper propagation before viscosification.

Lalehrokh et al. (2008) investigates the concept of using pH-Sensitive Polymer Microgels to improve sweep in fractured rock by plugging fractures. Their experimental investigations made use of artificially fractured outcrop cores, of both sandstone and carbonate types. It was found that treated cores yielded significantly lower permeabilities,

and when the treated core permeability was lower than the matrix permeability, the matrix was invaded as well as the fracture. An important observation was that the shut-in time significantly affected residual resistance factor (permeability reduction). This is because the polymer microgel residence time through the artificial fracture was too small to significantly increase pH without the aid of a shut-in period. Lalehrokh et al. (2008) also concluded, through their experimental work, that the polymer microgel solution could propagate much deeper into a fractured sandstone reservoir (on the order of 1000 ft) than into fractured carbonate reservoirs (on the order of 40-50 ft) before gelation. This is because pH increases much faster in carbonates due to the large quantity of carbonate compounds (depth of gel placement is a function of rate of pH increase and rate of fluid propagation). Acid pre-flushes were thus deemed more important in carbonates than in sandstones. In fact, acid pre-flushes had no significant impact on residual resistance factor in sandstones. One final observation worth noting is that polymer microgel precipitation/gelation could be triggered by divalent cations (such as calcium) in reservoir rock, even at pH values below the critical pH value. Ultimately, pH-Sensitive Polymer Microgels were deemed worthy candidates for conformance control in fractured reservoirs, as they could potentially divert flow from fractures to surrounding matrix, through controlled permeability reduction. Lalehrokh and Bryant (2009) further investigate the potential use of pH-Sensitive Polymer Microgels in fractured formations. They studied the effects of polymer concentration, salinity, salt types, and aging on permeability reduction. Their results also suggested that pH-Sensitive Polymer Microgels are good conformance control candidates in fractured formations of different types. (Lalehrokh et al. 2008; Lalehrokh and Bryant 2009)

Despite the strong working knowledge of pH-Sensitive Polymer Microgels, demonstrated by the surveyed literature, no field implementations have been reported to

date. However, their numerous advantages and their potential to improve vertical sweep efficiency render them worth considering as a conformance control agent. The literature discussed above provides a decent start for those looking to optimally utilize this technology to increase hydrocarbon recovery efficiency and decrease water production.

3.5 CONCLUSION

The above polymer microgel literature survey was presented in an attempt to consolidate the abundance of information on polymer microgel technology. Four different types of polymer microgels (Colloidal Dispersion Gels, Preformed Particle Gels, Temperature-Sensitive Microgels, and pH-Sensitive Polymer Microgels) were discussed. Table 3.3 can be referred to for a quick overview of some of the important characteristics of the different microgels discussed. The survey focused on the microgel characteristics, lab observations, field applications, microgel merits and controversies. The rheology and plugging mechanism of polymer microgels was discussed in some detail, but plenty of research is still needed as the plugging mechanism is still generally uncertain and there is controversy in the literature. The presented literature survey is by no means all inclusive, but an attempt was made to provide references to appropriate pieces of work where relevant, so readers are able to expand their polymer microgel knowledge even further. Polymer microgel flooding is an increasingly popular EOR method and an effective means of conformance control. It is as important as ever to optimally utilize such technology to maximize hydrocarbon recovery efficiency, and thus prolong the life of mature hydrocarbon reservoirs – our single greatest source of today's energy supply.

Parallel Core Flood Experiments

Test No.	Core No	Permeability (D)	Porosity (%)	Water-cut (%)		Flow distribution (%)		Recovery efficiency (%)	
				before	after	before	after	before	after
1	1.1	8.23	40	70	75	91	20	46.8	64.9
	1.2	0.541	40	22	54	9	80		
2	2.1	13.5	40	72	76	98	87	40.1	62.5
	2.2	0.61	40	6	48	2	13		

Table 3.1: PPG Parallel Core Flood Experiment Results (Coste et al. 2000)

Table from Coste et al. (2000).

Products	Description	Advantage	Disadvantage	Field Applications
PPG	• A crosslinked polyacrylimide particle • Gel is formed on surface facilities. • Particle dispersion is injected into formation. • Swell 20-200 times of its original size when mixing with water. • Commerical particle size can be controlled from a few hundred micron to a few centimeter.	• Strength- and size-controlled, environment-friendly; • Gelation is affected by shear, chromatographic adsorption of chemicals, dilution, dispersion and diffusion. • High temperature (120 °C) and high salinity (300,000 mg/L) resistance; • High salinity (300,000 mg/L) resistance; • Alternated slug injection of gel/water.	• Particle size is relatively large. • Cannot be penetrate into formation below 1D • Can only be used in the reservoirs with extreme permeability contrast	• Around 2000 treatments in chinese mature oilfield since 1999 • Covers both naturally fratured and unfractured reservoirs with temperature from 20 to 110 C and salinity from 2000 to 280,000 mg/l.
Weak Bulk Gel	• Gelant (Polymer + Crosslinker + Additives) is injected into formation. • Gelant forms gel under reservoir conditions. • Polymer conc. usually between 1,000 to 3,000 mg/l	• Bulk gel • Can penetrate in-depth before gelling. • Can be used to reduce permeability of fractures or channels	• Gelation is affected by shear and reaction of chemicals with reservoir rocks and fluids. • Difficult to predict gelation time and strength due to the flowing and reservoir effect.	Widely used in most China oilfields
CDG	• Dispersed colloid gel formed in reservoir. • Polymer conc. below 1000 mg/l • Cannot be used in reservoirs with fractures or extremely high channels	• Dispersion weak gel • Low chemical cost • Microsize particle after forming gel. • High injectivity due to relative low polymer concentration	• Easily penetrate and damage low permeability oil zones before gelling • Thermal and salt resistance depends on polymer properties.	A few pilots in Daqing and Shengli oilfields.

Table 3.2: Comparison of PPGs, CDGs, and Weak Bulk Gel

Table taken from Liu et al. (2006).

Name	Gelation	At Surface	Trigger	In Situ	Size Before	Size After	Stimulation
CDG	In-Situ	Polymer and Crosslinker	Transition Pressure	Swollen Microgel	nm to µm-sized Particles	µm-sized Particles	Far From Well
Preformed CDG	Preformed	Microgel	Transition Pressure	Swollen Microgel	nm to µm-sized Particles	µm-sized Particles	Far From Well
PPG	Preformed	Particle Gel	Transition Pressure	Swollen Particle Gel	µm to cm-sized Particles	20-200 Times Larger	Far From Well
Bright Water	Preformed	Microgel	Temperature	Swollen Microgel	0.1 to 1 µm	1 to 10 µm	Far From Well
pH-Sensitive	Preformed	Microgel	pH	Swollen Microgel	µm-sized Particles	Up to 1000 Times Larger	Far From Well

Table 3.3: Comparison of the Different Microgels Discussed

Table's information pulled from the literature survey.

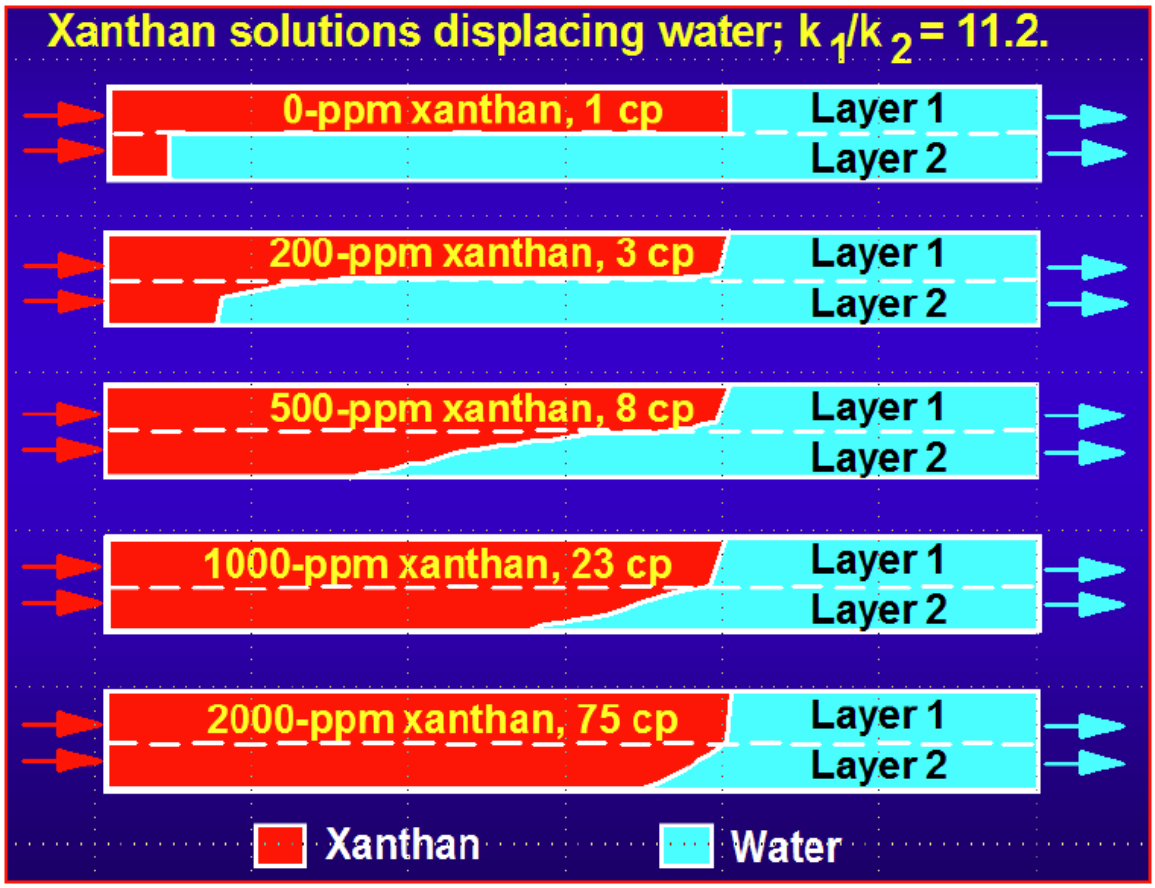

Figure 3.1: Illustration of Polymer Flooding as a Means of Mobility Control

Figure from Seright et al. (2011).

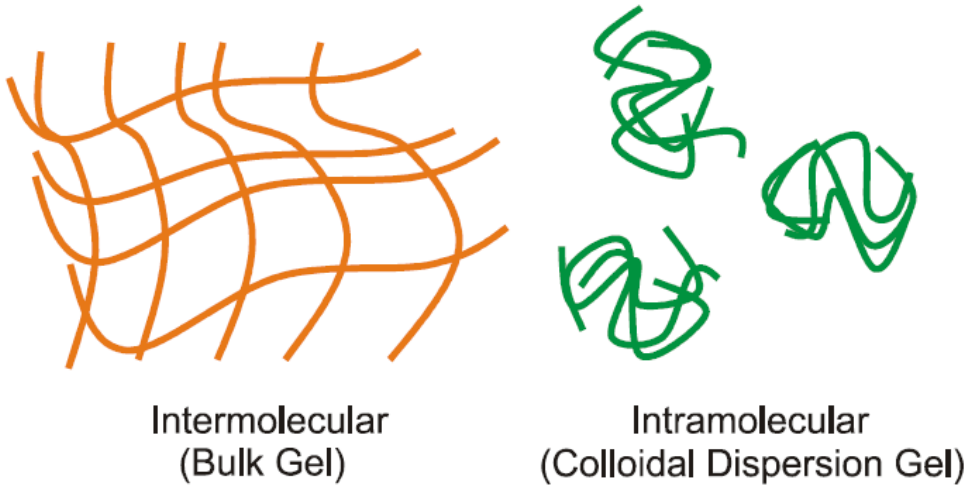

Figure 3.2: Difference between Bulk Gel and CDG

Figure from Diaz et al. (2008).

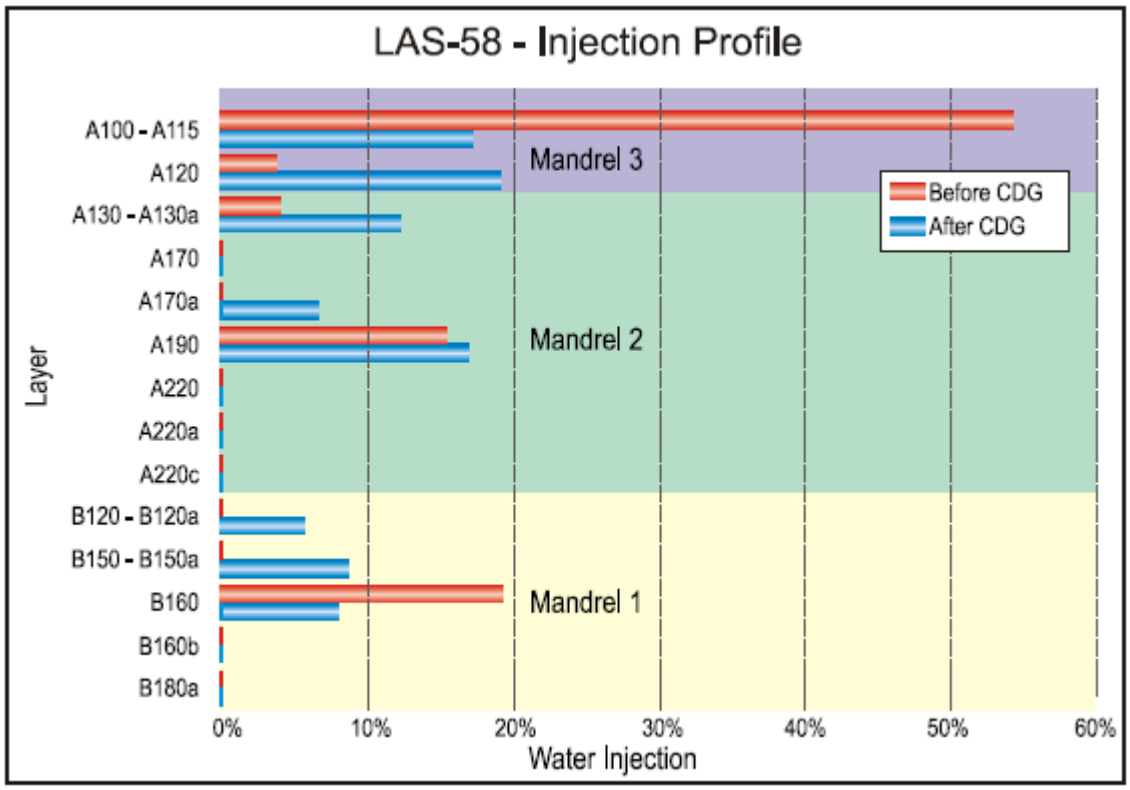

Figure 3.3: Improved Sweep Profile after CDG use in Loma Alta Sur Field

Figure from Diaz et al. (2008).

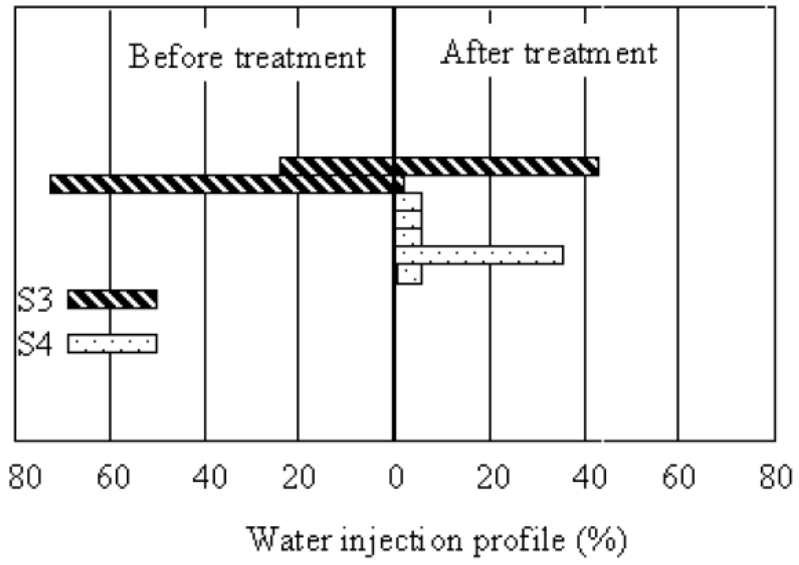

Figure 3.4: Improved Injection Distribution from PPG-Treated Injector (I)

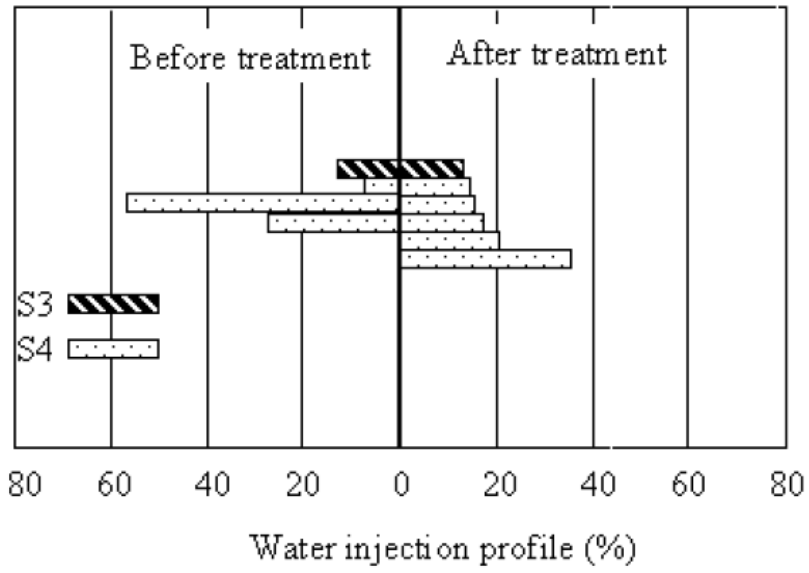

Figure 3.5: Improved Injection Distribution from PPG-Treated Injector (II)

Above figures from Coste et al. (2000). S3 represents a high permeability layer. S4 represents a low permeability layer.

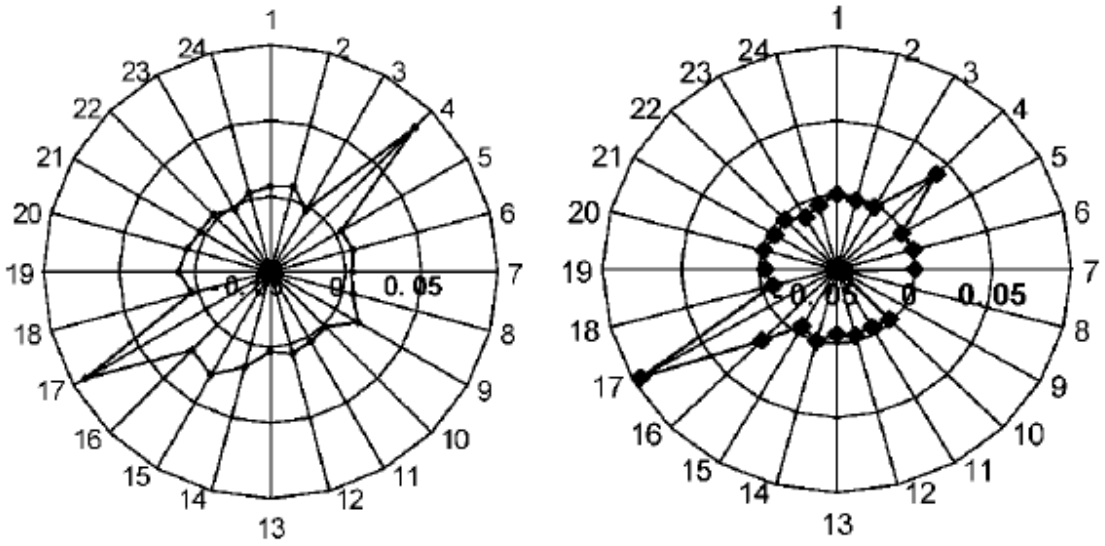

Figure 3.6: Heterogeneous Injection Profile prior to PPG Treatment

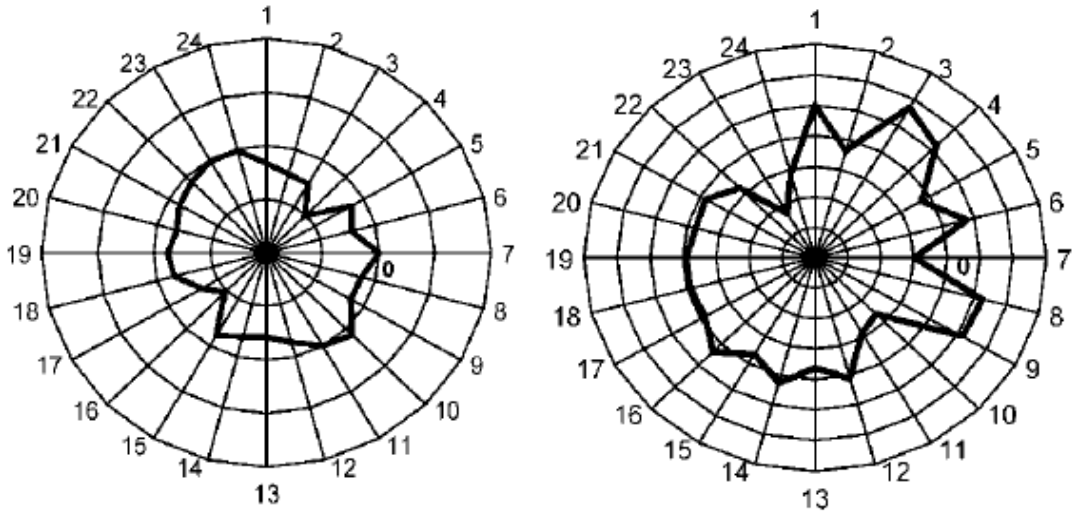

Figure 3.7: Improved Injection Profile after PPG Treatment

Above figures from He et al. (2004).

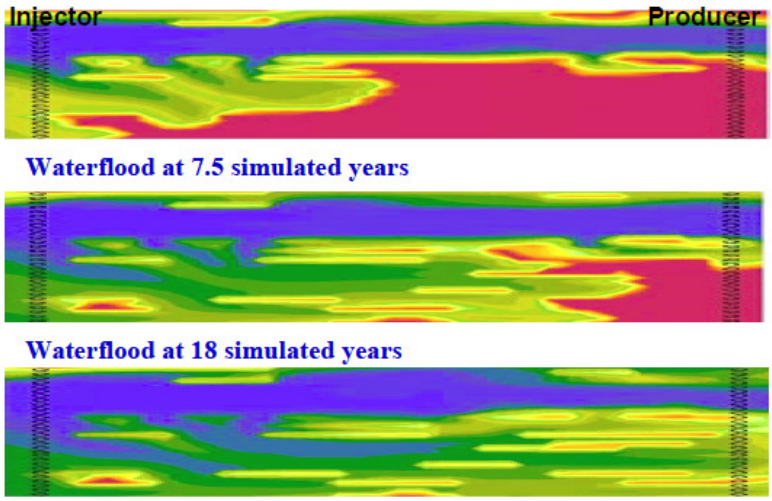

Figure 3.8: Simulated Vertical Sweep Improvement due to BW Treatment

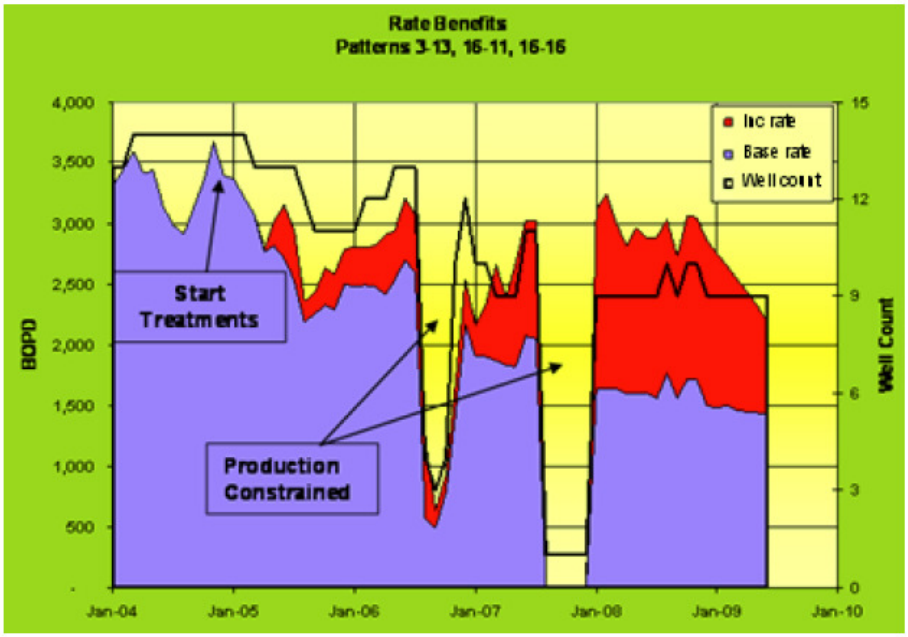

Figure 3.9: Actual Rate Benefits due to Bright Water Treatment

Above figures from Husband et al. (2010). In Figure 3.8, blue represents water while red represents oil (BW treatment applied at the 7.5 year mark). In Figure 3.9, red represents incremental oil over the base line in blue.

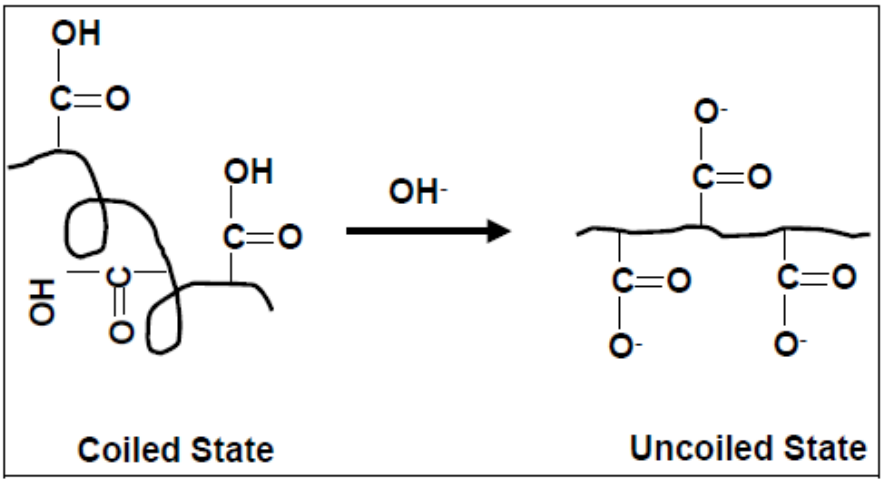

Figure 3.10: Illustration of Polyacrylic Acid Swelling With Ionization

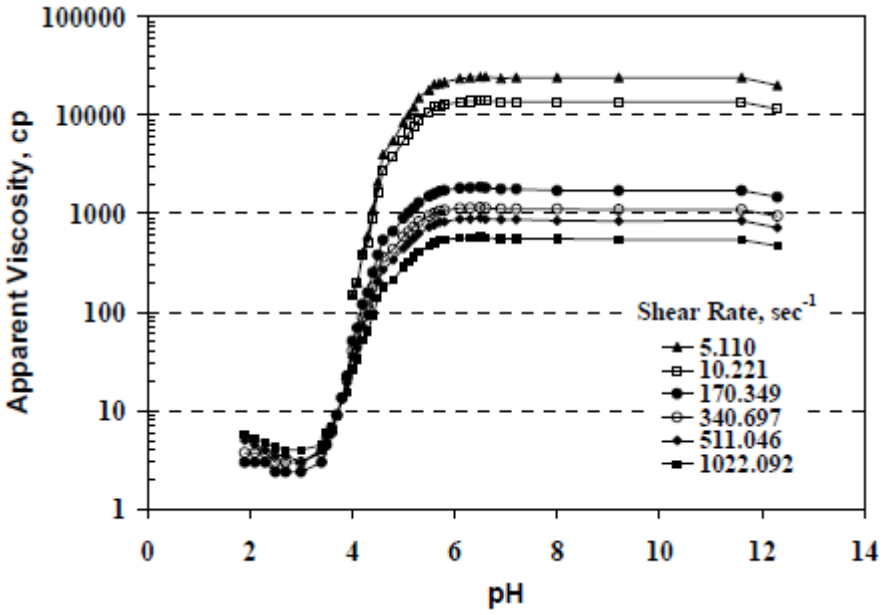

Figure 3.11: Effect of pH on Apparent Viscosity of Polyacrylic Acid

Above figures from Al-Anazi and Sharma (2002). Note that Figure 3.11's corresponding experiment utilized 3 wt% Polyacrylic Acid and 3 wt% NaCl, all at 24˚C.

Chapter 4: Microgel Experimental Case & Matching

This chapter outlines the methodology and results of simulating the use of polymer microgels in a core flooding experiment. Specifically, the microgels under investigation were Colloidal Dispersion Gels (CDGs). During the extensive literature survey already conducted (Chapter 3), one reported experiment on CDGs was selected for subsequent simulation. Simulations were conducted with the intent of matching this reported experiment, and these simulations are the subject of this chapter. Similar simulations and matching attempts for BrightWater and pH-sensitive microgels were conducted at UT Austin at the same time as the work reported here; these simulations were performed by Ulan Onbergenov, and are to be reported in his Master's thesis (Onbergenov 2012).

First, the reported CDG experiment is described in detail. This is followed by the description of the respective simulations, and an outlining of the matching attempts. To conclude, the results and the final match are discussed. It is important to note that one of the major objectives of these matching attempts was to obtain a full set of simulation parameters for use in subsequent synthetic simulations cases (Chapter 5). These synthetic simulations were used to provide additional insight on the polymer microgel flooding process, as well as to determine optimal conditions for polymer microgel use. This ultimately enables engineers to improve the design of polymer microgel floods, and thus to maximize hydrocarbon recovery efficiency and reservoir lifespan.

The simulations discussed in this chapter as well as in subsequent chapters were performed using UTGEL, an in-house reservoir simulator recently developed in the Petroleum & Geosystems Department at The University of Texas at Austin.

4.1 CDG EXPERIMENT DESCRIPTION AND SIMULATION SETUP

Lu et al. (2000)'s article was the source on CDG experiments that was selected for simulation and matching attempts. Lu et al. (2000) conducted CDG experiments so as to evaluate the potential of CDGs for enhanced oil recovery in the highly heterogeneous Daqing field in China, where uncrosslinked polymer typically channeled through high permeability streaks. The same experiments were used for the design of pilot tests in Daqing. This work was selected due to the fairly rigorous reporting of most of the experimental setup parameters. This enabled simulation of the experimental procedure with very few required assumptions. Lu et al. (2000)'s work addresses the characteristics, flow, and performance of CDGs through a variety of different experiments. The particular experiment that was simulated was conducted so as to obtain insight on the diverting performance of the microgel. Lu et al. (2000)'s work can be referred to for a detailed description of the experimental setup and procedure. However, this will also be briefly outlined within this section.

Lu et al. (2000) performed an experiment to investigate the diverting performance of CDGs. This experiment was an isothermal parallel core flood involving three homogeneous artificial cores of three different permeabilities (high, medium, and low permeability layers). The dimensions, permeabilities, porosities, and initial oil saturations for each core are reported in Table 4.1 below. A simplified schematic of the experimental setup can be seen in Figure 4.1 below.

The CDG experiment can be divided into 5 different parts:

1. Waterflooding the three artificial cores until 98% water cut in the effluent.
2. Uncrosslinked polymer flooding for 0.19 pore volumes.
3. Waterflooding until 98% water cut in the effluent.

4. CDG flooding for 0.19 pore volumes.
5. Waterflooding until 98% water cut in the effluent.

Each of these 5 different stages/steps required a matching attempt. Each core/layer's oil recovered and effluent water cut was reported by Lu et al. (2000) at the end of each flooding stage, and these results are displayed in Table 4.2. Table 4.2 also highlights the volume fraction of flow into each layer, so as to easily infer and compare the diverting performance of uncrosslinked polymer and of CDGs. As can be seen from the volume percent values in Table 4.2, the waterflood in stage 1 of the CDG experiment almost exclusively flowed into the high permeability core, as would be expected. Uncrosslinked polymer temporarily increased the volume percent flowing into the lower permeability layers, demonstrating uncrosslinked polymer's ability to act as a conformance control agent. This effect, however, was *short-term* as the waterflood following polymer injection still favorably flowed through the high permeability layer. On the other hand, CDGs diverted flow into the lower permeability layers for a longer time stretching into the post-CDG waterflood, demonstrating their *long-term* conformance control capabilities (through the plugging of the high permeability layer). Lu et al. (2000)'s reporting of volume percent enabled this observation that the CDG flood yielded a more dramatic *long-term* sweep improvement.

The overall oil recovered, effluent water cut, and injection pressure at the end of each flooding stage was reported by Lu et al. (2000), and these results are displayed in Table 4.3. Ultimately, the matching attempts were primarily aimed at matching each core/layer's oil recovery and water cut at the end of each stage. Injection pressure was also attempted to be matched, though this was of secondary importance.

Table 4.4 lists the important reservoir parameters taken or inferred from Lu et al. (2000)'s paper. Asides from Endpoint Mobility Ratio, none of these parameters were varied to obtain a match. The parameters varied for matching purposes are discussed separately in the section below. The three artificial cores were modeled as one "reservoir" with three layers and no crossflow between the layers. Table 4.5 lists the important simulation parameters. As can be seen in Table 4.5, four wells were needed to effectively model the experiment: one injector and three producers (one producer for each layer, mimicking each core's characteristic effluent). Figure 4.2 is an illustration of the reservoir model used for the undergone simulations; it should effectively model the experimental setup shown in Figure 4.1.

Some important given information regarding Lu et al. (2000)'s CDG experiment is listed below:

- The experiment was isothermal at 45˚C, and the experiment oil viscosity was roughly 9 cp at this temperature.
- There were two water solutions of different ionic compositions used for this experiment: produced water and river water. Produced water contained 0.05184 meq anions/mL solution and 0.0008 meq divalent cations/mL solution, while river water contained 0.01082 meq anions/mL solution and 0.001 meq divalent cations/mL solution. Table 4.6 can be referred to for a precise breakdown of the ions in each water solution.
- HPAM was the polymer of use in this experiment. The polymer had a molecular weight of 12M Dalton, 25% hydrolysis, and a purity of 89%.
- The uncrosslinked polymer solution was a mixture of river water and 800 ppm polymer, and possessed a viscosity of 25.6 cp.

- The CDG solution was a mixture of produced water, 800 ppm polymer, 8 ppm aluminum citrate crosslinker and 200 ppm unspecified additive. The solution possessed a viscosity of 12.7 cp.
- Injection rate was not specified for this particular experiment. The rate was taken to be 0.4 mL/min, as this was the rate used for one of the other experiments carried out by Lu et al. (2000).

4.2 CDG EXPERIMENT MATCHING

A large number of simulation parameters had to be varied until a match was obtained. This section outlines the parameters varied as well as the final set of parameters with which the CDG diverting experiment performed by Lu et al. (2000) was matched.

As previously mentioned, Tables 4.4 and 4.5 list the reservoir and simulation parameters respectively. Table 4.7 lists the well data used to model the parallel core flood experiment performed by Lu et al. (2000).

Some of the **assumptions** made in performing the CDG experiment simulation include:

- The cores initially contained produced water (see Table 4.6).
- River water was the injected water solution for all stages of the parallel core flood experiment *except* for the CDG flooding stage (where produced water was used instead).
- The cores were not perfectly homogeneous, despite Lu et al. (2000) stating this was the case. A match could only be obtained when a very small degree of

heterogeneity (V_{DP} = 0.2) was introduced. The concept of V_{DP} is introduced shortly.

- The three cores were at residual water saturation when Lu et al. (2000) set up the cores prior to the diverting performance experiment. This assumption is a reasonable one given the experimental procedure followed. This assumption was made because residual water saturations are a required simulation input parameter in UTGEL.
- The three cores were at residual oil saturation after Lu et al. (2000) completed all five flooding stages. This assumption was made because residual oil saturations are a required simulation input parameter in UTGEL.
- In matching the parallel core flood results, divalent cations were neglected in determining effective salinity. In addition, the effect of effective salinity on polymer solution viscosity was also neglected.
- In reporting simulation results, injection pressure was taken as the average of the pressures in each core's first gridblock.

In matching Lu et al. (2000)'s experiment, many parameters had to be varied. The list below outlines the main parameters varied in each step of the core flooding experiment. Note that Tables 4.8a and 4.8b should be referred to for the full list of simulation parameters and their final values. The values within these tables are those which yielded the closest match.

1. **Waterflood:** The main parameters varied in this step of the diverting experiment were the end point permeabilities (and thus end-point mobility ratio) and saturation exponents. These variations ultimately affect relative permeability

values, computed using Corey-type equations. Initially, a match could not be obtained. It became clear that flow allocation very strongly depended on the permeability of the first gridblock in each core/layer. Thus, a very slight heterogeneity was introduced, so as to help get a match. Heterogeneity (permeability variation/variance) is most commonly quantified using the Dykstra-Parsons coefficient, V_{DP}. This coefficient is zero for "perfectly" homogeneous reservoirs and one for "infinitely" heterogeneous reservoirs (Jensen 2000). A match was obtained with a low V_{DP} of 0.2. Note that longitudinal and transverse dispersivities of all phases were set to 0, to get a match, which is reasonable given the very small dimensions of the gridblocks in this simulation (dispersivities usually set to 10% of gridblock dimensions). Since pore volumes injected was not indicated by Lu et al. (2000), this was one of the matching parameters as well. The final set of Corey-type parameters that yielded a match suggested that the cores were water-wet.

2. **Polymer Flood:** The main parameters varied here were polymer parameters. Specifically, the parameters varied control the effects of salinity, polymer concentration, shear, adsorption, and permeability reduction on polymer properties and the polymer flooding profile. The effect of salinity on polymer properties was neglected, as explained in the assumptions listed previously. The parameters controlling the effect of polymer concentration on polymer solution viscosity were set so that an 800 ppm polymer solution possessed a viscosity of 25.6 cP, as indicated by Lu et al. (2000). The other parameters that control the polymer flood were matched using some of the experimental results produced by Lu et al. (2000) and Smith et al. (2000). Note that pore volumes flooded was not a matching parameter here as Lu et al. (2000) specified it was set to 0.19 PV.

Ultimately, a match was obtained for this step, having used a shear-thinning model. Note that Wreath's correlation (Wreath 1989) was added to UTGEL during this step, so that polymer solutions, under shear, were more accurately modeled in cores of different permeabilities.

3. **Waterflood:** The only parameter that could be varied here was pore volumes flooded. Despite this, a good match was obtained, supporting the parameters input to match the steps prior to this one.
4. **CDG Flood:** The main parameters varied here were CDG parameters. Specifically, the parameters varied control the effects of CDG concentration, shear, permeability, and permeability reduction on CDG properties and the CDG flooding profile. The parameters controlling the effect of CDG concentration on CDG solution viscosity were set so that an 800 ppm CDG solution possessed a viscosity of 12.7 cP, as indicated by Lu et al. (2000). The other parameters that control the CDG flood were matched solely using the results of the CDG flood (oil recovery, water cut, and flow allocation) as there was a shortage of information provided in the literature. Note that pore volumes flooded was not a matching parameter here as Lu et al. (2000) specified it was set to 0.19 PV. Ultimately, a match was obtained for this step, after making several changes to UTGEL. Shi et al. (2011a, 2011b) as well as UTGEL's technical manual can be referred to for additional insight on UTGEL's CDG viscosity and transport models. The most significant change was that a second *long-term* permeability reduction model was incorporated for CDGs, so that CDGs could have a *long-term* effect lasting into the post-CDG waterflood flush, as was evident in Lu et al. (2000)'s experiment. This additional permeability reduction model for CDGs made use of as a Langmuir-type isotherm for CDG adsorption. Without including

this second model, all the CDG was produced very quickly and there were no long-term permeability reduction effects. Updating UTGEL, as such, enabled the matching of this portion of the CDG diverting experiment.

5. **Waterflood:** Again, the only parameter that could be varied here was pore volumes flooded. A decent match was obtained. However, there were some discrepancies here, namely with the oil recovery and water cut in the low permeability core. This is outlined in more detail below.

4.3 CDG EXPERIMENT MATCHING RESULTS

The results of the simulation that yielded the closest match are displayed in Tables 4.9a and 4.9b. These results should be compared to those within Tables 4.2 and 4.3. After close comparison, it can be seen that oil recoveries were very closely matched. This was the main priority in matching Lu et al. (2000)'s experiment. Water cuts were also very closely matched, with the exception of the water cut in the low permeability core in the very last stage of the experiment. The simulation yielded water breakthrough at this point, which was not evident in Lu et al. (2000)'s experiment. However, this could not be rectified without significantly altering the oil recovery for the worse. In addition, injection pressures were not matched well. This was given the lowest priority in the matching process. The priority was to match oil recoveries and CDG diverting performance. With this in mind, the matching attempt can be deemed successful given the very good matches of oil recovery and the decent volume percent allocation matches. Figure 4.3 can help illustrate the final simulation's effective matching of Lu et al. (2000)'s experiment, in terms of oil recovery.

4.4 DISCUSSION

As Figure 4.3 illustrates, oil recovery was very well matched. Comparing Tables 4.9a and 4.9b to Tables 4.2 and 4.3 also shows that volume percent allocations were well matched as well. Despite the poor injection pressure matches, and the one poorly matched water cut value, the experiment was considered successfully matched. Thus, the final input parameters were deemed worth carrying forward for subsequent simulation sensitivity studies, to be outlined in the following chapter. Appendix A can be referred to for the final Input File used to obtain the CDG experiment match.

The fact that a good match was obtained also speaks to the validity of the CDG models incorporated into UTGEL. This was one of the incentives for such a matching attempt. However, in the following chapter, an interesting finding is raised. It was found that it was best to rework the CDG permeability reduction model. As previously mentioned, a second *long-term* permeability reduction model (that made use of a Langmuir-type adsorption curve) had to be added to UTGEL for CDGs, in order to get a match. This is because CDGs have shown the ability to induce *long-term* permeability reductions, as was witnessed in Lu et al. (2000)'s experiment, for example. However, it was later realized that in this matched experiment, the permeability reduction post-CDG flood was much larger than the permeability reduction during the CDG flood. This is essentially similar to saying that RRF was greater than RF. Figure 4.3 helps highlight this fact; it can clearly be seen that CDGs improved oil recovery in the low permeability core mostly during the post-CDG flood, with only some improvement *during* the CDG flooding stage. RRF being greater than RF is reasonable in a lab setting where low flow rates are typical. However, this is not realistic on a field scale, where flow rates are higher. Figure 4.4 can attest to the fact that at high flow rates CDGs induce an RRF that is lower than the induced RF.

In light of this finding, the CDG permeability reduction model was reworked. The new model still makes use of two permeability reduction equations, one for short-term effects and another for long-term effects. However, the long-term permeability reduction equation is modified. Long-term permeability reduction was made to be a factor of the short-term permeability reduction, ensuring it is always lower than RF. The modified model is presented in the subsequent chapter, along with a more detailed discussion. The modified model guarantees that RRF is lower than RF so that field-scale simulations possess more realistic results. This was important as the model prior to this modified one (that which was used in this chapter) yielded unrealistic results when conducting the sensitivity analysis in the following chapter. A more detailed discussion follows shortly.

Layers	Geometric size L×W×H (cm)	Permeability (μm^2)	Porosity (%)	Oil saturation (%)
High	32×3.6×3.6	1.78	25.3	77.4
Middle	32×3.6×3.6	0.57	23.2	73.2
Low	32×3.6×3.6	0.21	20.8	70.0

Table 4.1: Core Parameters for Lu et al. (2000)'s CDG Experiment

End of flooding	Water cut(%)			Oil recovery (%)			Volume percent(%)		
	H	M	L	H	M	L	H	M	L
Water	99.4	85.7	0.0	54.6	41.8	3.4	90.6	9.4	0.0
Polymer	95.3	98.4	0.0	55.5	42.7	9.5	63.3	26.6	10.0
Subsequent water	100.0	94.7	0.0	65.2	56.5	23.2	93.0	6.3	0.7
Gel	100.0	93.0	0.0	65.2	57.3	26.9	74.8	19.4	5.8
Subsequent water	100.0	99.4	0.0	66.5	61.5	53.8	70.7	26.1	3.2
Note: H means high permeable layer, M middle, and L low.									

Table 4.2: Layer Results of Lu et al. (2000)'s CDG Experiment

End of flooding procedure	Water cut (%)	Oil recovery (%)	Injection pressure (at)
Water	97.9	35.5	0.61
Polymer	86.5	37.9	5.20
Subsequent water	99.0	50.0	0.78
Gel	96.1	51.4	2.49
Subsequent water	96.7	61.2	4.44

Table 4.3: Overall Results of Lu et al. (2000)'s CDG Experiment

Tables from Lu et al. (2000).

Reservoir Property	Unit	Quantity			Comments
Reservoir Length	cm	32			
Reservoir Width	cm	3.6			
Reservoir Thickness	cm	10.8			
Depth of Top Layer	ft	0			
Initial Reservoir Pressure	psia	14.696			*Throughout Reservoir*
Oil Viscosity	cp	9.0			*Constant*
Water Viscosity	cp	0.60			*Constant*
Endpoint Mobility Ratio	-	10.7			*From Match*
Initial [Cl^-]	meq/ml H_20	0.05184			
Initial [Ca^{2+}]	meq/ml H_20	0.00080			
		Layer 1	**Layer 2**	**Layer 3**	
Thickness	ft	3.6	3.6	3.6	
X-Permeability	mD	1803.58	577.55	212.78	*Perm. Contrast ≈ 3*
Y-Permeability	mD	1803.58	577.55	212.78	*Perm. Contrast ≈ 3*
Z-Permeability	mD	0	0	0	*No Cross-flow*
Porosity	%	25.3	23.2	20.8	
Initial Oil Saturation	%	77.4	73.2	70.0	
Residual Oil Saturation	%	25.9	28.1	32.3	
Residual Water Saturation	%	22.6	26.8	30.0	

Table 4.4: Reservoir Data for Lu et al. (2000)'s CDG Experiment

Number of Grid-blocks (in x, y, z Directions)	15 x 1 x 3	*Variable Grid Size*
Coordinate System	Cartesian	
Temperature Variation	Not Considered	*Isothermal*
Simulation Time (PV)	7.45	*From Match*
Number of Wells	4	*1 Injector & 3 Producers*

Table 4.5: Simulation Data for Lu et al. (2000)'s CDG Experiment

Ion Compositions	Produced water		River water	
	Ppm	meg/L	ppm	meg/L
CO_3^{2-}	76.53	2.55	15.31	0.51
HCO_3^{1-}	1820.53	28.84	389.00	6.12
CL^{1-}	719.92	20.25	106.36	2.99
SO_4^{2-}	9.61	0.20	57.66	1.20
Ca^{2+}	8.02	0.40	12.02	0.60
Mg^{2+}	4.68	0.40	4.68	0.40
$Na^{1+}+K^{1+}$	1196.81	52.04	231.96	10.08
Total	3836.10	104.68	816.99	21.90

Table 4.6: Ionic Composition Breakdown of the Different Waters Used

Table from Lu et al. (2000).

Cumulative Time (PV)		Injector	Producer (High Perm)	Producer (Med Perm)	Producer (Low Perm)
1: Waterflood **1.13**	**Well Control**	Q_i = 0.4 mL/min	BHP = 14.696 psia	BHP = 14.696 psia	BHP = 14.696 psia
	Completion	Fully Completed	High Perm Layer Only	Med Perm Layer Only	Low Perm Layer Only
	Fluid	River Water	-	-	-
2: Polymer Flood **1.32**	**Well Control**	Q_i = 0.4 mL/min	BHP = 14.696 psia	BHP = 14.696 psia	BHP = 14.696 psia
	Completion	Fully Completed	High Perm Layer Only	Med Perm Layer Only	Low Perm Layer Only
	Fluid	River Water, 800 ppm Polymer	-	-	-
3: Waterflood **5.26**	**Well Control**	Q_i = 0.4 mL/min	BHP = 14.696 psia	BHP = 14.696 psia	BHP = 14.696 psia
	Completion	Fully Completed	High Perm Layer Only	Med Perm Layer Only	Low Perm Layer Only
	Fluid	River Water	-	-	-
4: CDG Flood **5.45**	**Well Control**	Q_i = 0.4 mL/min	BHP = 14.696 psia	BHP = 14.696 psia	BHP = 14.696 psia
	Completion	Fully Completed	High Perm Layer Only	Med Perm Layer Only	Low Perm Layer Only
	Fluid	Produced Water, 800 ppm CDG	-	-	-
5: Waterflood **7.45**	**Well Control**	Q_i = 0.4 mL/min	BHP = 14.696 psia	BHP = 14.696 psia	BHP = 14.696 psia
	Completion	Fully Completed	High Perm Layer Only	Med Perm Layer Only	Low Perm Layer Only
	Fluid	River Water	-	-	-

Table 4.7: Well Data for Simulation of CDG Experiment

Parameter (Unit)	Quantity	Comments	Experiment Stage
V_{DP}	0.2	Matched	*1: Waterflood*
α_L	0	Matched	*1: Waterflood*
α_T	0	Matched	*1: Waterflood*
k_{rw}^o	0.25	Matched	*1: Waterflood*
k_{ro}^o	0.35	Matched	*1: Waterflood*
n_w	5	Matched	*1: Waterflood*
n_o	2.5	Matched	*1: Waterflood*
Cumulative PV_1	1.13	Matched	*1: Waterflood*
S_P	0	Neglected Salinity Effect on μ	*2: Polymer Flood*
β_P	0	Neglected Divalent Cations	*2: Polymer Flood*
A_{P1}	520.8	Matched	*2: Polymer Flood*
A_{P2}	0	Matched	*2: Polymer Flood*
A_{P3}	0	Matched	*2: Polymer Flood*
$\gamma_{1/2}$	13.7	Matched	*2: Polymer Flood*
γ_c	3.97	From UTGEL Manual	*2: Polymer Flood*
P_α	1.6	Matched	*2: Polymer Flood*
a_{41}	1.153	Matched	*2: Polymer Flood*
a_{42}	0	Matched	*2: Polymer Flood*
b_4	100	Typical	*2: Polymer Flood*
b_{rk}	100	Typical	*2: Polymer Flood*
c_{rk}	0.32	Matched	*2: Polymer Flood*
R_{kmax}	10	Matched	*2: Polymer Flood*
PV_2	0.19	Given	*2: Polymer Flood*
Cumulative PV_3	5.26	Matched	*3: Waterflood*

Table 4.8a: Matched Parameters from Simulation of CDG Experiment

Parameter (Unit)	Quantity	Comments	Experiment Stage
[η]	2730.183	Matched	*4: CDG Flood*
K_H	1.0177	From UTGEL Manual	*4: CDG Flood*
a	0.004621	From UTGEL Manual	*4: CDG Flood*
b	996.9207	From UTGEL Manual	*4: CDG Flood*
n	0.859	From UTGEL Manual	*4: CDG Flood*
d	0.00047	From UTGEL Manual	*4: CDG Flood*
e	1.5804	From UTGEL Manual	*4: CDG Flood*
B	-0.06	From UTGEL Manual	*4: CDG Flood*
$\dot{\gamma}_c$	85.2	From UTGEL Manual	*4: CDG Flood*
μ	-0.18	Matched	*4: CDG Flood*
σ	2.44	Matched	*4: CDG Flood*
c	56.9	Matched	*4: CDG Flood*
f	-0.06	Matched	*4: CDG Flood*
R_{kcut}	200	Matched	*4: CDG Flood*
ADCDG	0.015302	Matched	*4: CDG Flood*
BDCDG	0.01293	Matched	*4: CDG Flood*
ADCDGILM	1.25	Matched	*4: CDG Flood*
TolCcdgRk	1d-1	Matched	*4: CDG Flood*
PV_4	0.19	Given	*4: CDG Flood*
Cumulative PV_5	7.45	Matched	*5: Waterflood*

Table 4.8b: Matched Parameters from Simulation of CDG Experiment

End of Flooding Stage	Water Cut (%)			Oil Recovery (%)			Volume Percent (%)		
	High	Med	Low	High	Med	Low	High	Med	Low
1: Waterflood	98.9	86.8	0.0	53.9	41.5	3.4	89.6	9.8	0.6
2: Polymer Flood	99.0	92.9	0.0	54.4	42.9	8.6	73.7	20.6	5.7
3: Waterflood	99.9	99.8	0.0	64.2	58.0	23.2	84.4	14.8	0.8
4: CDG Flood	99.9	99.7	0.0	64.3	58.1	30.9	67.5	24.2	8.3
5: Waterflood	99.9	99.0	95.5	65.9	60.2	48.4	69.5	22.1	8.3

Table 4.9a: Final Simulation Results Compared to Lu et al. (2000)'s Results

End of Flooding Stage	Cumulative PV	Water Cut (%)	Oil Recovery (%)	Inj. Pressure (atm)
1: Waterflood	1.13	96.8	35.4	1.04
2: Polymer Flood	1.32	93.3	37.5	1.51
3: Waterflood	5.26	97.8	50.5	1.13
4: CDG Flood	5.45	92.7	52.6	1.87
5: Waterflood	7.45	99.5	59.0	3.91

Table 4.9b: Final Simulation Results Compared to Lu et al. (2000)'s Results

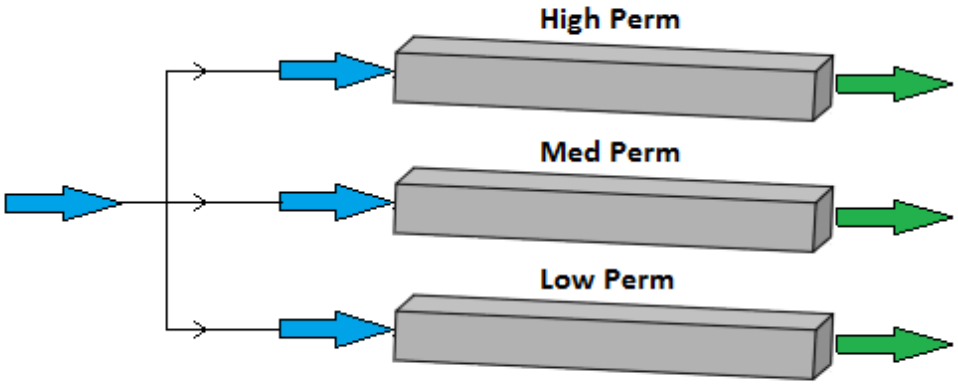

Figure 4.1: Simplified Schematic of Lu et al. (2000)'s Experimental Setup

Figure adapted from Smith et al. (2000).

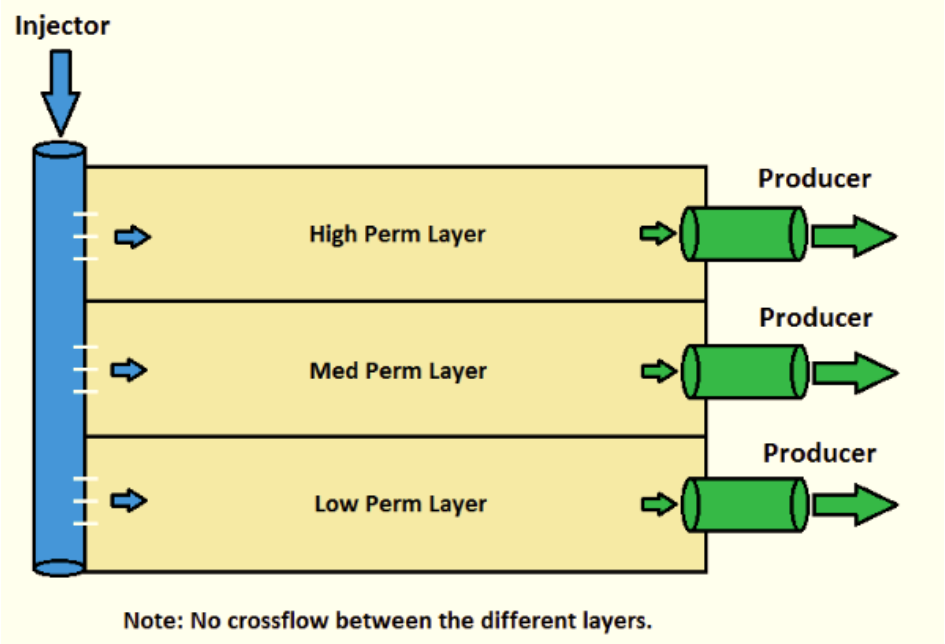

Figure 4.2: Illustration of Reservoir Model used for Matching Attempts

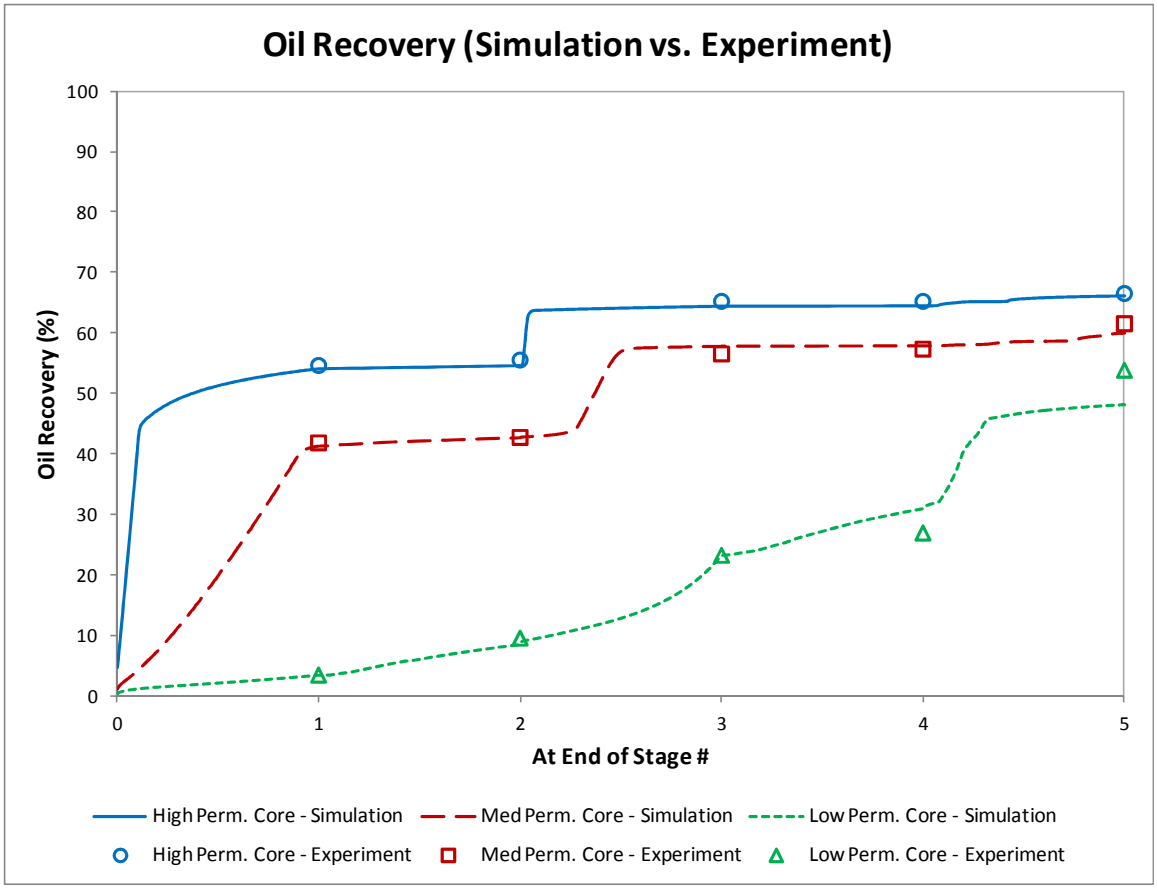

Figure 4.3: Illustration of CDG Experiment's Oil Recovery Match

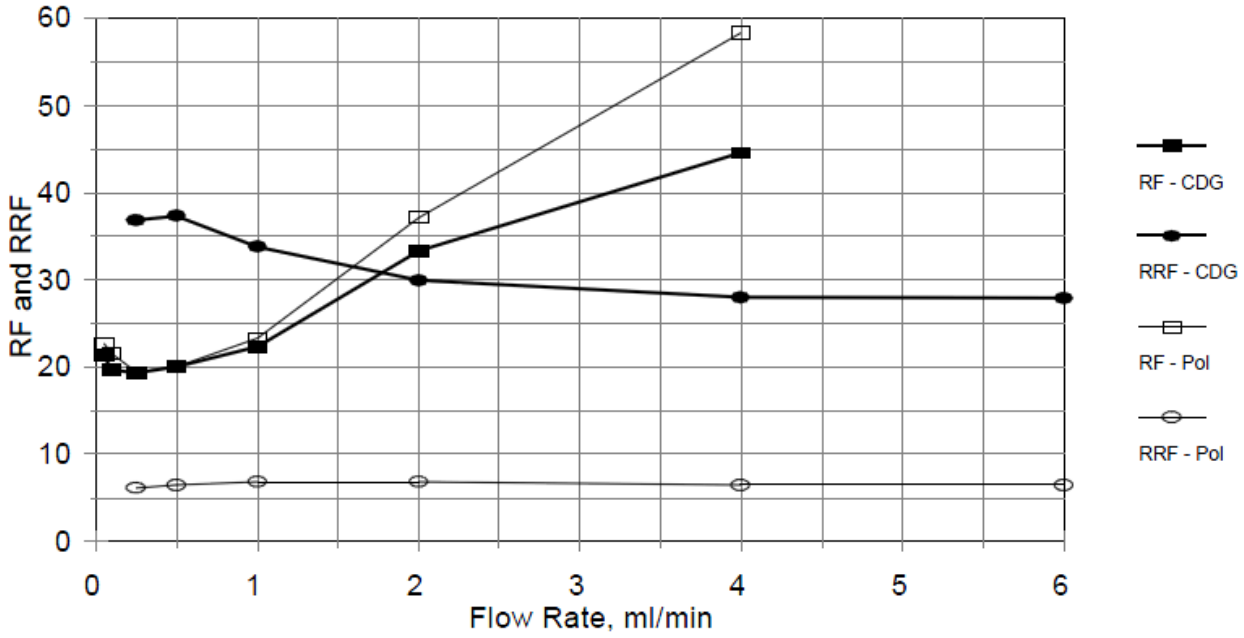

Figure 4.4: Smith et al. (2000)'s Comparison of RF and RRF

Figure taken from Smith et al. (2000).

Chapter 5: Synthetic Simulation Cases - Sensitivity Analysis

The objective of this chapter is to investigate the effect of certain key parameters on the effectiveness of a polymer microgel flood, and to compare the polymer microgel flood performance to a waterflooding base case and even a polymer flood. Such a sensitivity analysis is a vital means of determining when polymer microgel technology is an appropriate conformance control method to consider. The main variables studied in this chapter include:

1. Permeability contrast in a layered reservoir
2. Ratio of vertical to horizontal permeability, k_v/k_h
3. Concentration of polymer microgel injected

The first two points in the above list are variables that are unique to each reservoir, and that are beyond an engineer's control. They are highly relevant to such a sensitivity study, as they have a strong impact on the effectiveness of a conformance control attempt. The third point is one that an engineer is capable of controlling to optimize oil recovery. Altogether, these parameters were studied to determine what conditions are ideal for a polymer microgel flood, and what concentration of polymer microgel to inject so as to maximize oil recovery in an economic manner. It is important to note that the specific microgel investigated in this study was the Colloidal Dispersion Gel (CDG). CDGs were chosen over PPGs as, to date, UTGEL has a more complete model describing CDG behavior. Onbergenov (2012) performed similar investigations for Bright Water and pH-Sensitive polymer microgels.

Many synthetic simulation studies, similar to the one carried out in this chapter, already exist in the literature. Examples of such sensitivity analyses can be found in the

works of Bai et al. (2004c), Seright et al. (2011), Garmeh et al. (2011), as well as Izgec and Shook (2012). In each of these studies, polymer microgels were seen to improve oil recovery. However, not all studies deemed polymer microgels more effective than conventional polymer floods at improving ultimate oil recovery. Some common findings include that polymer microgels were most effective at increasing oil recovery whenever the reservoir was characterized by high permeability contrasts, and low k_v/k_h (Bai et al. 2004c; Seright et al. 2011; Garmeh et al. 2011). However, Izgec and Shook (2012) showed that k_v/k_h has a more complicated effect on oil recovery that depends on where the microgel bank is placed. Increased microgel concentration was shown to improve oil recovery (Garmeh et al. 2011); however, the economics would also need to be considered here. Izgec and Shook (2012)'s study demonstrated that it may be more beneficial to inject polymer microgel at lower concentrations but for longer periods of time (larger injection slugs). Ideally, the results of this chapter's sensitivity study would support these previous findings. However, as will soon be made clear, the results of this sensitivity study were highly dependent on the model incorporated in UTGEL. The model had to be reworked in order for the results to be more realistic. The results of several sensitivities, using several different models, are illustrated in this chapter. The most realistic sensitivity, and thus model, is highlighted at the end of the chapter when discussing the results.

5.1 SYNTHETIC SIMULATION BASE CASE SETUP

In order to carry out this chapter's sensitivity study, a three-dimensional synthetic field case was created. This synthetic case was designed so as to be a quarter of a five-spot pattern, containing an injector at one corner and a producer at the opposite corner. The reservoir model was set to possess two layers, a high permeability layer (thief zone) and a low permeability layer, both of equal thickness. For the sake of simplicity, each of

these layers was set to have constant permeability values, i.e. they were made homogeneous. A top- and side-profile of this reservoir model can be seen in Figures 5.1 and 5.2 respectively.

Since the experiment match in Chapter 4 was based on Lu et al. (2000)'s experiment carried out for the Daqing field in China, it was desirable to mimic Daqing's reservoir conditions as much as possible. As such, the base synthetic case's reservoir details are based on Lu et al. (2000)'s description of one of the reservoirs in Daqing field. More specifically, the reservoir is within Daqing field's Putaohua zone. The tabular description of the reservoir was also included in this chapter (Table 5.1) for reference. The reservoir characteristics that were incorporated in the synthetic base case include: well spacing (between producer and injector), average depth, average porosity, average water saturation, bottom hole temperature, original reservoir pressure, and oil viscosity. The average permeability was not considered since permeability contrast and k_v/k_h ratio were variables to be altered as part of the sensitivity analysis.

The base case reservoir parameters can be found in Table 5.2. As can be seen in this table, the base synthetic case has a permeability contrast of 10 (and k_v/k_h ratio of 0.1). As part of the subsequent sensitivity analyses, values smaller and larger than these were investigated in hopes of finding a trend. Table 5.3 displays the base case simulation parameters. It can be seen that the simulation is carried out until 2 pore volumes are flooded. It is also worth noting that two overlapping producers are included in the reservoir model; one that is completed in the high permeability layer, and one completed in the low permeability layer. This was done so that the production profile can be divided by layer for a more rigorous analysis. These two producers effectively act as one vertical producer completed throughout the reservoir thickness.

Table 5.4 describes the well data for the base synthetic case (waterflood). Note that the base case merely involves 2 pore volumes of waterflooding. Initially, the injectors were set to be pressure constrained. However, it was found that this made it difficult to compare the simulation results. This is because different subsequent sensitivity cases (with different permeabilities/microgel injection concentrations) yielded large injection rate differences, and so required very different time scales to complete 2 pore volumes of injection. Hence, injection was set to a constant rate instead, to allow easier comparison between different cases. This was similarly done in some previous sensitivity analyses, for example that carried out by Bai et al. (2004c). Note that the value specified for injection rate (Table 5.4) was chosen so that 1 pore volume of the entire reservoir was flooded in 1000 days, and so the entire simulation was 2000 days long. It can also be seen in Table 5.4 that the injector was fully completed throughout the thickness of the reservoir; this corresponds to bullhead injection, i.e. no zonal isolation. This yields more pessimistic results when polymer microgel flooding compared to zonal isolation with the treatment only in the high permeability layer.

Tables 5.5 and 5.6 describe the well data for a polymer flood and a CDG flood respectively. As can be seen, the well data is almost identical to that of the base synthetic waterflooding case. The only difference is that after 0.5 PV of waterflooding, 0.1 PV of polymer or CDG solution is flooded. This is then followed by a waterflooding flush for the remainder of the total 2 PV injected. Note that 0.1 PV polymer or CDG solution injected corresponds to 0.2 PV of the high-permeability layer. At this point the sensitivity analysis methodology should be clear. Tables 5.4, 5.5, and 5.6 describe the well data for a waterflood case, a polymer flood case, and a CDG flood case respectively. These cases are compared at varying permeability contrasts, k_v/k_h ratios, and CDG injection concentrations. Note that permeability contrast is controlled by changing the permeability

of the high-permeability layer/thief zone only. The ratio of k_v/k_h is controlled by changing the vertical permeability only. The results of the sensitivity analyses are discussed in the following sections.

5.2 SENSITIVITY ANALYSIS #1

This section reports the results of the first CDG sensitivity analysis conducted. The key characteristic that distinguishes this sensitivity analysis from the subsequent one is that the relative permeability, polymer, and microgel parameters here were all taken as exactly the same as those determined in Chapter 4 for the match of the CDG experiment. Essentially, the reason for doing this was so that the sensitivity analysis would be representative for the polymer and CDG used at Daqing. This is also why there was an attempt to mimic Daqing's reservoir characteristics. Tables 4.8a and 4.8b highlight the matched parameters from Chapter 4, and thus the parameters that were used in this sensitivity analysis. The polymer and CDG parameters are exactly the same. However, V_{DP} is set to zero here (homogeneous). In addition, dispersivities are no longer zero here; this is because dispersivities are generally set to 10% of the grid-block size, and the grid-blocks are much larger here. Also, the pore volumes injected in Tables 4.8a and 4.8b should be ignored as they are unique to that particular experiment. Appendix B can be referred to for the Input File that represents the base case (waterflood) of Sensitivity Analysis #1. The sensitivity cases all required simple alterations of this base case Input File.

Ultimately, when analyzing the results of this sensitivity study, it was found that the results were unrealistic. There was good reason for why this was the case, and it will be discussed below. However, this requires an understanding of the CDG permeability reduction model utilized by UTGEL. This is briefly outlined now.

As discussed in Chapter 4, the CDG permeability reduction model incorporated into UTGEL includes two distinct parts, one to account for short-term permeability reductions and another for long-term reductions. Long-term permeability reduction capabilities were added to UTGEL so as to enable a successful match of the CDG experiment outlined in the previous chapter.

The short-term and long-term permeability reductions are computed using two different equations. The short-term permeability reduction equation takes the following form:

$$R_k = 1.5 + \left[\frac{c}{(JR-1)*\sqrt{2*\pi*\sigma^2}} * \exp\left(-\frac{(ln(JR-1)-\mu)^2}{2*\sigma^2}\right)\right]^f, \quad \text{(Eqn. 5.1)}$$

where c, σ, μ, and f are input parameters that can be attained from matching experiments. In this particular sensitivity study, the input parameters obtained from the previous experiment match (Chapter 4) were used. The JR in Eqn. 5.1 above refers to the jamming ratio, and is represented by the following equation:

$$JR = \frac{2*r_h}{\epsilon_h} = \frac{2*\left(1.15*\sqrt{8*\bar{k}*\phi^{-1}}\right)}{\left(d*C_{m,fluid}+e\right)*\left(\dot{\gamma_{eq}}\right)^B}, \quad \text{(Eqn. 5.2)}$$

where r_h represents the pore throat radius, and ϵ_h represents the CDG adsorbed layer thickness. Notice that the jamming ratio is a function of average permeability $(\bar{k})$, porosity (ϕ), microgel concentration in the fluid $\left(C_{m,fluid}\right)$, and equivalent shear rate $\left(\dot{\gamma_{eq}}\right)$. The other variables ($d$, e, and B) are input parameters also obtained from the experiment match in Chapter 4. The UTGEL Technical manual can be referred to for more specifics regarding this model.

The important aspect of the short-term permeability reduction equation (Eqn. 5.1) is that it is a function of microgel *fluid* concentration, and is independent of microgel *adsorbed* concentration. As a result, it does not yield a long-term permeability reduction by itself. Instead, there will be no permeability reduction as soon as the CDG in the fluid is produced. This is the motivation for the second, long-term permeability reduction equation that was incorporated into UTGEL. Recall that this additional equation makes use of a Langmuir-type adsorption curve. The long-term permeability reduction equation is expressed as follows:

$$R_k = 1 + \left(R_{k,cut} - 1\right) * \frac{C_{m,ads}}{C_{m,ads,max}}, \qquad \text{(Eqn. 5.3)}$$

where $R_{k,cut}$ and $C_{m,ads,max}$ are input parameters obtained from the experiment match carried out in the previous chapter (R_{kcut} and ADCDGILM respectively). $C_{m,ads}$ is the concentration of CDG adsorbed to the rock surface, and is determined using the following equation:

$$C_{m,ads} = \min\left(C_{m,fluid}, \frac{a_1 * (C_{m,fluid} - C_{m,ads})}{1 + b_1 * (C_{m,fluid} - C_{m,ads})}\right), \qquad \text{(Eqn. 5.4)}$$

where a_1 and b_1 are input parameters determined from the experiment match carried out in the previous chapter (ADCDG and BDCDG respectively). Eqns. 5.3 and 5.4 are not unique to UTGEL; Garmeh et al. (2011) and Izgec and Shook (2012) also made use of such a permeability reduction model for their respective sensitivity studies. Note that it is the fact that Eqn. 5.3 is a function of *adsorbed* CDG concentration that renders it capable of modeling *long-term* permeability reduction. UTGEL switches from short-term

permeability reduction (Eqn. 5.1) to long-term permeability reduction (Eqn. 5.3) when the concentration of CDG in fluid ($C_{m,fluid}$) is below a certain concentration tolerance. This tolerance was also determined in Chapter 4's experiment match. Note that this concentration tolerance used to be hard-wired into UTGEL, but was made an input parameter during Chapter 4's experiment match instead (for greater control).

The reason this sensitivity analysis yielded unreasonable results relates to the differences between permeability reductions computed in the short-term and in the long-term. In Chapter 4's matched experiment, the long-term permeability reduction (post-CDG flood) was much larger than the short-term permeability reduction (during the CDG flood). This is similar to saying that RRF was greater than RF. As can be seen in Figure 4.4, this is reasonable in a lab setting where low flow rates are typical. However, on a field scale, where flow rates are higher, this is not realistic. RRF should be lower than RF in such cases. However, since the parameters for CDG were taken from Chapter 4, this was not the case here. As such, the results of this sensitivity are unrealistic. With this in mind, the results of this analysis will still be presented, but should not be given too much attention. In light of this problem, some of the CDG parameters were altered and the CDG permeability reduction model was also reworked. A second sensitivity analysis was subsequently conducted. The reader may skip to Section 5.3 (Sensitivity Analysis #2) for results that are more reliable and representative.

5.2.1 Permeability Contrast Study

First, the permeability contrast was investigated. Permeability contrast was varied simply by changing the permeability of the higher permeability upper layer. The base case permeability contrast was 10:1. Simulations were run with permeability contrasts of 5:1 and 15:1 as well. In order to analyze the effect of permeability contrast on

incremental oil recovery, simulations were run with and without CDG use. This resulted in six total simulations run, for this particular study.

Figure 5.3 shows the oil recovery profiles of these six simulations. The first noticeable trend in this graph is that for the cases without CDG use, decreased permeability contrasts yielded more oil recovery. For these waterflooding cases, this is to be expected. The reason for this is that decreased permeability contrast results in a more even sweep of the two layers, and thus improved oil recovery. Looking at the oil recovery profiles of the cases with CDG use, also on Figure 5.3, it can be seen that CDG improved oil recovery for all different permeability contrasts investigated. However, it was seen that decreasing permeability contrast yielded greater *incremental* oil recoveries. Incremental oil recovery is the oil recovered due to CDG over the waterflooding case with the same permeability contrast. Table 5.7 can be referred to for an easier comparison of the incremental oil recoveries.

It is important to note that the above trend of greater incremental oil recovery with decreasing permeability contrast is the opposite of the expected result from previous sensitivity studies. This helped with the realization of the problem discussed earlier.

5.2.2 Vertical to Horizontal Permeability Ratio Study

Next, the vertical to horizontal permeability ratio was investigated. This variable was varied simply by changing the vertical permeability of both layers. The base case k_v/k_h ratio was 0.1. Simulations were run with k_v/k_h ratios of 0.02 and 0.2 as well. In order to analyze the effect of k_v/k_h ratio on *incremental oil recovery*, simulations were run with and without CDG use. This resulted in six total simulations run, for this particular study.

Figure 5.4 shows the oil recovery profiles of these six simulations. The first noticeable trend in this graph is that for the cases without CDG use, increased k_v/k_h ratio

yielded more oil recovery. For these waterflooding cases, the reason for this is that increased vertical permeability leads to more of the denser flooding water phase migrating down to the deeper lower permeability layer. This results in a modestly improved sweep of the two layers, and thus improved oil recovery. This trend may be reversed had the higher permeability layer been on the bottom. Looking at the oil recovery profiles of the cases with CDG use, also on Figure 5.4, it can be seen that CDG improved oil recovery for all different k_v/k_h ratios investigated. However, it was seen that decreasing k_v/k_h ratios yielded greater *incremental* oil recoveries over the respective waterflooding cases. Table 5.8 can be referred to for an easier comparison of the incremental oil recoveries.

The above trend of greater incremental oil recovery with decreasing k_v/k_h ratio is reasonable. Izgec and Shook (2012) claimed that low k_v/k_h ratios are ideal if the microgel is activated near the injector, which is what was seen here. However, this was the only studied variable within this particular sensitivity analysis that yielded realistic results. Upon reworking of the permeability reduction model (in Sensitivity Analysis #2), all the studied variables yielded reasonable results.

5.2.3 Microgel Injection Concentration Study

Lastly, the concentration of injected microgel solution was investigated. Simulations were run with injected microgel concentrations of 200, 500, 800, 1100, and 1400 ppm. In order to analyze the effect of injected microgel concentration on *incremental oil recovery*, a simulation was run without CDG use as well. The base waterflooding case for this particular study is the same for each varied microgel concentration case. This resulted in six total simulations run, for this particular study.

All CDG concentrations yielded incremental oil recovery over the base waterflood case. In this particular sensitivity analysis, however, microgel concentration

yielded almost no impact on the *magnitude* of incremental oil recovery. This result is unreasonable, and this was one of the indicators that a second sensitivity analysis had to be conducted. Increasing CDG concentration should yield larger values of incremental oil recovery. The reworking of the permeability reduction model and the changes in CDG input parameters are addressed in more detail in the following section.

5.3 SENSITIVITY ANALYSIS #2

This section reports the results of the second CDG sensitivity analysis conducted. This sensitivity analysis was conducted after realizing that the first sensitivity analysis had a number of faults, as previously discussed. This sensitivity analysis is similar to the subsequent one in that the relative permeability and polymer parameters are exactly the same. As such, they are the same as those determined in Chapter 4 as part of the CDG experiment match. The base case reservoir and simulation setups are also the same (Tables 5.2 and 5.3). However, the two major differences are that the permeability reduction model was reworked, and that the CDG parameters had to be altered slightly.

In light of the problem discussed earlier, the CDG permeability reduction model was reworked. The new model still makes use of two permeability reduction equations, one for short-term effects and another for long-term effects. However, the long-term permeability reduction equation was modified. Long-term permeability reduction was made to be a factor of the short-term permeability reduction, ensuring it is always lower than RF. The modified *long-term* permeability reduction equation is expressed below:

$$R_k = R_{k,factor} * R_{k,max,gridblock}\ , \qquad \text{(Eqn. 5.5)}$$

where $R_{k,factor}$ is a factor set as an input parameter and $R_{k,max,gridblock}$ is the maximum permeability reduction that is calculated in a particular grid-block. As was the case with

the previous model, the long-term permeability reduction equation is still activated when the fluid concentration of CDG is less than a specified tolerance value. The modified long-term permeability reduction equation guarantees that RRF is lower than RF (as long as $R_{k,factor}$ is set to a value less than one) so that field-scale simulations possess more realistic results. To reiterate, this was important as the model prior to this modified one yielded unrealistic results when conducting Sensitivity Analysis #1.

Some of the CDG input parameters also were changed from those determined in the last chapter's CDG experiment match. CDG input matching parameters that are used to determine solution viscosity and jamming ratio were kept the same. The only parameters that were changed were the input matching parameters used to compute short-term permeability reduction (c, σ, μ, and f). These input parameters were altered so as to moderately increase the short-term permeability reduction values. This is because the short-term permeability reduction values attained in the experiment match were lower than the typical values witnessed throughout literature on CDGs. By making this change, the results of this sensitivity analysis are no longer perfectly representative of the CDGs used for Daqing's lab and field implementations, but the results may be more broadly applicable to CDG treatments. Tables 5.9a and 5.9b can be referred to for the set of simulation parameters used for all the cases of this sensitivity analysis (Sensitivity Analysis #2). Appendix C can be referred to for the Input File that represents the base case (waterflood) of Sensitivity Analysis #2. The only changes over the Input File in Appendix B can be found in the section of CDG input parameters. The sensitivity cases all required simple alterations of this base case Input File in Appendix C.

Ultimately, the results of this sensitivity study were realistic. The findings were also in agreement with findings from the literature, as will be discussed in more detail below.

5.3.1 Permeability Contrast Study

First, the permeability contrast was investigated. Permeability contrast was varied simply by changing the permeability of the higher permeability upper layer. The base case permeability contrast was 10:1. Simulations were run with permeability contrasts of 5:1 and 15:1 as well. In order to analyze the effect of permeability contrast on *incremental oil recovery*, simulations were run with and without CDG use. This resulted in six total simulations run, for this particular study.

Figure 5.5 shows the oil recovery profiles of these six simulations. The first noticeable trend in this graph is that for the cases without CDG use, decreased permeability contrasts yielded more oil recovery. For these waterflooding cases, this is to be expected. The reason for this is that decreased permeability contrast results in a more even sweep of the two layers, and thus improved oil recovery. Looking at the oil recovery profiles of the cases with CDG use, also on Figure 5.5, it can be seen that CDG improved oil recovery for all different permeability contrasts investigated. In addition, it was seen that increasing permeability contrast yielded greater *incremental* oil recoveries. Incremental oil recovery is the oil recovered due to CDG over the waterflooding case with the same permeability contrast. Table 5.10 can be referred to for an easier comparison of the incremental oil recoveries.

The above trend of greater incremental oil recovery with increasing permeability contrast is the result that was expected, due to the results of previous sensitivity studies (such as Garmeh et al. 2011 as well as Izgec and Shook 2012). There are a couple of different explanations for this trend. One explanation is that cases of greater permeability contrast have poorer sweep efficiency to start with, and so conformance control agents like CDGs have greater potential to improve oil recovery. Another plausible explanation

is that higher permeability contrasts induce a greater concentration of CDGs to penetrate the high permeability layer, and this thief layer is plugged more effectively.

5.3.2 Vertical to Horizontal Permeability Ratio Study

Next, the vertical to horizontal permeability ratio was investigated. This variable was varied simply by changing the vertical permeability of both layers. The base case k_v/k_h ratio was 0.1. Simulations were run with k_v/k_h ratios of 0.02 and 0.2 as well. In order to analyze the effect of k_v/k_h ratio on *incremental oil recovery*, simulations were run with and without CDG use. This resulted in six total simulations run, for this particular study.

Figure 5.6 shows the oil recovery profiles of these six simulations. The first noticeable trend in this graph is that for the cases without CDG use, increased k_v/k_h ratio yielded more oil recovery. For these waterflooding cases, the reason for this is that increased vertical permeability leads to more of the denser flooding water phase migrating down to the deeper lower permeability layer. This results in a modestly improved sweep of the two layers, and thus improved oil recovery. This trend may be reversed had the higher permeability layer been on the bottom. Looking at the oil recovery profiles of the cases with CDG use, also on Figure 5.6, it can be seen that CDG improved oil recovery for all different k_v/k_h ratios investigated. However, it was seen that decreasing k_v/k_h ratios yielded greater *incremental* oil recoveries over the respective waterflooding cases. Table 5.11 can be referred to for an easier comparison of the incremental oil recoveries.

The above trend of greater incremental oil recovery with decreasing k_v/k_h ratio is reasonable, and is a common finding in the literature (Bai et al. 2004c; Garmeh et al. 2011). Izgec and Shook (2012) also claimed that low k_v/k_h ratios are ideal if the microgel is activated near the injector, which is what was seen here (microgel is activated

throughout the thief zone, starting near the injector). One reason for this witnessed trend is that decreased k_v/k_h ratios make it less likely that CDG can cross into the lower permeability layer and induce damage therein. Another reason could be that low k_v/k_h ratios make it less likely that the injected water can cross back into the thief zone after CDGs served their diversion purpose.

5.3.3 Microgel Injection Concentration Study

Lastly, the concentration of injected microgel solution was investigated. Simulations were run with injected microgel concentrations of 400, 800, and 1200 ppm. In order to analyze the effect of injected microgel concentration on *incremental oil recovery*, a simulation was run without CDG use as well. The base waterflooding case for this particular study is the same for each varied microgel concentration case. This resulted in four total simulations run, for this particular study.

Figure 5.7 shows the oil recovery profiles of these four simulations. It can very easily be seen that increased CDG concentrations yield greater *incremental* oil recoveries over the waterflooding base case. This trend is reasonable and was to be expected. Table 5.12 can be referred to for an easier comparison of the incremental oil recoveries. It is interesting to note that although CDGs yield significant incremental oil recoveries, the CDG concentration has a relatively mild effect on the *magnitude* of this incremental recovery.

5.4 DISCUSSION

This chapter served as a means of gaining insight on the effect of certain key variables on the effectiveness of a polymer microgel flood. Namely, the key variables included: permeability contrast between a thief zone and the adjacent layer, vertical to horizontal permeability ratio, and injected microgel concentration. Again, of the two

sensitivity analyses conducted, Sensitivity Analysis #2 yielded the realistic and representative results. The main reason for Sensitivity Analysis #1's failure to achieve reasonable results involves the long-term permeability reductions computed for that particular analysis, as previously discussed.

Sensitivity Analysis #2 enables us to draw some important conclusions and points of discussion:

- Increased permeability contrast enables CDG treatments to achieve greater *incremental* oil recoveries over waterfloods.
- Decreased k_v/k_h ratio enables CDG treatments to achieve greater *incremental* oil recoveries over waterfloods.
- Increased CDG concentrations enable CDG treatments to achieve greater *incremental* oil recoveries over waterfloods.
- Permeability contrast is the most important factor, of those studied, as it most significantly determines the effectiveness of a CDG treatment.
- Of the variables studied, CDG concentration has the smallest effect on the effectiveness of a CDG treatment, i.e. it has the least impact on the magnitude of *incremental* oil recovery. This conclusion is supported by Izgec and Shook (2012)'s claim that it is a variable of "secondary importance".

The above results are in agreement with the findings in the literature (Bai et al. 2004c; Garmeh et al. 2011; Seright et al. 2011; Izgec and Shook 2012). This further supports the above conclusions, and also supports UTGEL's CDG modeling capabilities. It is important to note that the above findings for CDGs likely extend to polymer microgels of other types as well (such as PPGs and BrightWater). This is because these

other microgel types are similar conformance control agents. Though similar sensitivity analyses for these other types may be warranted, the conclusions will likely be the same.

It is important to illustrate that polymer microgels have added potential over the use of polymer floods. Figure 5.8 compares the oil recovery profile of an 800ppm CDG flood to an 800ppm polymer flood, with a permeability contrast of 10:1 and a k_v/k_h ratio of 0.1. The reservoir and simulation parameters were identical to those used for the simulations in Sensitivity Analysis #2. As can be seen in Figure 5.8, both polymer and CDG floods improve oil recovery over a waterflood. The CDG flood under these conditions did yield more oil recovery than the polymer flood, yet this was only by 1% of the original oil in place. However, when a similar comparison was conducted with a permeability contrast of 15:1 and a k_v/k_h ratio of 0.02, the CDG flood recovered almost 5% more of the original oil in place than the polymer flood. Figure 5.9 can be referred to for a graphical representation of this finding. This demonstrates a case where CDG is substantially more effective at improving sweep efficiency than polymer flooding. As discussed in Chapter 3, and as shown above, large permeability contrasts render conformance control agents (like microgels) more capable of improving sweep than mobility control agents (like polymer). Utilizing zonal isolation to focus CDG penetration solely to the high permeability layer could have improved sweep, and thus oil recovery, to an even greater extent.

It is important to discuss the different potential ways of modeling permeability reduction induced by CDGs. Prior to the work reported in this thesis, UTGEL's CDG model only considered short-term permeability reduction. During the CDG experiment matching attempts, a long-term permeability reduction equation was added to the model. This equation is Eqn. 5.3 shown earlier. Based on the work in this chapter, and the

realization that long-term permeability reduction should be smaller than short-term permeability reduction at a field-scale, this equation was replaced by Eqn. 5.5.

There are a number of other possible means of modeling long-term permeability reduction induced by CDGs. Some potential long-term permeability reduction equations include:

$$R_k = R_{k,factor} * R_{k,max,gridblock} * \frac{C_{m,ads}}{C_{m,ads,max}} \text{ ,} \qquad \text{(Eqn. 5.6)}$$

$$R_k = 1 + \left(R_{k,factor} * R_{k,max,gridblock} - 1\right) * \left(\frac{C_{m,ads}}{C_{m,ads,max}}\right). \qquad \text{(Eqn. 5.7)}$$

The above two equations have the advantage that they are functions of adsorbed CDG concentrations, and are not simply factors of the maximum gridblock permeability reduction. Another potential equation that ensures that long-term permeability reduction is a function of adsorbed CDG concentration can be developed by simply replacing $C_{m,fluid}$ in Eqn. 5.2 with $C_{m,total}$. This also yields the advantage that only one equation for permeability reduction (Eqn. 5.1) is needed for both short-term and long-term effects.

It is important that the chosen equation can yield a long-term permeability reduction that is either smaller or greater than short-term permeability reduction, for field or lab applications respectively. This enables it to be used regardless of the scale of the simulation. The current long-term permeability reduction equation, that which was used in Sensitivity Analysis #2 (Eqn. 5.5), allows for this possibility. $R_{k,factor}$ can simply be set to be greater than one if the long-term permeability reduction is expected to be greater than short-term reduction, as may be the case in a lab experiment.

As it can be seen, there are numerous options for modeling CDG long-term permeability reduction. Additional studies are necessary to determine the optimal equation for UTGEL.

General		Average porosity	23%
Discovery date	1959	Average water saturation	25%
Producing formation	P_I 1-4	Bottom hole temperature	45℃
Reservoir type	Un-saturated	Original reservoir pressure	13Mpa
Average depth	1100m	Fluid Properties	
Primary producing mechanism	Expansion	Bubble point	12Mpa
Well space	250m	Formation volume factor	1.05
Formation Data		Oil viscosity at BHT	9.3mpa.s
Lithology	Sandstone	Oil specific gravity in surface	0.897
Permeability range	196md to 736md	Recovery Data	
Average permeability	387md	Original oil in place	1000×10^4 tons
Permeability variation(D-P)	0.70	Original oil recovery	35%

Table 5.1: Daqing Oil Field Putaohua Zone - Reservoir Characteristics

Table from Lu et al. (2000).

Reservoir Property	Unit	Quantity	Comments
Reservoir Length	ft	580	
Reservoir Width	ft	580	
Reservoir Thickness	ft	20	
Depth of Top Layer	ft	3600	
Initial Reservoir Pressure	psia	1885	*Throughout Reservoir*
Oil Viscosity	cp	9.0	*Constant*
Water Viscosity	cp	0.60	*Constant*
Endpoint Mobility Ratio	-	10.7	*From Match*
Initial [Cl^-]	meq/ml H_20	0.05184	
Initial [Ca^{2+}]	meq/ml H_20	0.00080	
		Layer 1	**Layer 2**	
Thickness	ft	10	10	
X-Permeability	mD	1000	100	*Perm. Contrast ≈ 10*
Y-Permeability	mD	1000	100	*Perm. Contrast ≈ 10*
Z-Permeability	mD	100	10	*Kv/Kh = 0.1*
Porosity	%	23.0	23.0	
Initial Oil Saturation	%	75.0	75.0	
Residual Oil Saturation	%	25.0	25.0	
Residual Water Saturation	%	25.0	25.0	

Table 5.2: Reservoir Data for CDG Synthetic Study - Base Case

Number of Grid-blocks (in x, y, z Directions)	20 x 20 x 2	*Variable Grid Size*
Coordinate System	Cartesian	
Temperature Variation	Not Considered	*Isothermal*
Simulation Time (PV)	2.0	
Number of Wells	3	*1 Injector & 2 Producers*

Table 5.3: Simulation Data for CDG Synthetic Study - Base Case

Cumulative Time (PV)		Injector	Producer (High Perm)	Producer (Low Perm)
1: Waterflood **2.00**	**Well Control**	Q_i = 1547.44 ft^3/day	BHP = 1885 psia	BHP = 1885 psia
	Completion	Fully Completed	High Perm Layer Only	Low Perm Layer Only
	Fluid	River Water	-	-

Table 5.4: Well Data for CDG Synthetic Study - Base Case (Waterflood)

Cumulative Time (PV)		Injector	Producer (High Perm)	Producer (Low Perm)
1: Waterflood **0.50**	**Well Control**	Q_i = 1547.44 ft^3/day	BHP = 1885 psia	BHP = 1885 psia
	Completion	Fully Completed	High Perm Layer Only	Low Perm Layer Only
	Fluid	River Water	-	-
2: Polymer Flood **0.60**	**Well Control**	Q_i = 1547.44 ft^3/day	BHP = 1885 psia	BHP = 1885 psia
	Completion	Fully Completed	High Perm Layer Only	Low Perm Layer Only
	Fluid	River Water, 800 ppm Polymer	-	-
3: Waterflood **2.00**	**Well Control**	Q_i = 1547.44 ft^3/day	BHP = 1885 psia	BHP = 1885 psia
	Completion	Fully Completed	High Perm Layer Only	Low Perm Layer Only
	Fluid	River Water	-	-

Table 5.5: Well Data for CDG Synthetic Study - Polymer Flood

Cumulative Time (PV)		Injector	Producer (High Perm)	Producer (Low Perm)
1: Waterflood **0.50**	**Well Control**	Q_i = 1547.44 ft^3/day	BHP = 1885 psia	BHP = 1885 psia
	Completion	Fully Completed	High Perm Layer Only	Low Perm Layer Only
	Fluid	River Water	-	-
2: CDG Flood **0.60**	**Well Control**	Q_i = 1547.44 ft^3/day	BHP = 1885 psia	BHP = 1885 psia
	Completion	Fully Completed	High Perm Layer Only	Low Perm Layer Only
	Fluid	Produced Water, 800 ppm CDG	-	-
3: Waterflood **2.00**	**Well Control**	Q_i = 1547.44 ft^3/day	BHP = 1885 psia	BHP = 1885 psia
	Completion	Fully Completed	High Perm Layer Only	Low Perm Layer Only
	Fluid	River Water	-	-

Table 5.6: Well Data for CDG Synthetic Study - CDG Flood

Permeability Contrast	Incremental Oil Recovered (BBLS)	Incremental Oil Recovered (% OOIP)
5:1	15,980	7.7
10:1	8,910	4.3
15:1	6,640	3.2

Table 5.7: Perm. Contrast Effect on CDG Incremental Oil Recovery, #1

K_v/K_h Ratio	Incremental Oil Recovered (BBLS)	Incremental Oil Recovered (% OOIP)
0.02	11,030	5.3
0.1	8,940	4.3
0.2	8,840	4.2

Table 5.8: k_v/k_h Ratio Effect on CDG Incremental Oil Recovery, #1

Parameter (Unit)	Quantity	Comments
V_{DP}	0	Set
α_L (ft)	2.9	10% GB Dimension
α_T (ft)	2.9	10% GB Dimension
k_{rw}^{o}	0.25	From Match
k_{ro}^{o}	0.35	From Match
n_w	5	From Match
n_o	2.5	From Match
S_P	0	From Match
β_P	0	From Match
A_{P1}	520.8	From Match
A_{P2}	0	From Match
A_{P3}	0	From Match
$\gamma_{1/2}$	13.7	From Match
γ_c	3.97	From UTGEL Manual
P_α	1.6	From Match
a_{41}	1.153	From Match
a_{42}	0	From Match
b_4	100	Typical
b_{rk}	100	Typical
c_{rk}	0.32	From Match
R_{kmax}	10	From Match

Table 5.9a: Simulation Parameters for CDG Sensitivity Analysis #2

Parameter (Unit)	Quantity	Comments
[η]	2730.183	From Match
K_H	1.0177	From UTGEL Manual
a	0.004621	From UTGEL Manual
b	996.9207	From UTGEL Manual
n	0.859	From UTGEL Manual
d	0.00047	From UTGEL Manual
e	1.5804	From UTGEL Manual
B	-0.06	From UTGEL Manual
$\dot{\gamma}_c$	85.2	From UTGEL Manual
μ	-0.52	Set
σ	2.30	Set
c	56.89	Set
f	-2.06	Set
R_{kcut}	200	From Match
ADCDG	0.015302	No Longer Relevant*
BDCDG	0.01293	No Longer Relevant*
ResRkFact	0.80	Set
TolCcdgRk	1d-1	From Match

Table 5.9b: Simulation Parameters for CDG Sensitivity Analysis #2

*These variables were rendered “no longer relevant” as they ceased to have any effect on CDG permeability reduction, as a result of editing UTGEL’s model.

Permeability Contrast	Incremental Oil Recovered (BBLS)	Incremental Oil Recovered (% OOIP)
5:1	18,700	9.0
10:1	29,160	14.1
15:1	34,860	16.9

Table 5.10: Perm. Contrast Effect on CDG Incremental Oil Recovery, #2

K_v/K_h Ratio	Incremental Oil Recovered (BBLS)	Incremental Oil Recovered (% OOIP)
0.02	36,040	17.4
0.1	29,160	14.1
0.2	24,170	11.7

Table 5.11: k_v/k_h Ratio Effect on CDG Incremental Oil Recovery, #2

CDG Conc. (ppm)	Incremental Oil Recovered (BBLS)	Incremental Oil Recovered (% OOIP)
400	28,080	13.6
800	29,120	14.1
1200	31,630	15.3

Table 5.12: CDG Concentration Effect on Incremental Oil Recovery, #2

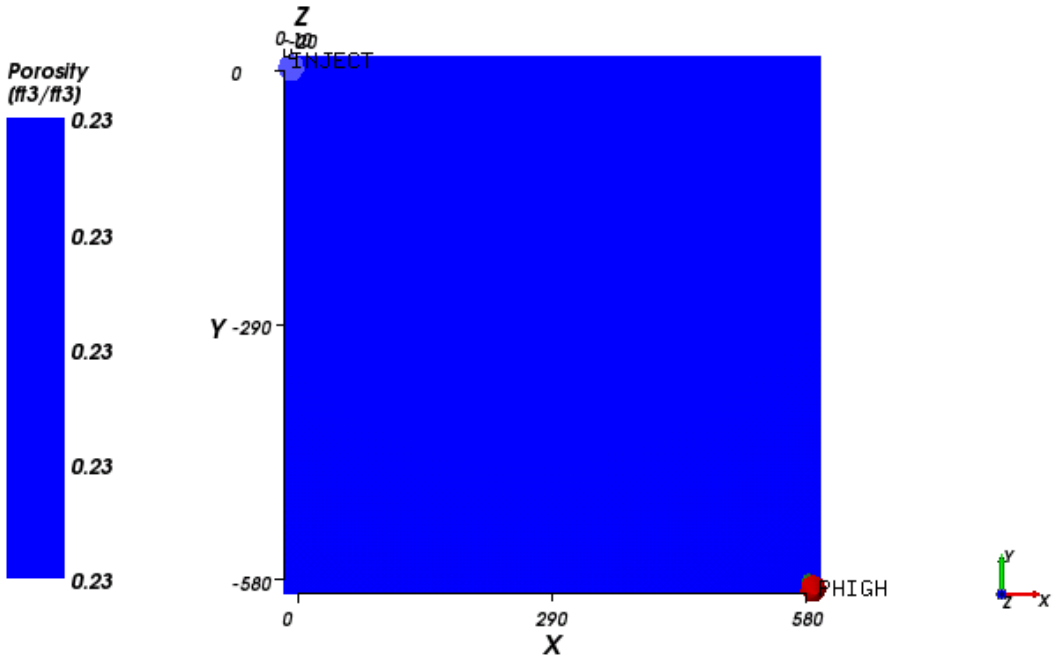

Figure 5.1: Top View of CDG Synthetic Study's Base Case Reservoir Model

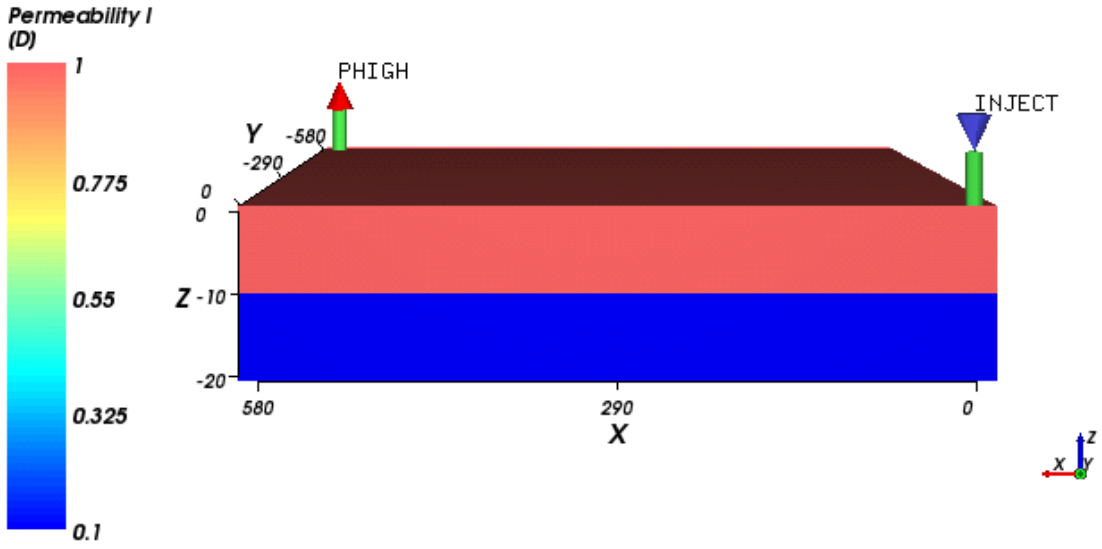

Figure 5.2: Side View of CDG Synthetic Study's Base Case Reservoir Model

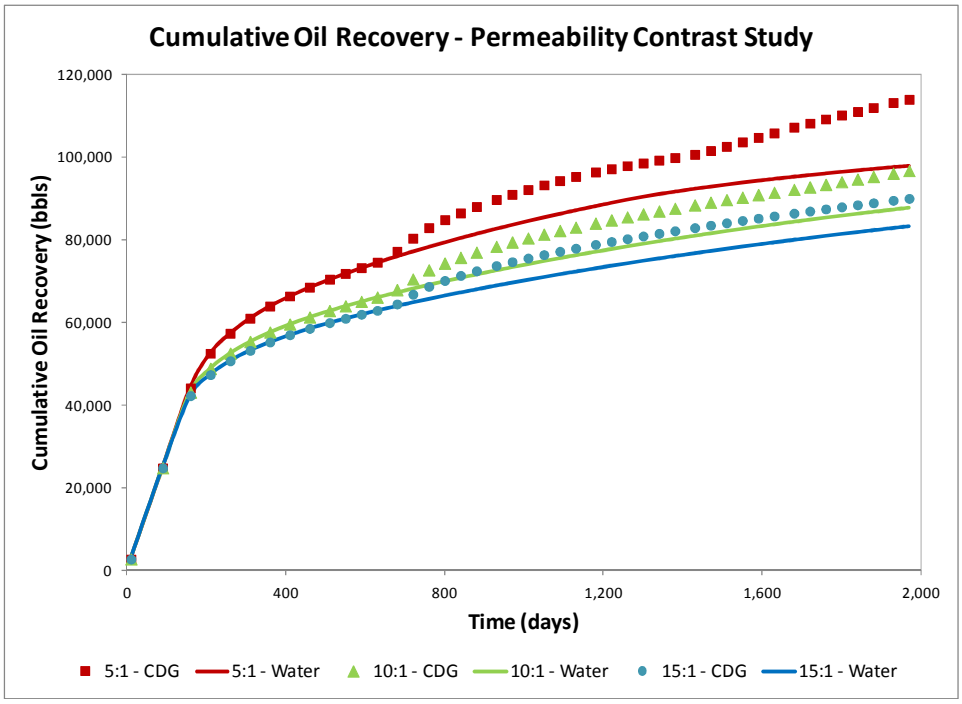

Figure 5.3: Perm. Contrast Effect on CDG Incremental Oil Recovery, #1

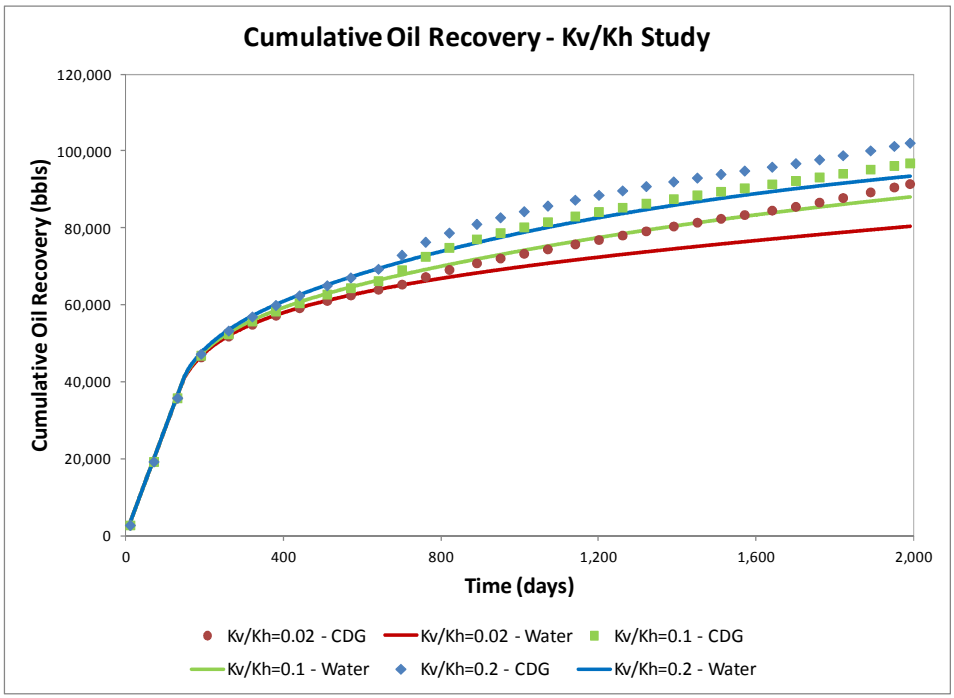

Figure 5.4: k_v/k_h Ratio Effect on CDG Incremental Oil Recovery, #1

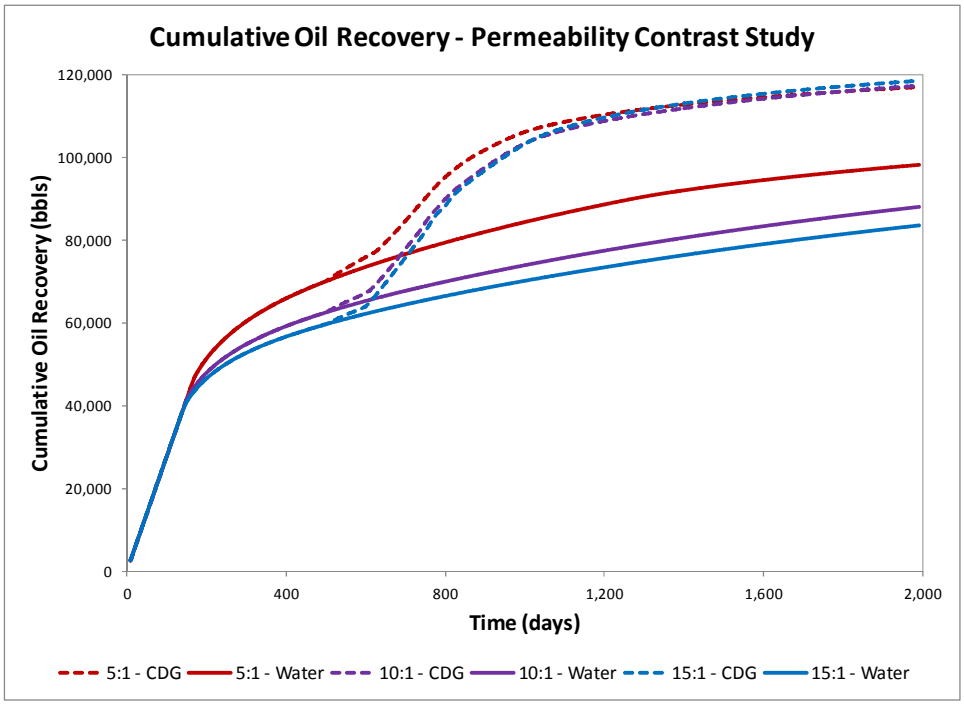

Figure 5.5: Perm. Contrast Effect on CDG Incremental Oil Recovery, #2

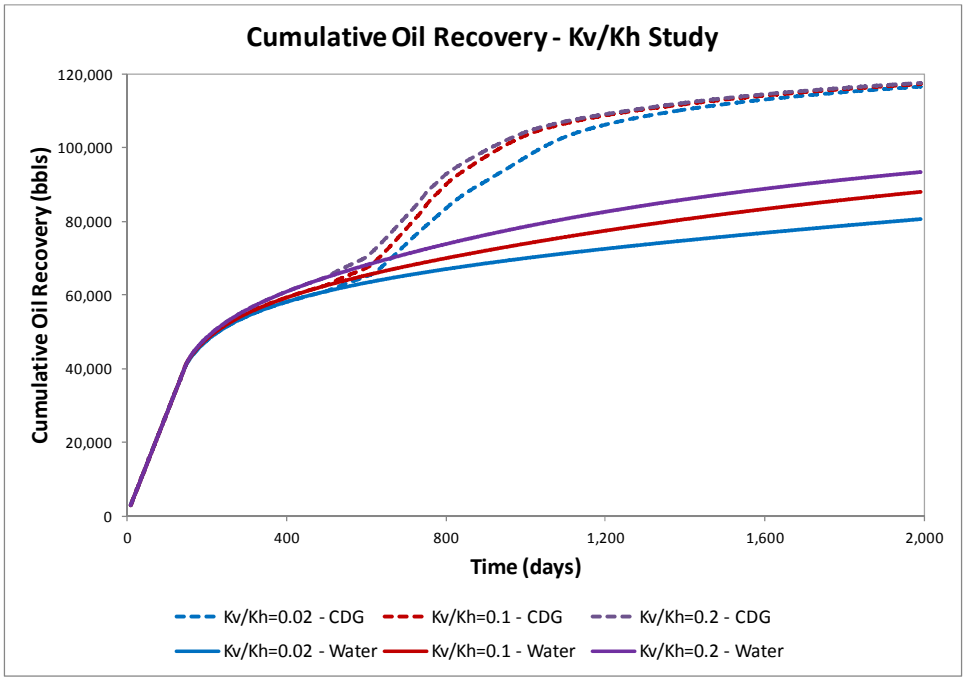

Figure 5.6: k_v/k_h Ratio Effect on CDG Incremental Oil Recovery, #2

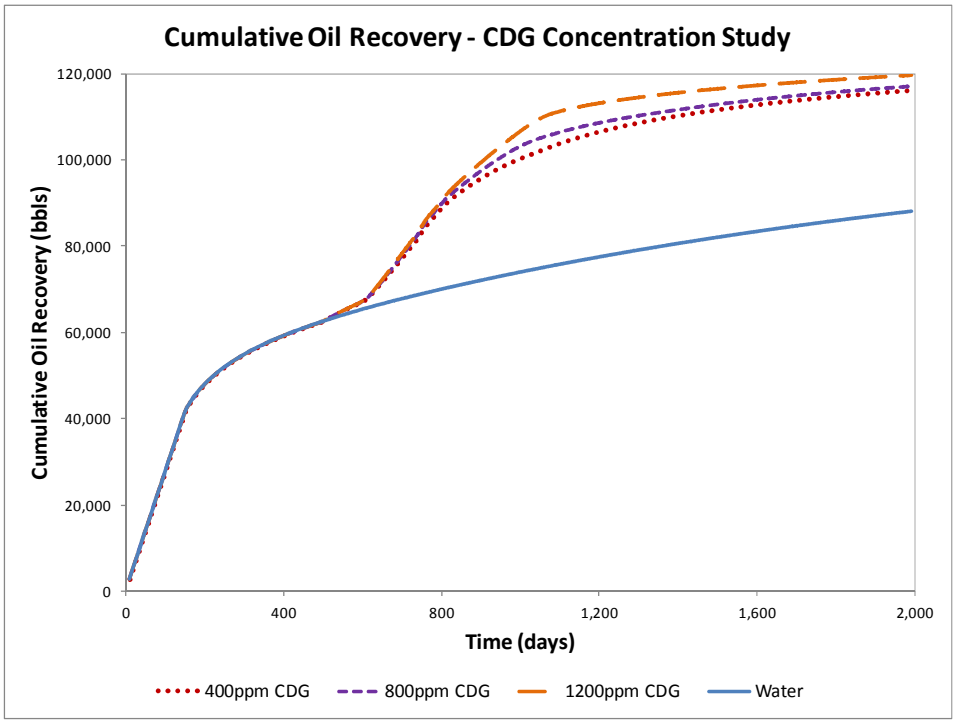

Figure 5.7: CDG Concentration Effect on Incremental Oil Recovery, #2

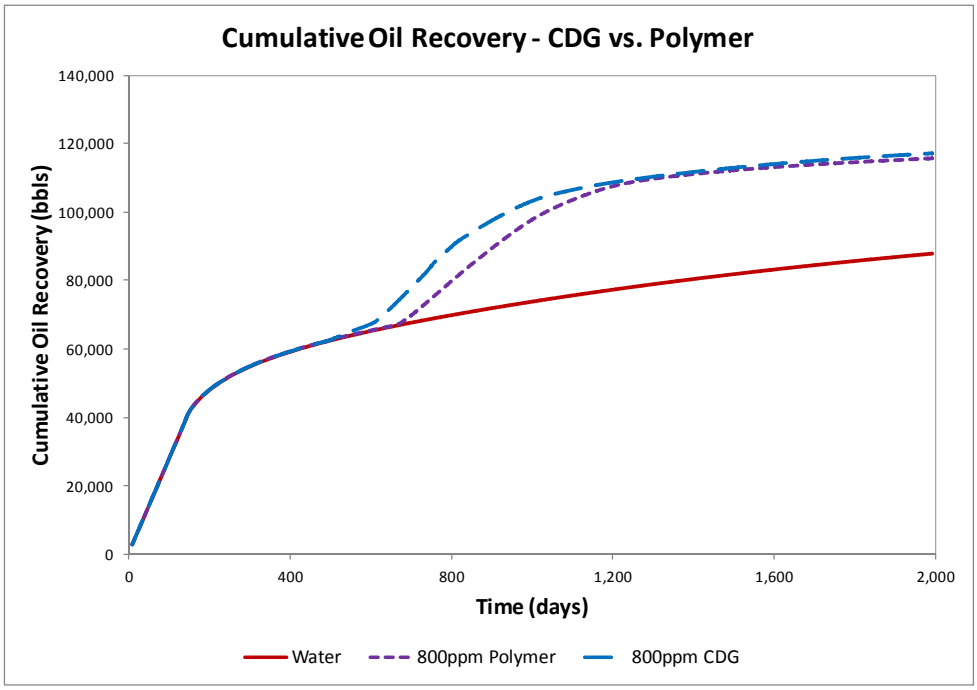

Figure 5.8: CDG vs. Polymer; 10:1 Perm. Contrast & 0.1 k_v/k_h

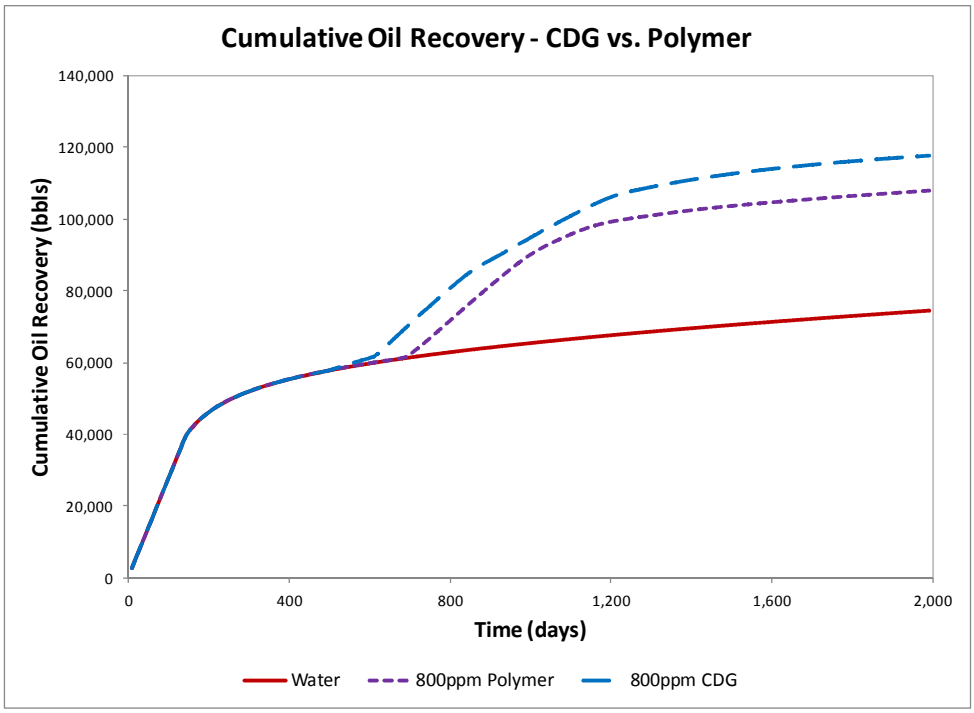

Figure 5.9: CDG vs. Polymer; 15:1 Perm. Contrast & 0.02 k_v/k_h

Chapter 6: Microgel Field Case

The objective of this chapter is to investigate polymer microgel potential to improve oil recovery and decrease water cut on a field scale. This investigation is carried out using a simulation study of a real field case, and the specific polymer microgel used is the Colloidal Dispersion Gel (CDG). Through the work carried out in the last two chapters, a strong understanding of CDGs, as a conformance control agent, has been developed. The previous two chapters also served to support the CDG models incorporated into UTGEL.

The conclusions reached in the last chapter, regarding CDG dependence on certain key variables, were determined using a simple, two-layer, homogeneous reservoir model. It was found that CDGs can be more effective than polymers at improving sweep efficiency under certain conditions. One of the most influential variables is permeability contrast. The existence of very high permeability thief zones (high permeability contrast) can severely inhibit the effectiveness of a polymer flood, as polymer may simply channel through the thief zones. Unlike polymers, CDGs prosper in such high permeability contrast (heterogeneous) environments. This is because they serve as conformance control agents, plugging high permeability zones and diverting flow to low permeability zones, improving sweep efficiency. One of the incentives for the field simulations carried out within this chapter is to ensure that CDGs can perform as intended on a field-level. A moderately heterogeneous field case was simulated, and is described below. This field is a real field, yet it will not be named. As usual, all simulations were performed using UTGEL.

CDGs have been shown to improve oil recovery and decrease water cut in numerous real field applications, as highlighted in Chapter 3's literature survey. This

chapter serves to demonstrate similar positive outcomes in a simulated field. This would not only further support CDG technology, but would also serve to support UTGEL's CDG modeling capabilities.

6.1 FIELD SIMULATION BASE CASE SETUP

Ultimately, the incentive to the subsequent field simulation is to investigate the viability/potential of CDG treatments in a field setting. As such, the simulation conducted is a forward simulation. In any case, there is not enough data in the literature to match a field case. Such a field-scale match, however, would be valuable should the possibility arise in the future.

In order to carry out this chapter's field simulation, a field case was obtained. This real field case had been previously simulated for prior work at UT Austin. The Input file for the field case was intended for UTCHEM simulation, and so was converted in order to be compatible with UTGEL. The reservoir model's grid also had to be made coarser, since the UTCHEM model was finer than necessary for the purpose of this chapter's simulations. Figures 6.1 and 6.2 present the original fine-gridded UTCHEM reservoir model. Figures 6.3 and 6.4 illustrate the modified coarser-gridded reservoir model for use in UTGEL. None of the reservoir, fluid, or polymer parameters were varied. Wreath's correlation parameters (Wreath 1989) were added to the Input file, since UTGEL has this capability. CDG parameters were also added to the Input file; these parameters are identical to those used in Sensitivity Analysis #2 in Chapter 5.

Table 6.1 provides the reservoir data for the base case of the CDG field simulation. Table 6.2 provides the key simulation data for this same base case. Note that none of the parameters in Tables 6.1 and 6.2 were changed throughout the simulations carried out in this chapter. As can be seen in Table 6.2, the field case contained 17 wells,

10 of which are injectors with the remaining wells being producers. These wells are arranged in a typical seven-spot pattern (Producer:Injector ratio of 1:2), as can be visualized in Figure 6.3.

The base case for the field simulation is simply 7.3 PV of waterflooding. Appendix D can be referred to for the base case Input file. Polymer flooding and CDG flooding cases will be compared to this waterflooding base case. In these simulations, the chemical treatment is injected after 5 PV of waterflooding, which is when the water cut reaches close to 99%. Following the chemical treatment slug, a waterflooding flush is carried out until the simulation reaches a cumulative injection of 7.3 PV, so as to enable a fair comparison with the waterflooding base case. All injecting wells were rate constrained, and all producing wells were pressure constrained. For more specific information regarding the performed simulations, Appendix D should be referenced. The only difference between the chemical treatment simulations and the base case simulation described in Appendix D is the chemical introduced. Injection rates, producer bottom-hole flowing pressure constraints, and injected fluid salinities are the same in all simulations compared.

6.2 SIMULATION RESULTS

Figures 6.5 and 6.6 present the results of the first simulations investigated. These plots both display the results of three distinct simulations: a waterflooding base case, a polymer flooding case, and a CDG flooding case. The two chemical treatment simulations had the respective treatments begin after 5 PV of waterflooding, corresponding to roughly 99% water cut. The respective chemical treatments were introduced in the form of a 0.3 PV slug, and the chemical was injected at 800 ppm concentration. The chemical treatment was followed by a water flush up until a

cumulative flooded volume of 7.3 PV. Figure 6.5 shows the cumulative oil recovery profiles of the three simulations performed (waterflooding base case, polymer treatment case, and CDG treatment case). Figure 6.6 shows the water cut profiles of the same three simulations. Note that the reason the CDG treatment water cut curve was somewhat jagged was likely because of the presence of many (highly heterogeneous) layers within this field, rendering the resulting profile significantly more complicated than that of the two-layer synthetic case in Chapter 5.

From these figures, it can be seen that the CDG treatment case yielded significant improvement in cumulative oil recovery (≈350,000 bbls), and a moderate (but somewhat long-lasting) decrease in water cut. This demonstrates the successful application of CDG. Figures 6.5 and 6.6 also enable comparison of the CDG profiles with the polymer profiles. Despite the polymer flooding treatment yielding some incremental oil recovery over the waterflooding base case, it can be seen that CDG yielded significantly more incremental oil than the polymer case. As previously explained, this may be the result of severe heterogeneity; very high permeability streaks may cause polymer solution to channel through and be produced quickly, while CDGs thrive in such environments and yield sweep efficiency improvements. The simulation results point towards this being the likely situation. Figures 6.7, 6.8, and 6.9 further support this hypothesis. These figures show the final oil saturation profiles, after 7.3 PV, for the waterflooding base case, the polymer flood case, and the CDG flood case respectively. From these figures, it can be seen that the final oil saturation profile that resulted after a polymer flood was almost the same as that of the waterflooding base case. However, it can be seen that the CDG flooding case yielded a modestly different final oil saturation profile with clearly improved sweep efficiency.

For the sake of comparison, some other simulations were run with different chemical treatment conditions. For example, simulations were run with chemical treatment slug sizes of 0.1 PV instead of 0.3 PV. The results of these simulations can be seen in Figures 6.10 and 6.11. Simulations were also run with chemical treatment concentrations of 1600 ppm instead of 800 ppm. The results of these simulations can be seen in Figures 6.12 and 6.13. Slug size and injection concentrations were varied as these are some of the most easily controlled aspects of a chemical treatment. In a real field case, permeability contrast and k_v/k_h are obviously beyond an engineer's control. And so injection conditions are the most important elements to consider when designing a chemical treatment.

As was expected, reducing slug size yielded decreased chemical treatment benefits for both the polymer and CDG cases. Increasing chemical concentrations improved the effectiveness of both the chemical treatments. The differences are quantified, and more easily comparable, in Table 6.3. Though it seems preferential to increase slug size and injection concentration, an economic analysis need be conducted on a case-to-case basis to determine the true optimums.

6.3 DISCUSSION

The simulations performed in this chapter demonstrate the potential benefits to a CDG treatment in real field applications. CDGs have been clearly found to be a viable technology for increasing oil recovery and decreasing associated water production, through improved sweep efficiency. In this particular field case, CDGs out-performed polymer fairly significantly.

Despite this chapter's simulation efforts, every field will have a unique outcome with regards to CDG effectiveness. Some situations may render polymers more

advantageous from an economic standpoint, or possibly even a technical standpoint as well. Some fields may not even be adequate options for CDG use. Simulation studies similar to the ones carried out within this chapter need be conducted on a case-to-case basis. Ultimately, the success of a CDG treatment depends on an array of different variables: reservoir heterogeneity (permeability contrasts), k_v/k_h, polymer/microgel availability (affecting project economics), to name just a few variables.

Reservoir Property	Unit	Quantity	Comments
Reservoir Length	ft	2100	
Reservoir Width	ft	2400	
Reservoir Thickness	ft	37	
Depth of Top Layer	ft	Variable	*Real Field Values*
Initial Reservoir Pressure	psia	550	*At 1966 ft Depth*
Porosity	%	Variable	*Real Field Values*
X-,Y-, and Z-Permeability	mD	Variable	*Real Field Values*
Initial Oil Saturation	%	80.0	*Constant*
Residual Oil Saturation	%	Variable	*Real Field Values*
Residual Water Saturation	%	Variable	*Real Field Values*
Oil Viscosity	cp	3.40	*Constant*
Water Viscosity	cp	0.37	*Constant*
Endpoint Mobility Ratio	-	3.9	
Initial [Cl^-]	meq/ml H_20	0.0513	
Initial [Ca^{2+}]	meq/ml H_20	0	

Table 6.1: Reservoir Data for CDG Field Simulation - Base Case

Number of Grid-blocks (in x, y, z Directions)	11 x 12 x 19	*Variable Grid Size*
Coordinate System	Cartesian	
Temperature Variation	Not Considered	*Isothermal*
Simulation Time (PV)	7.3	
Number of Wells	17	*10 Inj. & 7 Prod.*

Table 6.2: Simulation Data for CDG Field Simulation - Base Case

Chemical Concentration; Slug Size	Polymer – Incremental Oil Recovered (BBLS)	CDG – Incremental Oil Recovered (BBLS)
800 PPM; 0.1 PV	18,690	320,230
800 PPM; 0.3 PV	40,930	358,700
1600 PPM; 0.3 PV	84,570	379,910

Table 6.3: Incremental Oil Recovery over Waterflood – Polymer vs. CDG

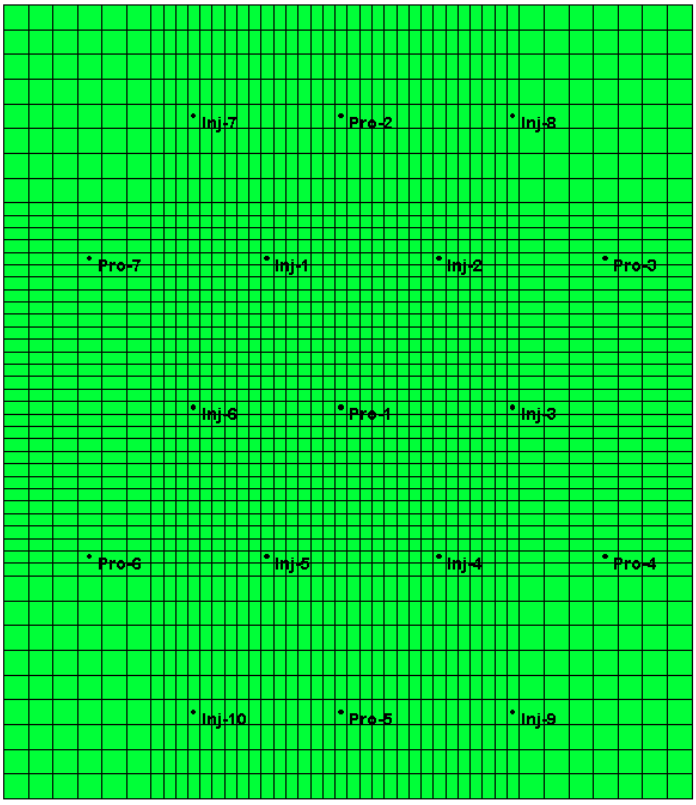

Figure 6.1: Top View of Fine-Gridded Reservoir Model (UTCHEM)

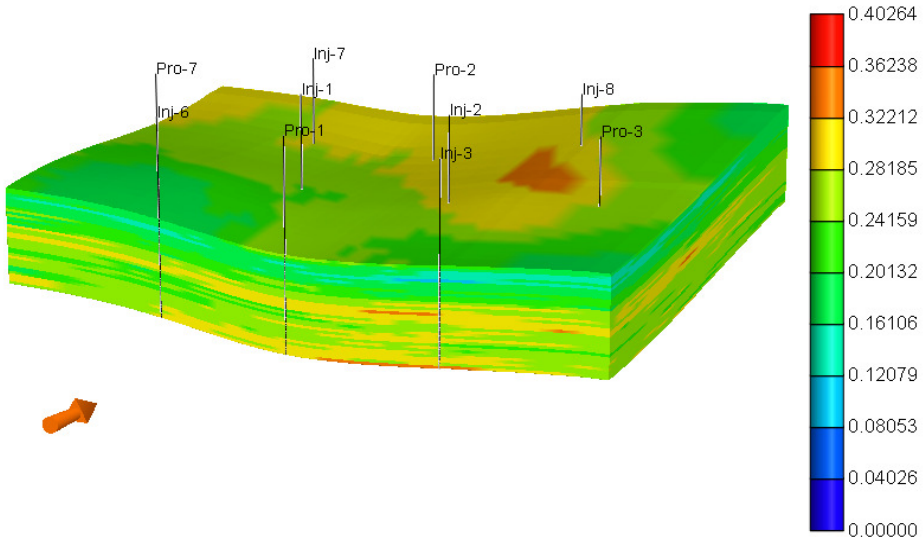

Figure 6.2: Side View of Fine Reservoir Model's Porosity (UTCHEM)

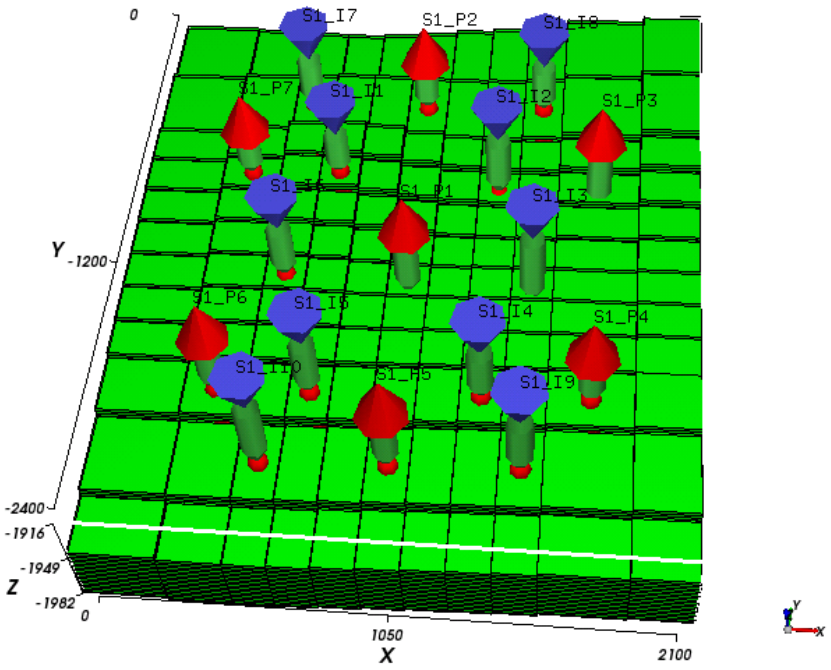

Figure 6.3: Top View of Coarse-Gridded Reservoir Model (UTGEL)

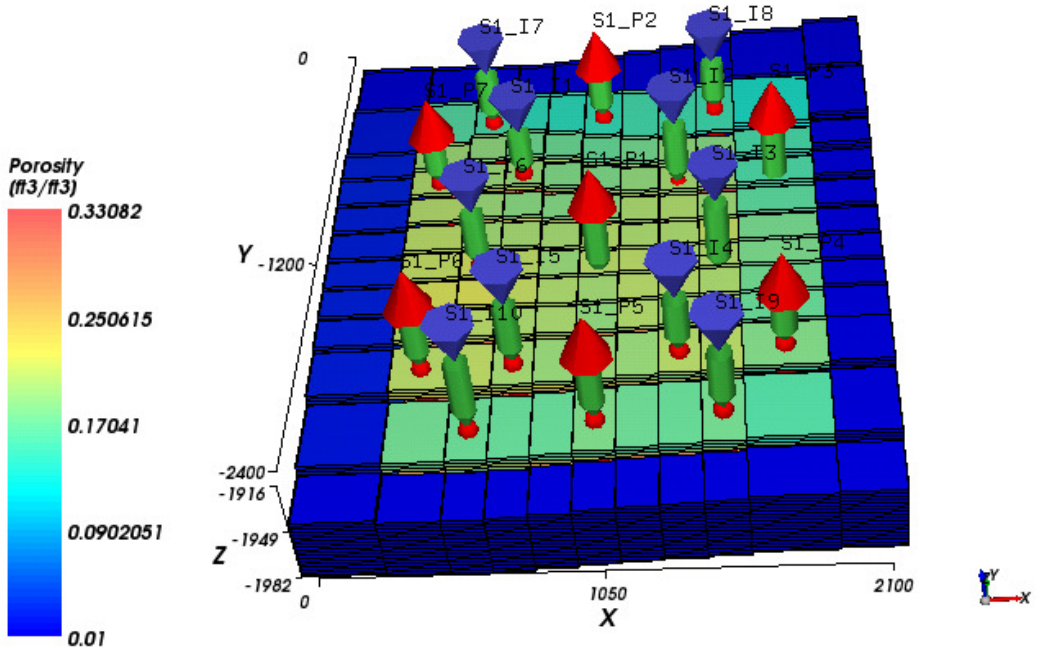

Figure 6.4: Coarse-Gridded Reservoir Model's Porosity (UTGEL)

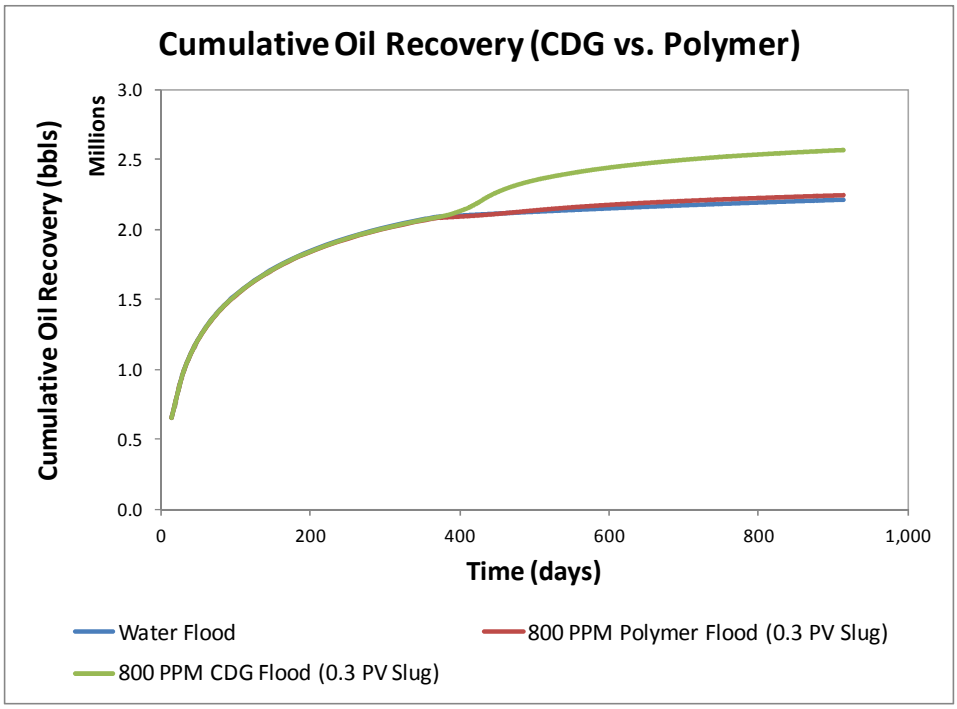

Figure 6.5: Oil Recovery – Polymer vs. CDG (800PPM, 0.3PV Slug)

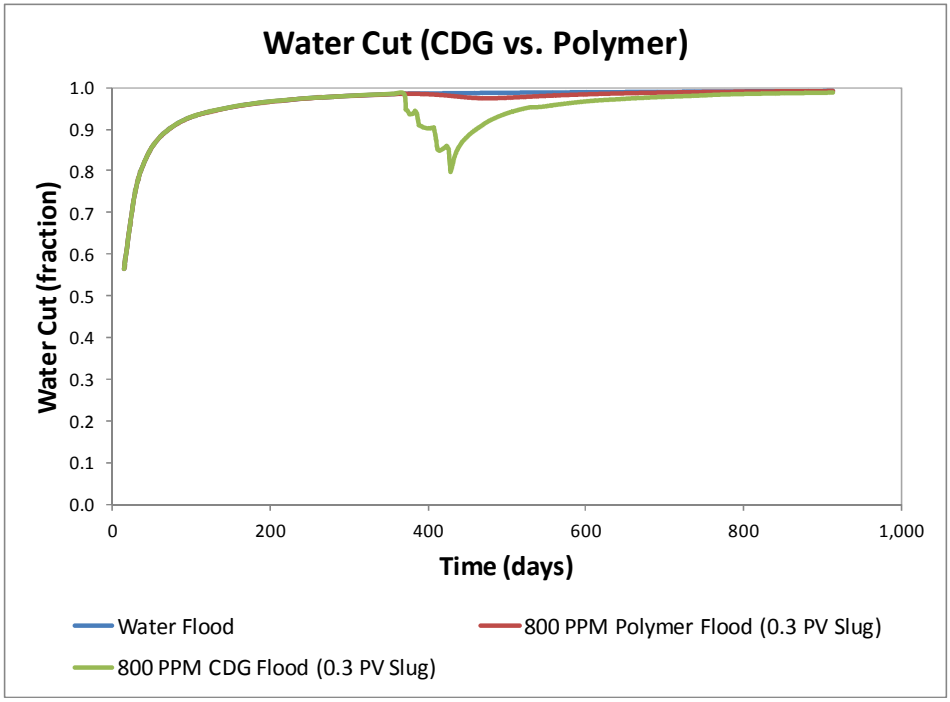

Figure 6.6: Water Cut – Polymer vs. CDG (800PPM, 0.3PV Slug)

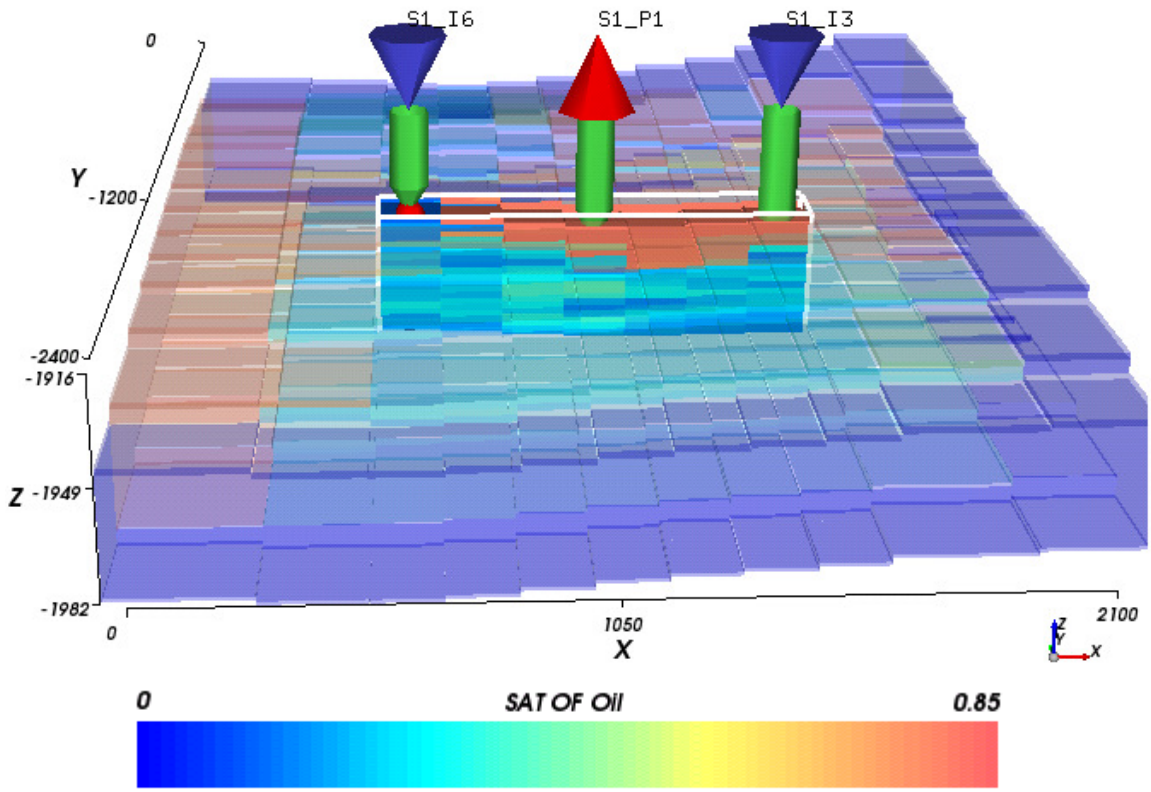

Figure 6.7: Final Oil Saturation Profile for Waterflooding Base Case

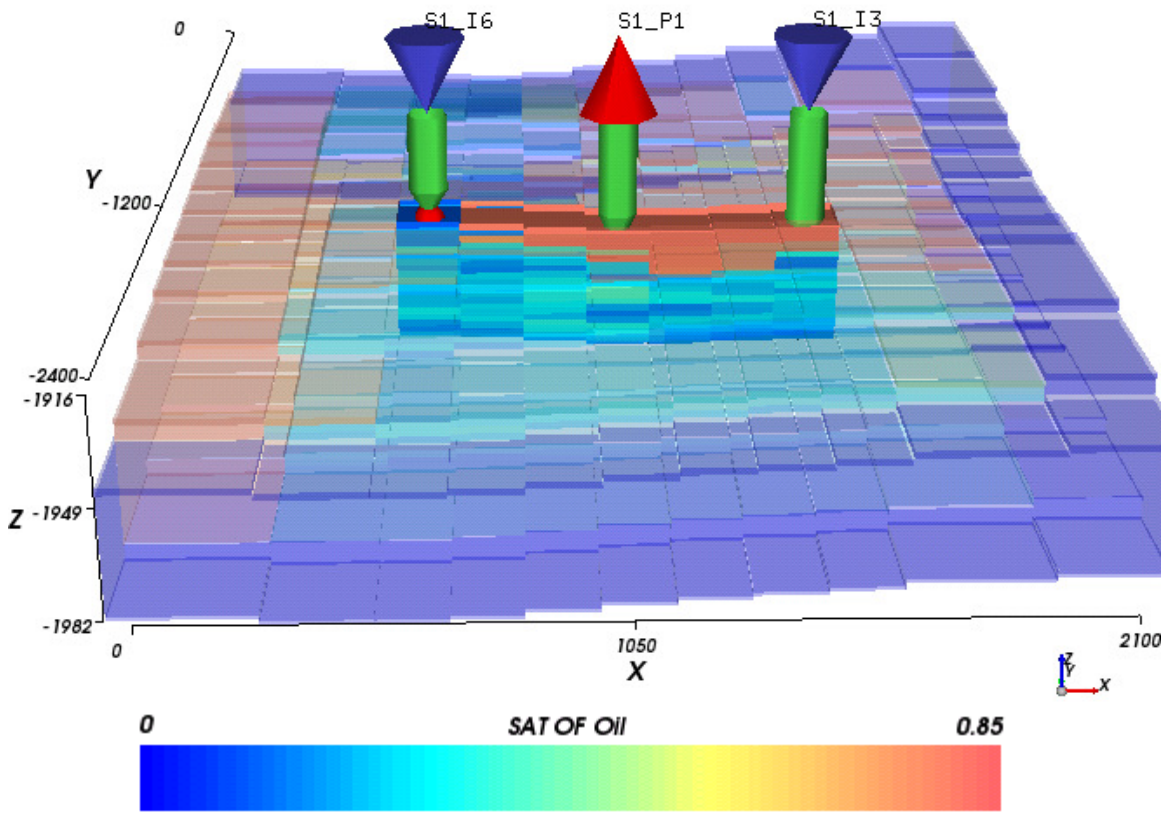

Figure 6.8: Final Oil Saturation Profile for Polymer Flood Case

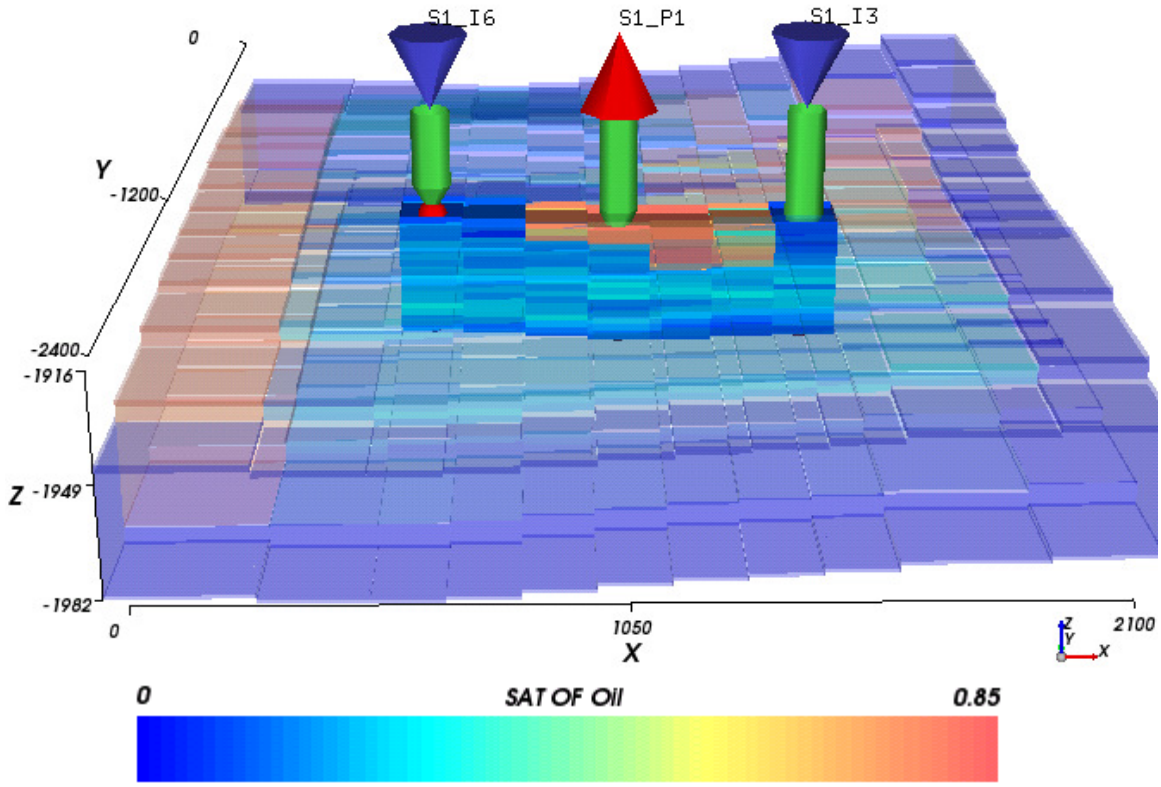

Figure 6.9: Final Oil Saturation Profile for CDG Flood Case

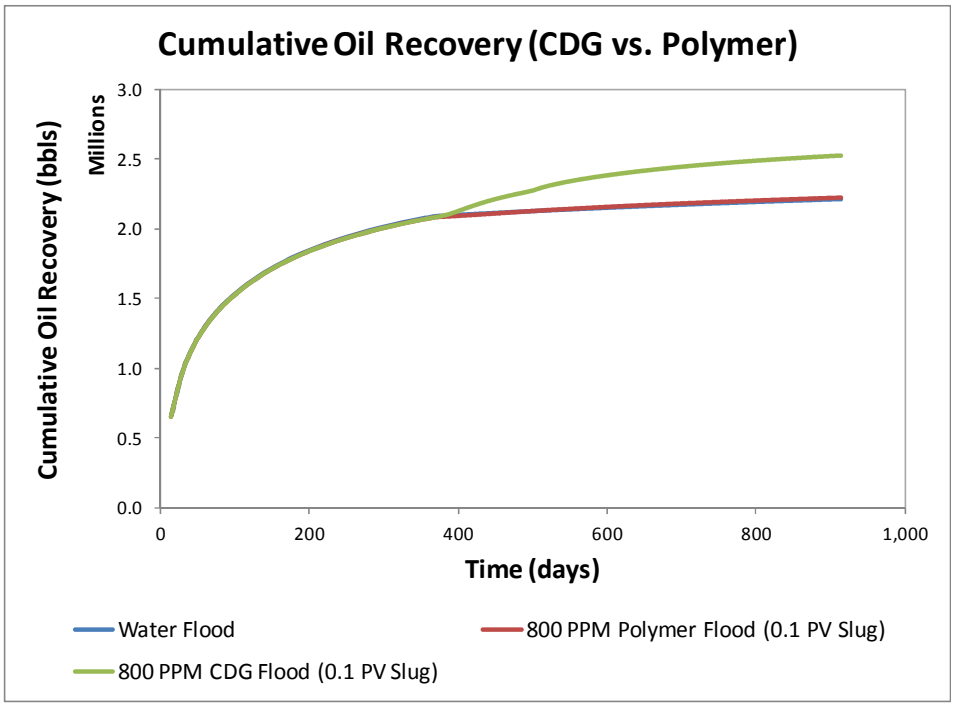

Figure 6.10: Oil Recovery – Polymer vs. CDG (800PPM, 0.1PV Slug)

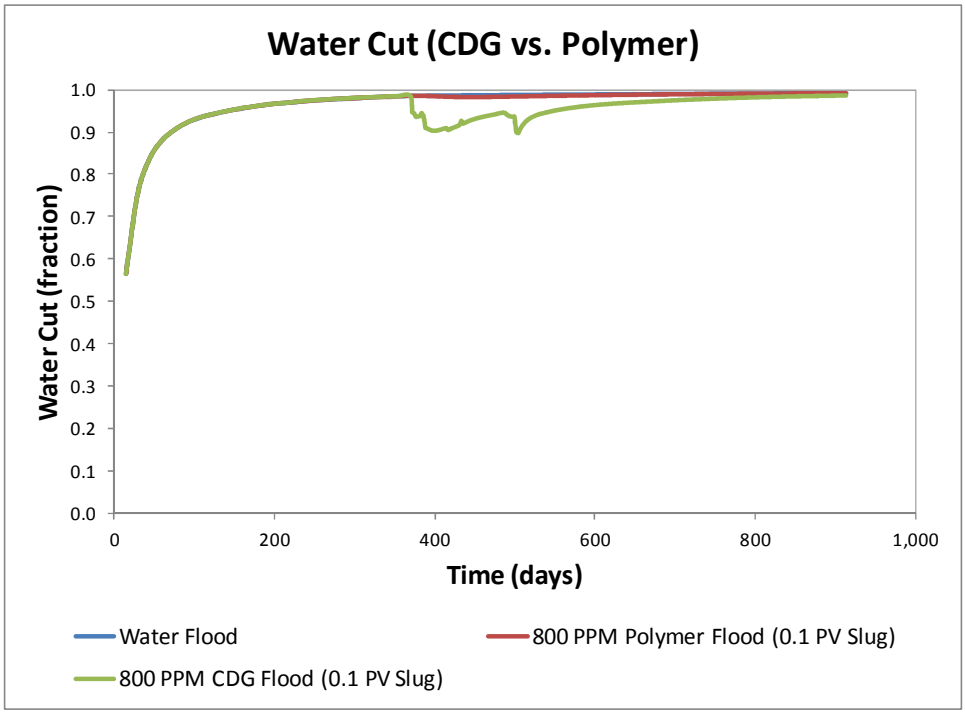

Figure 6.11: Water Cut – Polymer vs. CDG (800PPM, 0.1PV Slug)

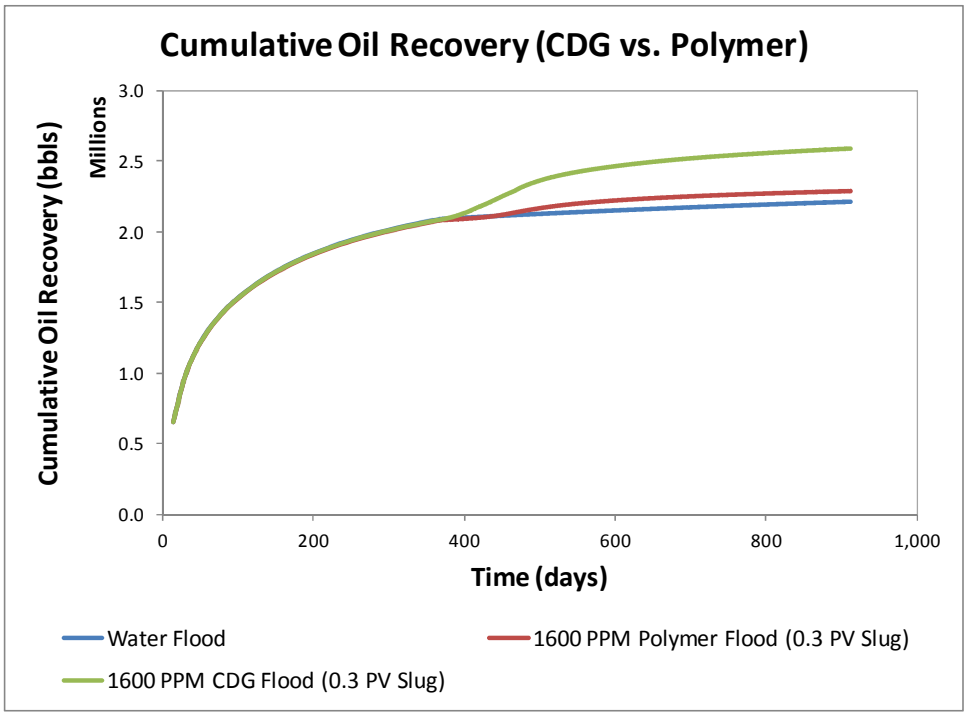

Figure 6.12: Oil Recovery – Polymer vs. CDG (1600PPM, 0.3PV Slug)

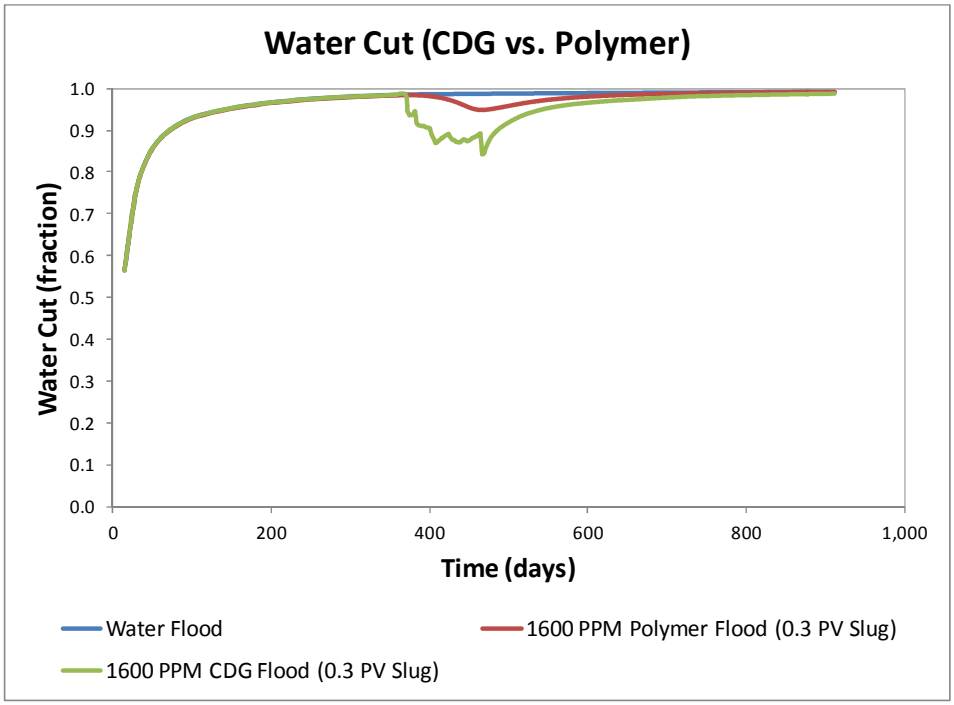

Figure 6.13: Water Cut – Polymer vs. CDG (1600PPM, 0.3PV Slug)

Chapter 7: Summary, Conclusions, and Recommendations

This chapter summarizes some of the major findings of the work carried out in this thesis. To close, recommendations are made for future consideration.

7.1 SUMMARY

This thesis involved a simulation study of polymer microgels as conformance control agents capable of plugging high permeability streaks, diverting flow, and subsequently improving reservoir sweep efficiency. Chapter 3 provided an extensive literature survey on polymer microgel technology. Topics addressed include laboratory studies, field applications, and potential mechanisms by which polymer microgels improve oil recovery. Colloidal Dispersion Gels, Preformed Particle Gels, Temperature-Sensitive Polymer Microgels (BrightWater), and pH-Sensitive Polymer Microgels were all discussed.

In the Chapters following the literature survey, the simulation studies focused on Colloidal Dispersion Gel (CDG) applications. Onbergenov (2012)'s work can be referred to for similar simulation studies for BrightWater and pH-Sensitive Polymer Microgels. Chapter 4 presented the results of the successful matching attempts of a CDG experiment carried out by Lu et al. (2000) in China. UTGEL, a novel reservoir simulator developed at UT Austin, was the tool of choice for these simulations. UTGEL was developed for polymer gel and microgel simulations; the work within this thesis served to support the models for CDGs.

Chapter 5 presented the results of simulation sensitivity studies. This chapter led to the updating of CDG's permeability reduction model, and also provided greater insight on the influence of certain key variables on CDG treatment effectiveness. Lastly, Chapter 6 presented the results of a real field case simulation, aimed at investigating CDG

viability on a field-scale. Throughout the simulation studies within this thesis, CDGs were seen to improve oil recovery and decrease associated water production.

7.2 CONCLUSIONS

A number of conclusions can be drawn from the work outlined within this thesis. Most noticeably, it is clear that polymer microgels can bear significant merits. Though this thesis focused on Colloidal Dispersion Gels, similar merits have been demonstrated in the work of many others, as can be seen in the literature. As conformance control agents, they have definitely shown to be one noteworthy means of extending the life of mature hydrocarbon reservoirs.

One conclusion that can be made, as a result of Chapter 5's sensitivity analyses, involves the effects of permeability contrast (heterogeneity), k_v/k_h, and microgel injection concentration on the extent to which CDGs can improve sweep efficiency. It was found that CDGs, and likely polymer microgels of other types by extension, are most effective in conditions of high permeability contrast, decreased k_v/k_h, and increased microgel injection concentration. Permeability contrast was found to be the most influential variable of those studied. Severe permeability contrast levels render polymer floods ineffective as polymers simply channel through thief zones, yet polymer microgels thrive under such heterogeneous conditions. The effect of k_v/k_h on the efficiency of a polymer microgel treatment is a complicated one that depends on the microgel activation location within the reservoir, as illustrated by Izgec and Shook (2012). Decreased k_v/k_h was advantageous in the CDG sensitivity study since the CDG corrected permeability variation close to the treating injector. Microgel injection concentration was found to be the least influential variable of the variables studied.

Another conclusion that can be drawn from the simulation studies addressed within this thesis is that UTGEL is an effective tool for polymer microgel simulation. Polymer microgel flow can be appropriately modeled with microgel solution effective viscosity and induced permeability reduction models. This is the method by which UTGEL models the flow of the different polymer microgels, and the induced recovery profiles. Such a simulation tool provides engineers with the means of studying polymer microgel potential on a case-to-case basis, by conducting simulation studies similar to the ones carried out within this thesis. UTGEL's forecasting capabilities can thus enable engineers to determine if polymer microgels are a more suitable option than conventional polymers for a particular field application, or if they are a viable option at all.

7.3 RECOMMENDATIONS

There are a number of suitable areas for future work. Firstly, and most importantly, research need be performed on the mechanisms by which polymer microgels improve oil recovery and decrease water cut. Though some insight was provided in this thesis's literature survey (Chapter 3), the mechanisms are still not entirely clear. Most of the literature on polymer microgel technology focuses on successful lab or field applications of the microgels. Though such works are highly valuable, more focus need be made on the means by which said microgels successfully improve sweep efficiency and, in turn, oil recovery. In addition, the reporting of failed polymer microgel treatments are just as valuable as successful implementations, if not more so. Investigating the means by which polymer microgels plug pores and increase sweep efficiency is an imperative next step. Without a strong and complete understanding of novel technology, risks are higher than need be.

Another recommendation for an area of future work involves the new UTGEL simulator. Throughout the course of the work outlined in this thesis, UTGEL was modified a number of times. For example, Wreath's correlation was incorporated into UTGEL during Chapter 4's experimental matching attempts. Additionally, CDG's permeability reduction model was modified a number of times, to account for and to fine-tune *long-term* permeability reduction. As such, it is clear that UTGEL development, though in the final stages, is still a work in progress. More simulation studies and matching attempts need be conducted to further validate and improve UTGEL. Note that this applies for CDGs (the long-term permeability reduction model can still be further improved, as discussed in Chapter 5's Discussion section) as well as the other polymer microgels not simulated within this thesis. Only when UTGEL has been extensively validated can it be reliably used for polymer microgel predictive simulations. This would enable the optimization of polymer microgel treatments, so as to maximize hydrocarbon recovery, decrease associated water production, and lengthen the lifespan of mature hydrocarbon reservoirs.

Appendix A: Input Data for Chapter 4 Run

```
CC*********************************************************************
CC                                                                     *
CC   BRIEF DESCRIPTION OF DATA SET                                     *
CC                                                                     *
CC*********************************************************************
CC                                                                     *
CC  Daqing Lab. Study - Parallel Core Test - Matching Attempt          *
CC                                                                     *
CC  LENGTH (FT) : 32 cm          PROCESS : PROFILE CONTROL (CDG)       *
CC  THICKNESS (FT) : 3.6 cm      INJ. RATE (ML/MIN) : 0.4              *
CC  WIDTH (FT) : 3.6 cm          COORDINATES : CARTESIAN               *
CC  POROSITY : LAYERED                                                 *
CC  GRID BLOCKS : 15x1x3                                               *
CC  DATE : Dec. 22nd, 2011                                             *
CC                                                                     *
CC*********************************************************************
CC
CC*********************************************************************
CC                                                                     *
CC   RESERVOIR DESCRIPTION                                             *
CC                                                                     *
CC*********************************************************************
CC
CC
*----RUNNO
CDGLAB
CC
CC
*----HEADER
Daqing Laboratory Study, Parallel Core Diverting Experiment
Attempt to Match Results
SPE #59466
CC
CC SIMULATION FLAGS
*---- IMODE IMES IDISPC IREACT  ICOORD ITREAC ITC  IENG
     1    2   3     1      1     0     0   0
CC
CC NUMBER OF GRID BLOCKS AND FLAG SPECIFIES CONSTANT OR VARIABLE GRID
SIZE
*----NX   NY  NZ  IDXYZ  IUNIT
    15   1   3   2     0
CC
CC  VARIABLE GRID BLOCK SIZE IN X
*----DX(I)
    15*0.0699912511
CC
```

```
CC  VARIABLE GRID BLOCK SIZE IN Y
*----DY(J)
    0.118110236
CC
CC  VARIABLE GRID BLOCK SIZE IN Z
*----DZ(K)
    3*0.118110236
CC
CC TOTAL NO. OF COMPONENTS, NO. OF TRACERS, NO. OF GEL COMPONENTS
*----N   NTW  NG
    14  0    6
CC
CC
*---- SPNAME(I),I=1,N
WATER
OIL
none
POLYMER
CHLORIDE
CALCIUM
none
none
none
none
none
none
none
CDG
CC
CC FLAG INDICATING IF THE COMPONENT IS INCLUDED IN CALCULATIONS OR NOT
*----ICF(KC) FOR KC=1,N
    1  1  0  1  1  1  0 0 0 0 0 0 0 1
CC
CC*********************************************************************
CC                                                                    *
CC    OUTPUT OPTIONS                                                   *
CC                                                                    *
CC*********************************************************************
CC
CC
CC  FLAG FOR PV OR DAYS FOR OUTPUT AND STOP THE RUN
*----ICUMTM  ISTOP
    1       1
CC
CC FLAG INDICATING IF THE PROFILE OF KCTH COMPONENT SHOULD BE WRITTEN
*----IPRFLG(KC),KC=1,N
    1  1  0  1  1  1 0 0 0 0 0 0 0  1
CC
CC FLAG FOR PRES,SAT.,TOTAL CONC.,TRACER CONC.,CAP.,GEL, ALKALINE PROFILES
```

```
*----IPPRES IPSAT IPCTOT IPGEL  ITEMP
   1     1    1     1     0
CC
CC FLAG FOR WRITING SEVERAL PROPERTIES
*----ICKL IVIS IPER ICNM  ICSE
   0   1   0   0    0
CC
CC FLAG FOR WRITING SEVERAL PROPERTIES TO PROF
*----IADS  IVEL IRKF IPHSE
   0    0   1   0
CC
CC*************************************************************************
CC                                                                        *
CC   RESERVOIR PROPERTIES                                                 *
CC                                                                        *
CC*************************************************************************
CC
CC
CC MAX. SIMULATION TIME (PV)
*---- TMAX
    7.45
CC
CC ROCK COMPRESSIBILITY (1/psi), STAND. PRESSURE(psi)
*----COMPR   PSTAND
   0.      14.696
CC
CC FLAGS INDICATING CONSTANT OR VARIABLE POROSITY, X,Y,AND Z
PERMEABILITY
*----IPOR1 IPERMX IPERMY IPERMZ  IMOD  ITRNZ  INTG
   2    2     3     0      0    0     0
CC
CC VARIABLE POROSITY
*----POR(I), for I = 1 to NX*NY*NZ
   15*0.253  15*0.232  15*0.208
CC
CC VARIABLE X-PERMEABILITY (MILIDARCY)
*----PERMX(I), for I=1 TO NX * NY * NZ
   2076.459  2402.501  2279.240  2522.318  1859.127
   1885.744  2475.336  2420.361  1923.401  2453.187
   1164.489  1585.904  1659.956  1616.417  1594.720
   531.6455  658.2313  681.4122  698.8215  692.7637
   465.1804  655.2278  574.5653  443.0055  483.6843
   858.4789  483.2423  630.2346  487.6963  823.9859
   108.7342  180.9330  200.0003  159.5862  148.3232
   226.6217  177.1981  214.4596  161.1565  282.1228
   326.5077  207.5728  179.7417  241.3352  164.6030
CC
CC VARIABLE Y-PERMEABILITY
*----FACTY
```

```
    1
CC
CC CONSTANT Z-PERMEABILITY
*----PERMZC
    0
CC
CC FLAG FOR CONSTANT OR VARIABLE DEPTH, PRESSURE, WATER SATURATION
*----IDEPTH  IPRESS  ISWI
    0      0      2
CC
CC CONSTANT DEPTH (ft)
*----D111
    0.0
CC
CC CONSTANT PRESSURE (psi)
*----PRESS1
    14.696
CC
CC VARIABLE INITIAL WATER SATURATION
*----S(I,1), for I = 1 to NX*NY*NZ
    15*0.226  15*0.268  15*0.300
CC
CC CONSTANT CHLORIDE AND CALCIUM CONCENTRATIONS (MEQ/ML)
*----C50       C60
    0.05184   0.0008
CC
CC*********************************************************************
CC                                                                    *
CC    PHYSICAL PROPERTY DATA                                          *
CC                                                                    *
CC*********************************************************************
CC
CC
CC CMC
*----  EPSME
     .0001
CC SLOPE AND INTERCEPT OF BINODAL CURVE AT ZERO, OPT., AND 2XOPT SALINITY
CC FOR ALCOHOL 1
*----HBNS70 HBNC70 HBNS71 HBNC71 HBNS72 HBNC72
    0.     .030    0.   .030     0.0   .030
CC SLOPE AND INTERCEPT OF BINODAL CURVE AT ZERO, OPT., AND 2XOPT SALINITY
CC FOR ALCOHOL 2
*----HBNS80 HBNC80 HBNS81 HBNC81 HBNS82 HBNC82
    0.     0.     0.     0.     0.     0.
CC
CC LOWER AND UPPER EFFECTIVE SALINITY FOR ALCOHOL 1 AND ALCOHOL 2
*----CSEL7  CSEU7  CSEL8  CSEU8
    .65   .9   0.     0.
CC
```

```
CC THE CSE SLOPE PARAMETER FOR CALCIUM AND ALCOHOL 1 AND ALCOHOL 2
*----BETA6  BETA7  BETA8
   0.0   0.    0.
CC
CC FLAG FOR ALCOHOL PART. MODEL AND PARTITION COEFFICIENTS
*----IALC  OPSK7O  OPSK7S  OPSK8O  OPSK8S
   0    0.     0.     0.     0.
CC
CC NO. OF ITERATIONS, AND TOLERANCE
*----NALMAX   EPSALC
   20      .0001
CC
CC ALCOHOL 1 PARTITIONING PARAMETERS IF IALC=1
*----AKWC7   AKWS7  AKM7  AK7    PT7
   4.671   1.79   48.   35.31   .222
CC
CC ALCOHOL 2 PARTITIONING PARAMETERS IF IALC=1
*----AKWC8   AKWS8  AKM8  AK8    PT8
   0.     0.    0.   0.     0.
CC
CC
*----IFT MODEL FLAG
   0
CC
CC INTERFACIAL TENSION PARAMETERS
*----G11  G12    G13   G21   G22    G23
   13.  -14.8   .007  13.2   -14.5  .010
CC
CC LOG10 OF OIL/WATER INTERFACIAL TENSION
*----XIFTW
   1.477
CC
CC CAPILLARY DESATURATION PARAMETERS FOR PHASE 1, 2, AND 3
*----ITRAP   T11       T22       T33
   0      1865.     28665.46     364.2
CC
CC REL. PERM. AND PC CURVES
*---- IPERM    IRTYPE
    0       0
CC
CC FLAG FOR CONSTANT OR VARIABLE REL. PERM. PARAMETERS
*----ISRW  IPRW  IEW
   2    0    0
CC
CC AQUEOUS PHASE (1) RESIDUAL SATURATION AT LOW CAPILLARY NO.
*----S1RW(I), for I = 1 to NX*NY*NZ
   15*0.226  15*0.268  15*0.300
CC
CC OLEIC PHASE (2) RESIDUAL SATURATION AT LOW CAPILLARY NO.
```

```
*----S2RW(I), for I = 1 to NX*NY*NZ
   15*0.259  15*0.281  15*0.323
CC
CC MICROEMULSION PHASE (3) RESIDUAL SATURATION AT LOW CAPILLARY NO.
*----S3RW(I), for I = 1 to NX*NY*NZ
   45*0.147
CC
CC CONSTANT ENDPOINT REL. PERM. OF PHASES 1,2,AND 3 AT LOW CAPILLARY NO.
*----P1RW  P2RW   P3RW
   .25   .35    .13771
CC
CC CONSTANT REL. PERM. EXPONENT OF PHASES 1,2,AND 3 AT LOW CAPILLARY NO.
*----E1W   E2W   E3W
   5.0   2.5   2.1817
CC
CC WATER AND OIL VISCOSITY , RESERVOIR TEMPERATURE
*----VIS1   VIS2  TEMPV
   0.6    9.0   113
CC
CC VISCOSITY PARAMETERS
*----ALPHA1 ALPHA2  ALPHA3  ALPHA4  ALPHA5
   0.0     0.0      0.0   0.000865    4.153
CC
CC PARAMETERS TO CALCULATE POLYMER VISCOSITY AT ZERO SHEAR RATE
*----AP1     AP2     AP3
   520.8   0.0     0.0
CC
CC PARAMETER TO COMPUTE CSEP,MIN. CSEP, AND SLOPE OF LOG VIS. VS. LOG CSEP
*----BETAP CSE1  SSLOPE
   .0    .01   .0
CC
CC PARAMETER FOR SHEAR RATE DEPENDENCE OF POLYMER VISCOSITY
*----GAMMAC  GAMHF  POWN    IPMOD   ishear  rweff   GAMHF2   IWREATH
   3.97    13.7   1.6     0       0       0.25    0        1
CC
CC WREATH CORRELATION PARAMETERS
*----WREATHM  WREATHB  WREATHN  WREATHT
   4.7      0.18     0.48     1.0
CC
CC FLAG FOR POLYMER PARTITIONING, PERM. REDUCTION PARAMETERS
*----IPOLYM EPHI3 EPHI4 BRK    CRK    RKCUT
   1      1.    1     100.   0.32   10
CC
CC SPECIFIC WEIGHT FOR COMPONENTS 1,2,3,7,AND 8 , AND GRAVITY FLAG
*----DEN1    DEN2    DEN3    DEN7    DEN8  IDEN
   62.899  49.857  62.399  49.824  0     2
CC
CC  FLAG FOR CHOICE OF UNITS ( 0:BOTTOMHOLE CONDITION , 1: STOCK TANK)
*-----ISTB
```

```
    0
CC
CC COMPRESSIBILITY FOR VOL. OCCUPYING COMPONENTS 1,2,3,7,AND 8
*----COMPC(1)  COMPC(2)  COMPC(3)  COMPC(7)  COMPC(8)
   0.       0.       0.       0.       0.
CC
CC CONSTANT OR VARIABLE PC PARAM., WATER-WET OR OIL-WET PC CURVE FLAG
*----ICPC   IEPC  IOW
   0     0    0
CC
CC CAPILLARY PRESSURE PARAMETERS, CPC
*---- CPC
    0.
CC
CC CAPILLARY PRESSURE PARAMETERS, EPC
*---- EPC
    2.
CC
CC MOLECULAR DIFFUSIVITY OF KCTH COMPONENT IN PHASE 1 (D(KC),KC=1,N)
*----D(1) D(2) D(3) D(4) D(5) D(6)
   0.  0.  0.  0.  0.  0. 0.0 0.0 0.0 0.0 0.0 0.0 0.0 0.0
CC
CC MOLECULAR DIFFUSIVITY OF KCTH COMPONENT IN PHASE 2 (D(KC),KC=1,N)
*----D(1) D(2) D(3) D(4) D(5) D(6)
   0.  0.  0.  0.  0.  0. 0.0 0.0 0.0 0.0 0.0 0.0 0.0 0.0
CC
CC MOLECULAR DIFFUSIVITY OF KCTH COMPONENT IN PHASE 3 (D(KC),KC=1,N)
*----D(1) D(2) D(3) D(4) D(5) D(6)
   0.  0.  0.  0.  0.  0. 0.0 0.0 0.0 0.0 0.0 0.0 0.0 0.0
CC
CC LONGITUDINAL AND TRANSVERSE DISPERSIVITY OF PHASE 1
*----ALPHAL(1)    ALPHAT(1)
   0.0         0.0
CC
CC LONGITUDINAL AND TRANSVERSE DISPERSIVITY OF PHASE 2
*----ALPHAL(2)    ALPHAT(2)
   0.0         0.0
CC
CC LONGITUDINAL AND TRANSVERSE DISPERSIVITY OF PHASE 3
*----ALPHAL(3)    ALPHAT(3)
   2.0         0.4
CC
CC SURFACTANT AND POLYMER ADSORPTION PARAMETERS
*----AD31    AD32  B3D   AD41  AD42   B4D  IADK, IADS1, FADS refk
   0.      .0   1000.  1.153  0.     100  0    0     0    0
CC
CC PARAMETERS FOR CATION EXCHANGE OF CLAY AND SURFACTANT
*----QV    XKC   XKS  EQW
   0     0.   0.   804
```

```
CC
CC
*----KGOPT
   5
CC
CC PARAMETERS FOR CDG GEL OPTION
*----IRKCDG, RKCUTCDG, CDGD,   CDGE,   CDGB,  GAMMACG
   2      200.0    0.00047  1.5804  -0.06  85.22242182
CC
CC PARAMETERS FOR CDG GEL OPTION
*----CDGMU, CDGSIG, CDGC, CDGF
   -0.18  2.44    56.9  -0.06
CC
CC PARAMETERS FOR CDG RETENTION
*----ADCDG,     BDCDG    ADCDGILM   TolCcdgRk
   0.015302   0.01293   1.25       1d-1
CC
CC CDG viscosity parametrs
*----CDGETA,   CDGKH,  VISCDGA,  VISCDGB,  CDGPOWN
   2730.183  1.0177  0.004621  996.9207  0.859
CC
CC**********************************************************************
CC                                                                     *
CC   WELL DATA                                                         *
CC                                                                     *
CC**********************************************************************
CC
CC
CC TOTAL NUMBER OF WELLS, WELL RADIUS FLAG, FLAG FOR TIME OR COURANT
NO.
*----NWELL   IRO   ITIME  NWREL
   4      2    1     4
CC
CC WELL ID,LOCATIONS,AND FLAG FOR SPECIFYING WELL TYPE, WELL RADIUS, SKIN
*----IDW   IW    JW    IFLAG    RW       SWELL  IDIR   IFIRST  ILAST  IPRF
   1    1    1    1       .00164   0.    3     1      3     0
CC
CC WELL NAME
*---- WELNAM
INJECT
CC
CC ICHEK MAX. AND MIN. ALLOWABLE BOTTOMHOLE PRESSURE AND RATE
*----ICHEK   PWFMIN   PWFMAX  QTMIN   QTMAX
   0      0.0     5801.6  0.0     5615.
CC
CC WELL ID, LOCATION, AND FLAG FOR SPECIFYING WELL TYPE, WELL RADIUS, SKIN
*----IDW  IW   JW   IFLAG    RW       SWELL  IDIR  IFIRST   ILAST    IPRF
   2   15  1    2       .00164   0.    3     1       1       0
CC
```

```
CC WELL NAME
*---- WELNAM
P1800
CC
CC MAX. AND MIN. ALLOWABLE BOTTOMHOLE PRESSURE AND RATE
*----ICHEK  PWFMIN   PWFMAX  QTMIN   QTMAX
   0     0.0     5000.  0.0    50000.
C
CC WELL ID, LOCATION, AND FLAG FOR SPECIFYING WELL TYPE, WELL RADIUS, SKIN
*----IDW  IW   JW   IFLAG   RW      SWELL  IDIR  IFIRST   ILAST   IPRF
   3   15  1   2       .00164  0.    3    2       2       0
CC
CC WELL NAME
*---- WELNAM
P580
CC
CC MAX. AND MIN. ALLOWABLE BOTTOMHOLE PRESSURE AND RATE
*----ICHEK  PWFMIN   PWFMAX  QTMIN   QTMAX
   0     0.0     5000.  0.0    50000.
CC
CC WELL ID, LOCATION, AND FLAG FOR SPECIFYING WELL TYPE, WELL RADIUS, SKIN
*----IDW  IW   JW   IFLAG   RW      SWELL  IDIR  IFIRST   ILAST   IPRF
   4   15  1   2       .00164  0.    3    3       3       0
CC
CC WELL NAME
*---- WELNAM
P210
CC
CC MAX. AND MIN. ALLOWABLE BOTTOMHOLE PRESSURE AND RATE
*----ICHEK  PWFMIN   PWFMAX  QTMIN   QTMAX
   0     0.0     5000.  0.0    50000.
CC
CC ID,INJ. RATE AND INJ. COMP. FOR RATE CONS. WELLS FOR EACH PHASE (L=1,3)
*----ID  QI(M,L)  C(M,KC,L)
   1  0.020341 1.0  0.  0.  0.  0.01082  0.001  0.  0.  0.0  0.0  0.0  0.0  0.0  0.0
   1  0.      0.0  0.  0.  0.  0.      0.     0.  0.  0.0  0.0  0.0  0.0  0.0  0.0
   1  0.      0.0  0.  0.  0.  0.      0.     0.  0.  0.0  0.0  0.0  0.0  0.0  0.0
CC
CC ID, BOTTOM HOLE PRESSURE FOR PRESSURE CONSTRAINT WELL (IFLAG=2 OR 3)
*----ID   PWF
   2   14.696
CC
CC ID, BOTTOM HOLE PRESSURE FOR PRESSURE CONSTRAINT WELL (IFLAG=2 OR 3)
*----ID   PWF
   3   14.696
CC
CC ID, BOTTOM HOLE PRESSURE FOR PRESSURE CONSTRAINT WELL (IFLAG=2 OR 3)
*----ID   PWF
   4   14.696
```

```
CC
CC CUM. INJ. TIME , AND INTERVALS (PV) FOR WRITING TO OUTPUT FILES
*----TINJ    CUMPR1   CUMHI1     WRHPV   WRPRF      RSTC
    1.13    0.01     0.01       0.01    0.01       1
CC
CC FOR IMES=2, THE INI. TIME STEP,CONC. TOLERANCE,MAX.,MIN. COURANT NO.
*----DT      DCLIM     CNMAX   CNMIN
    0.0001  0.01      0.1     0.01
CC
CC IRO, ITIME, NEW FLAGS FOR ALL THE WELLS (SURF/POLYMER)
*---- IRO ITIME IFLAG
     2   1     1  2  2  2
CC
CC NUMBER OF WELLS CHANGES IN LOCATION OR SKIN OR PWF
*----NWEL1
    0
CC
CC NUMBER OF WELLS WITH RATE CHANGES, ID
*----NWEL2   ID
    1       1
CC
CC ID,INJ. RATE AND INJ. COMP. FOR RATE CONS. WELLS FOR EACH PHASE (L=1,3)
*----ID  QI(M,L)  C(M,KC,L)
    1   0.020341 1.0   0.  0.  0.08  0.01082  0.001   0.  0.  0.0  0.0  0.0  0.0  0.0  0.0
    1   0.       0.0   0.  0.  0.    0.       0.      0.  0.  0.0  0.0  0.0  0.0  0.0  0.0
    1   0.       0.0   0.  0.  0.    0.       0.      0.  0.  0.0  0.0  0.0  0.0  0.0  0.0
CC
CC CUM. INJ. TIME , AND INTERVALS (PV) FOR WRITING TO OUTPUT FILES
*----TINJ   CUMPR1  CUMHI1(PROFIL)  WRHPV(HIST) WRPRF(PLOT) RSTC
    1.32   0.01    0.01            0.01        0.01        0.1
CC
CC FOR IMES=2 ,THE INI. TIME STEP,CONC. TOLERANCE,MAX.,MIN. Courant No.
*----DT      DCLIM   CNMAX   CNMIN
    0.0001   0.01    0.1     0.01
CC
CC IRO, ITIME, NEW FLAGS FOR ALL THE WELLS (SURF/POLYMER)
*---- IRO ITIME IFLAG
     2   1     1  2  2  2
CC
CC NUMBER OF WELLS CHANGES IN LOCATION OR SKIN OR PWF
*----NWEL1
    0
CC
CC NUMBER OF WELLS WITH RATE CHANGES, ID
*----NWEL2   ID
    1       1
CC
CC ID,INJ. RATE AND INJ. COMP. FOR RATE CONS. WELLS FOR EACH PHASE (L=1,3)
*----ID  QI(M,L)  C(M,KC,L)
```

```
   1   0.020341 1.0   0.  0.  0.  0.01082  0.001  0.  0.  0.0  0.0  0.0  0.0  0.0  0.0
   1   0.       0.0   0.  0.  0.  0.       0.     0.  0.  0.0  0.0  0.0  0.0  0.0  0.0
   1   0.       0.0   0.  0.  0.  0.       0.     0.  0.  0.0  0.0  0.0  0.0  0.0  0.0
CC
CC CUM. INJ. TIME , AND INTERVALS (PV) FOR WRITING TO OUTPUT FILES
*----TINJ   CUMPR1  CUMHI1(PROFIL)  WRHPV(HIST) WRPRF(PLOT) RSTC
   5.26  0.01    0.01          0.01        0.01        1
CC
CC FOR IMES=2 ,THE INI. TIME STEP,CONC. TOLERANCE,MAX.,MIN. Courant No.
*----DT      DCLIM   CNMAX   CNMIN
   0.0001   0.01    0.1     0.01
CC
CC IRO, ITIME, NEW FLAGS FOR ALL THE WELLS (SURF/POLYMER)
*---- IRO ITIME IFLAG
    2   1     1  2  2  2
CC
CC NUMBER OF WELLS CHANGES IN LOCATION OR SKIN OR PWF
*----NWEL1
   0
CC
CC NUMBER OF WELLS WITH RATE CHANGES, ID
*----NWEL2   ID
   1       1
CC
CC ID,INJ. RATE AND INJ. COMP. FOR RATE CONS. WELLS FOR EACH PHASE (L=1,3)
*----ID  QI(M,L)  C(M,KC,L)
   1   0.020341 1.0   0.  0.  0.  0.05184  0.0008 0.  0.  0.0  0.0  0.0  0.0  0.0  800.0
   1   0.       0.0   0.  0.  0.  0.       0.     0.  0.  0.0  0.0  0.0  0.0  0.0  0.0
   1   0.       0.0   0.  0.  0.  0.       0.     0.  0.  0.0  0.0  0.0  0.0  0.0  0.0
CC
CC CUM. INJ. TIME , AND INTERVALS (PV) FOR WRITING TO OUTPUT FILES
*----TINJ   CUMPR1  CUMHI1(PROFIL)  WRHPV(HIST) WRPRF(PLOT) RSTC
   5.45  0.01    0.01          0.01        0.01        0.1
CC
CC FOR IMES=2 ,THE INI. TIME STEP,CONC. TOLERANCE,MAX.,MIN. Courant No.
*----DT      DCLIM   CNMAX   CNMIN
   0.0001   0.01    0.1     0.01
CC
CC IRO, ITIME, NEW FLAGS FOR ALL THE WELLS (SURF/POLYMER)
*---- IRO ITIME IFLAG
    2   1     1  2  2  2
CC
CC NUMBER OF WELLS CHANGES IN LOCATION OR SKIN OR PWF
*----NWEL1
   0
CC
CC NUMBER OF WELLS WITH RATE CHANGES, ID
*----NWEL2   ID
   1       1
```

```
CC
CC ID,INJ. RATE AND INJ. COMP. FOR RATE CONS. WELLS FOR EACH PHASE (L=1,3)
*----ID  QI(M,L)  C(M,KC,L)
    1   0.020341 1.0   0.  0.  0.  0.01082  0.001  0.  0.  0.0  0.0  0.0  0.0  0.0  0.0
    1   0.       0.0   0.  0.  0.  0.       0.     0.  0.  0.0  0.0  0.0  0.0  0.0  0.0
    1   0.       0.0   0.  0.  0.  0.       0.     0.  0.  0.0  0.0  0.0  0.0  0.0  0.0
CC
CC CUM. INJ. TIME , AND INTERVALS (PV) FOR WRITING TO OUTPUT FILES
*----TINJ   CUMPR1  CUMHI1(PROFIL)  WRHPV(HIST) WRPRF(PLOT) RSTC
    7.45   0.01    0.01            0.01        0.01        1
CC
CC FOR IMES=2 ,THE INI. TIME STEP,CONC. TOLERANCE,MAX.,MIN. Courant No.
*----DT       DCLIM   CNMAX   CNMIN
    0.0001   0.01    0.1     0.01
```

Appendix B: Input Data for Chapter 5 Base Case Run (#1)

```
CC*********************************************************************
CC                                                                     *
CC   BRIEF DESCRIPTION OF DATA SET                                      *
CC                                                                     *
CC*********************************************************************
CC  SENSITIVITY STUDY - CDG Flooding                                    *
CC  Polymer/CDG Parameters Based on SPE #59466 Match                    *
CC                                                                     *
CC  Water Flood BASE CASE:        Water (2PV)                           *
CC  GRID BLOCKS: 20*20*2          COORDINATES : CARTESIAN               *
CC  GRID SIZE (ft): 29*29*10      Reservoir Pressure: 1885 psi          *
CC  POROSITY : 0.23               Reservoir Depth: 3600 ft              *
CC  Perm Contrast (mD): 1000:100  Injection (ft^3/day): 1547.44         *
CC  DATE : May 14th, 2012         Kv/Kh = 0.1                           *
CC                                                                     *
CC*********************************************************************
CC
CC*********************************************************************
CC                                                                     *
CC   RESERVOIR DESCRIPTION                                             *
CC                                                                     *
CC*********************************************************************
CC
CC
*----RUNNO
CDGSYN
CC
CC
*----HEADER
CDG Sensitivity Study, Base Case
Studying: Perm Contrast; Kv/Kh; CDG Injection Concentration
Polymer & CDG Parameters Based on SPE #59466 Match
CC
CC SIMULATION FLAGS
*---- IMODE IMES IDISPC IREACT  ICOORD ITREAC ITC  IENG
     1    2   3     1      1     0     0   0
CC
CC NUMBER OF GRID BLOCKS AND FLAG SPECIFIES CONSTANT OR VARIABLE GRID
SIZE
*----NX   NY  NZ  IDXYZ  IUNIT
    20   20  2   2     0
CC
CC  VARIABLE GRID BLOCK SIZE IN X
*----DX(I)
    800*29
CC
```

```
CC  VARIABLE GRID BLOCK SIZE IN Y
*----DY(J)
    800*29
CC
CC  VARIABLE GRID BLOCK SIZE IN Z
*----DZ(K)
    800*10
CC
CC TOTAL NO. OF COMPONENTS, NO. OF TRACERS, NO. OF GEL COMPONENTS
*----N   NTW  NG
    14  0    6
CC
CC
*---- SPNAME(I),I=1,N
WATER
OIL
none
POLYMER
CHLORIDE
CALCIUM
none
none
none
none
none
none
none
CDG
CC
CC FLAG INDICATING IF THE COMPONENT IS INCLUDED IN CALCULATIONS OR NOT
*----ICF(KC) FOR KC=1,N
    1  1  0  1  1  1  0 0 0 0 0 0 0 1
CC
CC*****************************************************************
CC                                                                *
CC    OUTPUT OPTIONS                                               *
CC                                                                *
CC*****************************************************************
CC
CC
CC  FLAG FOR PV OR DAYS FOR OUTPUT AND STOP THE RUN
*----ICUMTM  ISTOP
    1       1
CC
CC FLAG INDICATING IF THE PROFILE OF KCTH COMPONENT SHOULD BE WRITTEN
*----IPRFLG(KC),KC=1,N
    1  1  0  1  1  1 0 0 0 0 0 0 0  1
CC
CC FLAG FOR PRES,SAT.,TOTAL CONC.,TRACER CONC.,CAP.,GEL, ALKALINE PROFILES
```

```
*----IPPRES IPSAT IPCTOT IPGEL  ITEMP
   1     1    1     1     0
CC
CC FLAG FOR WRITING SEVERAL PROPERTIES
*----ICKL IVIS IPER ICNM  ICSE
   0   1   0   0    0
CC
CC FLAG FOR WRITING SEVERAL PROPERTIES TO PROF
*----IADS  IVEL IRKF IPHSE
   0    0   1   0
CC
CC*********************************************************************
CC                                                                    *
CC   RESERVOIR PROPERTIES                                             *
CC                                                                    *
CC*********************************************************************
CC
CC
CC MAX. SIMULATION TIME (PV)
*---- TMAX
    2.00
CC
CC ROCK COMPRESSIBILITY (1/psi), STAND. PRESSURE(psi)
*----COMPR   PSTAND
   0.      1885.0
CC
CC  FLAGS  INDICATING  CONSTANT  OR  VARIABLE  POROSITY,  X,Y,AND  Z
PERMEABILITY
*----IPOR1 IPERMX IPERMY IPERMZ  IMOD  ITRNZ  INTG
   0    2     3     3      0    0     0
CC
CC CONSTANT POROSITY
*----PORC1
   800*0.23
CC
CC VARIABLE X-PERMEABILITY (MILIDARCY)
*----PERMX(I), for I=1 TO NX * NY * NZ
   400*1000 400*100
CC
CC Y-PERMEABILITY MULTIPLIER
*----FACTY
   1
CC
CC Z-PERMEABILITY MULTIPLIER
*----FACTZ
   0.1
CC
CC FLAG FOR CONSTANT OR VARIABLE DEPTH, PRESSURE, WATER SATURATION
*----IDEPTH  IPRESS  ISWI
```

```
   0      0      0
CC
CC CONSTANT DEPTH (ft)
*----D111
   3600.0
CC
CC CONSTANT PRESSURE (psi)
*----PRESS1
   1885.0
CC
CC CONSTANT INITIAL WATER SATURATION
*----SWI
   0.25
CC
CC CONSTANT CHLORIDE AND CALCIUM CONCENTRATIONS (MEQ/ML)
*----C50       C60
   0.05184   0.0008
CC
CC*********************************************************************
CC                                                                    *
CC   PHYSICAL PROPERTY DATA                                           *
CC                                                                    *
CC*********************************************************************
CC
CC
CC CMC
*----  EPSME
    .0001
CC SLOPE AND INTERCEPT OF BINODAL CURVE AT ZERO, OPT., AND 2XOPT SALINITY
CC FOR ALCOHOL 1
*----HBNS70 HBNC70 HBNS71 HBNC71 HBNS72 HBNC72
   0.    .030   0.   .030    0.0   .030
CC SLOPE AND INTERCEPT OF BINODAL CURVE AT ZERO, OPT., AND 2XOPT SALINITY
CC FOR ALCOHOL 2
*----HBNS80 HBNC80 HBNS81 HBNC81 HBNS82 HBNC82
   0.    0.    0.    0.    0.    0.
CC
CC LOWER AND UPPER EFFECTIVE SALINITY FOR ALCOHOL 1 AND ALCOHOL 2
*----CSEL7  CSEU7  CSEL8  CSEU8
   .65   .9   0.    0.
CC
CC THE CSE SLOPE PARAMETER FOR CALCIUM AND ALCOHOL 1 AND ALCOHOL 2
*----BETA6  BETA7  BETA8
   0.0   0.    0.
CC
CC FLAG FOR ALCOHOL PART. MODEL AND PARTITION COEFFICIENTS
*----IALC  OPSK7O  OPSK7S  OPSK8O  OPSK8S
   0    0.     0.     0.     0.
CC
```

```
CC NO. OF ITERATIONS, AND TOLERANCE
*----NALMAX   EPSALC
   20       .0001
CC
CC ALCOHOL 1 PARTITIONING PARAMETERS IF IALC=1
*----AKWC7   AKWS7  AKM7  AK7     PT7
   4.671   1.79   48.   35.31   .222
CC
CC ALCOHOL 2 PARTITIONING PARAMETERS IF IALC=1
*----AKWC8   AKWS8  AKM8  AK8     PT8
   0.      0.     0.    0.      0.
CC
CC
*----IFT MODEL FLAG
   0
CC
CC INTERFACIAL TENSION PARAMETERS
*----G11  G12     G13   G21   G22    G23
   13.  -14.8   .007  13.2   -14.5  .010
CC
CC LOG10 OF OIL/WATER INTERFACIAL TENSION
*----XIFTW
   1.477
CC
CC CAPILLARY DESATURATION PARAMETERS FOR PHASE 1, 2, AND 3
*----ITRAP   T11        T22        T33
   0       1865.      28665.46   364.2
CC
CC REL. PERM. AND PC CURVES
*---- IPERM    IRTYPE
    0        0
CC
CC FLAG FOR CONSTANT OR VARIABLE REL. PERM. PARAMETERS
*----ISRW  IPRW  IEW
   0     0     0
CC
CC CONSTANT RESIDUAL SATURATIONS OF PHASES 1,2,AND 3 AT LOW CAPILLARY
NO.
*----S1RWC   S2RWC   S3RWC
   0.25    0.25    0.147
CC
CC CONSTANT ENDPOINT REL. PERM. OF PHASES 1,2,AND 3 AT LOW CAPILLARY NO.
*----P1RW  P2RW   P3RW
   .25   .35    .13771
CC
CC CONSTANT REL. PERM. EXPONENT OF PHASES 1,2,AND 3 AT LOW CAPILLARY NO.
*----E1W   E2W   E3W
   5.0   2.5   2.1817
CC
```

```
CC WATER AND OIL VISCOSITY , RESERVOIR TEMPERATURE
*----VIS1   VIS2  TEMPV
   0.6    9.0   113
CC
CC VISCOSITY PARAMETERS
*----ALPHA1 ALPHA2  ALPHA3  ALPHA4    ALPHA5
   0.0    0.0     0.0     0.000865  4.153
CC
CC PARAMETERS TO CALCULATE POLYMER VISCOSITY AT ZERO SHEAR RATE
*----AP1     AP2     AP3
   520.8   0.0     0.0
CC
CC PARAMETER TO COMPUTE CSEP,MIN. CSEP, AND SLOPE OF LOG VIS. VS. LOG CSEP
*----BETAP CSE1  SSLOPE
   .0    .01   .0
CC
CC PARAMETER FOR SHEAR RATE DEPENDENCE OF POLYMER VISCOSITY
*----GAMMAC  GAMHF  POWN    IPMOD   ishear  rweff   GAMHF2   IWREATH
   3.97    13.7   1.6     0       0       0.25    0        1
CC
CC WREATH CORRELATION PARAMETERS
*----WREATHM  WREATHB  WREATHN  WREATHT
   4.7      0.18     0.48     1.0
CC
CC FLAG FOR POLYMER PARTITIONING, PERM. REDUCTION PARAMETERS
*----IPOLYM EPHI3 EPHI4 BRK    CRK    RKCUT
   1      1.    1     100.   0.32   10
CC
CC SPECIFIC WEIGHT FOR COMPONENTS 1,2,3,7,AND 8 , AND GRAVITY FLAG
*----DEN1    DEN2    DEN3    DEN7    DEN8  IDEN
   62.899  49.857  62.399  49.824  0     2
CC
CC  FLAG FOR CHOICE OF UNITS ( 0:BOTTOMHOLE CONDITION , 1: STOCK TANK)
*-----ISTB
     0
CC
CC COMPRESSIBILITY FOR VOL. OCCUPYING COMPONENTS 1,2,3,7,AND 8
*----COMPC(1)  COMPC(2)  COMPC(3)  COMPC(7)  COMPC(8)
   0.        0.        0.        0.        0.
CC
CC CONSTANT OR VARIABLE PC PARAM., WATER-WET OR OIL-WET PC CURVE FLAG
*----ICPC   IEPC  IOW
   0      0     0
CC
CC CAPILLARY PRESSURE PARAMETERS, CPC
*---- CPC
     0.
CC
CC CAPILLARY PRESSURE PARAMETERS, EPC
```

```
*---- EPC
     2.
CC
CC MOLECULAR DIFFUSIVITY OF KCTH COMPONENT IN PHASE 1 (D(KC),KC=1,N)
*----D(1) D(2) D(3) D(4) D(5) D(6)
    0.  0.  0.  0.  0.  0. 0.0 0.0 0.0 0.0 0.0 0.0 0.0 0.0
CC
CC MOLECULAR DIFFUSIVITY OF KCTH COMPONENT IN PHASE 2 (D(KC),KC=1,N)
*----D(1) D(2) D(3) D(4) D(5) D(6)
    0.  0.  0.  0.  0.  0. 0.0 0.0 0.0 0.0 0.0 0.0 0.0 0.0
CC
CC MOLECULAR DIFFUSIVITY OF KCTH COMPONENT IN PHASE 3 (D(KC),KC=1,N)
*----D(1) D(2) D(3) D(4) D(5) D(6)
    0.  0.  0.  0.  0.  0. 0.0 0.0 0.0 0.0 0.0 0.0 0.0  0.0
CC
CC LONGITUDINAL AND TRANSVERSE DISPERSIVITY OF PHASE 1
*----ALPHAL(1)     ALPHAT(1)
    2.9          2.9
CC
CC LONGITUDINAL AND TRANSVERSE DISPERSIVITY OF PHASE 2
*----ALPHAL(2)     ALPHAT(2)
    2.9          2.9
CC
CC LONGITUDINAL AND TRANSVERSE DISPERSIVITY OF PHASE 3
*----ALPHAL(3)     ALPHAT(3)
    2.0          0.4
CC
CC SURFACTANT AND POLYMER ADSORPTION PARAMETERS
*----AD31     AD32  B3D    AD41   AD42    B4D  IADK, IADS1, FADS refk
    0.       .0    1000.  1.153  0.      100  0     0      0    0
CC
CC PARAMETERS FOR CATION EXCHANGE OF CLAY AND SURFACTANT
*----QV     XKC   XKS  EQW
    0      0.    0.   804
CC
CC
*----KGOPT
    5
CC
CC PARAMETERS FOR CDG GEL OPTION
*----IRKCDG, RKCUTCDG, CDGD,    CDGE,   CDGB,  GAMMACG
    2       200.0     0.00047  1.5804  -0.06  85.22242182
CC
CC PARAMETERS FOR CDG GEL OPTION
*----CDGMU, CDGSIG, CDGC, CDGF
    -0.18  2.44    56.9  -0.06
CC
CC PARAMETERS FOR CDG RETENTION
*----ADCDG,      BDCDG     ADCDGILM   TolCcdgRk
```

```
   0.015302   0.01293   1.25      1d-1
CC
CC CDG viscosity parametrs
*----CDGETA,  CDGKH,  VISCDGA,  VISCDGB,  CDGPOWN
   2730.183  1.0177  0.004621  996.9207  0.859
CC
CC*********************************************************************
CC                                                                     *
CC   WELL DATA                                                         *
CC                                                                     *
CC*********************************************************************
CC
CC
CC TOTAL NUMBER OF WELLS, WELL RADIUS FLAG, FLAG FOR TIME OR COURANT
NO.
*----NWELL   IRO   ITIME  NWREL
   3      2    1     3
CC
CC WELL ID,LOCATIONS,AND FLAG FOR SPECIFYING WELL TYPE, WELL RADIUS, SKIN
*----IDW   IW    JW    IFLAG    RW       SWELL  IDIR   IFIRST  ILAST  IPRF
   1    1    1    1       .50      0.    3     1      2     0
CC
CC WELL NAME
*---- WELNAM
INJECT
CC
CC ICHEK MAX. AND MIN. ALLOWABLE BOTTOMHOLE PRESSURE AND RATE
*----ICHEK   PWFMIN   PWFMAX  QTMIN   QTMAX
   0      0.0     5801.6  0.0    5615.
CC
CC WELL ID, LOCATION, AND FLAG FOR SPECIFYING WELL TYPE, WELL RADIUS, SKIN
*----IDW  IW   JW   IFLAG    RW       SWELL  IDIR  IFIRST   ILAST    IPRF
   2   20   20   2       .50      0.    3    1       1       0
CC
CC WELL NAME
*---- WELNAM
PHIGH
CC
CC MAX. AND MIN. ALLOWABLE BOTTOMHOLE PRESSURE AND RATE
*----ICHEK  PWFMIN   PWFMAX  QTMIN   QTMAX
   0     0.0     5000.   0.0    50000.
C
CC WELL ID, LOCATION, AND FLAG FOR SPECIFYING WELL TYPE, WELL RADIUS, SKIN
*----IDW  IW   JW   IFLAG    RW      SWELL  IDIR  IFIRST   ILAST    IPRF
   3   20   20   2       .50     0.    3    2       2       0
CC
CC WELL NAME
*---- WELNAM
PLOW
```

```
CC
CC MAX. AND MIN. ALLOWABLE BOTTOMHOLE PRESSURE AND RATE
*----ICHEK  PWFMIN   PWFMAX  QTMIN   QTMAX
   0     0.0     5000.  0.0    50000.
CC
CC ID,INJ. RATE AND INJ. COMP. FOR RATE CONS. WELLS FOR EACH PHASE (L=1,3)
*----ID  QI(M,L)  C(M,KC,L)
   1  1547.44  1.0  0.  0.  0.  0.01082  0.001  0.  0.  0.0  0.0  0.0  0.0  0.0  0.0
   1  0.      0.0  0.  0.  0.  0.      0.     0.  0.  0.0  0.0  0.0  0.0  0.0  0.0
   1  0.      0.0  0.  0.  0.  0.      0.     0.  0.  0.0  0.0  0.0  0.0  0.0  0.0
CC
CC ID, BOTTOM HOLE PRESSURE FOR PRESSURE CONSTRAINT WELL (IFLAG=2 OR 3)
*----ID   PWF
   2   1885.0
CC
CC ID, BOTTOM HOLE PRESSURE FOR PRESSURE CONSTRAINT WELL (IFLAG=2 OR 3)
*----ID   PWF
   3   1885.0
CC
CC CUM. INJ. TIME , AND INTERVALS (PV) FOR WRITING TO OUTPUT FILES
*----TINJ   CUMPR1  CUMHI1    WRHPV  WRPRF     RSTC
   2.00   0.01    0.01      0.01   0.01      1
CC
CC FOR IMES=2, THE INI. TIME STEP,CONC. TOLERANCE,MAX.,MIN. COURANT NO.
*----DT     DCLIM    CNMAX  CNMIN
   0.0001  0.01     0.1    0.01
```

Appendix C: Input Data for Chapter 5 Base Case Run (#2)

```
CC*********************************************************************
CC                                                                     *
CC   BRIEF DESCRIPTION OF DATA SET                                      *
CC                                                                     *
CC*********************************************************************
CC  SENSITIVITY STUDY - CDG Flooding - WATERFLOODING BASE CASE       *
CC  Polymer/CDG Parameters Based on Previous Experiment Match         *
CC  CDG Rk Parameters Edited; Long-Term Rk Model Reworked             *
CC                                                                    *
CC  Water Flood BASE CASE:          Water (2 PV)                      *
CC  GRID BLOCKS: 20*20*2           COORDINATES : CARTESIAN           *
CC  GRID SIZE (ft): 29*29*10       Reservoir Pressure: 1885 psi      *
CC  POROSITY : 0.23                Reservoir Depth: 3600 ft          *
CC  Perm Contrast (mD): 1000:100   Injection (ft^3/day): 1547.44      *
CC  DATE : May 25th, 2012          Kv/Kh = 0.1                       *
CC*********************************************************************
CC
CC*********************************************************************
CC                                                                     *
CC   RESERVOIR DESCRIPTION                                             *
CC                                                                     *
CC*********************************************************************
CC
CC
*----RUNNO
CDGSYN
CC
CC
*----HEADER
CDG Sensitivity Study, WATERFLOODING Base Case
Studying: Perm Contrast; Kv/Kh; CDG Injection Concentration
Polymer & CDG Parameters Based on Experiment Match; CDG Rk Parameters Updated
CC
CC SIMULATION FLAGS
*---- IMODE IMES IDISPC IREACT  ICOORD ITREAC ITC  IENG
     1    2   3     1      1     0     0   0
CC
CC NUMBER OF GRID BLOCKS AND FLAG SPECIFIES CONSTANT OR VARIABLE GRID
SIZE
*----NX   NY  NZ  IDXYZ  IUNIT
    20   20  2   2     0
CC
CC  VARIABLE GRID BLOCK SIZE IN X
*----DX(I)
    800*29
```

```
CC
CC  VARIABLE GRID BLOCK SIZE IN Y
*----DY(J)
    800*29
CC
CC  VARIABLE GRID BLOCK SIZE IN Z
*----DZ(K)
    800*10
CC
CC TOTAL NO. OF COMPONENTS, NO. OF TRACERS, NO. OF GEL COMPONENTS
*----N   NTW  NG
    14  0    6
CC
CC
*---- SPNAME(I),I=1,N
WATER
OIL
none
POLYMER
CHLORIDE
CALCIUM
none
none
none
none
none
none
none
CDG
CC
CC FLAG INDICATING IF THE COMPONENT IS INCLUDED IN CALCULATIONS OR NOT
*----ICF(KC) FOR KC=1,N
    1  1  0  1  1  1  1  0 0 0 0 0 0 0 0 1
CC
CC**********************************************************************
CC                                                                     *
CC    OUTPUT OPTIONS                                                    *
CC                                                                     *
CC**********************************************************************
CC
CC
CC  FLAG FOR PV OR DAYS FOR OUTPUT AND STOP THE RUN
*----ICUMTM  ISTOP
    1       1
CC
CC FLAG INDICATING IF THE PROFILE OF KCTH COMPONENT SHOULD BE WRITTEN
*----IPRFLG(KC),KC=1,N
    1  1  0  1  1  1  1  0 0 0 0 0 0 0 0  1
CC
```

```
CC FLAG FOR PRES,SAT.,TOTAL CONC.,TRACER CONC.,CAP.,GEL, ALKALINE PROFILES
*----IPPRES IPSAT IPCTOT IPGEL  ITEMP
   1     1    1     1     0
CC
CC FLAG FOR WRITING SEVERAL PROPERTIES
*----ICKL IVIS IPER ICNM  ICSE
   0   1   0   0    0
CC
CC FLAG FOR WRITING SEVERAL PROPERTIES TO PROF
*----IADS  IVEL IRKF IPHSE
   0    0   1   0
CC
CC*************************************************************************
CC                                                                        *
CC   RESERVOIR PROPERTIES                                                  *
CC                                                                        *
CC*************************************************************************
CC
CC
CC MAX. SIMULATION TIME (PV)
*---- TMAX
    2.00
CC
CC ROCK COMPRESSIBILITY (1/psi), STAND. PRESSURE(psi)
*----COMPR   PSTAND
   0.      1885.0
CC
CC  FLAGS  INDICATING  CONSTANT  OR  VARIABLE  POROSITY,  X,Y,AND  Z
PERMEABILITY
*----IPOR1 IPERMX IPERMY IPERMZ  IMOD  ITRNZ  INTG
   0    2     3     3      0    0     0
CC
CC CONSTANT POROSITY
*----PORC1
   800*0.23
CC
CC VARIABLE X-PERMEABILITY (MILIDARCY)
*----PERMX(I), for I=1 TO NX * NY * NZ
   400*1000 400*100
CC
CC Y-PERMEABILITY MULTIPLIER
*----FACTY
   1
CC
CC Z-PERMEABILITY MULTIPLIER
*----FACTZ
   0.1
CC
CC FLAG FOR CONSTANT OR VARIABLE DEPTH, PRESSURE, WATER SATURATION
```

```
*----IDEPTH  IPRESS  ISWI
   0      0      0
CC
CC CONSTANT DEPTH (ft)
*----D111
   3600.0
CC
CC CONSTANT PRESSURE (psi)
*----PRESS1
   1885.0
CC
CC CONSTANT INITIAL WATER SATURATION
*----SWI
   0.25
CC
CC CONSTANT CHLORIDE AND CALCIUM CONCENTRATIONS (MEQ/ML)
*----C50       C60
   0.05184   0.0008
CC
CC*********************************************************************
CC                                                                    *
CC   PHYSICAL PROPERTY DATA                                           *
CC                                                                    *
CC*********************************************************************
CC
CC
CC CMC
*----  EPSME
    .0001
CC SLOPE AND INTERCEPT OF BINODAL CURVE AT ZERO, OPT., AND 2XOPT SALINITY
CC FOR ALCOHOL 1
*----HBNS70 HBNC70 HBNS71 HBNC71 HBNS72 HBNC72
   0.    .030   0.  .030    0.0  .030
CC SLOPE AND INTERCEPT OF BINODAL CURVE AT ZERO, OPT., AND 2XOPT SALINITY
CC FOR ALCOHOL 2
*----HBNS80 HBNC80 HBNS81 HBNC81 HBNS82 HBNC82
   0.    0.    0.    0.    0.    0.
CC
CC LOWER AND UPPER EFFECTIVE SALINITY FOR ALCOHOL 1 AND ALCOHOL 2
*----CSEL7  CSEU7  CSEL8  CSEU8
   .65   .9   0.    0.
CC
CC THE CSE SLOPE PARAMETER FOR CALCIUM AND ALCOHOL 1 AND ALCOHOL 2
*----BETA6  BETA7  BETA8
   0.0   0.    0.
CC
CC FLAG FOR ALCOHOL PART. MODEL AND PARTITION COEFFICIENTS
*----IALC  OPSK7O  OPSK7S  OPSK8O  OPSK8S
   0    0.     0.     0.     0.
```

```
CC
CC NO. OF ITERATIONS, AND TOLERANCE
*----NALMAX   EPSALC
   20       .0001
CC
CC ALCOHOL 1 PARTITIONING PARAMETERS IF IALC=1
*----AKWC7   AKWS7  AKM7  AK7     PT7
   4.671   1.79   48.   35.31   .222
CC
CC ALCOHOL 2 PARTITIONING PARAMETERS IF IALC=1
*----AKWC8   AKWS8  AKM8  AK8     PT8
   0.      0.     0.    0.      0.
CC
CC
*----IFT MODEL FLAG
   0
CC
CC INTERFACIAL TENSION PARAMETERS
*----G11  G12     G13   G21   G22    G23
   13.  -14.8   .007  13.2   -14.5  .010
CC
CC LOG10 OF OIL/WATER INTERFACIAL TENSION
*----XIFTW
   1.477
CC
CC CAPILLARY DESATURATION PARAMETERS FOR PHASE 1, 2, AND 3
*----ITRAP   T11        T22        T33
   0       1865.      28665.46   364.2
CC
CC REL. PERM. AND PC CURVES
*---- IPERM    IRTYPE
    0        0
CC
CC FLAG FOR CONSTANT OR VARIABLE REL. PERM. PARAMETERS
*----ISRW  IPRW  IEW
   0    0    0
CC
CC CONSTANT RESIDUAL SATURATIONS OF PHASES 1,2,AND 3 AT LOW CAPILLARY
NO.
*----S1RWC   S2RWC   S3RWC
   0.25    0.25    0.147
CC
CC CONSTANT ENDPOINT REL. PERM. OF PHASES 1,2,AND 3 AT LOW CAPILLARY NO.
*----P1RW  P2RW   P3RW
   .25   .35    .13771
CC
CC CONSTANT REL. PERM. EXPONENT OF PHASES 1,2,AND 3 AT LOW CAPILLARY NO.
*----E1W   E2W   E3W
   5.0   2.5   2.1817
```

```
CC
CC WATER AND OIL VISCOSITY , RESERVOIR TEMPERATURE
*----VIS1   VIS2  TEMPV
   0.6    9.0   113
CC
CC VISCOSITY PARAMETERS
*----ALPHA1 ALPHA2  ALPHA3  ALPHA4    ALPHA5
   0.0    0.0     0.0     0.000865  4.153
CC
CC PARAMETERS TO CALCULATE POLYMER VISCOSITY AT ZERO SHEAR RATE
*----AP1     AP2     AP3
   520.8   0.0     0.0
CC
CC PARAMETER TO COMPUTE CSEP,MIN. CSEP, AND SLOPE OF LOG VIS. VS. LOG CSEP
*----BETAP CSE1  SSLOPE
   .0    .01   .0
CC
CC PARAMETER FOR SHEAR RATE DEPENDENCE OF POLYMER VISCOSITY
*----GAMMAC  GAMHF  POWN    IPMOD   ishear  rweff   GAMHF2   IWREATH
   3.97    13.7   1.6     0       0       0.25    0        1
CC
CC WREATH CORRELATION PARAMETERS
*----WREATHM  WREATHB  WREATHN  WREATHT
   4.7      0.18     0.48     1.0
CC
CC FLAG FOR POLYMER PARTITIONING, PERM. REDUCTION PARAMETERS
*----IPOLYM EPHI3 EPHI4 BRK    CRK    RKCUT
   1      1.    1     100    0.32   10
CC
CC SPECIFIC WEIGHT FOR COMPONENTS 1,2,3,7,AND 8 , AND GRAVITY FLAG
*----DEN1    DEN2    DEN3    DEN7    DEN8  IDEN
   62.899  49.857  62.399  49.824  0     2
CC
CC  FLAG FOR CHOICE OF UNITS ( 0:BOTTOMHOLE CONDITION , 1: STOCK TANK)
*-----ISTB
     0
CC
CC COMPRESSIBILITY FOR VOL. OCCUPYING COMPONENTS 1,2,3,7,AND 8
*----COMPC(1)  COMPC(2)  COMPC(3)  COMPC(7)  COMPC(8)
   0.        0.        0.        0.        0.
CC
CC CONSTANT OR VARIABLE PC PARAM., WATER-WET OR OIL-WET PC CURVE FLAG
*----ICPC   IEPC  IOW
   0      0     0
CC
CC CAPILLARY PRESSURE PARAMETERS, CPC
*---- CPC
     0.
CC
```

```
CC CAPILLARY PRESSURE PARAMETERS, EPC
*---- EPC
     2.
CC
CC MOLECULAR DIFFUSIVITY OF KCTH COMPONENT IN PHASE 1 (D(KC),KC=1,N)
*----D(1) D(2) D(3) D(4) D(5) D(6)
    0.  0.  0.  0.  0.  0. 0.0 0.0 0.0 0.0 0.0 0.0 0.0 0.0
CC
CC MOLECULAR DIFFUSIVITY OF KCTH COMPONENT IN PHASE 2 (D(KC),KC=1,N)
*----D(1) D(2) D(3) D(4) D(5) D(6)
    0.  0.  0.  0.  0.  0. 0.0 0.0 0.0 0.0 0.0 0.0 0.0 0.0
CC
CC MOLECULAR DIFFUSIVITY OF KCTH COMPONENT IN PHASE 3 (D(KC),KC=1,N)
*----D(1) D(2) D(3) D(4) D(5) D(6)
    0.  0.  0.  0.  0.  0. 0.0 0.0 0.0 0.0 0.0 0.0 0.0  0.0
CC
CC LONGITUDINAL AND TRANSVERSE DISPERSIVITY OF PHASE 1
*----ALPHAL(1)     ALPHAT(1)
    2.9           2.9
CC
CC LONGITUDINAL AND TRANSVERSE DISPERSIVITY OF PHASE 2
*----ALPHAL(2)     ALPHAT(2)
    2.9           2.9
CC
CC LONGITUDINAL AND TRANSVERSE DISPERSIVITY OF PHASE 3
*----ALPHAL(3)     ALPHAT(3)
    2.0           0.4
CC
CC SURFACTANT AND POLYMER ADSORPTION PARAMETERS
*----AD31     AD32  B3D    AD41   AD42    B4D  IADK, IADS1, FADS refk
    0.       .0    1000.  1.153  0.      100  0     0      0    0
CC
CC PARAMETERS FOR CATION EXCHANGE OF CLAY AND SURFACTANT
*----QV     XKC   XKS  EQW
    0      0.    0.   804
CC
CC
*----KGOPT
    5
CC
CC PARAMETERS FOR CDG GEL OPTION
*----IRKCDG, RKCUTCDG, CDGD,    CDGE,   CDGB,  GAMMACG
    2       200.0     0.00047  1.58    -0.06  85.0
CC
CC PARAMETERS FOR CDG GEL OPTION
*----CDGMU, CDGSIG, CDGC,  CDGF
    -0.52  2.30    56.9   -2.06
CC
CC PARAMETERS FOR CDG RETENTION
```

```
*----ADCDG,     BDCDG    ResRkFact   TolCcdgRk
   0.015302   0.01293   0.80        1d-1
CC
CC CDG viscosity parametrs
*----CDGETA,   CDGKH,  VISCDGA,  VISCDGB,  CDGPOWN
   2730.183  1.0177  0.004621  996.9207  0.859
CC
CC*********************************************************************
CC                                                                     *
CC   WELL DATA                                                         *
CC                                                                     *
CC*********************************************************************
CC
CC
CC TOTAL NUMBER OF WELLS, WELL RADIUS FLAG, FLAG FOR TIME OR COURANT
NO.
*----NWELL   IRO   ITIME  NWREL
   3      2    1     3
CC
CC WELL ID,LOCATIONS,AND FLAG FOR SPECIFYING WELL TYPE, WELL RADIUS, SKIN
*----IDW   IW    JW    IFLAG    RW       SWELL  IDIR   IFIRST  ILAST  IPRF
   1     1     1     1        .50      0.    3     1      2     0
CC
CC WELL NAME
*---- WELNAM
INJECT
CC
CC ICHEK MAX. AND MIN. ALLOWABLE BOTTOMHOLE PRESSURE AND RATE
*----ICHEK   PWFMIN   PWFMAX  QTMIN   QTMAX
   0       0.0      5801.6  0.0     5615.
CC
CC WELL ID, LOCATION, AND FLAG FOR SPECIFYING WELL TYPE, WELL RADIUS, SKIN
*----IDW  IW   JW   IFLAG    RW       SWELL  IDIR  IFIRST   ILAST    IPRF
   2    20   20   2        .50      0.    3     1       1       0
CC
CC WELL NAME
*---- WELNAM
PHIGH
CC
CC MAX. AND MIN. ALLOWABLE BOTTOMHOLE PRESSURE AND RATE
*----ICHEK  PWFMIN   PWFMAX  QTMIN   QTMAX
   0      0.0      5000.   0.0     50000.
C
CC WELL ID, LOCATION, AND FLAG FOR SPECIFYING WELL TYPE, WELL RADIUS, SKIN
*----IDW  IW   JW   IFLAG    RW       SWELL  IDIR  IFIRST   ILAST    IPRF
   3    20   20   2        .50      0.    3     2       2       0
CC
CC WELL NAME
*---- WELNAM
```

```
PLOW
CC
CC MAX. AND MIN. ALLOWABLE BOTTOMHOLE PRESSURE AND RATE
*----ICHEK  PWFMIN   PWFMAX  QTMIN   QTMAX
   0     0.0     5000.   0.0     50000.
CC
CC ID,INJ. RATE AND INJ. COMP. FOR RATE CONS. WELLS FOR EACH PHASE (L=1,3)
*----ID  QI(M,L)  C(M,KC,L)
   1   1547.44  1.0   0.  0.  0.  0.01082  0.001   0.  0.  0.0  0.0  0.0  0.0  0.0  0.0
   1   0.       0.0   0.  0.  0.  0.       0.      0.  0.  0.0  0.0  0.0  0.0  0.0  0.0
   1   0.       0.0   0.  0.  0.  0.       0.      0.  0.  0.0  0.0  0.0  0.0  0.0  0.0
CC
CC ID, BOTTOM HOLE PRESSURE FOR PRESSURE CONSTRAINT WELL (IFLAG=2 OR 3)
*----ID   PWF
   2    1885.0
CC
CC ID, BOTTOM HOLE PRESSURE FOR PRESSURE CONSTRAINT WELL (IFLAG=2 OR 3)
*----ID   PWF
   3    1885.0
CC
CC CUM. INJ. TIME , AND INTERVALS (PV) FOR WRITING TO OUTPUT FILES
*----TINJ    CUMPR1   CUMHI1     WRHPV   WRPRF      RSTC
   2.00    0.01     0.01       0.01    0.01       1
CC
CC FOR IMES=2, THE INI. TIME STEP,CONC. TOLERANCE,MAX.,MIN. COURANT NO.
*----DT      DCLIM     CNMAX   CNMIN
   0.0001  0.01      0.1     0.01
```

Appendix D: Input Data for Chapter 6 Field Case

```
CC*************************************************************************
CC                                                                       *
CC    BRIEF DESCRIPTION OF DATA SET : UTGEL                               *
CC                                                                       *
CC*************************************************************************
CC XYZ AREA 7 spot                                                        *
CC Injection Details and other properties from DW's Input for coreflood C *
CC                                                                       *
CC LENGTH (FT) : 2100          PROCESS: WATERFLOODING BASE CASE (7.3 PV)  *
CC THICKNESS (FT) : 37         INJ. RATE (FT3/DAY) :                      *
CC WIDTH (FT) : 2400           COORDINATES : CARTESIAN                    *
CC POROSITY : variable         PROD. RATE (FT3/DAY):                      *
CC GRID BLOCKS : 11x12x19      1BBL=5.615 cubic feet                      *
CC DATE : 06/15/2009           A1 Sand - original grid size               *
CC                                                                       *
CC*************************************************************************
CC                                                                       *
CC*************************************************************************
CC                                                                       *
CC   RESERVOIR DESCRIPTION                                               *
CC                                                                       *
CC*************************************************************************
CC
CC
*----RUNNO
FIELD
CC
CC
*----HEADER
s-1119
Alcohol Included-DW' paper
Waterflood BASE CASE
CC
CC SIMULATION FLAGS
*---- IMODE IMES IDISPC IREACT ICOORD ITREAC ITC IENG
     1    2   3     0     1     0     0  0
CC
CC NUMBER OF GRID BLOCKS AND FLAG SPECIFIES CONSTANT OR VARIABLE GRID
SIZE
*----NX   NY  NZ  IDXYZ  IUNIT
    11   12  19  2     0
CC Grid Properties Given By Chevron
CC CONSTANT GRID BLOCK SIZE IN X, Y, AND Z  (in ft)
*----DX
300       225       150       150       150
```

```
150       150       150       150       300
225
CC Grid Properties Given By Chevron
CC  CONSTANT GRID BLOCK SIZE IN X, Y, AND Z  (in ft)
*----DY
300       300       150       150.00006         149.99994
150       150       150       150       225
300       225
CC
CC Grid Properties Given By Chevron
*----DZ  (this is mean from NET from ecl2gocad) total thickness is about 68 ft
2 2 2 2 2 2 2 2 2 2 2 2 2 2 2 2 2 1
CC
CC TOTAL NO. OF COMPONENTS, NO. OF TRACERS, NO. OF GEL COMPONENTS
*----N   NTW   NG
    14  0     6
CC
CC  All species must be present even for standard waterflood.
*---- species name
water
oil
surf(M3+IOS)
polymer(AN-125)
anion
calcium
alc(EGBE+t-Pent)
none
none
none
none
none
none
CDG
CC
CC FLAG INDICATING IF THE COMPONENT IS INCLUDED IN CALCULATIONS OR NOT
*----ICF(KC) FOR KC=1,N
    1  1  1  1  1  0  1  0  0  0  0  0  0  0  1
CC
CC*************************************************************************
CC                                                                        *
CC    OUTPUT OPTIONS                                                       *
CC                                                                        *
CC*************************************************************************
CC
CC ICUMTM=0==>TIME PRINTING;istop=1==>PV SPEC
CC FLAGS FOR PV OR DAYS
*----ICUMTM  ISTOP
    1       1
CC
```

```
CC FLAG INDICATING IF THE PROFILE OF KCTH COMPONENT SHOULD BE WRITTEN
*----IPRFLG(KC),KC=1,N
   1 1 1 1 1 0 1 0 0 0 0 0 0 1
CC
CC FLAG FOR PRES,SAT.,TOTAL CONC.,TRACER CONC.,CAP.,GEL, ALKALINE PROFILES
*----IPPRES IPSAT IPCTOT IPGEL IPTEMP
   1     1    1     0    0
CC  ICKL is phase conc.  (K is component and L is phase)
CC FLAG FOR WRITING SEVERAL PROPERTIES TO UNIT 6 (PROFIL)
*----ICKL IVIS IPER ICNM ICSE
   1   1   1   1   1
CC
CC FLAG FOR WRITING SEVERAL PROPERTIES TO UNIT 6 (PROFIL)
*----IADS  IVEL IRKF IPHSE
   1    0   1   1
CC
CC*********************************************************************
CC                                                                     *
CC   RESERVOIR PROPERTIES                                               *
CC                                                                     *
CC*********************************************************************
CC
CC
CC MAX. SIMULATION TIME
*---- TMAX
     7.3
CC
CC ROCK COMPRESSIBILITY (1/PSI), STAND. PRESSURE(PSIA)
*----COMPR      PSTAND
   0.000008   14.7
CC  Porosity Values For Each Grid Input Given Through Include Files
CC      FLAGS  INDICATING  CONSTANT  OR  VARIABLE  POROSITY,  X,Y,AND  Z
PERMEABILITY
*----IPOR1 IPERMX IPERMY IPERMZ  IMOD  ITRANZ  INTG
   4    4     4     4      1    0      0
CC Depth To The Top Layer Input Given Through Include Files
CC FLAG FOR CONSTANT OR VARIABLE DEPTH, PRESSURE, WATER SATURATION
*----IDEPTH  IPRESS  ISWI
   4      1      0
CC
CC  4/10/2009 - Chevron
*----PINIT    HINIT
   550.     1965.77185
CC  4/10/2009 - Chevron
CC WATER SATURATION
*----SWI
   0.2
CC
CC FLAG FOR RESERVOIR PROPERTY MODIFICATION
```

```
*----IMPOR  IMKX  IMKY  IMKZ  IMSW
   0     1     1     1     0
CC
CC NUMBER OF REGIONS WITH MODIFIED X PERMEABILITY
*---- NMOD1
    17
CC
CC FIRST AND LAST INDEX IN X,Y,Z DIRECTION,MODIFIED METHOD,CONSTANT
VALUE.
*---- IMIN   IMAX   JMIN   JMAX   KMIN   KMAX   IFACT   FACTX
     4  4      4      4      19     19     2      0.3826
        8      8      4      4      19     19     2      0.6546
        9      9      7      7      19     19     2      0.3729
        8      8      10     10     19     19     2      0.3708
        4      4      10     10     19     19     2      0.3561
        3      3      7      7      19     19     2      0.3739
        3      3      2      2      19     19     2      0.3117
        9      9      2      2      19     19     2      0.734
        9      9      11     11     19     19     2      0.5459
        3      3      11     11     19     19     2      0.637
        6      6      7      7      19     19     2      0.5878
        6      6      2      2      19     19     2      0.2139
        10     10     4      4      19     19     2      0.6652
        10     10     10     10     19     19     2      0.3931
        6      6      11     11     19     19     2      0.4183
        2      2      10     10     19     19     2      0.5491
        2      2      4      4      19     19     2      0.6232
CC
CC NUMBER OF REGIONS WITH MODIFIED Y PERMEABILITY
*---- NMOD2
    17
CC
CC FIRST AND LAST INDEX IN X,Y,Z DIRECTION,MODIFIED METHOD,CONSTANT
VALUE.
*---- IMIN   IMAX   JMIN   JMAX   KMIN   KMAX   IFACT   FACTX
     4  4      4      4      19     19     2      0.3826
        8      8      4      4      19     19     2      0.6546
        9      9      7      7      19     19     2      0.3729
        8      8      10     10     19     19     2      0.3708
        4      4      10     10     19     19     2      0.3561
        3      3      7      7      19     19     2      0.3739
        3      3      2      2      19     19     2      0.3117
        9      9      2      2      19     19     2      0.734
        9      9      11     11     19     19     2      0.5459
        3      3      11     11     19     19     2      0.637
        6      6      7      7      19     19     2      0.5878
        6      6      2      2      19     19     2      0.2139
        10     10     4      4      19     19     2      0.6652
        10     10     10     10     19     19     2      0.3931
```

```
          6       6       11      11      19      19      2       0.4183
          2       2       10      10      19      19      2       0.5491
          2       2       4       4       19      19      2       0.6232
CC
CC NUMBER OF REGIONS WITH MODIFIED Z PERMEABILITY
*---- NMOD3
     17
CC
CC  FIRST  AND  LAST  INDEX  IN  X,Y,Z  DIRECTION,MODIFIED  METHOD,CONSTANT
VALUE.
*---- IMIN   IMAX   JMIN   JMAX   KMIN   KMAX   IFACT   FACTX
      4  4       4       4       19      19      2       0.3826
          8       8       4       4       19      19      2       0.6546
          9       9       7       7       19      19      2       0.3729
          8       8       10      10      19      19      2       0.3708
          4       4       10      10      19      19      2       0.3561
          3       3       7       7       19      19      2       0.3739
          3       3       2       2       19      19      2       0.3117
          9       9       2       2       19      19      2       0.734
          9       9       11      11      19      19      2       0.5459
          3       3       11      11      19      19      2       0.637
          6       6       7       7       19      19      2       0.5878
          6       6       2       2       19      19      2       0.2139
          10      10      4       4       19      19      2       0.6652
          10      10      10      10      19      19      2       0.3931
          6       6       11      11      19      19      2       0.4183
          2       2       10      10      19      19      2       0.5491
          2       2       4       4       19      19      2       0.6232
CC formation water  (3000 ppm NaCl)
CC CONSTANT CHLORIDE AND CALCIUM CONCENTRATIONS (MEQ/ML)
*----C50       C60
    0.0513    0.0
CC
CC*************************************************************************
CC utchem requires 2 alochols                                                 *
CC PHYSICAL PROPERTY DATA                                                     *
CC                                                                           *
CC*************************************************************************
CC
CC DW
CC OIL CONC. AT PLAIT POINT FOR TYPE II(+) AND TYPE II(-), CMC (do not change)
*---- EPSME
     0.0001
CC SLOPE AND INTERCEPT OF BINODAL CURVE AT ZERO, OPT., AND 2XOPT SALINITY
CC  DW'S INPUT FILE FOR CORE FLOOD C (SPE 113965)
*----HBNS70 HBNC70 HBNS71 HBNC71 HBNS72 HBNC72
    0.0    0.055  0      0.035  0.     0.055
CC SLOPE AND INTERCEPT OF BINODAL CURVE AT ZERO, OPT., AND 2XOPT SALINITY
CC FOR ALCOHOL 2
```

```
*----HBNS80 HBNC80 HBNS81 HBNC81 HBNS82 HBNC82
   0.    0.    0.    0.    0.    0.
CC DW'S INPUT FILE FOR CORE FLOOD C (SPE 113965)
CC LOWER AND UPPER EFFECTIVE SALINITY FOR ALCOHOL 1(7) AND ALCOHOL 2 (8)
*----CSEL7    CSEU7    CSEL8  CSEU8
   0.5      0.85     0.    0.
CC DW'S INPUT FILE FOR CORE FLOOD C (SPE 113965)
CC THE CSE SLOPE PARAMETER FOR CALCIUM AND ALCOHOL 1 AND ALCOHOL 2
*----BETA6  BETA7  BETA8
   0.0    0    0.0
CC DW'S INPUT FILE FOR CORE FLOOD C (SPE 113965)
CC FLAG FOR ALCOHOL PART. MODEL AND PARTITION COEFFICIENTS
*----IALC  OPSK7O  OPSK7S  OPSK8O  OPSK8S
   0    0.0     0     0.     0.
CC
CC NO. OF ITERATIONS, AND TOLERANCE
*----NALMAX   EPSALC
   20       .0001
CC DW'S INPUT FILE FOR CORE FLOOD C (SPE 113965)
CC ALCOHOL 1 PARTITIONING PARAMETERS IF IALC=1  (leave as is)
*----AKWC7   AKWS7  AKM7  AK7    PT7
   4.671    1.79   48   35.31  0.222
CC
CC ALCOHOL 2 PARTITIONING PARAMETERS IF IALC=1
*----AKWC8   AKWS8  AKM8  AK8    PT8
   0.      0.    0.    0.     0.
CC
CC  0 = Healy and Reed and 1 is Chun-Huh
*--- ift
   1
CC
CC INTERFACIAL TENSION PARAMETERS
*----CHUH  AHUH
   0.3   10.
CC
CC LOG10 OF OIL/WATER INTERFACIAL TENSION
*----XIFTW
   1.48
CC
CC CAPILLARY DESATURATION PARAMETERS FOR PHASE 1, 2, AND 3
*----ITRAP   T11        T22        T33
   2      2000.      75000.     365.
CC  UTCHEM9P9: new input data
CC relative perm. flag (0:imbibition corey,1:first drainage corey
*----iperm     IRTYPE
   0          0
CC RESIDUAL SATURATION FOR EACH PHASE INPUT GIVEN THROUGH INCLUDE FILES
CC FLAG FOR CONSTANT OR VARIABLE REL. PERM. PARAMETERS
*----ISRW  IPRW  IEW
```

```
   4     0   0
CC  CHEVRON - 04/10/2009
CC CONSTANT ENDPOINT REL. PERM. OF PHASES 1,2,AND 3 AT LOW CAPILLARY NO.
*----P1RW  P2RWZ P3RW
   .30  0.7  0.30
CC CHEVRON - 04/10/2009
CC CONSTANT REL. PERM. EXPONENT OF PHASES 1,2,AND 3 AT LOW CAPILLARY NO.
*----E1W   E2W  E3W
   2    2   2
CC
CC  RES. SATURATION OF PHASES 1,2,AND 3 AT HIGH CAPILLARY NO.
*----S1RC(=SWIR)  S2RC(=SORCHEM)  S3RC(SMER=SWIR)
   0.0001    0.0001   0.0001
CC
CC ENDPOINT REL. PERM. OF PHASES 1,2,AND 3 AT HIGH CAPILLARY NO.
*----P1RC P2RC P3RC
   1.   1.   1.
CC
CC REL. PERM. EXPONENT OF PHASES 1,2,AND 3 AT HIGH CAPILLARY NO.
*----E13CW  E23C E31C
   1   1   1
CC SPE 113965
CC  WATER  AND  OIL  VISCOSITY  at  reference  temperature,  RESERVOIR  TEMPERATURE
(leave zero)
*----VIS1   VIS2  TEMPV
   0.37   3.4    0.
CC DW'S INPUT FILE FOR CORE FLOOD C (SPE 113965)
CC MICROEMULSION VISCOSITY PARAMETERS
*----ALPHA1 ALPHA2  ALPHA3  ALPHA4  ALPHA5
     .1    2.5    0.1      0.1    0.1
CC DW'S INPUT FILE FOR CORE FLOOD C (SPE 113965)
CC PARAMETERS TO CALCULATE POLYMER VISCOSITY AT ZERO SHEAR RATE
*----AP1     AP2    AP3
  45       625    1000
CC  DW'S INPUT FILE FOR CORE FLOOD C (SPE 113965)
CC PARAMETER TO COMPUTE CSEP,MIN. CSEP, AND SLOPE OF LOG VIS. VS. LOG CSEP
*----BETAP CSE1  SSLOPE
   1.   .01   -0.377
CC  DW'S INPUT FILE FOR CORE FLOOD C (SPE 113965)
CC PARAMETER FOR SHEAR RATE DEPENDENCE OF POLYMER VISCOSITY (50% shear ~
10 cP)
*----GAMMAC  GAMHF  POWN   IPMOD  ISHEAR   RWEFF  GAMHF2  IWREATH
    4      30   1.8    0       1      0.4   0.0    1
CC
CC WREATH CORRELATION PARAMETERS
*----WREATHM  WREATHB  WREATHN  WREATHT
   4.7     0.18    0.48    1.0
CC
CC FLAG FOR POLYMER (4) PARTITIONING, PERM. REDUCTION PARAMETERS
```

```
*----IPOLYM EPHI3 EPHI4   BRK    CRK    rkcut
    1      1.   1       100   0.04      10
CC
CC SPECIFIC WEIGHT FOR COMPONENTS 1,2,3,7,AND 8 , AND GRAVITY FLAG
*----DEN1  DEN2  DEN3 DEN7 DEN8 IDEN
    .433  .377  .433 .346  0.  2
CC
CC  FLAG FOR CHOICE OF UNITS ( 0:BOTTOMHOLE CONDITION , 1: STOCK TANK)
*-----ISTB
     1
CC
CC  FVF FOR PHASE 1,2,3
*-----(FVF(L),L=1,NPHAS)
     1    1.083    1
CC
CC COMPRESSIBILITY FOR VOL. OCCUPYING COMPONENTS 1,2,3,7,AND 8
*----COMPC(1)  COMPC(2)  COMPC(3)  COMPC(7)  COMPC(8)
    0.000003   0.00001        0.        0.        0.
CC
CC CONSTANT OR VARIABLE PC PARAM., WATER-WET OR OIL-WET PC CURVE FLAG
*----ICPC   IEPC  IOW
    0       0     0
CC
CC CAPILLARY PRESSURE PARAMETERS, CPC
*----CPC
    0.
CC
CC CAPILLARY PRESSURE PARAMETERS, EPC
*---- EPC
     2.
CC
CC MOLECULAR DIFFUSIVITY OF KCTH COMPONENT IN PHASE 1 (D(KC),KC=1,N)
*----D(1) D(2) D(3) D(4) D(5) D(6) D(7) D(8) D(9) D(10) D(1
    0.   0.   0.   0.    0.  0.  8*0.
CC
CC MOLECULAR DIFFUSIVITY OF KCTH COMPONENT IN PHASE 2 (D(KC),KC=1,N)
*----D(1) D(2) D(3) D(4) D(5) D(6) D(7) D(8) D(9)  D(10)  D(11)
    0.   0.   0.   0.   0.   0.  8*0.
CC
CC MOLECULAR DIFFUSIVITY OF KCTH COMPONENT IN PHASE 3 (D(KC),KC=1,N)
*----D(1) D(2) D(3) D(4) D(5) D(6) D(7) D(8) D(9) D(10)  D(11)
    0.   0.   0.   0.   0.   0.   8*0.
CC  Mojdeh
CC LONGITUDINAL AND TRANSVERSE DISPERSIVITY (ft) OF PHASE 1
*----ALPHAL(1)     ALPHAT(1)
    4             0.4
CC Mojdeh
CC LONGITUDINAL AND TRANSVERSE DISPERSIVITY OF PHASE 2
*----ALPHAL(2)     ALPHAT(2)
```

```
    4            0.4
CC Mojdeh
CC LONGITUDINAL AND TRANSVERSE DISPERSIVITY OF PHASE 3
*----ALPHAL(3)     ALPHAT(3)
    4            0.4
CC   Polymer (7 microg/g), surf. (0.3 mg/g)
CC SURFACTANT AND POLYMER ADSORPTION PARAMETERS
*----AD31  AD32  B3D    AD41   AD42  B4D      iadk   iads1   fads refk(mD)
    0.125     0.0  1000.  1   0.    100.       0       0     0   0.
CC
CC PARAMETERS FOR CATION EXCHANGE OF CLAY AND SURFACTANT MW (needed for
cation exch)
*----QV      XKC   XKS  EQW
    0.0     0.0   0.0  429.
CC
CC
*----KGOPT
    5
CC
CC PARAMETERS FOR CDG GEL OPTION
*----IRKCDG, RKCUTCDG, CDGD,    CDGE,   CDGB,  GAMMACG
    2       200.0     0.00047  1.58    -0.06  85.0
CC
CC PARAMETERS FOR CDG GEL OPTION
*----CDGMU, CDGSIG, CDGC,  CDGF
    -0.52  2.30    56.9   -2.06
CC
CC PARAMETERS FOR CDG RETENTION
*----ADCDG,      BDCDG     ResRkFact   TolCcdgRk
    0.015302    0.01293   0.80        1d-1
CC
CC CDG viscosity parametrs
*----CDGETA,   CDGKH,  VISCDGA,  VISCDGB,  CDGPOWN
    2730.183  1.0177  0.004621  996.9207  0.859
CC
CC**************************************************************************
CC                                                                         *
CC  WELL DATA                                                               *
CC                                                                          *
CC**************************************************************************
CC
CC
CC TOTAL NUMBER OF WELLS, WELL RADIUS FLAG, FLAG FOR TIME OR COURANT
NO.
*----NWELL   IRO   ITIME  NWELR
     17     2     1     17
CC 4/10/2009
CC WELL ID,LOCATIONS,AND FLAG FOR SPECIFYING WELL TYPE, WELL RADIUS, SKIN
*----IDW  IW   JW   IFLAG    RW     SWELL  IDIR  IFIRST   ILAST    IPRF
```

```
    1  4    4    1    0.4    0    3    1       19       1
cc
cc
*----kprf
    1 1 1 1 1 1 1 1 1 1 1 1 1 1 1 1 1 1 1 1
CC
CC WELL NAME
*---- WELNAM
S1_I1
CC Maximum allowable rate of 2500b/d= 44916.8 cubic feet per day
CC MAX. AND MIN. ALLOWABLE BOTTOMHOLE PRESSURE AND RATE
*----ICHEK   PWFMIN   PWFMAX  QTMIN   QTMAX
   0      300.0    1300.0  0.0     84219
CC
CC WELL ID,LOCATIONS,AND FLAG FOR SPECIFYING WELL TYPE, WELL RADIUS, SKIN
*----IDW  IW   JW   IFLAG    RW     SWELL  IDIR  IFIRST   ILAST    IPRF
    2  8    4    1      0.4    0    3     1      19       1
cc
cc
*----kprf
    0 0 1 1 0 0 1 1 1 1 1 1 1 1 1 1 1 1 1 1
CC
CC WELL NAME
*---- WELNAM
S1_I2
CC
CC MAX. AND MIN. ALLOWABLE BOTTOMHOLE PRESSURE AND RATE
*----ICHEK   PWFMIN   PWFMAX  QTMIN   QTMAX
   0      300.0    1300.0  0.0     84219
CC
CC WELL ID,LOCATIONS,AND FLAG FOR SPECIFYING WELL TYPE, WELL RADIUS, SKIN
*----IDW  IW   JW   IFLAG    RW     SWELL  IDIR  IFIRST   ILAST    IPRF
    3  9    7    1      0.4    0    3     1      19       1
cc
cc
*----kprf
    0 0 0 0 0 0 0 1 1 1 1 1 1 1 1 1 1 1 1 1
CC
CC WELL NAME
*---- WELNAM
S1_I3
CC
CC MAX. AND MIN. ALLOWABLE BOTTOMHOLE PRESSURE AND RATE
*----ICHEK   PWFMIN   PWFMAX  QTMIN   QTMAX
   0      300.0    1300.0  0.0     84219
CC
CC WELL ID,LOCATIONS,AND FLAG FOR SPECIFYING WELL TYPE, WELL RADIUS, SKIN
*----IDW  IW   JW   IFLAG    RW     SWELL  IDIR  IFIRST   ILAST    IPRF
    4  8    10   1      0.4    0    3     1      19       1
```

```
cc
cc
*----kprf
    1 1 0 1 0 0 0 1 1 1 1 1 1 1 1 1 1 1
CC
CC WELL NAME
*---- WELNAM
S1_I4
CC
CC MAX. AND MIN. ALLOWABLE BOTTOMHOLE PRESSURE AND RATE
*----ICHEK   PWFMIN   PWFMAX  QTMIN   QTMAX
   0      300.0    1300.0  0.0     84219
CC
CC WELL ID,LOCATIONS,AND FLAG FOR SPECIFYING WELL TYPE, WELL RADIUS, SKIN
*----IDW  IW   JW   IFLAG    RW     SWELL  IDIR  IFIRST   ILAST    IPRF
    5  4    10    1    0.4   0      3      1       19       1
cc
cc
*----kprf
    1 1 1 1 0 1 1 1 1 1 1 1 1 1 1 1 1 1
CC
CC WELL NAME
*---- WELNAM
S1_I5
CC
CC MAX. AND MIN. ALLOWABLE BOTTOMHOLE PRESSURE AND RATE
*----ICHEK   PWFMIN   PWFMAX  QTMIN   QTMAX
   0      300.0    1300.0  0.0     84219
CC
CC WELL ID,LOCATIONS,AND FLAG FOR SPECIFYING WELL TYPE, WELL RADIUS, SKIN
*----IDW  IW   JW   IFLAG    RW     SWELL  IDIR  IFIRST   ILAST    IPRF
    6  3    7     1    0.4     0      3      1       19       1
cc
cc
*----kprf
    0 1 1 1 1 1 1 1 1 1 1 1 1 1 1 1 1 1
CC
CC WELL NAME
*---- WELNAM
S1_I6
CC
CC MAX. AND MIN. ALLOWABLE BOTTOMHOLE PRESSURE AND RATE
*----ICHEK   PWFMIN   PWFMAX  QTMIN   QTMAX
   0      300.0    1300.0  0.0     84219
CC
CC WELL ID,LOCATIONS,AND FLAG FOR SPECIFYING WELL TYPE, WELL RADIUS, SKIN
*----IDW  IW   JW   IFLAG    RW     SWELL  IDIR  IFIRST   ILAST    IPRF
    7  3     2     1    0.4     0      3      1       19       1
cc
```

```
cc
*----kprf
    1 1 1 1 1 1 1 1 1 1 1 1 1 1 1 1 1 1 1 1 1
CC
CC WELL NAME
*---- WELNAM
S1_I7
CC
CC MAX. AND MIN. ALLOWABLE BOTTOMHOLE PRESSURE AND RATE
*----ICHEK   PWFMIN   PWFMAX  QTMIN   QTMAX
   0      300.0    1300.0  0.0     84219
CC
CC WELL ID,LOCATIONS,AND FLAG FOR SPECIFYING WELL TYPE, WELL RADIUS, SKIN
*----IDW  IW   JW   IFLAG    RW     SWELL  IDIR  IFIRST   ILAST    IPRF
    8  9    2     1     0.4       0      3      1       19        1
cc
cc
*----kprf
    1 1 0 1 0 0  1 1 1 1 1 1 1 1 1 1 1 1 1
CC
CC WELL NAME
*---- WELNAM
S1_I8
CC
CC MAX. AND MIN. ALLOWABLE BOTTOMHOLE PRESSURE AND RATE
*----ICHEK   PWFMIN   PWFMAX  QTMIN   QTMAX
   0      300.0    1300.0  0.0     84219
CC
CC WELL ID,LOCATIONS,AND FLAG FOR SPECIFYING WELL TYPE, WELL RADIUS, SKIN
*----IDW  IW   JW   IFLAG    RW     SWELL  IDIR  IFIRST   ILAST    IPRF
    9  9    11     1     0.4     0      3      1       19        1
cc
cc
*----kprf
    1 1 1 1 1 1 1 1 1 1 1 1 1 1 1 1 1 1 1 1 1
CC
CC WELL NAME
*---- WELNAM
S1_I9
CC
CC MAX. AND MIN. ALLOWABLE BOTTOMHOLE PRESSURE AND RATE
*----ICHEK   PWFMIN   PWFMAX  QTMIN   QTMAX
   0      300.0    1300.0  0.0     84219
CC
CC WELL ID,LOCATIONS,AND FLAG FOR SPECIFYING WELL TYPE, WELL RADIUS, SKIN
*----IDW  IW   JW   IFLAG    RW     SWELL  IDIR  IFIRST   ILAST    IPRF
   10  3    11     1     0.4     0      3      1       19        1
cc
cc
```

```
*----kprf
    1 1 1 1 0 1 1 1 1 1 1 1 1 1 1 1 1 1 1
CC
CC WELL NAME
*---- WELNAM
S1_I10
CC
CC MAX. AND MIN. ALLOWABLE BOTTOMHOLE PRESSURE AND RATE
*----ICHEK   PWFMIN   PWFMAX  QTMIN   QTMAX
   0      300.0    1300.0  0.0     84219
CC
CC WELL ID,LOCATIONS,AND FLAG FOR SPECIFYING WELL TYPE, WELL RADIUS, SKIN
*----IDW  IW   JW   IFLAG    RW    SWELL  IDIR  IFIRST   ILAST    IPRF
    11  6    7     2      0.4    0     3     1       19       1
cc
cc
*----kprf
    0 0 0 0 0 1 1 1 1 1 1 1 1 1 1 1 1 1 1
CC
CC WELL NAME
*---- WELNAM
S1_P1
CC   DW, max 10000 bbls/d
CC MAX. AND MIN. ALLOWABLE BOTTOMHOLE PRESSURE AND RATE
*----ICHEK   PWFMIN   PWFMAX  QTMIN   QTMAX
   0      300.0      1300.   0.0     -56146.0
CC
CC WELL ID,LOCATIONS,AND FLAG FOR SPECIFYING WELL TYPE, WELL RADIUS, SKIN
*----IDW  IW   JW   IFLAG    RW    SWELL  IDIR  IFIRST   ILAST    IPRF
    12  6    2     2      0.4    0     3     1       19       1
cc
cc
*----kprf
    1 1 1 1 1  0 1 1 1 1 1 1 1 1 1 1 1 1 1
CC
CC WELL NAME
*---- WELNAM
S1_P2
CC
CC MAX. AND MIN. ALLOWABLE BOTTOMHOLE PRESSURE AND RATE
*----ICHEK   PWFMIN   PWFMAX  QTMIN   QTMAX
   0      300.0      1400.   0.0     -28073
CC
CC WELL ID,LOCATIONS,AND FLAG FOR SPECIFYING WELL TYPE, WELL RADIUS, SKIN
*----IDW  IW   JW   IFLAG    RW    SWELL  IDIR  IFIRST   ILAST    IPRF
    13  10   4     2      0.4    0     3     1       19       1
cc
cc
*----kprf
```

```
    0 0 0 0 0 0 0 0 0 0 0 0 0 0 0 0 0 0 1 1 1
CC
CC WELL NAME
*---- WELNAM
S1_P3
CC
CC MAX. AND MIN. ALLOWABLE BOTTOMHOLE PRESSURE AND RATE
*----ICHEK   PWFMIN   PWFMAX  QTMIN   QTMAX
   0      300.0      1400.   0.0     -28073
CC
CC WELL ID,LOCATIONS,AND FLAG FOR SPECIFYING WELL TYPE, WELL RADIUS, SKIN
*----IDW  IW   JW   IFLAG    RW    SWELL  IDIR  IFIRST   ILAST    IPRF
    14  10   10    2     0.4    0     3     1       19       1
cc
cc
*----kprf
    1 1 1 1 0 0 1 1 1 1 1 1 1 1 1 1 1 1 1
CC
CC WELL NAME
*---- WELNAM
S1_P4
CC
CC MAX. AND MIN. ALLOWABLE BOTTOMHOLE PRESSURE AND RATE
*----ICHEK   PWFMIN   PWFMAX  QTMIN   QTMAX
   0      300.0      1400.   0.0     -28073
CC
CC WELL ID,LOCATIONS,AND FLAG FOR SPECIFYING WELL TYPE, WELL RADIUS, SKIN
*----IDW  IW   JW   IFLAG    RW    SWELL  IDIR  IFIRST   ILAST    IPRF
    15  6    11     2     0.4    0     3     1       19       1
cc
cc
*----kprf
    1 1 1 1 0 1 1 1 1 1 1 1 1 1 1 1 1 1 1
CC
CC WELL NAME
*---- WELNAM
S1_P5
CC
CC MAX. AND MIN. ALLOWABLE BOTTOMHOLE PRESSURE AND RATE
*----ICHEK   PWFMIN   PWFMAX  QTMIN   QTMAX
   0      300.0      1400.   0.0    -28073
CC
CC WELL ID,LOCATIONS,AND FLAG FOR SPECIFYING WELL TYPE, WELL RADIUS, SKIN
*----IDW  IW   JW   IFLAG    RW    SWELL  IDIR  IFIRST   ILAST    IPRF
    16  2    10    2     0.4    0     3     1       19       1
cc
cc
*----kprf
    1 1 1 0 1 1 1 1 1 1 1 1 1 1 1 1 1 1 1
```

```
CC
CC WELL NAME
*---- WELNAM
S1_P6
CC
CC MAX. AND MIN. ALLOWABLE BOTTOMHOLE PRESSURE AND RATE
*----ICHEK   PWFMIN   PWFMAX  QTMIN   QTMAX
    0       300.0      1400.   0.0     -28073
CC
CC WELL ID,LOCATIONS,AND FLAG FOR SPECIFYING WELL TYPE, WELL RADIUS, SKIN
*----IDW  IW   JW   IFLAG    RW     SWELL  IDIR  IFIRST   ILAST    IPRF
     17   2   4     2       0.4    0      3     1        19       1
cc
cc
*----kprf
     1 1 1 1 1 1 1 1 1 1 1 1 1 1 1 1 1 1 1 1 1
CC
CC WELL NAME
*---- WELNAM
S1_P7
CC
CC MAX. AND MIN. ALLOWABLE BOTTOMHOLE PRESSURE AND RATE
*----ICHEK   PWFMIN   PWFMAX  QTMIN   QTMAX
    0       300.0      1400.   0.0     -28073
CC
CC
*----ID   QI    C
    1  44916.8     1.    0.   0.    0.    0.05130 0.     2*0  4*0  2*0
    1    0.        0.    0.   0.    0.    0.      0.     6*0   2*0
    1    0.        0.    0.   0.    0.    0.      0.     6*0   2*0
CC
CC
*----ID   QI    C
    2  44916.8     1.    0.   0.    0.    0.05130 0.     2*0  4*0  2*0
    2    0.        0.    0.   0.    0.    0.      0.     6*0   2*0
    2    0.        0.    0.   0.    0.    0.      0.     6*0   2*0
CC
CC
*----ID   QI    C
    3  44916.8     1.    0.   0.    0.    0.05130 0.     2*0  4*0 2*0
    3    0.        0.    0.   0.    0.    0.      0.     6*0   2*0
    3    0.        0.    0.   0.    0.    0.      0.     6*0   2*0
CC
CC id,INJ. RATE AND INJ. COMP. FOR RATE CONS. WELLS FOR EACH PHASE(L=1,3)
*----id  QI(M,L)  C(M,KC,L) (need to keep 2nd and 3rd lines for oil and ME)
    4  44916.8     1.    0.   0.    0.    0.05130 0.     2*0  4*0  2*0
    4    0.        0.    0.   0.    0.    0.      0.     6*0   2*0
    4    0.        0.    0.   0.    0.    0.      0.     6*0   2*0
CC
```

```
CC
*----id  QI(M,L)  C(M,KC,L) (need to keep 2nd and 3rd lines for oil and ME)
    5  44916.8     1.    0.   0.    0.    0.05130 0.     2*0  4*0  2*0
    5   0.        0.    0.   0.    0.    0.      0.     6*0   2*0
    5   0.        0.    0.   0.    0.    0.      0.     6*0   2*0
CC
CC id,INJ. RATE AND INJ. COMP. FOR RATE CONS. WELLS FOR EACH PHASE(L=1,3)
*----id  QI(M,L)  C(M,KC,L) (need to keep 2nd and 3rd lines for oil and ME)
    6  44916.8     1.    0.   0.    0.    0.05130 0.     2*0  4*0 2*0
    6   0.        0.    0.   0.    0.    0.      0.     6*0   2*0
    6   0.        0.    0.   0.    0.    0.      0.     6*0   2*0
CC
CC id,INJ. RATE AND INJ. COMP. FOR RATE CONS. WELLS FOR EACH PHASE(L=1,3)
*----id  QI(M,L)  C(M,KC,L) (need to keep 2nd and 3rd lines for oil and ME)
    7  22458.4     1.    0.   0.    0.    0.05130 0.     2*0  4*0 2*0
    7   0.        0.    0.   0.    0.    0.      0.     6*0   2*0
    7   0.        0.    0.   0.    0.    0.      0.     6*0   2*0
CC
CC
*----id  QI(M,L)  C(M,KC,L) (need to keep 2nd and 3rd lines for oil and ME)
    8  22458.4     1.    0.   0.    0.    0.05130 0.     2*0  4*0 2*0
    8   0.        0.    0.   0.    0.    0.      0.     6*0   2*0
    8   0.        0.    0.   0.    0.    0.      0.     6*0   2*0
CC
CC id,INJ. RATE AND INJ. COMP. FOR RATE CONS. WELLS FOR EACH PHASE(L=1,3)
*----id  QI(M,L)  C(M,KC,L) (need to keep 2nd and 3rd lines for oil and ME)
    9  22458.4     1.    0.   0.    0.    0.05130 0.     2*0  4*0  2*0
    9   0.        0.    0.   0.    0.    0.      0.     6*0   2*0
    9   0.        0.    0.   0.    0.    0.      0.     6*0   2*0
CC
CC id,INJ. RATE AND INJ. COMP. FOR RATE CONS. WELLS FOR EACH PHASE(L=1,3)
*----id  QI(M,L)  C(M,KC,L) (need to keep 2nd and 3rd lines for oil and ME)
   10  22458.4     1.    0.   0.    0.    0.05130 0.     2*0  4*0  2*0
   10   0.        0.    0.   0.    0.    0.      0.     6*0   2*0
   10   0.        0.    0.   0.    0.    0.      0.     6*0   2*0
CC
CC   Pressure constrained producer
*----WELL ID   PWF
   11         300.0
CC
CC   Pressure constrained producer
*----WELL ID   PWF
   12         300.0
CC
CC   Pressure constrained producer
*----WELL ID   PWF
   13         300.0
CC
CC   Pressure constrained producer
```

```
*----WELL ID   PWF
    14         300.0
CC
CC   Pressure constrained producer
*----WELL ID   PWF
    15         300.0
CC
CC   Pressure constrained producer
*----WELL ID   PWF
    16         300.0
CC
CC   Pressure constrained producer
*----WELL ID   PWF
    17         300.0
CC
CC CUM. INJ. TIME , AND INTERVALS (PV OR DAY) FOR WRITING TO OUTPUT FILES
(3.7.8)
*----TINJ      CUMPR1  CUMHI2  WRHPV(HIST) WRPRF(PLOT) RSTC
   5        4.9     4.9     0.2          0.5        4.9
CC
CC FOR IMES=2 ,THE INI. TIME STEP,CONC. TOLERANCE,MAX.,MIN. time steps
*----DT             DCLIM     CNMAX   CNMIN
    0.00001        0.001     0.2     0.01
CC
CC IRO, ITIME, NEW FLAGS FOR ALL THE WELLS
*---- IRO ITSTEP IFLAG
      2   1     10*1  7*2
CC
CC NUMBER OF WELLS CHANGES IN LOCATION OR SKIN OR PWF
*----NWEL1
    0
CC
CC NUMBER OF WELLS WITH RATE CHANGES, ID - SP FLOOD INTO 10 INJECTORS
*----NWEL2   ID
    10       1 2 3 4 5 6 7 8 9 10
CC
CC id,INJ. RATE AND INJ. COMP. FOR RATE CONS. WELLS FOR EACH PHASE(L=1,3)
*----id  QI(M,L)  C(M,KC,L) (need to keep 2nd and 3rd lines for oil and ME)
    1  14036.5     1.    0.   0.    0.    0.7116  0  0  7*0
    1    0.        0.    0.   0.    0.    0.      0.        6*0   2*0
    1    0.        0.    0.   0.    0.    0.      0.        6*0   2*0
CC
CC id,INJ. RATE AND INJ. COMP. FOR RATE CONS. WELLS FOR EACH PHASE(L=1,3)
*----id  QI(M,L)  C(M,KC,L) (need to keep 2nd and 3rd lines for oil and ME)
    2  14036.5     1.    0.   0.    0.    0.7116  0  0  7*0
    2    0.        0.    0.   0.    0.    0.      0.        6*0   2*0
    2    0.        0.    0.   0.    0.    0.      0.        6*0   2*0
CC
CC
```

```
*----id  QI(M,L)  C(M,KC,L) (need to keep 2nd and 3rd lines for oil and ME)
    3 14036.5      1.    0.   0.    0.    0.7116  0  0  7*0
    3    0.        0.    0.   0.    0.    0.      0.        6*0   2*0
    3    0.        0.    0.   0.    0.    0.      0.        6*0   2*0
CC
CC
*----id  QI(M,L)  C(M,KC,L) (need to keep 2nd and 3rd lines for oil and ME)
    4  14036.5     1.     0.   0.    0.    0.7116  0  0  7*0
    4    0.        0.     0.   0.    0.    0.      0.        6*0   2*0
    4    0.        0.     0.   0.    0.    0.      0.        6*0   2*0
CC
CC id,INJ. RATE AND INJ. COMP. FOR RATE CONS. WELLS FOR EACH PHASE(L=1,3)
*----id  QI(M,L)  C(M,KC,L) (need to keep 2nd and 3rd lines for oil and ME)
    5  14036.5     1.    0.   0.    0.    0.7116  0  0  7*0
    5    0.        0.    0.   0.    0.    0.      0.        6*0  2*0
    5    0.        0.    0.   0.    0.    0.      0.        6*0  2*0
CC
CC id,INJ. RATE AND INJ. COMP. FOR RATE CONS. WELLS FOR EACH PHASE(L=1,3)
*----id  QI(M,L)  C(M,KC,L) (need to keep 2nd and 3rd lines for oil and ME)
    6  14036.5     1.    0.   0.    0.    0.7116  0  0  7*0
    6    0.        0.    0.   0.    0.    0.      0.        6*0  2*0
    6    0.        0.    0.   0.    0.    0.      0.        6*0  2*0
CC
CC id,INJ. RATE AND INJ. COMP. FOR RATE CONS. WELLS FOR EACH PHASE(L=1,3)
*----id  QI(M,L)  C(M,KC,L) (need to keep 2nd and 3rd lines for oil and ME)
    7  7018.25     1.    0.   0.    0.    0.7116  0  0  7*0
    7    0.        0.    0.   0.    0.    0.      0.        6*0  2*0
    7    0.        0.    0.   0.    0.    0.      0.        6*0  2*0
CC
CC id,INJ. RATE AND INJ. COMP. FOR RATE CONS. WELLS FOR EACH PHASE(L=1,3)
*----id  QI(M,L)  C(M,KC,L) (need to keep 2nd and 3rd lines for oil and ME)
    8   7018.25    1.    0.   0.    0.    0.7116  0  0  7*0
    8    0.        0.    0.   0.    0.    0.      0.        6*0  2*0
    8    0.        0.    0.   0.    0.    0.      0.        6*0  2*0
CC
CC id,INJ. RATE AND INJ. COMP. FOR RATE CONS. WELLS FOR EACH PHASE(L=1,3)
*----id  QI(M,L)  C(M,KC,L) (need to keep 2nd and 3rd lines for oil and ME)
    9   7018.25    1.    0.   0.    0.    0.7116  0  0  7*0
    9    0.        0.    0.   0.    0.    0.      0.        6*0  2*0
    9    0.        0.    0.   0.    0.    0.      0.        6*0  2*0
CC
CC id,INJ. RATE AND INJ. COMP. FOR RATE CONS. WELLS FOR EACH PHASE(L=1,3)
*----id  QI(M,L)  C(M,KC,L) (need to keep 2nd and 3rd lines for oil and ME)
   10   7018.25    1.    0.   0.    0.    0.7116  0  0  7*0
   10    0.        0.    0.   0.    0.    0.      0.        6*0  2*0
   10    0.        0.    0.   0.    0.    0.      0.        6*0  2*0
CC
CC CUM. INJ. TIME , AND INTERVALS (PV OR DAY) FOR WRITING TO OUTPUT FILES
(3.7.8)
```

```
*----TINJ    CUMPR1  CUMHI2 WRHPV(HIST) WRPRF(PLOT) RSTC
    5.3     0.01    0.1   0.01        0.1        0.05
CC Water Inj.
CC FOR IMES=2 ,THE INI. TIME STEP,CONC. TOLERANCE,MAX.,MIN. time steps
*----DT            DCLIM     CNMAX   CNMIN
    0.00001       0.005     0.05   0.001
CC
CC IRO, ITIME, NEW FLAGS FOR ALL THE WELLS
*---- IRO ITIME IFLAG
      2   1     10*1  7*2
CC
CC NUMBER OF WELLS changes IN LOCATION OR SKIN OR PWF
*----NWEL1
     0
CC
CC NUMBER OF WELLS WITH RATE changes, id
*----NWEL2   Id
    10      1 2 3 4 5 6 7 8 9 10
CC
CC id,INJ. RATE AND INJ. COMP. FOR RATE CONS. WELLS FOR EACH PHASE(L=1,3)
*----id  QI(M,L)  C(M,KC,L) (need to keep 2nd and 3rd lines for oil and ME)
    1  14036.5     1.    0.   0.    0.0  0.0513   0.     0  7*0
    1    0.        0.    0.   0.    0.    0.      0.      6*0   2*0
    1    0.        0.    0.   0.    0.    0.      0.      6*0   2*0
CC
CC id,INJ. RATE AND INJ. COMP. FOR RATE CONS. WELLS FOR EACH PHASE(L=1,3)
*----id  QI(M,L)  C(M,KC,L) (need to keep 2nd and 3rd lines for oil and ME)
    2  14036.5     1.    0.   0.    0.0  0.0513   0.      0   7*0
    2    0.        0.    0.   0.    0.    0.      0.       6*0   2*0
    2    0.        0.    0.   0.    0.    0.      0.       6*0   2*0
CC
CC id,INJ. RATE AND INJ. COMP. FOR RATE CONS. WELLS FOR EACH PHASE(L=1,3)
*----id  QI(M,L)  C(M,KC,L) (need to keep 2nd and 3rd lines for oil and ME)
    3  14036.5     1.    0.   0.    0.0  0.0513   0.      0    7*0
    3    0.        0.    0.   0.    0.    0.      0.       6*0   2*0
    3    0.        0.    0.   0.    0.    0.      0.       6*0   2*0
CC
CC id,INJ. RATE AND INJ. COMP. FOR RATE CONS. WELLS FOR EACH PHASE(L=1,3)
*----id  QI(M,L)  C(M,KC,L) (need to keep 2nd and 3rd lines for oil and ME)
    4  14036.5     1.    0.   0.    0.0  0.0513   0.      0   7*0
    4    0.        0.    0.   0.    0.    0.      0.       6*0   2*0
    4    0.        0.    0.   0.    0.    0.      0.       6*0   2*0
CC
CC id,INJ. RATE AND INJ. COMP. FOR RATE CONS. WELLS FOR EACH PHASE(L=1,3)
*----id  QI(M,L)  C(M,KC,L) (need to keep 2nd and 3rd lines for oil and ME)
    5  14036.5    1.    0.   0.    0.0  0.0513   0.      0    7*0
    5    0.        0.    0.   0.    0.    0.      0.       6*0  2*0
    5    0.        0.    0.   0.    0.    0.      0.       6*0  2*0
CC
```

```
CC id,INJ. RATE AND INJ. COMP. FOR RATE CONS. WELLS FOR EACH PHASE(L=1,3)
*----id  QI(M,L)  C(M,KC,L) (need to keep 2nd and 3rd lines for oil and ME)
    6  14036.5     1.    0.   0.    0.0  0.0513   0.      0   7*0
    6    0.        0.    0.   0.    0.    0.      0.       6*0  2*0
    6    0.        0.    0.   0.    0.    0.      0.       6*0  2*0
CC
CC id,INJ. RATE AND INJ. COMP. FOR RATE CONS. WELLS FOR EACH PHASE(L=1,3)
*----id  QI(M,L)  C(M,KC,L) (need to keep 2nd and 3rd lines for oil and ME)
    7  7018.25     1.    0.   0.    0.0  0.0513   0.      0    7*0
    7    0.        0.    0.   0.    0.    0.      0.       6*0   2*0
    7    0.        0.    0.   0.    0.    0.      0.       6*0   2*0
CC
CC id,INJ. RATE AND INJ. COMP. FOR RATE CONS. WELLS FOR EACH PHASE(L=1,3)
*----id  QI(M,L)  C(M,KC,L) (need to keep 2nd and 3rd lines for oil and ME)
    8  7018.25       1.    0.   0.    0.0  0.0513   0.      0   7*0
    8    0.        0.    0.   0.    0.    0.      0.       6*0   2*0
    8    0.        0.    0.   0.    0.    0.      0.       6*0   2*0
CC
CC id,INJ. RATE AND INJ. COMP. FOR RATE CONS. WELLS FOR EACH PHASE(L=1,3)
*----id  QI(M,L)  C(M,KC,L) (need to keep 2nd and 3rd lines for oil and ME)
    9  7018.25       1.    0.   0.    0.0  0.0513   0.      0   7*0
    9    0.        0.    0.   0.    0.    0.      0.       6*0    2*0
    9    0.        0.    0.   0.    0.    0.      0.       6*0    2*0
CC
CC id,INJ. RATE AND INJ. COMP. FOR RATE CONS. WELLS FOR EACH PHASE(L=1,3)
*----id  QI(M,L)  C(M,KC,L) (need to keep 2nd and 3rd lines for oil and ME)
    10  7018.25       1.    0.   0.    0.0  0.0513   0.      0  7*0
    10    0.        0.    0.   0.    0.    0.      0.       6*0  2*0
    10    0.        0.    0.   0.    0.    0.      0.       6*0  2*0
CC post flush formation water injection
CC CUM. INJ. TIME , AND INTERVALS (PV OR DAY) FOR WRITING TO OUTPUT FILES
(3.7.8)
*----TINJ      CUMPR1  CUMHI2 WRHPV(HIST) WRPRF(PLOT) RSTC
    7.3       0.5    0.5   0.01        0.3        0.3
CC
CC FOR IMES=2 ,THE INI. TIME STEP,CONC. TOLERANCE,MAX.,MIN. time steps
*----DT            DCLIM     CNMAX   CNMIN
    0.000001       0.001     0.05   0.001
```

Nomenclature

English Symbols

a	Parameter to Calculate CDG Solution Viscosity
ADCDG	CDG Adsorption Parameter
ADCDGILM	Parameter to Calculate CDG Long-Term Permeability Reduction Factor (see $C_{m,ads,max}$)
a_1	CDG Adsorption Parameter (this is ADCDG)
a_{41}	Polymer Adsorption Parameter
a_{42}	Polymer Adsorption Parameter
A_{P1}	Parameter Used to Calculate Polymer Solution Viscosity at Zero Shear Rate as Function of Polymer and Electrolyte Concentrations
A_{P2}	Parameter Used to Calculate Polymer Solution Viscosity at Zero Shear Rate as Function of Polymer and Electrolyte Concentrations
A_{P3}	Parameter Used to Calculate Polymer Solution Viscosity at Zero Shear Rate as Function of Polymer and Electrolyte Concentrations
b	Parameter to Calculate CDG Solution Viscosity
B	Parameter to Calculate Adsorbed Layer Thickness of Microgels
BDCDG	CDG Adsorption Parameter
b_1	CDG Adsorption Parameter (this is BDCDG)
b_4	Polymer Adsorption Parameter
b_{rk}	Parameter for Calculating Polymer Permeability Reduction Factor
c	Parameter to Calculate CDG Short-Term Permeability Reduction Factor
c	Polymer Concentration in Solution
c*	Polymer Overlap Concentration in Solution

$C_{m,ads}$	Microgel Concentration Adsorbed to Rock Surface
$C_{m,ads,max}$	Maximum Microgel Concentration Adsorbed (this is ADCDGILM)
$C_{m,fluid}$	Microgel Concentration in the Fluid
$C_{m,total}$	Total Microgel Concentration ($C_{m,fluid} + C_{m,ads}$)
c_{rk}	Parameter for Calculating Polymer Permeability Reduction Factor
d	Parameter to Calculate Adsorbed Layer Thickness of Microgels
D	Center-of-Mass Diffusion Coefficient of Polymer Chain or Suspension
e	Parameter to Calculate Adsorbed Layer Thickness of Microgels
f	Parameter to Calculate CDG Short-Term Permeability Reduction Factor
f_o	Fractional Flow of Oil
f_w	Fractional Flow of Water
G'	Storage or Elastic Modulus
G''	Loss or Viscous Modulus
h_i	Thickness of a Geological Layer i
JR	Jamming Ratio used to Quantify Microgel Pore Plugging Tendency
$\bar{k}$	Average Permeability
k_B	Boltzmann Constant
k_i	Permeability of a Geological Layer i
k_h	Permeability in Horizontal Direction
K_H	Huggins Constant
k_o	Permeability to Oil
k_p	Permeability to Polymer Solution
k_{ro}^{o}	End-Point Relative Permeability to Oil
k_{rw}^{o}	End-Point Relative Permeability to Water
k_v	Permeability in Vertical Direction

k_w	Permeability to Water
M	Mobility Ratio
n	Parameter to Calculate CDG Solution Viscosity
n_o	Relative Permeability Exponent of Oleic Phase
n_w	Relative Permeability Exponent of Aqueous Phase
PV	Pore Volumes Flooded
P_α	Exponent to Calculate the Shear Rate Dependence of Polymer Solution Viscosity
q_i	Flow Allocation into a Geological Layer i
Q_i	Injection Rate
ResRkFact	See $R_{k,factor}$
RF	Resistance Factor
RRF	Residual Resistance Factor
r_h	Pore Throat Radius
R_k	Permeability Reduction
R_{kcut}	Maximum CDG Permeability Reduction Factor
R_{kmax}	Polymer Permeability Reduction Cutoff
$R_{k,factor}$	Factor for Calculating CDG Long-term Permeability Reduction
$R_{k,max,gridblock}$	Maximum Permeability Reduction Calculated in a Particular Grid-block
S_P	Slope of Polymer Solution Viscosity vs. Effective Salinity on log-log Plot
T	Temperature
TolCcdgRk	CDG Concentration Tolerance (Cutoff between Short- & Long-Term R_k)
V_{DP}	Dykstra-Parsons Coefficient

Greek Symbols

α_L	Longitudinal Dispersivity
α_T	Transverse Dispersivity
β_P	Parameter for Calculating Effective Divalent Salinity to Compute Polymer Solution Viscosity
$\gamma_{1/2}$	Shear Rate at which Polymer Solution Viscosity is half the Corresponding Polymer Solution Viscosity at Zero Shear Rate
γ_c	Shear Rate Equation Coefficient
$\dot{\gamma}_c$	Coefficient in CDG Shear Rate Equation
$\dot{\gamma}_{eq}$	Equivalent Shear Rate
ϵ_h	CDG Adsorbed Layer Thickness
η	Polymer Solution Viscosity
$[\eta]$	Intrinsic Viscosity
η_r	Relative Viscosity
η_{red}	Reduced Viscosity
η_s	Solvent Viscosity
η_{sp}	Specific Viscosity
μ	Parameter to Calculate CDG Short-Term Permeability Reduction Factor
μ_o	Oil Viscosity
μ_p	Polymer Solution Viscosity
μ_w	Water Viscosity
σ	Parameter to Calculate CDG Short-Term Permeability Reduction Factor
ϕ	Porosity

References

Abdo M.K., Chung H.S. and Phelps C.H.: "Field Experience with Floodwater Diversion by Complexed Biopolymers", SPE/DOE Fourth Symposium on Enhanced Oil Recovery, 15-18 April 1984, Tulsa, Oklahoma, U.S.A. (SPE 12642)

Al-Anazi H.A. and Sharma M.M.: "Use of a pH Sensitive Polymer for Conformance Control", SPE International Symposium and Exhibition on Formation Damage Control, 20-21 February 2002, Lafayette, Louisiana, U.S.A. (SPE 73782)

Al-Assi A.A., Willhite G.P., Green D.W. and McCool C.S.: "Formation and Propagation of Gel Aggregates using Partially Hydrolyzed Polyacrylamide and Aluminum Citrate", SPE/DOE Symposium on Improved Oil Recovery, 22-26 April 2006, Tulsa, Oklahoma, U.S.A. (SPE 100049)

Al-Mutairi S.M. and Kokal S.L.: "EOR Potential in the Middle East: Current and Future Trends", SPE EUROPEC/EAGE Annual Conference and Exhibition, 23-26 May 2011, Vienna, Austria. (SPE 143287)

Ali, Syed A.: "Mature Fields and Well Revitalization", Journal of Petroleum Technology (January 2012), pp. 74.

Avery M.R., Burkholder L.A. and Gruenenfelder M.A., "Use of Crosslinked Xanthan Gels in Actual Profile Modification Field Projects", SPE 1986 International Meeting on Petroleum Engineering, 17-20 March 1986, Beijing, China. (SPE 14114)

Bai B., Huang F., Liu Y., Seright R.S. and Wang Y.: "Case Study on Preformed Particle Gel for In-depth Fluid Diversion", 2008 SPE/DOE Improved Oil Recovery Symposium, 19-23 April 2008, Tulsa, Oklahoma, U.S.A. (SPE 113997)

Bai B., Li L., Liu Y., Wang Z. and Liu H.: "Preformed Particle Gel for Conformance Control: Factors Affecting its Properties and Applications", 2004 SPE/DOE Fourteenth Symposium on Improved Oil Recovery, 17-21 April 2004a, Tulsa, Oklahoma, U.S.A. (SPE 89389)

Bai B., Liu Y., Coste J.P. and Li L.: "Preformed Particle Gel for Conformance Control: Transport Mechanism through Porous Media", 2004 SPE/DOE Fourteenth Symposium on Improved Oil Recovery, 17-21 April 2004b, Tulsa, Oklahoma, U.S.A. (SPE 89468)

Bai B., Wang Q., Du Y. and Liu Y.Z.: "Factors Affecting In-Depth Gel Treatment for Reservoirs with Thick Heterogeneous Oil Layers", Petroleum Society's 5th Canadian International Petroleum Conference (55th Annual Technical Meeting), 8-10 June 2004c, Calgary, Alberta, Canada. (PAPER 2004-140)

Benson I., Nghiem L.X., Bryant S.L., Sharma M.M. and Huh C.: "Development and Use of a Simulation Model for Mobility/Conformance Control Using a pH-Sensitive Polymer", 2007 SPE Annual Technical Conference and Exhibition, 11-14 November 2007, Anaheim, California, U.S.A. (SPE 109665)

Bjorsvik M., Hoiland H. and Skauge A.: "Formation of Colloidal Dispersion Gels from Aqueous Polyacrylamide Solutions", Colloids and Surfaces A: Physicochem. Eng. Aspects (2008), pp. 504-511.

Borling D., Chan K., Hughes T. and Sydansk R.: "Pushing Out the Oil with Conformance Control", Oilfield Review (1994), Vol. 6, No. 2, pp. 44-58.

Bourdarot G. and Ghedan S.: "Modified EOR Screening Criteria as Applied to a Group of Offshore Carbonate Oil Reservoirs", SPE Reservoir Characterization and Simulation Conference and Exhibition, 9-11 October 2011, Abu Dhabi, U.A.E. (SPE 148323)

Chang H.L., Sui X., Xiao L., Liu H., Guo Z., Yao Y., Xiao Y., Chen G., Song K. and Mack J.C.: "Successful Field Pilot of In-Depth Colloidal Dispersion Gel (CDG) Technology in Daqing Oil Field", 2004 SPE/DOE Fourteenth Symposium on Improved Oil Recovery, 17-21 April 2004, Tulsa, Oklahoma, U.S.A. (SPE 89460)

Chang H.L., Zhang Z.Q., Wang Q.M., Xu Z.S., Guo Z.D., Sun H.Q., Cao X.L. and Qiao Q.: "Advances in Polymer Flooding and Alkaline/Surfactant/Polymer Processes as Developed and Applied in the People's Republic of China", Journal of Petroleum Technology (February 2006), pp. 84-89. (SPE 89175)

Chang K.T., Frampton H., and Morgan J.C. 2002. Composition and Method for Recovering Hydrocarbon Fluids from a Subterranean Reservoir. US Patent No. 6,454,003.

Chauveteau G. and Kohler N.: "Polymer Flooding: The Essential Elements for Laboratory Evaluation", Improved Oil Recovery Symposium of the Society of Petroleum Engineers of AIME, 22-24 April 1974, Tulsa, Oklahoma, U.S.A. (SPE 4745)

Chauveteau G., Omari A., Tabary R., Renard M. and Rose J.: "Controlling Gelation Time and Microgel Size for Water Shutoff", 2000 SPE/DOE Improved Oil Recovery Symposium, 3-5 April 2000, Tulsa, Oklahoma, U.S.A. (SPE 59317)

Chauveteau G., Omari A., Tabary R., Renard M., Veerapen J. and Rose J.: "New Size-Controlled Microgels for Oil Production", 2001 SPE International Symposium on Oilfield Chemistry, 13-16 February 2001, Houston, Texas, U.S.A. (SPE 64988)

Chauveteau G., Tabary R., Blin N., Renard M., Rousseau D. and Faber R.: "Disproportionate Permeability Reduction by Soft Preformed Microgels", 2004 SPE/DOE Fourteenth Symposium on Improved Oil Recovery, 17-21 April 2004, Tulsa, Oklahoma, U.S.A. (SPE 89390)

Chauveteau G., Tabary R., Le Bon C., Renard M., Feng Y. and Omari A.: "In-Depth Permeability Control by Adsorption of Soft Size-Controlled Microgels", SPE European Formation Damage Conference, 13-14 May 2003, The Hague, The Netherlands. (SPE 82228)

Choi S.K., Ermel Y.M., Bryant S.L., Huh C. and Sharma M.M.: "Transport of a pH-Sensitive Polymer in Porous Media for Novel Mobility-Control Applications", 2006 SPE/DOE Symposium on Improved Oil Recovery, 22-26 April 2006, Tulsa, Oklahoma, U.S.A. (SPE 99656)

Choi S.K., Sharma M.M., Bryant S.L. and Huh C.: "pH-Sensitive Polymers for Novel Conformance Control and Polymerflood Applications", 2009 SPE International Symposium on Oilfield Chemistry, 20-22 April 2009, The Woodlands, Texas, U.S.A. (SPE 121686)

Choi, S.K.: "*pH Sensitive Polymers for Novel Conformance Control and Polymer Flooding Applications*", Ph.D. Dissertation, The University of Texas at Austin, August 2008.

Coste J.P., Liu Y., Bai B., Li Y., Shen P., Wang Z. and Zhu G.: "In-Depth Fluid Diversion by Pre-Gelled Particles. Laboratory Study and Pilot Testing.", 2000 SPE/DOE Improved Oil Recovery Symposium, 3-5 April 2000, Tulsa, Oklahoma, U.S.A. (SPE 59362)

Cohen Y. and Christ F.R.: "Polymer Retention and Adsorption in the Flow of Polymer Solutions through Porous Media", SPE Reservoir Engineering (March 1986), pp. 113-118. (SPE 12942)

Cozic C., Rousseau D. and Tabary R.: "Broadening the Application Range of Water Shutoff / Conformance Control Microgels: An Investigation of their Chemical Robustness", 2008 SPE Annual Technical Conference and Exhibition, 21-24 September 2008, Denver, Colorado, U.S.A. (SPE 115974)

Cozic C., Rousseau D. and Tabary R.: "Novel Insights into Microgel Systems for Water Control", SPE Production & Operations (November 2009), pp. 590-601. (SPE 115974)

Cui X.H., Li Z.Q., Cao X.L., Song X.W. and Zhang X.: "A Novel PPG Enhanced Surfactant-Polymer System for EOR", SPE Enhanced Oil Recovery Conference, 19-21 July 2011, Kuala Lumpur, Malaysia. (SPE 143506)

Delshad, Mojdeh. "Fundamentals of Enhanced Oil Recovery". The University of Texas at Austin. Austin, Texas, U.S.A. 17 January 2012. Lecture.

Diaz D., Somaruga C., Norman C. and Romero J.: "Colloidal Dispersion Gels Improve Oil Recovery in a Heterogeneous Argentina Waterflood", SPE/DOE Improved Oil Recovery Symposium, 19-23 April 2008, Tulsa, Oklahoma, U.S.A. (SPE 113320)

Dickson J.L., Leahy-Dios A. and Wylie P.L.: "Development of Improved Hydrocarbon Recovery Screening Methodologies", 2010 SPE Improved Oil Recovery Symposium, 24-28 April 2010, Tulsa, Oklahoma, U.S.A. (SPE 129768)

Dominguez J.G. and Willhite G.P.: "Retention and Flow Characteristics of Polymer Solutions in Porous Media", SPE-AIME Fourth Symposium on Improved Oil Recovery, 22-24 March 1976, Tulsa, Oklahoma, U.S.A. (SPE 5835)

Dovan H.T. and Hutchins R.D.: "Development of a New Aluminum/Polymer Gel System for Permeability Adjustment", SPE Reservoir Engineering (May 1987), pp. 177-183. (SPE 12641)

Espinosa, D.R.: "*Nanoparticle-Stabilized Supercritical CO_2 Foams for Potential Mobility Control Applications*", M.S.E. Thesis, The University of Texas at Austin, May 2011.

Feng Y., Tabary R., Renard M., Le Bon C., Omari A. and Chauveteau G.: "Characteristics of Microgels Designed for Water Shutoff and Profile Control", SPE International Symposium on Oilfield Chemistry, 5-7 February 2003, Houston, Texas, U.S.A. (SPE 80203)

Fielding R.C. Jr., Gibbons D.H. and Legrand F.P.: "In-Depth Drive Fluid Diversion Using an Evolution of Colloidal Dispersion Gels and New Bulk Gels: An Operational Case History of North Rainbow Ranch Unit", SPE/DOE Ninth Symposium on Improved Oil Recovery, 17-20 April 1994, Tulsa, Oklahoma, U.S.A. (SPE/DOE 27773)

Fletcher A.J.P., Flew S., Forsdyke I.N., Morgan J.C., Rogers C. and Suttles D.: "Deep Diverting Gels for Very Cost-Effective Waterflood Control", Journal of Petroleum Science and Engineering (1992), pp. 33-43.

Frampton H., Morgan J.C., Cheung S.K., Munson L., Chang K.T. and Williams D.: "Development of a Novel Waterflood Conformance Control System", 2004 SPE/DOE Fourteenth Symposium on Improved Oil Recovery, 17-21 April 2004, Tulsa, Oklahoma, U.S.A. (SPE 89391)

Garmeh R., Izadi M., Salehi M., Romero J.L., Thomas C.P. and Manrique E.J.: "Thermally Active Polymer to Improve Sweep Efficiency of Water Floods: Simulation and Pilot Design Approaches", SPE Enhanced Oil Recovery Conference, 19-21 July 2011, Kuala Lumpur, Malaysia. (SPE 144234)

Ghaddab F., Kaddour K., Tesconi M., Brancolini A., Carniani C. and Galli G.: "El Borma - Bright Water: A Tertiary Method for Enhanced Oil Recovery for a Mature Field", SPE Production and Operations Conference and Exhibition, 8-10 June 2010, Tunis, Tunisia. (SPE 136140)

Grattoni C.A., Al-Sharji H.H., Yang C., Muggeridge A.H. and Zimmerman R.W.: "Rheology and Permeability of Crosslinked Polyacrylamide Gel", Journal of Colloid and Interface Science (2001), pp. 601-607.

He L., Hongxue H., Zhuling L. and Wang B.: "Granular-Polymer-Gel Treatment Successful in the Daqing Oil Field", 2004 SPE Asia Pacific Conference on Integrated Modeling for Asset Management, 29-30 March 2004, Kuala Lumpur, Malaysia. (SPE 87071)

Hirasaki G.J. and Pope G.A.: "Analysis of Factors Influencing Mobility and Adsorption in the Flow of Polymer Solution through Porous Media", SPE-AIME 47th Annual Fall Meeting, 8-11 October 1972, San Antonio, Texas, U.S.A. (SPE 4026)

Huh C., Choi S.K. and Sharma M.M.: "A Rheological Model for pH-Sensitive Ionic Polymer Solutions for Optimal Mobility-Control Applications", 2005 SPE Annual Technical Conference and Exhibition, 9-12 October 2005, Dallas, Texas, U.S.A. (SPE 96914)

Huh C., Lange E.A. and Cannella W.J.: "Polymer Retention in Porous Media", SPE/DOE Seventh Symposium on Enhanced Oil Recovery, 22-25 April 1990, Tulsa, Oklahoma, U.S.A. (SPE 20235)

Huh, Chun. "Fundamentals of Enhanced Oil Recovery". The University of Texas at Austin. Austin, Texas, U.S.A. 24 January 2012. Lecture.

Husband M., Ohms D., Frampton H., Carhart S., Carlson B., Morgan J.C. and Chang K.T.: "Results of a Three-Well Waterflood Sweep Improvement Trial in the Prudhoe Bay Field Using a Thermally Activated Particle System", 2010 SPE Improved Oil Recovery Symposium, 24-28 April 2010, Tulsa, Oklahoma, U.S.A. (SPE 129967)

Izgec O. and Shook G.M.: "Design Considerations of Waterflood Conformance Control with Temperature-Triggered Low Viscosity Sub-Micron Polymer", SPE Western Regional Meeting, 19-23 March 2012, Bakersfield, California, U.S.A. (SPE 153898)

Jennings R.R., Rogers J.H. and West T.J.: "Factors Influencing Mobility Control by Polymer Solutions", SPE Ninth Biennial Production Symposium, 14-15 May 1970, Wichita Falls, Texas, U.S.A. (SPE 2867)

Jensen, Jerry L. *Statistics for Petroleum Engineers and Geoscientists*. Amsterdam: Elsevier, 2000. Print.

Kabir A.H.: "Chemical Water & Gas Shutoff Technology - An Overview", SPE Asia Pacific Improved Oil Recovery Conference, 8-9 October 2001, Kuala Lumpur, Malaysia. (SPE 72119)

Kim, H.S.: "*Simulation Study of Gel Conformance Treatments*", Ph.D. Dissertation, The University of Texas at Austin, May 1995.

Lake, Larry W. "Fundamentals of Enhanced Oil Recovery". The University of Texas at Austin. Austin, Texas, U.S.A. 20 January 2012. Lecture.

Lake, Larry W. *Enhanced Oil Recovery*. Englewood Cliffs, NJ: Prentice Hall, 1989. Print.

Lalehrokh F. and Bryant S.L.: "Application of pH-Triggered Polymers for Deep Conformance Control in Fractured Reservoirs", 2009 SPE Annual Technical Conference and Exhibition, 4-7 October 2009, New Orleans, Louisiana, U.S.A. (SPE 124773)

Lalehrokh F., Bryant S.L., Huh C. and Sharma M.M.: "Application of pH-Triggered Polymers in Fractured Reservoirs to Increase Sweep Efficiency", 2008 SPE/DOE Improved Oil Recovery Symposium, 19-23 April 2008, Tulsa, Oklahoma, U.S.A. (SPE 113800)

Larkin R. and Creel P.: "Methodologies and Solutions to Remediate Inter-Well Communication Problems on the SACROC CO_2 EOR Project – A Case Study", 2008 SPE/DOE Improved Oil Recovery Symposium, 19-23 April 2008, Tulsa, Oklahoma, U.S.A. (SPE 113305)

Li M.Y., Dong Z.X., Lin M.Q. and Wu Z.L.: "A Study on the Size and Conformation of Linked Polymer Coils", Journal of Petroleum Science and Engineering (2004), pp. 213-219.

Liang J. and Seright R.S.: "Further Investigations of Why Gels Reduce Water Permeability More Than Oil Permeability", 1997 SPE International Symposium on Oilfield Chemistry, 18-21 February 1997, Houston, Texas, U.S.A. (SPE 37249)

Liang J., Sun H. and Seright R.S.: "Reduction of Oil and Water Permeabilities Using Gels", SPE/DOE Eighth Symposium on Enhanced Oil Recovery, 22-24 April 1992, Tulsa, Oklahoma, U.S.A. (SPE/DOE 24195)

Liu Y., Bai B. and Shuler P.J.: "Application and Development of Chemical-Based Conformance Control Treatments in China Oil Fields", 2006 SPE/DOE Symposium on Improved Oil Recovery, 22-26 April 2006, Tulsa, Oklahoma, U.S.A. (SPE 99641)

Lu X., Song K., Niu J. and Chen F.: "Performance and Evaluation Methods of Colloidal Dispersion Gels in the Daqing Oil Field", 2000 SPE Asia Pacific Conference on Integrated Modeling for Asset Management, 25-26 April 2000, Yokohama, Japan. (SPE 59466)

Mack J.C. and Smith J.E.: "In-Depth Colloidal Dispersion Gels Improve Oil Recovery Efficiency", SPE/DOE Ninth Symposium on Improved Oil Recovery, 17-20 April 1994, Tulsa, Oklahoma, U.S.A. (SPE 27780)

Maerker, J.M.: "Dependence of Polymer Retention on Flow Rate", Journal of Petroleum Technology (November 1973), pp. 1307-1308. (SPE 4423)

Manrique E., Thomas C., Ravikiran R., Izadi M., Lantz M., Romero J. and Alvarado V.: "EOR: Current Status and Opportunities", 2010 SPE Improved Oil Recovery Symposium, 24-28 April 2010, Tulsa, Oklahoma, U.S.A. (SPE 130113)

Mohan H., Biglarbigi K., Carolus M. and Van Wagener D.: "Assessing the EOR Potential of the United States", SPE Enhanced Oil Recovery Conference, 19-21 July 2011, Kuala Lumpur, Malaysia. (SPE 145073)

Morgan N.: "Pop Goes the Polymer", BP Frontiers (December 2007), pp. 6-9.

Morrow, Norman R. "Improved Oil Recovery by Waterflooding: Past and Future". Claude R. Hocott and Sylvain Pirson Lectureship Graduate Student Seminar. The University of Texas at Austin. Austin, Texas, U.S.A. 5 March 2012. Guest Lecture.

Muruaga E., Flores M., Norman C. and Romero J.: "Combining Bulk Gels and Colloidal Dispersion Gels for Improved Volumetric Sweep Efficiency in a Mature Waterflood", 2008 SPE/DOE Improved Oil Recovery Symposium, 19-23 April 2008, Tulsa, Oklahoma, U.S.A. (SPE 113334)

Mustoni J.L., Norman C.A. and Denyer P.: "Deep Conformance Control by a Novel Thermally Activated Particle System to Improve Sweep Efficiency in Mature Waterfloods of the San Jorge Basin", 2010 SPE Improved Oil Recovery Symposium, 24-28 April 2010, Tulsa, Oklahoma, U.S.A. (SPE 129732)

Needham R.B. and Doe P.H.: "Polymer Flooding Review", Journal of Petroleum Technology (December 1987), pp. 1503-1507. (SPE 17140)

Norman C., Turner B., Romero J.L., Centeno G. and Muruaga E.: "A Review of Over 100 Polymer Gel Injection Well Conformance Treatments in Argentina and Venezuela: Design, Field Implementation, and Evaluation", First International Oil Conference and Exhibition, 31 August - 2 September 2006, Cancun, Mexico. (SPE 101781)

Norman C.A., Smith J.E. and Thompson R.S.: "Economics of In-Depth Polymer Gel Processes", 1999 SPE Rocky Mountain Regional Meeting, 15-18 May 1999, Gillette, Wyoming, U.S.A. (SPE 55632)

Ohms D., McLeod J., Graff C.J., Frampton H., Morgan J.C., Cheung S., Yancey K. and Chang K.T.: "Incremental Oil Success from Waterflood Sweep Improvement in Alaska", SPE International Symposium on Oilfield Chemistry, 20-22 April 2009, The Woodlands, Texas, U.S.A. (SPE 121761)

Onbergenov, U.: "*Simulation of Thermally Active and pH-Sensitive Polymers for Conformance Control*", M.S.E. Thesis, The University of Texas at Austin, May 2012.

Pritchett J., Frampton H., Brinkman J., Cheung S., Morgan J., Chang K.T., Williams D. and Goodgame J.: "Field Application of a New In-Depth Waterflood

Conformance Improvement Tool", SPE International Improved Oil Recovery Conference, 20-21 October 2003, Kuala Lumpur, Malaysia. (SPE 84897)

Pye D.J.: "Improved Secondary Recovery by Control of Water Mobility", SPE Secondary Recovery Symposium, 4-5 May 1964, Wichita Falls, Texas, U.S.A. (SPE 845)

Pyziak D. and Smith D.D.: "Update on Anton Irish Conformance Efforts", 6th International Conference on Production Optimization, 7-9 November 2007, Houston, Texas, U.S.A.

Ranganathan R., Lewis R., McCool C.S., Green D.W. and Willhite G.P.: "Experimental Study of the Gelation Behavior of a Polyacrylamide/Aluminum Citrate Colloidal-Dispersion Gel System", Society of Petroleum Engineering Journal (December 1998), pp. 337-343. (SPE 52503)

Rousseau D., Chauveteau G., Renard M., Tabary R. and Zaitoun A.: "Rheology and Transport in Porous Media of New Water Shutoff/Conformance Control Microgels", SPE International Symposium on Oilfield Chemistry, 2-4 February 2005, Houston, Texas, U.S.A. (SPE 93254)

Roussennac B. and Toschi C.: "Brightwater Trial in Salema Field (Campos Basin, Brazil)", SPE EUROPEC/EAGE Annual Conference and Exhibition, 14-17 June 2010, Barcelona, Spain. (SPE 131299)

Schulte W.M.: "Challenges and Strategy for Increased Oil Recovery", International Petroleum Technology Conference, 21-23 November 2005, Doha, Qatar. (IPTC 10146)

Seright, R.S. "ARE COLLOIDAL DISPERSION GELS REALLY A VIABLE TECHNOLOGY?" *New Mexico Petroleum Recovery and Research Center (PRRC)*. 2006. Web. 14 Jan. 2012. <http://baervan.nmt.edu/randy/>.

Seright, R.S. "Propagation of an Aluminum-Citrate-HPAM 'Colloidal-Dispersion' Gel through Berea Sandstone" *New Mexico PRRC*. 1995. Web. 19 Jan. 2012. <http://baervan.nmt.edu/research_groups/reservoir_sweep_improvement/pages/Annual%20reports/1994%20Annual/Improved%20Techniques%2094%205.pdf>.

Seright R.S.: "Disproportionate Permeability Reduction with Pore-Filling Gels", Society of Petroleum Engineering Journal (March 2009), pp. 5-13. (SPE 99443)

Seright R.S.: "Impact of Permeability and Lithology on Gel Performance", SPE/DOE Eighth Symposium on Enhanced Oil Recovery, 22-24 April 1992, Tulsa, Oklahoma, U.S.A. (SPE/DOE 24190)

Seright R.S.: "Use of Polymers to Recover Viscous Oil from Unconventional Reservoirs", Oil & Natural Gas Technology (October 12, 2011), pp. 48-52.

Seright R.S. and Liang J.: "A Survey of Field Applications of Gel Treatments for Water Shutoff", III Latin American/Caribbean Petroleum Engineering Conference, 27-29 April 1994, Buenos Aires, Argentina. (SPE 26991)

Seright R.S., Lane R.H. and Sydansk R.D.: “A Strategy for Attacking Excess Water Production”, SPE Production & Facilities (August 2003), pp. 158-169. (SPE 84966)

Seright R.S., Seheult M. and Talashek, T.: “Injectivity Characteristics of EOR Polymers”, SPE Annual Technical Conference and Exhibition, 21-24 September 2008, Denver, Colorado, U.S.A. (SPE 115142)

Seright R.S., Zhang G., Akanni O.O. and Wang D.: “A Comparison of Polymer Flooding with In-Depth Profile Modification”, Canadian Unconventional Resources Conference, 15-17 November 2011, Calgary, Alberta, Canada. (CSUG/SPE 146087)

Sheng, James J. *Modern Chemical Enhanced Oil Recovery: Theory and Practice*. Amsterdam: Elsevier, 2011. Print.

Shi J., Varavei A., Huh C., Delshad M., Sepehrnoori K. and Li X.: “Transport Model Implementation and Simulation of Microgel Processes for Conformance and Mobility Control Purposes”, Energy & Fuels (September 2011a), pp. 5063-5075. (DOI: 10.1021/ef200835c)

Shi J., Varavei A., Huh C., Delshad M., Sepehrnoori K. and Li X.: “Viscosity Model of Preformed Microgels for Conformance and Mobility Control”, Energy & Fuels (September 2011b), pp. 5033-5037. (DOI: 10.1021/ef200408u)

Silverman, Dennis. "Energy Units and Conversions." University of California (UC) Irvine Department of Physics and Astronomy. 2007. Web. 25 June 2011. <http://www.physics.uci.edu/~silverma/units.html>.

Smith D.D., Giraud M.J., Kemp C.C., McBee M., Taitano J.A., Winfield M.S., Portwood J.T. and Everett D.M.: “The Successful Evolution of Anton Irish Conformance Efforts”, 2006 SPE Annual Technical Conference and Exhibition, 24-27 September 2006, San Antonio, Texas, U.S.A. (SPE 103044)

Smith J.E.: “Performance of 18 Polymers in Aluminum Citrate Colloidal Dispersion Gels”, SPE International Symposium on Oilfield Chemistry, 14-17 February 1995, San Antonio, Texas, U.S.A. (SPE 28989)

Smith J.E.: “The Transition Pressure: A Quick Method for Quantifying Polyacrylamide Gel Strength”, SPE International Symposium on Oilfield Chemistry, 8-10 February 1989, Houston, Texas, U.S.A. (SPE 18739)

Smith J.E., Lui H. and Guo Z.D.: “Laboratory Studies of In-Depth Colloidal Dispersion Gel Technology for Daqing Oil Field”, 2000 SPE/AAPG Western Regional Meeting, 19-23 June 2000, Long Beach, California, U.S.A. (SPE 62610)

Smith J.E., Mack J.C. and Nicol A.B.: “The Adon Road - An In-Depth Gel Case History”, 1996 SPE/DOE Tenth Symposium on Improved Oil Recovery, 21-24 April 1996, Tulsa, Oklahoma, U.S.A. (SPE/DOE 35352)

Sorbie, Kenneth S. *Polymer-Improved Oil Recovery*. London: Boca Raton, Flor.: Blackie and Son, CRC., 1991. Print.

Spildo K., Skauge A., Aarra M.G. and Tweheyo M.T.: "A New Polymer Application for North Sea Reservoirs", SPE Reservoir Evaluation & Engineering (June 2009), pp. 427-432. (SPE 113460)

Spildo K., Skauge A. and Skauge T.: "Propagation of Colloidal Dispersion Gels (CDG) in Laboratory Corefloods", 2010 SPE Improved Oil Recovery Symposium, 24-28 April 2010, Tulsa, Oklahoma, U.S.A. (SPE 129927)

Stahl, G. A., and D. N. Schulz. *Water-Soluble Polymers for Petroleum Recovery*. New York: Plenum, 1988. Print.

Stoffer, James O. "Polymer Chemistry Hypertext" University of Missouri - Rolla Chemistry Department. 1998a. Web. 21 May 2012. <http://web.mst.edu/~wlf/MW/huggins.html?huggins+parameter+viscosity>.

Stoffer, James O. "Polymer Chemistry Hypertext" University of Missouri - Rolla Chemistry Department. 1998b. Web. 21 May 2012. <http://web.mst.edu/~wlf/MW/kraemer.html>.

Stoffer, James O. "Polymer Chemistry Hypertext" University of Missouri - Rolla Chemistry Department. 1998c. Web. 21 May 2012. <http://web.mst.edu/~wlf/MW/Mark.html>.

Stosur G.J.: "EOR: Past, Present and What the Next 25 Years May Bring", SPE International Improved Oil Recovery Conference, 20-21 October 2003, Kuala Lumpur, Malaysia. (SPE 84864)

Stosur G.J., Hite J.R., Carnahan N.F. and Miller K.: "The Alphabet Soup of IOR, EOR and AOR: Effective Communication Requires a Definition of Terms", SPE International Improved Oil Recovery Conference, 20-21 October 2003, Kuala Lumpur, Malaysia. (SPE 84908)

Sydansk R.D.: "A New Conformance-Improvement-Treatment Chromium (III) Gel Technology", SPE/DOE Enhanced Oil Recovery Symposium, 17-20 April 1988, Tulsa, Oklahoma, U.S.A. (SPE/DOE 17329)

Sydansk R.D. and Southwell G.P.: "More than 12 Years of Experience with a Successful Conformance-Control Polymer Gel Technology", 2000 SPE/AAPG Western Regional Meeting, 19-23 June 2000, Long Beach, California, U.S.A. (SPE 62561)

Szabo M.T.: "Some Aspects of Polymer Retention in Porous Media Using a C^{14}-Tagged Hydrolyzed Polyacrylamide", Society of Petroleum Engineering Journal (August 1975), pp. 323-337. (SPE 4668)

Teraoka, Iwao. *Polymer Solutions: An Introduction to Physical Properties*. New York: Wiley-Interscience, 2002. Print.

Urbissinova T.S., Trivedi J.J. and Kuru E.: "Effect of Elasticity During Viscoelastic Polymer Flooding: A Possible Mechanism of Increasing the Sweep Efficiency", Journal of Canadian Petroleum Technology (December 2010), Vol. 49, No. 12, pp. 49-56. (SPE 133471)

Wang D., Han P., Shao Z., Chen J., Seright R.S.: "Sweep Improvement Options for the Daqing Oil Field", 2006 SPE/DOE Symposium on Improved Oil Recovery, 22-26 April 2006, Tulsa, Oklahoma, U.S.A. (SPE 99441)

Wreath, D.G.: "*A Study of Polymer Flooding and Residual Oil Saturation*", M.S.E. Thesis, The University of Texas at Austin, December 1989.

Wu Y.S. and Bai B.: "Modeling Particle Gel Propagation in Porous Media", 2008 SPE Annual Technical Conference and Exhibition, 21-24 September 2008, Denver, Colorado, U.S.A. (SPE 115678)

Yanez P.A.P., Mustoni J.L., Relling M.F., Chang K.T., Hopkinson P. and Frampton H.: "New Attempt in Improving Sweep Efficiency at the Mature Koluel Kaike and Piedra Clavada Waterflooding Projects of the S. Jorge Basin in Argentina", 2007 SPE Latin American and Caribbean Petroleum Engineering Conference, 15-18 April 2007, Buenos Aires, Argentina. (SPE 107923)

Yang C., Grattoni C.A., Muggeridge A.H. and Zimmerman R.W.: "Flow of Water through Channels Filled with Deformable Polymer Gels", Journal of Colloid and Interface Science (2002), pp. 466-470.

Zaitoun A., Tabary R., Rousseau D., Pichery T., Nouyoux S., Mallo P. and Braun O.: "Using Microgels to Shut Off Water in a Gas Storage Well", 2007 SPE International Symposium on Oilfield Chemistry, 28 February - 2 March 2007, Houston, Texas, U.S.A. (SPE 106042)

Zhang H. and Bai B.: "Preformed Particle Gel Transport through Open Fractures and its Effect on Water Flow", 2010 SPE Improved Oil Recovery Symposium, 24-28 April 2010, Tulsa, Oklahoma, U.S.A. (SPE 129908)

"EIA - 2010 International Energy Outlook - Liquid Fuels." Web. 25 June 2011. <http://www.eia.gov/oiaf/ieo/liquid_fuels.html>.

"EIA - 2010 International Energy Outlook - World Energy Demand and Economic Outlook." Web. 20 June 2011. <http://www.eia.gov/oiaf/ieo/world.html>.

"EIA - Appendix A - Reference Case Projection Tables." Web. 25 June 2011. <http://www.eia.gov/oiaf/ieo/ieorefcase.html>.

"EIA's Energy in Brief: How Much Renewable Energy Do We Use?" Web. 20 June 2011. <http://www.eia.gov/energy_in_brief/renewable_energy.cfm>.

"EIA Renewable Energy-U.S. Energy Consumption by Energy Source." Web. 25 June 2011. <http://www.eia.gov/cneaf/alternate/page/renew_energy_consump/table1.html>.

“Oil & Gas Journal - EOR Continues to Unlock Oil Resources.” Web. 12 April 2004. <http://www.ogj.com/articles/print/volume-102/issue-14/special-report/eor-continues-to-unlock-oil-resources.html>.

"World Population: 1950-2050 - U.S. Census Bureau." Census Bureau Home Page. Web. 20 June 2011. <http://www.census.gov/ipc/www/idb/worldpopgraph.php>.

Vita

Mazen Ramzi Abdulbaki attended The International School of Choueifat in Abu Dhabi. In 2007, he graduated and went on to enroll in Rice University as an undergraduate student. He received a B.S. degree in Chemical Engineering from Rice University, in 2010. Later that year, he joined the Department of Petroleum & Geosystems Engineering at The University of Texas at Austin, as a graduate student pursuing a Master's of Science in Petroleum Engineering. Throughout his time as a graduate student, he worked as a graduate research assistant, under the supervision of Dr. Kamy Sepehrnoori.

Permanent e-mail address: mazen.r.abdulbaki@gmail.com

This thesis was typed by Mazen Ramzi Abdulbaki.